FOLATE RECEPTOR MEDIATED GENE TARGETING: COMPARATIVE EVALUATION OF NATURAL AND SYNTHETIC POLYMER BASED NANOPARTICLES

A THESIS PRESENTED BY
VIOLA B MORRIS
TO

SREE CHITRA TIRUNAL INSTITUTE FOR MEDICAL SCIENCES AND TECHNOLOGY, TRIVANDRUM
Thiruvananthapuram

IN PARTIAL FULFILMENT OF THE REQUIREMENTS
FOR THE AWARD OF
DOCTOR OF PHILOSOPHY

2010

To My Eternal Supervisor

Holy Mother Mary.....

CERTIFICATE

*"I Viola B Morris, hereby certify that I had personally carried out the work depicted in the thesis entitled, "**Folate receptor mediated gene targeting: Comparative evaluation of natural and synthetic polymer based nanoparticles**", to the best of my knowledge and belief, it contains no material previously published or written by another person nor material which has been accepted for the award of any other degree or diploma of the university or other institute of higher learning, except where due acknowledgment has been made in the text".*

Place: Trivandrum
Date: 11-11-2010

Signature : 
Name : Viola B Morris
Reg.No: 5672

Tel: (91) 471 234 0801
Fax: (91) 471 234 1814

Grams: CHITRAMET
Telex: 0435 6290

श्री चित्रा तिरुनाल आयुर्विज्ञान तथा प्रौद्योगिकी संस्थान
बायो मेडिकल टैक्नोलॉजी विंग
पूजापुरा, तिरुवनन्तपुरम-695 012, इन्डिया

SREE CHITRA TIRUNAL INSTITUTE FOR MEDICAL SCIENCES AND TECHNOLOGY
BIOMEDICAL TECHNOLOGY WING
POOJAPPURA, THIRUVANANTHAPURAM 695012, INDIA
(An Institute of National Importance under Govt. of India)

Dr. Chandra P. Sharma
Senior Scientist G & Head, Biosurface Technology Division
Associate Dean, PhD Programme
sharmacp@sctimst.ac.in

November 11, 2010

This is to certify that Ms. Viola B Morris in the division of Bio-Surface Technology of this Institute has fulfilled the requirements prescribed for the Ph.D degree of the Sree Chitra Tirunal Institute for Medical Sciences and Technology, Trivandrum.

The thesis entitled, "Folate Receptor Mediated Gene Targeting: Comparative Evaluation of Natural and Synthetic Polymer based Nanoparticles" was carried out under my direct supervision. No part of the thesis was submitted for the award of any degree or diploma prior to this date.

*Clearance was obtained from the Institutional Ethics Committee/ Institutional Animal Ethics for carrying out the study

Chandra P. Sharma
(Research Supervisor)

The thesis entitled

FOLATE RECEPTOR MEDIATED GENE TARGETING: COMPARATIVE EVALUATION OF NATURAL AND SYNTHETIC POLYMER BASED NANOPARTICLES

Submitted by

Viola B Morris

for the degree of

Doctor of Philosophy

of

SREE CHITRA TIRUNAL INSTITUTE FOR MEDICAL SCIENCES AND TECHNOLOGY, TRIVANDRUM
Thiruvananthapuram

Is evaluated and approved by

Dr. Chandra P Sharma
(Research Supervisor)

Examiner

Acknowledgements

It is a pleasure to thank many people for their support during the last three years which made this thesis possible.

First of all, I wish to thank my supervisor, Dr. Chandra P. Sharma who always inspired me through his valuable guidance, cheerful enthusiasm and encouragement during the entire course of this work. It was only due to his understanding, personal support and great patience that I was able to complete my research work in a respectable manner. I am very grateful to Dr. C.K.S. Pillai, my earlier research supervisor at Regional Research Laboratory, Trivandrum, and Emeritus Scientist at SCTIMST, from whom I got the fundamentals of my present research. His sound advice and parenting support encouraged me a lot.

I owe my most sincere gratitude to Dr. K. Radhakrishnan, Director of our Institute, Dr. K. Mohandas, earlier director of our institute, Dr. G.S. Bhuvaneshwar, Head of BMT wing for all the facilities provided during the course of my work. I am thankful to The Registrar and Deputy Registrar for their academic assistance. I would like to thank my doctoral advisory committee members Dr. A.K. Gupta, Dr. K. Sreenivasan, Dr. T Anoopkumar and Dr. M.R. Rekha for valuable suggestions and critical comments in each stage of the work. I appreciate Dr. M.R. Rekha for her patience in answering and discussing all the small and bigger problems aroused during my daily lab life.

I am grateful to Council of Scientific and Industrial Research, India for the research fellowship and financial assistance from Department of Science & Technology, Govt. of India through the project Facility for nano/microparticles based biomaterials- advanced drug delivery systems #8013, under the Drugs &Pharmaceuticals Research Programme.

I have received a lot of help from many people during my research. First of all I have to thank Dr. E. Sreekumar, Scientist at Rajiv Gandhi Centre for Biotechnology from whom I learned the fundamentals of plasmid isolation. He also kindly provided me green fluorescent plasmid for which I am extremely grateful. I warmly thank Dr. Anoopkumar and his students Ms. Sunitha and Ms. Vrinda for further plasmid isolations works. I am grateful to Dr. T.V. Anilkumar for giving me training in confocal microscopy and letting me use the equipment. My warm thanks to Mr. Willi Paul for his support during my course and patience in doing Atomic force microscopy studies. I leave a grateful note to Dr. T.V. Kumary for allowing me to use equipments at common instrument room. I wish to thank Dr. Lissy K. Krishnan and Mr. Renjith Nair for FACS analysis. My sincere thanks to Dr. H.K. Varma and Mr. Suresh Babu S. for Infrared spectroscopy studies. My warm thanks to Dr. K.Sreenivasan and Mr. Hari P.R. for gel permeation chromatography studies. I gratefully acknowledge Dr. Annie John, Dr. Harisrishnan V.S. and all the staff of Division of Laboratory Animal Science for the help during my animal experiments. My sincere thanks to Dr. Mira Mohanty and Mr. Joseph Sebastian for cryosectioning of tissues and Ms. Susan for TEM studies.

I express my sincere gratitude for library facility especially to Mr. J.C. Das and Mr Suresh N. Above all I deeply grateful to my sincere friend Mr. Arun Anirudhan for the preparation of whole thesis in the present form and Mr. Muraleedharan C. V for the facilities provided.

I am thankful to all staff of Biosurface Technology for their support and encouragement. I thank Ms. Shelma, Ms. Sonia, Ms. Susan, Ms. Nimi, Mr. Durga Das, Dr. Sunitha, Dr. Raj Mohan, Ms. Joshy, Ms. Radhika, Ms Thasneem, Ms.Vijila and Ms Mini for all their good

friendship and support, and special thanks to Ms. Jane Joy Thomas for her language help. I wish to extend thanks to my senior Ph.D colleagues Dr. Kaladhar Kamalasanan and Dr. Sajeesh S. for their timely advice and suggestion.

I am really privileged to have my sincere friend Dr. Nirmal Ravi, for helping me to get through the difficult times and for the constant encouragement. I owe my loving thanks to my beloved friends Ms. Dimple, Dr. Prasanth R. Krishna Dr. Divya P, Dr.Manju Pradeep, Dr. Viji Mary and Mr. Shine Joseph for their love and caring. I extend my warm thanks to Ms. Beena, Ms. Soumya, Ms. Manju, Ms Rathikala and Ms. Ragaseema for their good company while sharing home.

Lastly, and most importantly, I wish to thank my parents Mr. S. Ben Morris and Mrs. Elizabeth Ben Morris. Without their prayer, encouragement and love I could not have finished my research. I extend my warm gratitude to my grandmother, brother, sister and their family.

This life is not enough to thank Lord my God for all his divine mercy. **"I am always aware of the Lord's presence; He is near, and nothing can shake me."(Psalms: 16:8)**. For God says **"I will always guide you and satisfy you with good things. I will keep you strong and well"(Isai: 58: 11)** .

Viola B. Morris

Contents

List of Figures

List of Tables

Abbreviations

Abs	Absorbance
AFM	Atomic force microscopy
ATFP	Arginine modified trimethylated chitosan having folic acid-polyethylene glycol conjugation.
ATMC	Arginine modified trimethylated chitosan
BCA	Bicinchoninic acid
BSA	Bovine serum albumin
Chito	Chitosan
DLS	Dynamic light scattering
DM	Degree of dimethylation
DMSO	Dimethyl sulphoxide
DNA	Deoxyribonucleic acid
DOM	Degree of O-methylation
DQ	Degree of quaternisation
DSC	Differential scanning calorimetry
EDC	1-Ethyl-3-(3-dimethylaminopropyl) carbodiimide hydrochloride
EDTA	Ethylene diamine tetra acetic acid
FA	Folic acid
FBS	Foetal bovine serum
FFRPMI	Folate free RPMI
FITC	Fluorescein isothiocyanate
FTIR	Fourier transform infrared spectroscopy
GFP	Green fluorescent protein

GPC	Gel permeation chromatography
h	hours
HBSS	Hanks buffered salt solution
HTFP	Histidine modified trimethylated chitosan having folic acid-polyethylene glycol conjugation
HTMC	Histidine modified trimethylated chitosan
kDa	kilo Dalton
kV	kilo volt
MEM	Minimal essential medium
MTT	3-(4, 5-Dimethylthiazol-2-yl)-2, 5-diphenyltetrazolium bromide
mV	milli Volt
Mv	Viscosity average molecular weight
Mw	Weight average molecular weight
MWCO	Molecular weight cut- off
NHS	N-hydroxy succinimidyl ester
nm	nano meter
NMR	Nuclear magnetic spectroscopy
PBS	Phosphate buffered saline
pDNA	plasmid DNA
PEG	Polyethylene glycol
PEI	Polyethyleneimine
ppm	parts per million
PRP	Platelet rich plasma
RES	Reticulo endothelial system
RLU	Relative light units
RT	Room temperature
TEM	Transmission electron microscopy
TMC	Trimethyl chitosan
TNBS	Trinitrobenzenesulfonic acid
UV	Ultraviolet

SYNOPSIS

According to the World Health Organisation, cancer continues to be the leading cause of death. The American Cancer Society estimated that the global burden of cancer cases is expected to grow to 27 million and cancer death to 17.5 million by 2050. The cause of cancer by mutation of genes in transformed cells created a great interest in the application of gene therapy techniques to cancer treatment. Many human tumors including cancers of the brain, lung, ovary, uterus, kidney, testis, colon and myelocytic blood cells, are over expressed by folate receptors, which is absent in most of the normal tissues. Similarly, folate receptor density appears to increase as the stage or grade of the cancer worsens. These factors enlighten the use of folate mediated gene delivery vectors in the treatment of cancers which are difficult to treat by classical methods. In the present study, we have evaluated natural and synthetic based polymers for tumor targeted gene delivery. On the basis of transfection efficiency, biocompatibility, and in vivo tumor targeting efficiency, we have demonstrated that folate mediated arginine modified oligo(-alkylaminosiloxane)-graft-poly(ethyleneimine) as a potential vector for future cancer gene therapy.

This synopsis is subdivided into background and objectives, hypothesis, methods, major findings and significance of the findings.

Cancer is a group of diseases characterised by unrestrained cell growth, invasion followed by destruction of adjacent tissues and metastasis, being the spread to distant anatomic sites via blood or lymph. Cancer is caused by mutation in genes responsible for the cell cycle. Carcinogens mutate DNA which thus leads to cancer. Tobacco, asbestos, arsenic, radiation such as gamma and x-rays, the sun and compounds in car exhaust fumes are all examples of carcinogens. Tumor suppressor genes and proto oncogenes are two general classes of genes responsible for cancer development. Replacement of mutated cancer causing genes with healthy copy of therapeutic genes can help to exterminate the disease. Particularly, a short expression of therapeutically active proteins may be sufficient to get rid of tumors other than genetic diseases like cystic fibrosis, which need long term expression. Therefore, gene therapy is found to be more advantageous compared to chemotherapy and radiation. The first clinical study on gene therapy was carried out in 1989. Till date, out of the total 1579 gene therapy

clinical trials undergone, 1019 (64.5% of all gene therapy trials) clinical studies have been cancer related. Generally, gene transfer is achieved by delivering the gene expression plasmid directly to the patient with the help of a gene delivery system. An effective cancer gene delivery system requires the successful transport of the transgene from the site of administration to the nucleus of the target cells. In order to do so, the system has to overcome several barriers such as interaction with blood components and vascular endothelial cells, serum inactivation, degradation by nucleases, non specific uptake such as uptake by reticuloendothelial system and so on. Mainly two types of gene delivery systems including viral and non viral vectors are used for clinical applications. The disadvantages of viral vectors such as limited DNA loading capacity, toxicity, immunogenicity, inflammatory response, insertional mutagenesis and high cost encourages the development of non viral delivery systems. Compared to viral vectors, non-viral vectors are advantageous due to low immune response, unlimited size of insert DNA up to 52 kb and capability of large production with acceptable cost. The two major classes of non-viral systems are cationic liposomes and cationic polymers. Cationic liposomes can effectively interact electrostatically with negatively charged DNA and help to transfer it into the cell. However, these complexes are relatively toxic, widely distribute in the body and rapidly clear from the bloodstream. On the other hand, cationic polymer/DNA complexes are more stable than cationic lipids. Although cationic polymers do not exhibit high transfection efficiency compared to viral vectors, the structural variability and versatility for selected modifications make them promising in the field of gene delivery.

Biodistribution barriers for the systemic delivery of cancer genes include the interaction with blood components and nonspecific uptake. The objective of the present study is to synthesize a systemically stable tumor targeted gene delivery system. Systemic stability can be achieved by the introduction of steric stabilisation on conjugating neutral polymers such as polyethylene glycol(PEG) or (N-(2 -hydroxypropyl)methacrylamide) (pHPMA) with cationic polymers. Such modification changes the biodistribution pattern and enhances the prolonged circulation of the conjugates thereby, enabling their targeting to specific tissues. Since the reduced form of folic acid (Vit. B9) is essential for rapidly dividing cells including cancer cells for numerous bodily functions, an elevation in the appetite for physiological folates permit the cells to over express

folate receptors. The conjugation of folic acid (FA) ligand to neutral polymer like PEG assists in the achievement of both systemic stability and tumor targeting simultaneously. Therefore, in the present work, we hypothesized the synthesis of a systemically stable tumor targeted gene delivery vector by grafting PEG-FA conjugates to different cationic polymers such as arginine and histidine modified natural and synthetic based polymers.

High molecular weight chitosan was chosen as the natural polymer. Native chitosan was depolymerized into four different molecular weights such as 15 kDa, 50 kDa, 85 kDa and 120 kDa using $NaNO_2$ oxidative depolymerisation method. Each depolymerised chitosan was then trimethylated to two different degrees by varying the trimethylating agent,methyl iodide. The trimethylated products were further conjugated with arginine and histidine using EDC/NHS chemistry. The arginine and histidine modified trimethylated depolymerised chitosans were named as ATMC and HTMC derivatives respectively. Out of the two groups of ATMC and HTMC, the chitosan having low molecular weight such as 15 kDa and high degree of trimethylation was found to have the highest transfection efficiency and lowest cytotoxicity. They were further conjugated with PEG-FA using DCC and NHS in DMSO. The resultant polymers were named as ATFP15H and HTFP15H. Both the polymers were then characterized by means of IR and NMR for structural evaluation, TNBS assay to evaluate the degree of primary amines and acid-base titration to determine the buffering capacity. The derivatives were then bound with DNA, and the obtained nano sized complexes were characterised to evaluate its potential for gene delivery. The size and zeta potential of the particles were determined by dynamic light scattering method using Zetasizer Nano ZS. The morphology of the particles were analysed by transmission electron microscopy(TEM). Physical integrity of the DNA after complexation with polymers was determined using agarose gel electrophoresis. The protection of DNA by the polymers from degradation by cellular nucleases abundant in serum and extracellular matrix were also evaluated by electrophoretic shift assay in the presence of DNase1. Hemolysis and nanoparticles induced aggregation of erythrocytes under invitro conditions, were analyzed as a prerequisite for the intravenous administration of complexed nanoparticles in animals or humans. The cytotoxicity of nanoplexes of both ATFP15H and HTFP15H was tested using cancer cell lines. Transfection studies were performed on KB oral epidermoid cells expressing

high amount of folate receptors, by using pGL3-Luc and pEGFP as reporter genes in presence of 10% serum. *In vitro* targeting ability of the polymers was determined by estimating the percentage of cells with fluorescently labeled nanoparticles after 4 h of incubation using FACS. Nuclear localisation ability of the nanoparticles were also determined by labeling the nanoparticles and nucleus of the cells with different tags and observed by fluorescent microscope.

The synthetic polymer used was based on the commercially available branched PEI having a molecular weight of 25 kDa, also referred to as "Gold Standard". It was grafted with arginine and histidine modified oligoalkylaminosiloxane. Initially, the oligo- (alkylaminosiloxane) was prepared by polymerising 3-(2-aminoethylamino) propyl-methyl- dimethoxysilane in presence of 1 N NaOH. From the preliminary characterization, it was observed that the product formed was an oligomer of 5 siloxane group. Thus the resultant product was further conjugated with 5 equivalents of arginine and histidine using EDC and NHS to obtain SiDAAr and SiDAHs respectively. Using an aspartic acid molecule as a linker group, these oligomers were then grafted with PEI. By keeping the equivalents of PEI as constant and by varying the composition of SiDAAr or SiDAHs molecule, two groups having 4 polymers each were prepared. The derivatives synthesized by arginine group were P(SiDAAr)1, P(SiDAAr)5, P(SiDAAr)10, P(SiDAAr)15 and by histidine group were P (SiDAHs)1, P (SiDAHs)5, P (SiDAHs)10 and P (SiDAHs)15. From the physicochemical characterizations performed as given above, P (SiDAAr)5 from the arginine group and P(SiDAHs)1 from histidine group were chosen to induce tumor targeting. By varying the composition of PEG-FA conjugate to the P(SiDAAr)5 and P(SiDAHs)1 polymers, four different derivatives such as P(SiDAAr)5FP2, P(SiDAAr)5FP3, P(SiDAHs)1FP2 and P(SiDAHs)1FP3 were prepared. All the derivatives were again characterised for *in vitro* cytotoxicity, systemic stability, transfection efficiency and tumor targeting ability. From the characterizations determined, P(SiDAAr)5FP2 was selected for the examination of invivo tumor targeting.

Balb/C mice were selected for performing *in vivo* tumor targeting experiment. 25-30 gram weighed mice were injected subcutaneously with $2x10^6$ KB cells. After 2-3 weeks, the fluorescent labeled polymers were injected intravenously into the mice. The mice were sacrificed and tumor, liver and kidney were excised at 2, 4, 16, and 24 h interval post injection. The

frozen sections of the tissues were analyzed using confocal microscopy. The polymer without the targeting group was used as control.

Major findings and significance of the work were as follows. From the characterizations of tumor targeted natural based polymers, it was observed that both ATFP15H and HTFP15H derivatives exhibited endosomal disrupting capacity more than PEI. From dynamic light scattering measurement and transmission electron micrographs, it was clear that the derivative was able to condense the plasmid DNA effectively and form positively charged core-shell nanostructured particles having a size of less than 100 nm. Due to the presence of PEG group, both the derivatives were found to be compatible with blood in terms of percentage hemolysis, and erythrocyte aggregation. The PEG group could also improve the colloidal stability of polyplexes and cell viability to an extent of greater than 125% compared to control at the concentration of 10 μg of the derivative. Finally due to the large extent of cellular uptake and nuclear trafficking, ATFP15H and HTFP15H derivatives were found to exhibit improved transfection efficiency in KB cell lines even in the presence of 10% serum compared to native polymers as ATMC15H and HTMC15H respectively. The outstanding characteristics observed for ATFP15H derivative was its membrane permeability and nuclear localization ability. Similarly, HTFP15H derivative was characterised by its enhanced buffering capacity. Even though the derivatives exhibited better systemic stability and cell viability, the transfection efficiency of both the polymers were not better than the control PEI. Thus, our aim was to improve transfection efficiency by maintaining the systemic stability and cell viability. Based on the above objective, we synthesized arginine and histidine modified oligoalkyl amino siloxane grafted poly ethyleneimine. *In vitro* transfection efficiency studies revealed that P(SiDAAr)5 polymer exhibited much better transfection efficiency compared to PEI while P(SiDAHs)1 derivative showed almost similar transfection efficiency to that of PEI. However, both the polymers showed enhanced cell viability than PEI. They were further modified to induce tumor targeting ability. Due to the presence of PEG group, the transfection efficiency of the daughter polymer was evaluated to be less than the parent polymer. But it was found to be much better than the control polymers such as superfect and PEI. Out of the arginine and histidine group of polymers, P(SiDAAr)5FP2 derivative showed highest transfection efficiency, cell viability and systemic stability compared

to other derivatives and PEI. Therefore, the polymer was then further analyzed for *in vitro* and *in vivo* tumor targeting ability. From the above experiments, it was observed that the polymer showed very good tumor targeting ability systemically even at the 2^{nd} hour of nanoparticles injection. These observations led to the conclusion that the P(SiDAAr)5FP2 derivative is a promising candidate for futurecancer gene therapy.

1 INTRODUCTION

1.1 Cancer Gene Therapy.

The branch of medicine concerned with the study, diagnosis, treatment, and prevention of cancer is called oncology. Despite the recent advancements in oncology, cancer continues to be a significant medical problem. According to the World Health Organization, cancer is a leading cause of death worldwide. Cancer affects people at all age groups in which the risk increases with age. It was estimated that in 2007, 12 million new cancer cases were reported and about 7.6 million total cancer deaths worldwide. Cancer caused about 13% of all human deaths in 2007. In 2010, about 1,529,560 cancer cases have been diagnosed. By 2050, the global burden is expected to grow to 27 million new cancer cases and 17.5 million cancer deaths (Hernandez, Green, Cassel, Pobutsky, Vu & Wilkens 2010).

1.1.1 Cancer and its classification.

The abnormal proliferation of genetically altered cells is called neoplasm. Neoplasm can be benign or malignant. Cancer or malignant neoplasm is a class of disease that involve three malignant properties such as uncontrolled cell growth beyond the normal limits, invasion followed by destruction of adjacent tissues and metastasis, being the spread to distant anatomic sites via blood or lymph. Benign neoplasm or benign tumor are self limited. They neither invade other tissues nor form metastasis. Cancers are classified according to their cell type of origin such as histology and location. Examples of general categories include:

- **Carcinoma:** These are the malignant tumors derived from epithelial cells that cover internal and external parts of the body such as lung, breast, prostate and colon cancer.
- **Sarcoma:** Malignant tumors derived from the cells that are located in bone, cartilage, fat, muscle, connective tissue or mesenchymal cells.
- **Lymphoma:** cancers derived from lymph nodes and immune system tissues.
- **Leukemias:** are cancers that begin in the bone marrow and later accumulate in the blood stream.

- **Adenoma:** are cancers that arise in the thyroid, the pitutary gland, the adrenal gland and other glandular tissues.
- **Blastoma or Blastic tumor:** A tumor which resembles an immature or embryonic tissue. Many of these tumors are most common in children.
- **Germinoma:** Tumors derived from germ cell of ovary or testes in adults and in fetuses, babies and young children. These cancers are often found on the body midline, particularly at the tip of the tailbone.
- **Mesothelioma:** The tumor derived in mesothelial cells that line the peritoneal and pleural cavities.

1.1.2 Genetics of cancer.

In 1902, a German zoologist Theodor Boveri postulated that chromosomes were distinct and transmitted different inheritance factors (Jiao & Habib 2003). He suggested that mutations of the chromosomes could generate a cell with unlimited growth potential which could be passed onto its descendents. Cancers are caused by mutations in the genes of transformed cells responsible for the synthesis of proteins involved in the regulation of the cell cycle. Agents that cause DNA damage are known as mutagens and mutagens that cause cancers are known as carcinogens. Tobacco, asbestos, arsenic, radiation such as gamma and x-rays, the sun and compounds in car exhaust fumes are all examples of carcinogens. Particular substances have been linked to specific types of cancer. For example, tobacco smoking is associated with lung cancer and prolonged exposure to asbestos fibre is associated with mesothelioma (O'Reilly, Mclaughlin, Beckett & Sime 2007). Most forms of cancer are sporadic i.e. they have no inherited cause. However, it is estimated that 5%-10% of all cancers occur through errors in DNA replication or are inherited, meaning that individuals who inherit a specific genetic alteration have a very high risk of developing a particular cancer (Hernandez et al. 2010). For example, certain inherited mutation in the genes of BRCA1 and BRCA2 are associated with an elevated risk of breast cancer and ovarian cancer. Another well known cancer is retinoblastoma, which occur in young children, due to a hereditary mutation in the retinoblastoma gene. The heritability of these cancers is usually affected by complex interactions between environmental

factors and the hosts genome. Genetic abnormalities accountable for the cause of cancer typically affect two general classes of genes such as proto-oncogenes and tumor suppressor genes. Proto-oncogenes are normal genes that promote cell growth and mitosis. When proto-oncogenes are mutated to oncogenes by carcinogenic agents, it produces excessive levels of growth promoting proteins which give rise to the hyperactive growth and division, protection against programmed cell death, loss of respect for normal tissue boundaries and the ability to become established in diverse tissue environment. Tumor suppressor genes are genes which discourage growth, survival and other properties of cancer cells. Tumor suppressor gene products typified by p53 are frequently transcription factors that suppress mitosis and cell growth. In cancer cells, the tumor suppressor gene is inactivated, resulting in the loss of normal functions such as accurate DNA replication, control over cell cycle, orientation and adhesion within tissues, and interaction with protective cells of the immune system. Nearly half of all cancers are caused by altered p53 genes. Other suppressor genes include Rb (retinoblastoma family), APC (adenomatous polyposis coli), BRCA (breast cancer susceptibility protein) type 1 and 2, SMAD4, TP53, and p16/CDKN2A. Oncogenes are typically dominant because they provide gain-of-function i.e., only one copy of a proto-oncogene needs to mutate for gain-of-function, whereas suppressor genes are recessive. They contain loss-of function mutations i.e. both copies of a suppressor gene need to mutate to cause loss-of-suppressor function. Mutations of tumor suppressor genes can be inherited. Other potential therapeutic genes for cancer include suicide genes which control apoptosis and DNA- repair genes which instruct a cell to repair damaged DNA.

1.1.3 Treatment for cancer.

Treatment for cancer depends on many factors such as type of cancer, stage of cancer, age, health status and additional personal characteristics of patient. Based on these factors, patient often receive one or more combinations of therapies and palliative care. Usual treatments for cancer are surgery, radiation, chemotherapy, immunotherapy, hormone therapy or gene therapy. Surgery, the oldest known treatment for cancer, is effective only if cancer has not metastasized. After the disease has spread, it is nearly impossible to remove all the cancer cells by surgical means. Radiotherapy utilises high energy gamma rays that are emitted from

metals such as radium or high energy x-rays and is not specific in its action. It is capable of destroying both normal and malignant cells. However, radiotherapy is used as a standalone treatment to shrink a tumor or destroy cancer cells, and it is also used in combination with other cancer treatments. Chemotherapeutic agents are cytotoxic drugs that interfere with the cell division process so that cancer cells will commit suicide. These treatments target any rapidly dividing cells, not necessarily just cancer cells. Chemotherapy is generally used to treat cancer that has metastasized because the drug travels throughout the entire body. However, they suffer from significant adverse reactions to many organs. Immunotherapy aims to get the bodys immune system to fight the tumor. It can be done locally or systemically. Local immunotherapy causes local inflammation and tumor shrink, while, systemic immunotherapy treats the whole body by administrating agents such as the protein interferon alpha that can shrink tumors. Hormone therapy finds advantage on the relationship between cancer and hormone, most notably breast and prostate cancer. It is designed to alter hormone production in the body so that cancer cells stop growing or are killed completely. Breast cancer hormone therapy focuses on the reduction of estrogen levels and prostate cancer hormone therapies often focus on reduction of testosterone levels. Similarly, in the case of leukemia and lymphoma, the hormone cortisone has to be reduced. These therapies are in its initial stages.

1.1.4 Gene therapy for cancer.

The understanding of genetics of cancer created a great interest in applying gene therapy techniques for cancer treatment. The goal of gene therapy is the correction of genetic disorders by delivering therapeutic genes into the target cells of patients in order to compensate for the defective gene responsible for disease development. This approach provides a promising tool to eradicate the disease by treating it at its source. Particularly, a short expression of therapeutically active proteins may be sufficient to get rid of tumors other than genetic diseases like cystic fibrosis, which need long term expression. The first clinical study on gene therapy was carried out in 1989. Till date, out of the total 1579 gene therapy clinical trials undergone, 1019 (64.5% of all gene therapy trials) clinical studies have been related to cancer (Biesalski, Bueno de Mesquita, Chesson, Chytil, Grimble, Hermus, KÃhrle, Lotan, Norpoth, Pastorino & Thurnham 1998) (*Gene therapy clinical trials* 2010).

Researchers are studying several ways to treat cancer using gene therapy. In one approach, replacement of altered genes such as tumor suppressor genes or oncogenes with healthy genes result in the prevention of cell growth (Boveri 2008). In other approach researchers are trying to improve patient's immune response to cancer. These include the method such as ex vivo transfection of T-lymphocytes to tumors and the localized delivery of cytokines that mediate inflammation and an immune response at the tumor site (OMalley & Couch 1999). Scientists are investigating the insertion of genes into cancer cells to make them more sensitive to chemotherapy, radiation therapy or other treatments. In one such approach, researchers introduce "suicide genes" into a patient's cancer cells. A pro-drug is then given to the patient in order to activate the suicide genes, which leads to the destruction of those cancer cells (Kirn 2002). The most commonly investigated suicide genes are the herpes simplex virus thymidine kinase (HSV-tk) and cytosine deaminase (CD) (OMalley & Couch 1999). Other research is focused to prevent cancer cells from developing new blood vessels by the delivery of antiangiogenic genes capable of reducing the tumor vascularisation and reducing its proliferation (Lin, Buxton, Acheson, Radziejewski, Maisonpierre, Yancopoulos, Channon, Hale, Dewhirst, George & Peters 1998) (Goldman, Kendall, Cabrera, Soroceanu, Heike, Gillespie, Siegal, Mao, Bett, Huckle, Thomas & Curiel 1998).

1.2 Methods of Gene Transfer.

Gene transfer can be achieved by either *ex vivo* or *in vivo*. The *ex vivo* approach includes the following steps (a) isolation of healthy cells from either patients blood or bone marrow; (b) transferring these cells in cell culture with the gene expression plasmid; and (c) subsequently implanting the transfected cells back to the patient. In the *in vivo* gene therapy, the gene delivery system carrying the gene expression plasmid is directly introduced to the patient. Several systems are used to transfer foreign genetic material into human body. An effective cancer gene delivery system requires the successful transport of the transgene from the site of administration to the nucleus of the target cells. In order to do so the system have to overcome several barriers such as interaction with blood components, vascular endothelial cells, serum inactivation and degradation by nucleases, non specific uptake such as uptake by recticuloendothelial system and so on. Therefore the vector should be capable of protecting

DNA and render it inaccessible to degradative enzymes. Protection of the gene could be achieved by encapsulation in protein capsules such as viral vectors, by condensation in poly cationic lipid or polymers or by entrapping in controlled release hydrogels. While nonspecific uptake can be reduced by attaching targeting ligands to the surface of the DNA delivery vector.

1.2.1 Gene delivery vectors.

1.2.1.1 Direct injection of naked DNA.

One of the simple and successful approaches to gene delivery is the direct injection of naked DNA in to the tumor site (Wolff, Malone, Williams, Chong, Acsadi, Jani & Felgner 1990). This has been shown to produce high levels of gene expression, however the pattern of expression is non uniform (Choate & Khavari 1997). Naked DNA is also unstable for systemic administration due to the presence of serum nucleases. Therefore this approach is limited to tissues that are easily accessible such as skin and muscles.

1.2.1.2 Viral gene delivery vectors.

The use of genetically altered viruses is another highly efficient gene transfer method. The most common viral vectors used today are retrovirus, adenovirus, herpes simplex virus, lentivirus, adeno-associated virus, which have been modified by eliminating their viral coding sequence partially or completely with therapeutic genes (Mansouri, Lavigne, Corsi, Benderdour, Beaumont & Fernandes 2004) (El-Aneed 2004). These vectors show very high gene transfection efficiency with major drawbacks such as limited DNA loading capacity, toxicity, immunogenicity, inflammatory response, insertional mutagenesis and high cost (Morille, Passirani, Vonarbourg, Clavreul & Benoit 2008). The limitations of viral vectors encouraged the development of alternative vectors based on non-viral systems.

1.2.1.3 Non viral vectors.

Synthetic or non-viral gene delivery vectors are typically of cationic in nature especially cationic lipids and cationic polymers. They interact with negatively charged DNA through electrostatic interactions leading to lipoplexes and polyplexes respectively. Even though the transfection efficiency of non viral vectors are lower than that of their viral counterparts, these kind of vectors are associated with many advantages such as low immunogenic response,

the capacity to carry large inserts of DNA (52kb), possibility of selective modification using ligand and large scale manufacture. (Zhang, Xu, Wang, Qiao, Liu & Li 2004) (El-Aneed 2004) (Dass 2002). Among non-viral vectors, lipoplexes were the first delivery carriers used in clinical trials (Fernandez & Rice 2009). Out of the three basic constituents of cationic lipids, such as the polar head group, a linker and a hydrophobic moiety, cationic head group promotes interaction with DNA. Even though tremendous technical advances have been made by encapsulating DNA or RNA in liposomes, wide bio distribution and poor transfection efficiency focused on the development of polymeric gene delivery vectors.

Cationic polymers are able to condense more DNA with more stability than lipids. Irrespective of the cationic lipids, cationic polymers do not contain a hydrophobic moiety and therefore the complexes are completely soluble in water (Elouahabi & Ruysschaert 2005). In addition it has the ability to compress DNA molecule to a relatively small size. This could be an essential requirement for better transfection efficiency (Gershon, Ghirlando, Guttman & Minsky 1993). These vectors can be easily be modified by varying the molecular weight, geometry (linear vs. branched) and ligand attachment according to the end use (Elouahabi & Ruysschaert 2005) (Gershon et al. 1993) (Gao & Hui 2001). This opens the way to extensive structure/ function relationship studies. The following section will explain the hurdles which have to be overcome for the development of an ideal polymeric gene delivery vector for tumor targeted gene therapy.

1.3 Hurdles in Cancer Gene Therapy.

An ideal gene delivery vector is the one having an ability to transport therapeutic gene into targeted cells. For cancer gene therapy, treatment needs to be administered systemically. During systemic targeting of tumors the cationic systems have to survive in the bloodstream without being degraded or captured by cellular defence mechanisms (Sorgi, Bhattacharya & Huang 1997) (Schwartz, Ivanov, Pitard, Escriou, Rangara, Byk, Wils, Crouzet & Scherman 1999). Once at the tumor site, they have to extravasate into the tissue and bind specifically to the target cells. After their cellular internalization, large amounts of complexes are degraded in the endolysosomal compartment or in the cytoplasm. In the end, only a very small fraction of the applied dose has been observed to exhibit the desired effect. The following discussion highlights the diverse barriers to safe and efficient gene delivery.

1.3.1 Hurdles at the systemic gene delivery.

Systemic delivery of the cationic DNA carrier system is hindered by various factors. Extravasation of complexes beyond the endothelial barrier is one major problem. It depends on the size of the complex and the permeability of the endothelia at the specific sites. The physiological salt concentration of 150mM often causes the aggregation of cationic complexes and vascular blockage (Orig, Brunner, Schuller, Kircheis & Wagner 1999). The positive surface charge of the polyplex is thought to be important to adhere to the negatively charged cellular membrane leading to the intracellular uptake of the polyplex. But this cationic surface charge leads to the numerous unspecific interactions with cellular blood components, vessel endothelia and serum protein such as serum albumin. Protein binding hinders cellular uptake, promotes aggregation and encourages phagocytosis (Dash, Read, Fisher, Howard, Wolfert, Oupicky, Subr, Strohalm, Ulbrich & Seymour 2000). Such effects influences the biodistribution and gene expression patterns of polyplexes in vivo, resulting enhanced accumulation in the lung, due to a certain sieve effect of the pulmonary capillaries. Numerous biodistribution studies show an initial accumulation of cationic systems in the lung and subsequent rapid uptake predominantly into Kupffer cells of liver, and then to spleen, kidney intestine etc. In fact the clearance rate of these vectors from the circulatory system depends on their physicochemical surface characteristics. Hence, strategies must be developed to change this biodistribution pattern and to prolong circulation. To be stealthy i.e. undetectable by macrophages (Gref, Minamitake, Peracchia, Trubetskoy, Torchilin & Langer 1994), vectors have to be as small, hydrophilic and neutral as possible (Vonarbourg, Passirani, Saulnier & Benoit 2006). At the same time receptor mediated gene targeting enhances the gene uptake by pathologic cells by reducing the bio distribution into non- pathological cells.

1.3.2 Hurdles at the cellular level.

Once the gene delivery system is reached at the tumor site, the collagen and other proteins present in the tumor matrix is the further barrier to gene delivery (Pluen, Boucher, Ramanujan, McKee, Gohongi, di Tomaso, Brown, Izumi, Campbell, Berk & Jain 2001). Depending on the type of tumor, the influence of the extracellular matrix composition and structure on macromolecule mobility can vary significantly. On a cellular level, the first obstacle encountered by

the polyplexes is the cellular membrane, which composed of a lipid bilayer and containing various integral proteins as seen in Figure 1 (Morille et al. 2008). Depending on whether or not the complex is conjugated to targeting ligands, cellular entry is possible by one of two routes. Non targeted positively charged polyplexes are able to pass the cellular membrane via endocytosis through the electrostatic interactions with anionic cell surface proteoglycans (Merdan, Kunath, Fischer, Kopecek & Kissel 2002). There are a multitude of endocytic pathways that can be processed by the carrier systems: clathrin-mediated endocytosis via coated pits (adsorptive or receptor mediated), lipid-raft mediated endocytosis, phagocytosis and macropinocytosis. Carrier systems having a specific targeting moiety, which are specifically recognized by a cell surface receptor, could enter cells via both adsorptive endocytosis and receptor-mediated endocytosis (Mellman 1996). For most diseased conditions, the targeting receptors that are present only on certain cell populations have provided a useful tool in gene delivery. Selection of the appropriate targeting ligand can be influenced by several factors. Endogenous ligands, such as folate and transferrin, are the most widely used class of targeting moieties based on their biocompatibility and fairly well studied receptor distribution (Schatzlein 2003). In contrast, exogenous ligands, such as the peptide- and antibody-based targeting agents are susceptible to an immune response, which could limit their utility (Schatzlein 2003).

If cellular entry is gained by endocytosis, subsequent intracellular routing of vesicle-bound polyplexes will be a major barrier to efficient transfection. Two hypothesis have been suggested to explain the mechanisms involved in endosomal release of DNA by cationic polymer based vectors. The first one is based on the idea that a physical disruption of the negatively charged endosomal membrane occurs on direct interaction with the cationic polymer. This mechanism seems to depend on the target membrane composition (cell type). The second hypothesis is termed as "proton sponge" effect. For example, poly- (ethylenimine)s are believed to act as proton sponges: as the vesicle acidifies, the amino groups are thought to become protonated thus buffer the acidic pH of the lysosome, and protecting the DNA from degradation. As a result of this accumulation of protons in the vesicle results in an influx of counter ions which causes osmotic swelling and rupture of the endosomal membrane, in turn releasing the polyplexes into the cytoplasm (Boussif, Lezoualc'h, Zanta, Mergny, Scherman, Demeneix & Behr 1995*b*)

(Maxfield & Yamashiro 1987).

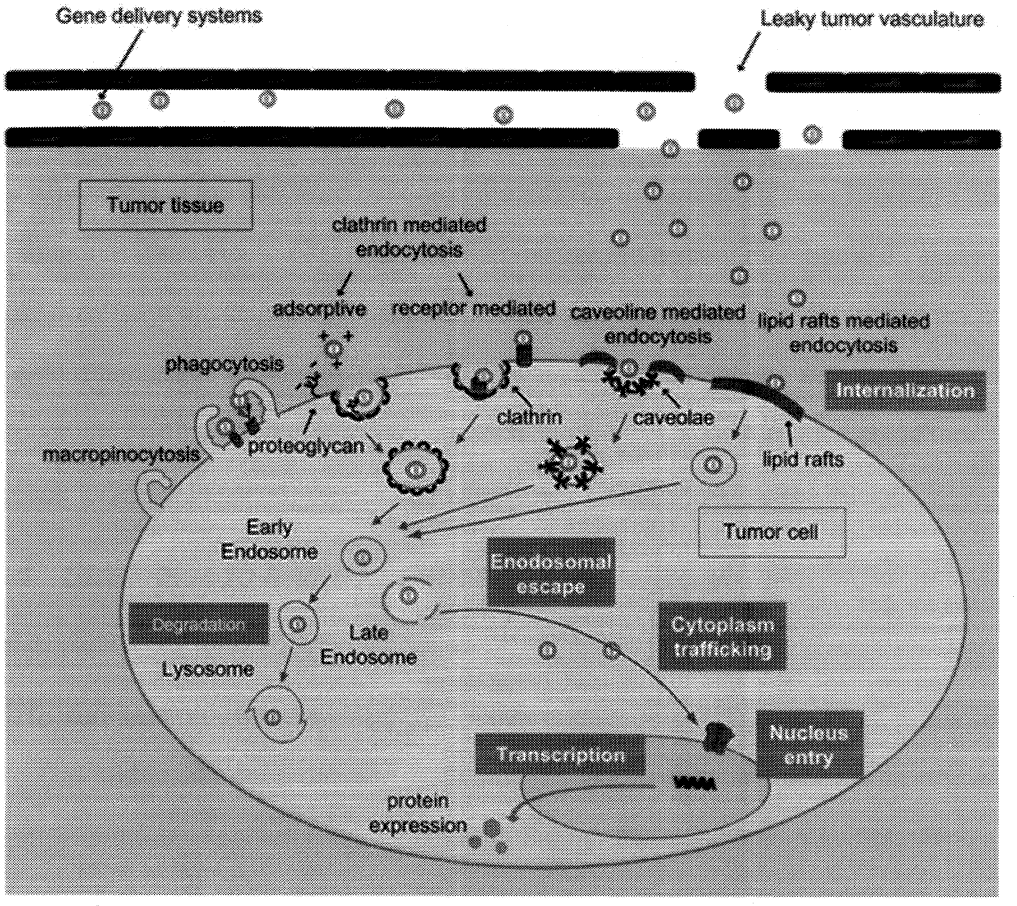

Figure 1: Schematic representation of the different hurdles encountered by a gene delivery system to enter and traffic into a tumour cell (Morille et al. 2008).

After endosomal escape, the nucleic acid must traffic through the additional barriers in the cytosol that hamper the delivery of the complex into the nucleus of the cell. Within the cytoplasm the nucleolytic enzymes ready to degrade unprotected nucleic acids are intermingle amongst microtubules, intermediate filaments, and microfilaments that are organized into a dense network to form the cytoskeleton (Lechardeur & Lukacs 2006). Therefore the mobility of large molecules, such as pDNA, is extremely low in the cytoplasm, making them an easy target for cytoplasmic nucleases (Lukacs, Haggie, Seksek, Lechardeur, Freedman & Verkman 2000). Thus pDNA has to be both protected and also available to enter the nucleus.

1.3.3 Hurdles at nuclear level.

In non-viral gene delivery the final barrier is the nucleus. The entry in to the nucleus enables the expression of the delivered gene and the desired therapeutic effect. There are two paths to enter into the nucleus. First path is during mitosis the nuclear membrane disassemble and thus, even large molecues, such as plasmids are able to gain access. Otherwise the only way to enter the nucleus is through the NPC. Small molecules or ions are able to diffuse passively through the NPC, while larger molecules such as proteins or DNA require some tags such as nuclear localisation sequences (NLS) to mediate their transport into the nucleus.

1.4 Strategies to Improve Cancer Gene Delivery.

1.4.1 Systemic delivery.

To surmount the hurdles described above numerous efforts have been made to obtain effective and stable gene delivery systems. The primary requirement for an efficient gene therapy is the unimpeded systemic delivery through the bloodstream and oftentimes to disseminated regions of the body. By introducing steric stabilisation, the positive charge gets shielded and create a steric barrier against aggregation with albumin, complement factors or cellular components in the bloodstream. Steric stabilization of polyplexes can be achieved by introducing poly(N-(2-hydroxypropyl)- methacrylamide) (pHPMA), poly(ethylene glycol) (PEG), and various oligosaccharides on cationic polymer. It is observed that small particles with size of ~ 100nm and surface charges close to neutrality could be obtained with PEG modification. Since the polymer is nontoxic, non-immunogenic, non-antigenic, and highly soluble in water the PEG conjugated complexes have several advantages: a prolonged residence in body, a decreased degradation by metabolic enzymes and a reduction or elimination of protein immunogenicity. PEGylated polymers are protected against proteolytic degradation and show increased serum half lives due to decreased elimination process such as renal excretion and opsonisation. Due to reduced opsonisation they are less phagocytosed by reticulo endothelial system. This effect is the result of high hydrophilic profile, combined with brush type polymer crowding and flexibility (Vonarbourg et al. 2006). The capacity of PEG group for repelling proteins and not interacting with macrophage plasma membrane is dependent on different pa-

rameters such as molecular weight, density, conformation and flexibility of chain (Vonarbourg et al. 2006). Most of the studies suggested that molecular weight in the range of 1500 to 3500 Da is appropriate for decreasing protein adsorption in vitro. While for reducing macrophage uptake, the chains have to be very long as 20,000 Da.

Similar to PEG, Poly (N-(2 -hydroxypropyl)methacrylamide) (pHPMA) reduces the interactions with albumin and reduces association with macrophages invitro (OupickÃ, Howard, KonÃ¡k, Dash, Ulbrich & Seymour 2000). Although the PEG or pHPMA moieties could stabilise the polyplexes in serum-rich environment; it may interfere with DNA complexation resulting in poorly condensed polyplexes and reduced transfection efficiencies (Erbacher, Bettinger, Belguise-Valladier, Zou, Coll, Behr & Remy 1999*a*) (OupickÃ, Konak, Dash, Seymour & Ulbrich 1999). This problem can be overcome by using multivalent chains which have the ability to cooperatively bind with multiple amino groups per hydrophilic chain forming a covalently cross linked coating that offers both steric and lateral stability (Dash et al. 2000) (Subr, KonÃ¡k, Laga & Ulbrich 2006). Gene transfer efficiency can also be improved by incorporating hetro-bifunctional PEG or multivalent HPMA chains with targeting groups (Blessing, Kursa, Holzhauser, Kircheis & Wagner 2001) (Fisher, Ulbrich, Subr, Ward, Mautner, Blakey & Seymour 2000). This results in active targeting and receptor-mediated endocytosis. Depending on the specific cell types to be targeted, the ligands can be varied from small molecules like folate, galactose, low-density lipoprotein (LDL), fibroblast growth factor (FGF) receptor binding peptides, etc to peptides and proteins like transferrin or antibodies. Transferrin and folate are the common ligands used to target tumor cells.

Oligosaccharides can be used for improving serum stability of polyplexes because of their inherent solubility, biocompatibility, biodegradability, and potential targeting capacity. For example Hwang et al. (Hwang, Bellocq & Davis 2001) developed a ternary system consisting of hybrid constructs of cationic polymer and cyclodextrin, one of the oligosaccharide for the complexation of nucleic acid. The cationic nature of cyclodextrin (CD) enables DNA complexation whereas cyclodextrin rings allow PEG binding. Liposome/protamine/DNA (LPD) is another example of ternary system developed for the systemic stability. Protamine is a naturally occurring polycation which condenses DNA in the head of spermatozoa. The nuclear localizing prop-

erty of protamine makes it particularly attractive for transfection applications. Also, protamine sulfate is a small defined peptide system (44.25 kDa), that possesses a high affinity for DNA structure (Warrant & Kim 1978) and contains a short runs of basic amino acids known to act as NLS (Sorgi et al. 1997). Compared to classic lipoplexes, LPD offers better nuclease protection and gives higher transfection efficiency in mice via tail vein injection (Li, Rizzo, Bhattacharya & Huang 1998).

1.4.2 Cellular uptake.

Cellular uptake of the polyplexes may occur in various ways, including adsorptive or fluid phase endocytosis, receptor mediated endocytosis, macropinocytosis or phagocytosis. Out of these adsorptive or fluid phase endocytosis is the major pathway following the clathrin coated pit mechanism (Godbey, Wu & Mikos 1999*a*). Due to the presence of negatively charged proteoglycans and glycoproteins on the cell surface, it will adsorb the positively charged polyplexes. Therefore the surface negative charge of the cell line and the positive charge of the polyplexes may influence the balance in favour of either one or the other route. By increasing the surface charge of the polyplexes cellular uptake can be improved (Blau, Jubeh, Haupt & Rubinstein 2000). While this may leads to the increased toxicity both on cellular and systemic level. Therefore the therapeutic use of this strategy is limited to local administration.

The use of protein trasnsduction domain (PTD) mediate an endocytosis independent cellular uptake (Elliott & O'Hare 1997) of proteins as well as other large molecules. The PTDs are able to accumulate in the cells in concentration dependent manner. Therefore physiological membranes do not hinder it. Besides, this type of cell entry helps to circumvent the harmful endolysosomal compartment with its acidic environment. The use of PTD increases the transfection efficiency in all cell lines as well as in vivo. For example the intra peritoneal injection of a 120 kDa beta-galactosidase protein coupled to the HIV-1 TAT protein led to significant delivery in virtually all tissues including brain (Schwarze, Ho, Vocero-Akbani & Dowdy 1999). The characteristic feature of PTD sequence is the presence of a high number of basic amino acids such as arginine and lysine which will interact with the negatively charged constitutes of cell membrane. Some examples of PTD having highest efficiencies are TAT protein derived from HIV-1 virus (Frankel & Pabo 1988), the drosophila antennapedia transcription factor ANTP (Joliot,

Pernelle, Deagostini-Bazin & Prochiantz 1991) and the herpes simplex virus type-1 VP22 transcription factor (Elliott & O'Hare 1997). The major physiological task of all these three peptides is the interaction with nucleic acids during transcription. In order to avoid electrostatic interactions of the PTD with the nucleic acids the ternary complexes can be formed. For example the ternary complexes using TAT peptide together with PEI and plasmid DNA has led to approximately 10 fold increase in reporter gene expression compared to PEI alone. While no increase in transfection was observed with poly L-arginine/DNA complex alone (Rudolph, Plank, Lausier, Schillinger & Rosenecker 2003).

In order to avoid unspecific cellular uptake, targeting can be achieved actively or passively. Active targeting can be achieved by incorporating a targeting moiety to the delivery vector. The targeted polyplexes will be taken up by the receptors present in the specific cell types via receptor mediated endocytosis. At the early endosome level the receptor is recycled back to the cell membrane. The targeted complexes having targeting moieties with a positive surface charge may also enter cells via adsorptive endocytosis. Therefore both routes of entry may be observed. Some examples of receptors present in the cell surfaces are transferrin, folate, integrins, asialoglycoprotein receptors ect.

The transferrin receptor was one of the first targeting structures used in non-viral gene delivery to target tumor cells. The fact that cerebra endothelial cells and hepatocytes possess significant levels of transferrin receptors, makes transferrin as an attractive target for systemic gene therapy. The incorporation of high amounts of transferrin with and without PEG spacers into polyplexes leads to both effective shielding of surface charge and tumor targeting (Kircheis, Wightman, Schreiber, Robitza, RÃssler, Kursa & Wagner 2001). Similar to transferrin receptor, folate receptor also represents an attractive structure to target cancer cells. Since the reduced form of folic acid (Vit. B9) is essential for rapidly dividing cells including cancer cells for numerous bodily functions, an elevation in the appetite for physiological folates permit the cells to over express folate receptors. Many human tumors including cancers of the brain, lung, ovary, uterus, kidney, testis, colon and myelocytic blood cells, are over expressed by folate receptors, which is absent in most of the normal tissues. Similarly, folate receptor density appears to increase as the stage or grade of the cancer worsens. These factors enlighten the

use of folate mediated gene delivery vectors in the treatment of cancers which are difficult to treat by classical methods.

Integrins are hetrodimeric membrane receptors having affinity towards RGD (arginine-glycine-aspartic acid) peptides. RGD peptides attached to polyplexes (Erbacher, Remy & Behr 1999*b*) (Hart, Harbottle, Cooper, Miller, Williamson & Coutelle 1995) have been shown to associate with cells much more readily than those without targeting moiety. Integrins are also highly over expressed in tumor tissues. The asialoglycoprotein receptors (ASGPr) is expressed abundantly in hepatocytes and selectively binds to galactose terminated glycoproteins. Various mono or oligo saccharide ligands such as lactose, galactose, mannose, fructose as well as larger carbohydrates like asialo- oromucoid etc shows affinity to ASGPr receptors. The hepatic disorders such as cirrhosis or liver cancer are the main target using these receptors.

Passive targeting to solid tumors occurs due to the effect known as enhanced permeability and retention (EPR) effect, which demonstrates that complexes or macromolecules may accumulate passively in solid tumors, due to an increased permeability of tumor endothelia and lack of normal lymphatic drainage in connection with hyper vasculature of the tissue (Matsumura & Maeda 1986). It has been exploited successfully to passively target polymers (Shiah, Sun, Peterson & Kopecek 1999) or liposomes (Yuan, Leunig, Huang, Berk, Papahadjopoulos & Jain 1994) to tumors without incorporating a more specific targeting moiety. The extent of accumulation depends on size and charge of the complexes.

1.4.2.1 Endosomal escape and crossing over cytoplasm.

In order to avoid the endo lysosomal degradation of the polyplexes, it has to escape from the endolysosomal pathway rapidly. Usually the vesicular escape of polyplexes occurs via pH dependent process. According to proton sponge hypothesis (Boussif, Lezoualc'h, Zanta, Mergny, Scherman, Demeneix & Behr 1995*a*) the buffering capacity of the polymer leads to increased influx of protons and chloride ions during endolysosomal acidification, which results in increased osmotic pressure in the vesicle. As a result passive diffusion of water into the vesicle increases which eventually leads to swelling and rupture of the vesicle. Therefore the complexes having higher density of amine groups possess a greater buffering potential, which results in higher transfection efficiencies (Godbey, Wu, Hirasaki & Mikos 1999*b*).

After release from endosomes/lysosomes the polyplexes has to cross the cytoplasm in order to reach the nucleus without being degraded by cytoplasmic nucleases. Since majority of the plasmid DNA enters the nucleus during cell division, DNA must be stable until the next disassembly of the nuclear envelope. As a result the rapidly dividing cell lines show more efficient gene expression than slowly dividing cells. In the case of polyplexes, the microinjection of PEI/pDNA complexes resulted in a 10-fold higher levels of transgene expression compared to naked DNA, and showed that the enhanced expression may be the consequence of increased cytoplasmic mobility, due to the smaller size of the compacted DNA (Pollard, Remy, Loussouarn, Demolombe, Behr & Escande 1998). Alternatively the cationic polymer could alter the structure of the cytoskeleton by widening the meshes and thus enhancing the permeability for large molecules. It is known that plasmids that are microinjected into the cytoplasm of cultured cells are poorly expressed whereas those that are microinjected directly in the nucleus are highly expressed (Dowty, Williams, Zhang, Hagstrom & Wolff 1995). These results indicate that nucleus entry is another important barrier for efficient transfection.

1.4.3 Nuclear entry.

The nuclear envelope is a double membrane that can be interrupted by proteins less than 40 kDa in MW or 9-11 nm in diameter, through channels known as nuclear pore complexes (NPCs) by passive diffusion. In the case of larger macromolecules, however requires the assistance of import proteins such as importins to actively shuttle them through the NPCs (Wente 2000). The NPC is able to mediate transport of ions, small molecules, proteins, RNA, and ribonucleoproteins in and out of the nucleus. For the trafficking of intracellular protein toward the nuclear pores, a specific sequence known as nuclear localization sequence (NLS) has to be present, which can be recognised by import proteins so as to direct their subsequent transport into the nucleus. The first NLS described was the derived sequence of the simian cancer virus large T antigen (Kalderon, Roberts, Richardson & Smith 1984). These NLSs are recognized in the cytoplasm by a soluble protein, importin-α (Gorlich & Mattaj 1996). The complex of NLS/importin-α connects to another protein, importin β, and these trimeric complex then docks at the NPC and can enter the nucleus (Moroianu, Blobel & Radu 1995). Because of the cationic peptide sequences of nuclear localization sequence (NLS) they can also be

used as DNA-binding agent (Kichler, Pages, Leborgne, Druillennec, Lenoir, Coulaud, Delain, Le Cam, Roques & Danos 2000). Alternatively, NLSs can be attached to a polymer vector that is subsequently complexed with its genetic cargo (Moffatt, Wiehle & Cristiano 2006). Even though their promising fitness for gene delivery, the extent to which NLSs can enhance cytosolic trafficking and nuclear uptake may be limited by the size and type of DNA such as linear or plasmid used, the method of NLS incorporation, type of NLS peptide employed, the number of NLSs incorporated, and the type of polymer vector used (e.g., liposomes, PEI).

1.5 Hypothesis.

It is hypothesised that by proper designing and modification a safe and efficient gene delivery vector having systemic stability, tumor targeting ability, cellular and nuclear uptake property can be synthesised. Moreover the vector should be capable of protecting DNA and render it inaccessible to degradative enzymes.

1.6 Objective of the Study.

- In order to evaluate the efficiency of natural and synthetic based cationic polymers having DNA complexation and protection properties, chitosan and poly (ethyleneimine) were chosen as the base polymer.
- In order to enhance the cellular and nuclear up-take efficiency, arginine and histidine functionalities were chosen to modify the base polymers.
- Poly (ethylene glycol) was used to improve the systemic stability of the cationic polymer.
- Since the rapidly dividing cells including cancer cells over expresses the folate receptors, folic acid was used to induce targeting ability for the cationic polymer.

The following chapters are summarised as below. The chapter 2, literature review, illustrates the significance of each modification and their literatures else where. Chapter 3, materials and methods explains the synthetic routes, physicochemical and biological characterisation methods involved in each modification. Chapter 4, shows the results of each modification in natural as well as synthetic polymer based delivery vectors, and chapter 4 describes the comparatives evaluation of natural and synthetic polymer based gene delivery vectors upon

its modification. Chapter 5, summary and conclusion demonstrates the most important results and concludes by highlighting the most important findings from the study.

2 LITERATURE REVIEW

2.1 *Natural Polymer based Gene Delivery Vectors: Significance of Chitosan as Gene Delivery Vector.*

Among the various natural polymer based gene delivery vectors, chitosan is the most prominent because of its biodegradability, biocompatibility and cationic potential (Hirano, Seino, Akiyama & Nonaka 1990) (Kim, Jiang, Jere, Park, Cho, Nah, Choi, Akaike & Cho 2007*c*). Chitosan, being a linear cationic polysaccharide, consists of $\beta\ 1 \rightarrow 4$ linked glucosamine partly containing N-acetylglucosamine. It was first described as a delivery system for plasmids by Mumper et.al (Mumper, Wang, Claspell & Rolland 1995). The role of chitosan in gene delivery was supported by its ability to protonate in acidic conditions and to form complexes with anionic DNA by electrostatic interactions (Zhao, Yu, Wu, Mao & Yu 2006). The biodegradable cationic polymer chitosan is capable of forming small and stable toroidal complexes with plasmid DNA and provide protection against DNase that is comparable to PEI (KÃping-HÃggÃrd, VÃrum, Issa, Danielsen, Christensen, Stokke & Artursson 2004). The transfection efficiency of chitosan depends on various factors such as molecular weight, degree of deacetylation, pH of the transfecting medium and cell type. Rolland et al. demonstrated that the size of the chitosan/DNA complexes increases with the increased molecular weight of chitosan (MacLaughlin, Mumper, Wang, Tagliaferri, Gill, Hinchcliffe & Rolland 1998). However high molecular weight chitosan forms more stable complexes with DNA due to a chain entanglement effect (Kiang, Wen, Lim & Leong 2004). For various cell lines increased deacetylation generally improves transfection efficiency. This may be due to the increased charge density and thus higher complex stability (Huang, Fong, Khor & Lim 2005). On the other hand, moderate deacetylation or more than 65% positively charged monomer units should be required to obtain stable complexes and for successful gene transfer (KÃping-HÃggÃrd, Tubulekas, Guan, Edwards, Nilsson, VÃrum & Artursson 2001). This results indicates that high levels of transfection can be achieved on maintaining a fine balance between extracellular DNA protection versus efficient intracellular un-packaging (KÃping-HÃggÃrd et al. 2004). The pH in between 6.8 to 7.0 was found to be optimum to achieve higher level of transfection (Sato, Ishii & Okahata 2001). Below pH 6.5, transfection efficiency was low, possibly due to hindered

endosomal release. The transfection efficiency of the chitosan based polyplexes showed variation with the cell type used. Higher gene transfer is seen in HEK293 cells as compared to other cell lines (KÃping-HÃggÃrd et al. 2004) (Corsi, Chellat, Yahia & Fernandes 2003). This variation may be due to difference in cellular uptake due to cell specific plasma membrane compositions as well as difference in chitosan degrading enzymes present within the endosomal compartments of the cells.

Even though chitosan displays a significantly better biocompatibility and protection against DNase degradation comparable to that of PEI, it exhibits low transfection efficiency. Due to the presence of easily modifiable primary amino group present in chitosan, several research groups have conducted numerous modifications to the polymer structure, including use of PEI grafted chitosan (Jiang, Kim, Arote, Nah, Cho, Choi, Akaike & Cho 2007), galactosylated chitosan (Erbacher, Zou, Bettinger, Steffan & Remy 1998) galactosylated chitosan-graft-poly(vinylpyrrolidone) (PVP) (Park, Jiang, Cook, Cho, Kim, Jeong, Akaike & Cho 2004), trimethylated chitosan oligomers (Thanou, Florea, Geldof, Junginger & Borchard 2002), N-dodecylated chitosan (Li, Liu & Yao 2002) deoxycholic acid modified chitosan (Kim, Gihm, Park, Lee, Kim, Kwon, Chung & Jeong 2001) or ligand attached chitosans for targeting cell membrane receptors (Sato et al. 2001).

Quaternisation of chitosan improved its transfection efficiency in spite of higher cytotoxicity (Thanou et al. 2002) (Kean, Roth & Thanou 2005). The higher cytotoxicity of the trimethylated chitosan derivatives were reduced by grafting the polymer with PEG (Germershaus, Mao, Sitterberg, Bakowsky & Kissel 2008*a*) or polylysine (Yu, Chen, Lu, Sun, Tian, Hu, Wang, Zhang & Jing 2007). The chitosan graft PLL polymer exhibited better DNA binding ability, reduced cytotoxicity, and increased transfection efficiency as compared to polylysine alone and the 'gold standard' 25 kDa PEI. Buffering capacity of the chitosan polyplexes were improved when chitosan conjugated with imidazole containing derivatives (Kim, Ihm, Choi, Nah & Cho 2003) or by conjugating with polyethyleneimine (Wong, Sun, Zhang, Dai, Liu, He & Leong 2006). The enhanced transfection efficiency in such modifications was due to proton sponge effect.

By modifying chitosans with deoxycholic acid (Kim et al. 2001), stearic acid, (Hu, Zhao, Yuan, You, Du & Zeng 2006) and alkyl chains, aggregation tendency of the chitosans were

reduced which leads to improved transfection. A thiolated derivative of chitosan with reducible disulfide linkages was synthesized. Due to the formation of disulfide bonds between the thiolated chitosan derivative and plasma membrane proteins cellular uptake was improved which leads to enhanced transfection (Loretz, Thaler & Bernkop-SchnÃrch 2007). Endosomal escape of chitosan was improved by coupling N-isopropylacrylamide/vinyl laurate copolymer (PNVLCS). At 20 ^{o}C after 18 h of transfection, the efficiency of PNVLCS-DNA was increased when compared to PNVLCS complexes that were incubated at 37 ^{o}C (Sun, Liu, Cheng, Zhang, Cao, Yao, Liang, Zuo, Guo & Zhang 2005).

The delivery of chitosan complexes to specific cell types was achieved by conjugating chitosan to various cell targeting ligands such as galactose, lactose (Erbacher et al. 1998), trisaccharide (Issa, KÃping-HÃggÃrd, TÃmmeraas, VÃrum, Christensen, Strand & Artursson 2006) etc which improved hepatic cell targeting. Folate targeting of chitosan promotes tumor targeting (Chan, Kurisawa, Chung & Yang 2007).

2.2 *Synthetic Polymer based Gene Delivery Vectors: Significance of Poly (ethyleneimine) as Gene Delivery Vector.*

Among the widely used cationic polymer based gene delivery vectors poly- ethyleneimine (PEI) is regarded as the most effective vector (Deng, Yue, Jin, Chen, Kung, Lin & Wu 2( )9). The commercially available branched PEI having a molecular weight of 25 kDa, has been widely used as 'gold standard'. In 1995 Behr et al. had introduced PEI as a successful delivery vector of oligonucleotide (Boussif et al. 1995*a*). There are mainly two types of structure: linear molecule and branched molecule. Branched PEI synthesized via acid catalyzed polymerization of aziridine, while the linear PEI is synthesized by ring opening polymerization of 2-ethyl-2-oxazoline followed by hydrolysis (Brissault, Kichler, Guis, Leborgne, Danos & Cheradame 2003). One of the important factors for the high transfection efficiencies obtained with these polymers is the property known as 'proton sponge effect'. Branched structure of PEI containing high density of primary, secondary and tertiary amino groups exhibits protonation on every third or fourth nitrogen at pH 7 confers significant buffering capacity to the polymers over a wide pH range. This buffering capacity allows PEI polyplexes to escape from the endo-lysosomal degradation.

Even though PEI is considered as 'gold standard' of gene transfection, major drawbacks of PEI are its non-degradability, cytotoxicity, and aggregation which strictly limit its application in clinical gene therapy (Yang, Li, Goh & Li 2007). High transfection efficiency of PEI, along with its cytotoxicity, strongly depends on its molecular weight, degree of branching, ionic strength of the solution, zeta potential and particle size (Kunath, von Harpe, Fischer, Petersen, Bickel, Voigt & Kissel 2003) (Kircheis, SchÃller, Brunner, Ogris, Heider, Zauner & Wagner 1999). Many studies have been attempted to reduce its cytotoxicity and maintain the transfection efficiency. Transfection efficiency of PEI has been studied over a wide range of molecular weights. Studies showed that linear PEI with low molecular weight was the most efficient in transfection and least cytotoxic (Breunig, Lungwitz, Liebl, Fontanari, Klar, Kurtz, Blunk & Goepferich 2005). One another study showed that moderately branched polymer having molecular weight of 10 kDa showed better transfection efficiency and low toxicity compared to high molecular weight PEI (Fischer, Bieber, Li, ElsÃsser & Kissel 1999) (Petersen, Kunath, Martin, Stolnik, Roberts, Davies & Kissel 2002*b*). Godbey et.al showed that transfection efficiency of PEI polyplexes increases with increased molecular weights (Godbey et al. 1999*b*). Again it is demonstrated that linear PEI (22 kDa) was more efficient in both salt and salt-free buffers than branched polymers (25 and 800 kDa) (Wightman, Kircheis, RÃssler, Carotta, Ruzicka, Kursa & Wagner 2001). Kissel et al. showed that increased toxicity is caused by aggregation and adherence on the cell surface, which results in significant necrosis. It was recognized that the optimal molecular weight for PEI polyplex formation is typically between 5 and 25 kDa. In addition to the molecular weight, degree of branching of PEI will also influence the complex formation and its transfection. It was reported that branched PEI is more effective in condensing DNA as well as for the formation of stable polyplex than the linear PEI (Reschel, KonÃ¡k, OupickÃ, Seymour & Ulbrich 2002).

By virtue of its amino functional group, the polymer enables researchers to successfully introduce ample modifications to reduce the toxicity and to improve transfection efficiency. Most exploited modification on PEI is PEGylation, which creates a hydrophilic exterior that reduces interactions of the polyplexes with plasma proteins and erythrocytes. Various synthetic strategies exist to conjugate PEG to PEI. For instance PEGylated PEI polyplexes were linked

to tumor specific ligand transferrin, an asialoglycoprotein and then applied intravenously, resulting in five-fold increase in the transfection efficiency with lower toxicity in comparison with PEGylated (transferrin-free) PEI polyplexes (Kircheis et al. 1999). Knorr et al. synthesized an acetal based PEGylation reagent with meleimide terminus that could be coupled to mercaptan modified PEI (Knorr, Allmendinger, Walker, Paintner & Wagner 2007). The resultant products showed improved transfection efficiency in vitro as well as in vivo.

Other than PEGylation, several other modificatios to PEI have been made to improve transfection efficiency. Rosenholm et.al. reported that conjugating PEI with folic acid and mesoporous silica could improve endosomal escape, reduce toxicity and enhance targetability (Rosenholm, Meinander, Peuhu, Niemi, Eriksson, Sahlgren & LindÃn 2009). Thomas and Klibanov have introduced quaternary amine structures by reacting PEI with methyl and ethyl iodide. The resultant product showed reduced transfection efficiency due to the lack of protonable amines, which support the "proton sponge" hypothesis. Various other groups have modified the functionality of PEI to improve transfection efficiency and reduce cytotoxicity. Some other examples are given in the Table 1.

2.3 Significance of Arginine and Histidine Modification on Cationic Polymers.

Arginine residues of Tat peptide and other cell-penetrating peptide (CPP) s containing cationic arginines and lysines, were known to deliver molecules efficiently by intracellular translocation (Brooks, Lebleu & VivÃs 2005) (Zhao & Weissleder 2004) (Tung & Weissleder 2003). Kim et al. reported that cholesteryl oligo-D-arginine (Chol-R9) was presented to reduce tumor growth efficiency by delivering VEGF siRNA. This may be due to membrane permeability and nuclear localization ability of arginine residues (il Kim, Ou, Lee & Kim 2009). Meanwhile, several studies have been performed on the cell-penetrating property of arginine modified polymers. Arginine residues when conjugated to dendrimers such as poly (amido amine) (PAMAM) dendrimer (Choi, Nam, Park, Kim, Lee & Park 2004), poly (propyleneimine) (PPI) dendrimer (Kim, Baek, Zhe Bai & Park 2007*b*), and poly (l-lysine) (PLL) dendrimer (Okuda, Sugiyama, Niidome & Aoyagi 2004), have shown enhanced transfection efficiency than unmodified den-

Table 1: Derivatives of polyethylenimine

No	Derivative	Transfection efficiency	Cytotoxicity	Additional advantage comparedto PEI	Reference
1	PEI-PEG-CTX	(P-PEG-AF-CTX> P-AF	(P-PEG-AF-CTX< P-AF	Tumor targeting	(Veiseh, Kievit, Gunn, Ratner & Zhang 2009)
2	PEI-PEG-Trastuzumab	PEI-PEG(2)-Trastuzumab> PEG-PEI	Not given	Improved pharmacokinetics and biodistribution	(Germershaus, Neu, Behe & Kissel 2008*b*)
3	Heparin-conjugated polyethylenimine	HCPEI > PEI25kIn presence of serum	HCPEI< PEI25k	High blood compatibility	(Jeon, Yang, Lee & Kim 2008)
4	Poly (ester amine)	PCL/PEI-1.2 (MW 1200)> PEI 25 K.	PCL/PEI-1.2 (MW 1200)<PEI 25 K	excellent transfection capability at alveolar region	(Arote, Kim, Kim, Hwang, Jiang, Song, Nah, Cho & Cho 2007)
5	α-cyclodextrin core and oligoethylenimine arms	α-CD-OEI >bPEI (25K).	α-CD- OEI< bPEI (25K).	The transfection efficiency increased with an increase in the OEI arm length.	(Yang et al. 2007)
6	chitosan-graft-polyethylenimine	CHI-g-PEI >PEI 25K	CHI-g-PEI< PEI 25K	Good DNA binding and high protection	(Jiang et al. 2007)
7	PEI crosslinked with small diacrylates	EGDMA-PEI 800-4h> bPEI25kDa	EGDMA-PEI 800-4h < bPEI25kDa	stable complexes with DNA and potential degradability	(Dong, Jin, Li, Sun, Ma & Hua 2006)
8	folate-PEI-PLLA	B-PEI, L-PEI > folate-PEI-PLLA.	B-PEI, L-PEI> folate-PEI-PLLA	cell permeability and biocompatibility	(Wang & Hsiue 2005)
9	PMMA-PEI core-shell nanoparticles	PMMA-PEI >PEI	PMMA-PEI <PEI	more stable complexed nanoparticles	(Zhu, Tang, Law, Feng, Ho, Lee, Harris & Li 2005)
10	PEI-g-PEG	bPEI(25k)-g-IPEG(550) >bPEI	bPEI(25k)-g-IPEG(550) <bPEI	Improved blood compatibility	(Petersen, Fechner, Martin, Kunath, Stolnik, Roberts, Fischer, Davies & Kissel 2002*a*)

drimers. Reports on linear polymers like, chitosan (Gao, Xu, Chen, Gu, Chen & Li 2008) and poly (ester-amide)s (Yamanouchi, Wu, Lazar, Craig Kent, Chu & Liu 2008) were also displayed high transfection efficiency on conjugation with arginine specifying their excellent gene delivery potency despite they do not exist as oligo-peptide forms. Kim et al (il Kim et al. 2009) described the enhanced transfection efficiency of arginine-grafted bioreducible poly (disulfide amine) (ABP) polymers with low cytotoxicity.

Hetrocyclic imidazole containing polymers have shown promising transfection efficiency. This is because polymers with imidazole moieties or two amines in close proximity were most efficient at avoiding lysosomal degradation due to higher buffering capacity. It was reported that chitosan when conjugated with varying ratio of imidazole containing urocanoic acid, the cytotoxicity was reduced and transfection efficiency enhanced compared to unmodified chitosan illustrating the role of proton sponge effect (Kim et al. 2003). The imidazole group of histidine plays a pKa around 6 thus absorb protons and possess buffering capacity in the endosomal pH range (pH 5-6.5). This leads to the osmotic swelling and membrane disruption and eventually the vesicular escape of DNA (Midoux & Monsigny 1999). The escape of DNA leads to more transfection. This enhanced buffering capacity is due to the lone pair of electrons on the unsaturated nitrogen that provides pH dependent amphoteric properties (Lee, Gao, Kim, Park, Kwon & Bae 2008) (Lee, Na & Bae 2005). Many research groups have been studied the improvement in transfection upon conjugation with histidine (Lee, Oh, Kim, Youn & Bae 2007) (Benns, Choi, Mahato, Park & Kim 2000) (Bikram, Ahn, Chae, Lee, Yockman & Kim 2004). Lee et al (Lee, Shin, Na & Bae 2003) established the amphoteric property and fusogenic activity of the imidazole group and its interaction in endosomal membrane. Therefore the incorporation of imidazole moieties represents a promising option for the improvement of the efficiency of polymers without increasing toxicity.

2.4 Significance of Siloxane Modification on Cationic Polymers.

Silicon derivatives, which belong to the largest class of industrial compounds, show generally low toxicity and biocompatibility (Pitt 1973) (Rose, Landavere & Kuppers 1996). Silica is an essential component of cells throughout the human body and amorphous silica is biodegradable and freely dispersible throughout the body which ultimately excreted by urine (Rosenholm

et al. 2009). Kichler et al reported that out of two main processes of siloxane synthesis such as hydrosilation and oligomerisation of alkoxysilanes, the oligoaminosiloxanes such as SiDA synthesised by alkoxysilane condensation gives useful products in the area of DNA vectorisation (Kichler, Sabourault, Décor, Leborgne, Schmutz, Valleix, Danos, Wagner & Mioskowski 2003). The oligoalkylaminosiloxane prepared by alkali hydrolysis delivers DNA into cells by adsorptive endocytosis through sulphated proteoglycans. Recently, several groups have reported the use of mesoporous silica matrix in carrying, protecting and releasing large amounts of cargo such as genes and membrane -impermeable chemicals (Rosenholm et al. 2009) (Slowing, Trewyn & Lin 2007) (Rosenholm, Duchanoy & Lindén 2007) (Fuller, Zugates, Ferreira, Ow, Nguyen, Wiesner & Langer 2008).

2.5 Significance of PEG-FA Modification on Cationic Polymers.

Polyethyleneglycol (PEG) is a linear, uncharged, hydrophilic and non- immunogenic polymer with low toxicity having size ranging from 200 to 40000 Da. It is a polyether with repetitive CH2-CH2-O- units with hydroxyl groups at the end. The attachment of polyethyleneglycol to polymers or drugs is called PEGylation which was first introduced by Davis et al. in the 1970s (Abuchowski & Davis 1979). When PEG is covalently linked to polymers it alters their properties extensively. Since the polymer is non-ionic and hydrophilic its conjugation to cationic polymers enhances biocompatibility and circulating half-life in bloodstream which leads to decrease interactions with plasma proteins or circulating cells (Abuchowski & Davis 1979) (Delgado, Francis & Fisher 1992) and alter its biodistribution. The PEGylation also facilitates conjugation of endosome-disrupting peptides for intracellular trafficking (Abuchowski, McCoy, Palczuk, van Es & Davis 1977) and conjugation of nuclear localization signal (NLS) peptides for nuclear delivery (Katre 1990).

PEGylation of liposomes were first reported by Klibanov et al. (Klibanov, Maruyama, Torchilin & Huang 1990) in 1990. Later on PEI was found to be a potent gene vector by J.P.Behr, which leads to the modification of PEI with PEG. Delivery of DNA safely by minimizing unspecific interactions of the positively charged polyplex with biological environment, is achieved by PEG shielding based on the so called stealth effect. Even after number of freeze-thawing cycles, the PEG shielding of polyplexes leads to improved stability (Ogris, Walker,

Blessing, Kircheis, Wolschek & Wagner 2003). It also increases the solubility of the DNA complexes. Embracher et al. reported that the steric stabilization of PEGylated polymers is due to the formation of brush corona layer of PEG on the surface of these polymers (Erbacher et al. 1999*a*). However, the transfection efficiency of the PEGylated PEI is significantly lower than that of the corresponding non-modified polymers due to charge masking properties (Kopatz, Remy & Behr 2004). In order to overcome this problem, two types of PEGylation were developed such as pre-PEGylation and post- PEGylation.

2.5.1 Pre-PEGylation.

In pre-PEGylation polyplexes with or without targeting ligand are prepared in one step reaction by mixing plasmid DNA with polycation and polycation coupled to PEG or to PEG-ligand. Pre PEGylation is easy to perform because it involves the mixing of DNA with PEGylated polymer solution. Although PEGylation of polymer up to 20% is appropriate for complexing DNA, otherwise the hydrophilic parts seem to hinder proper DNA condensation and particle formation (Kursa, Walker, Roessler, Ogris, Roedl, Kircheis & Wagner 2003).

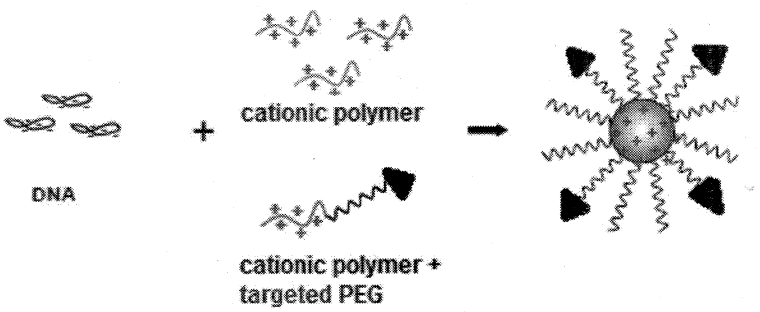

Figure 2: Schematic representation of pre-PEGylation

2.5.2 Post-PEGylation.

In post PEGylation, DNA is first condensed by polycations or partially PEGylated polycation having ligands. Then after complexation PEGylated reagents is again added to the reaction mixture to shield the cationic surfaces via active ester-(NHS) or tresyl-activated PEGs. Post-PEGylation is very effective in stabilizing the structure of the nanoparticles. Wagner et al. first condensed DNA with PEI 800 kDa and subsequently grafted on the hydrophilic polymer

to provide a better condensation of the DNA with the polycations (Ogris, Brunner, SchÃller, Kircheis & Wagner 1999) (Kircheis et al. 1999).

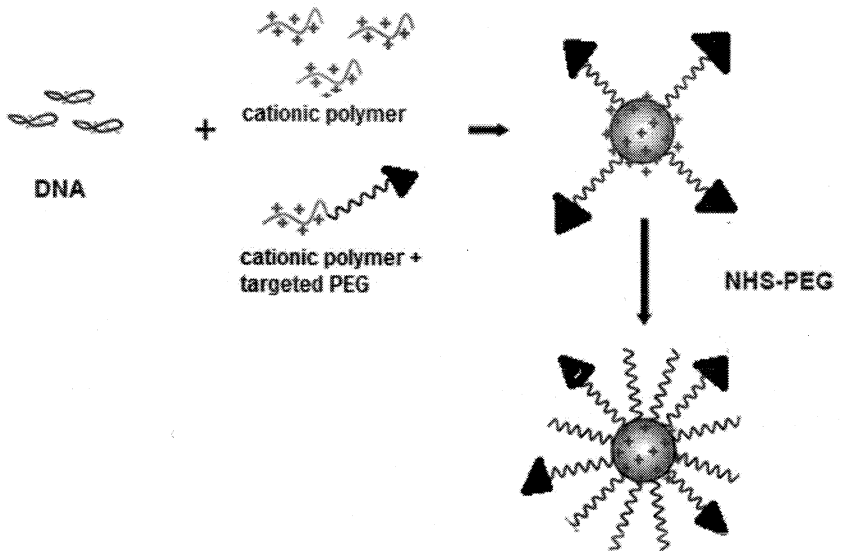

Figure 3: Schematic representation of post-PEGylation

2.5.3 Cell-specific targeting.

In order to avoid the problem of non-specific interaction and to overcome the difficulties associated with PEG coating, a target specific ligand can be added to the gene delivery system resulting in active targeting and receptor mediated endocytosis (Ogris et al. 2003) (Xu, Huang, Huang, Tang, Rait, Yin, Cruz, Xiang, Pirollo & Chang 2002) (Moffatt, Wiehle & Cristiano 2005). Ligand targeted therapies offer several advantages such as flexibility and adaptability. Gene delivery vectors should allow specific cell types to be targeted by utilizing the interactions between cell surface receptors and ligands present on their surface.

Folic acid or reduced form of vitamin B9 is essential for the proliferation and maintenance of all cells including cancer cells for numerous bodily functions. Therefore an elevation in the appetite for physiological folates permit the cells to over express folate receptors (FR). Folate receptors glycosylphosphtidylinositol (GPI), are known to be over expressed on many human cancer cell surface, such as brain, kidney, lung, and breast cancers, and, in particular, in epithelial carcinomas such as ovarian cancers (Low, Henne & Doorneweerd 2008). Therefore

folic acid has been covalently conjugated to anti-cancer drugs and gene delivery vectors for selective targeting towards tumors. Many researchers have used folic acid (FA) as a ligand for cationic liposomes (Kamaly, Kalber, Thanou, Bell & Miller 2009) and other polymers such as chitosan (Mansouri, Cuie, Winnik, Shi, Lavigne, Benderdour, Beaumont & Fernandes 2006), poly (l-lysine) (Park et al. 2004), and polyethyleneimine (Liang, He, Xiao, Li, Chan, Kung, Shuai & Peng 2008) to target cells expressing FRs.

Early efforts on folate receptor gene targeting was by Gottschalk et al. (Gottschalk, Cristiano, Smith & Woo 1994) and Reddy et al. (Reddy, Dean, Kennedy & Low 1999) (Reddy & Low 2000) using folate linked poly- lysine and poly lysine- polyethylene glycol complexes respectively, yielded only low levels of reporter activity despite good gene delivery to folate receptor expressing (FR+)cells. These studies indicated that efficient DNA delivery and gene expression required not only the active targeting but also an endosomal disruption mechanism to release DNA from its intracellular compartment as seen in Figure 4 (Wang & Low 1998). Therefore to achieve both targeted gene delivery and endosomal disruption with minimal collateral toxicity, Benns et al. linked folate to both ends of monofunctionalized PEG and then grafted it to PEI (FPF-g-PEI). The complex of plasmid DNA with the resultant product exhibits good transfection in FR+ cells (Benns, Maheshwari, Furgeson, Mahato & Kim 2001).

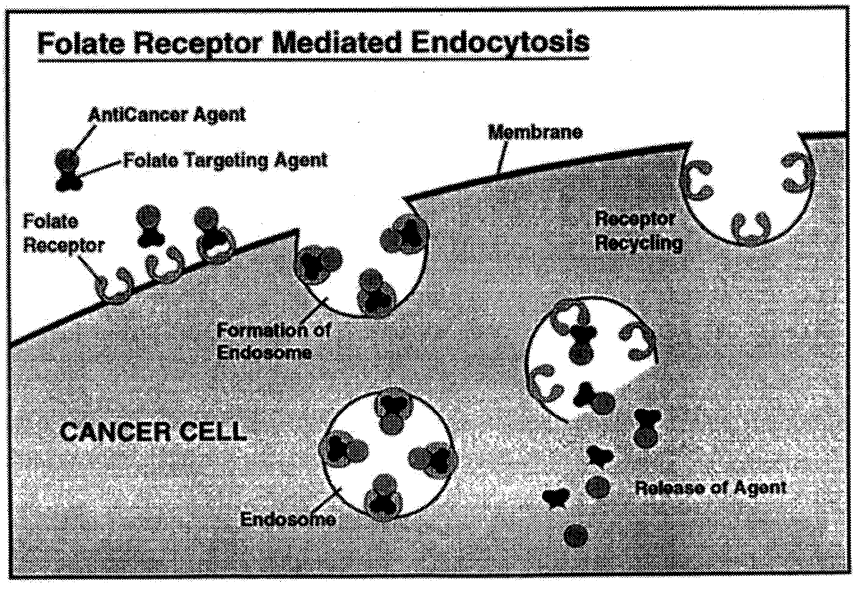

Figure 4: Diagramatic representation of folate receptor mediated endocytosis. (Wang & Low 1998)

Significant efforts have also been devoted to facilitate improved gene delivery, from titrating the use of PEG, which can reduce nonspecific uptake and increase transfection efficiency, to minimization of vector size, which can improve extravasation of the vector into the tumor. This may leads to the improved folate-targeted gene therapy vectors, as should research into enhancement of the efficiencies of endosomal escape and gene trafficking to the nucleus.

3 MATERIALS AND METHODS

3.1 *Synthesis and Characterisation of Natural Polymer based Nanoparticles.*

3.1.1 Materials.

High molecular weight chitosan polymer was obtained from CIFT Kochi, PEI (~25 kDa), Methyl iodide and 1- methyl-2-pyrrolidinone (NMP) arginine and histidine were purchased from Aldrich (USA). 1- Ethyl-3-(3- dimethylaminopropyl) carbodiimide hydrochloride (EDC), dicyclohexylcarbodiimide (DCC), N -hydroxysuccinimide (NHS), 3-[4,5-di-methylthiazol-2-yl]-2,5-diphenyltetrazolium bromide (MTT), were purchased from Sigma (USA). Fetal bovine serum (FBS), Minimal Essential Medium (MEM), and Trypsin/EDTA were obtained from Gibco (USA). Folate-free RPMI 1640 (FFRPMI), YOYO iodide and Hoechst 33342 were obtained from Invitrogen.

3.1.2 Depolymerisation of chitosan.

The low molecular weight chitosans were prepared by oxidative degradation with $NaNO_2$ at room temperature. The detailed procedures were given elsewhere (Mao, Shuai, Unger, Simon, Bi & Kissel 2004). Briefly, 1% (w/w) chitosan was dissolved in 1% acetic acid solution under magnetic stirring. When chitosan was completely dissolved, the appropriate amount of 0.1 M $NaNO_2$ was added drop wise and the reaction was performed at 4 ^oC for 3 h. The reaction mixture was subsequently neutralized with 1 N NaOH to pH 7 and reduced with $NaBH_4$. The reduction reaction was also carried out at 4 ^oC for 3 h. The reduced product was again precipitated using NaOH and the precipitated chitosan was recovered by filtration, washed several times with deionised water and then by methanol. Finally, it was dried in vacuum oven at 60 ^oC for 6 h.

3.1.3 Preparation of N-N-N trimethylated chitosan (TMC) polymer.

Trimethylation of chitosan was performed by a method described by Kean et.al. (Kean et al. 2005). Briefly depolymerised chitosan were dissolved in NMP with 2.4 g of sodium iodide at 60 ^oC under stirring. Addition of sufficient NaOH (15% w/v; aq) was made to maintain an alkaline environment throughout the reaction. Methylation was produced through nucleophillic

substitution by the addition of methyl iodide to the solution. Diethylether : ethanol (1:1 v/v) were used to precipitate the products. Products were dried, and redissolved in 0.5 M NaCl and precipitated again with diethylether : ethanol, centrifuged followed by thorough washing of the pellet with diethylether : ethanol. Finally, the derivative was dissolved in H_2O and freeze dried. The degree of trimethylation was varied by changing the concentration of the trimethylating reagents without changing the time of reaction. The reaction time was kept constant as 120 min. Chitosans having molecular weight of 15, 50, 85 and 125 kDa was used for trimethylation. Products were characterised by ^{1}HNMR (300 MHz, Spectrospin and Bruker).

3.1.4 Preparation of Arginine conjugated Trimethylated Chitosan (ATMC).

Arginine conjugated trimethylated chitosans were prepared by EDC/NHS chemistry. Briefly, the acid group of arginine is activated using EDC/NHS for one hour and it conjugated to the amino group of trimethylated chitosans in acetate buffer of pH 6 for 16 h at room temperature. Products were dialyzed (MWCO 12,000 Da) against deionised water for three days to remove un-reacted substrates and then lyophilized. Chitosans having molecular weight 15, 50, 85 and 120 kDa having two different degree of trimethylation were used for the reaction.

3.1.5 Preparation of Histidine conjugated Trimethylated Chitosan (HTMC).

Histidine conjugated trimethylated chitosans were prepared by EDC/NHS chemistry. Briefly, the acid group of histidine is activated using EDC/NHS for one hour and it conjugated to the amino group of trimethylated chitosans in acetate buffer of pH 6 for 16 h at room temperature. Products were dialyzed (MWCO 12,000 Da) against deionised water for three days to remove un-reacted substrates and then lyophilized. Chitosans having molecular weight 15, 50, 85 and 120 kDa having two different degree of trimethylation were used for the reaction.

3.1.6 Preparation of ATMCPEGFA (ATFP) conjugates.

The ATMC15HPEGFA (ATFP15H) conjugate was synthesized according to the method described elsewhere (Hwa Kim, Hoon Jeong, Joe & Gwan Park 2005). Briefly, folate (15 mg, 0.0375 mM), DCC (7.5 mg, 0.0375 mM), and NHS (4.25 mg, 0.0375 mM) were dissolved in anhydrous DMSO. The activation reaction proceeded under nitrogen for 1 h at room temperature. The insoluble dicyclohexylurea was removed by filtration. A hetero-functional PEG derivative

(COOHPEGNH2, 44.5 mg, 0.0125 mM) dissolved in DMSO was added into the activated folate solution. The PEGFA conjugate was dialyzed (MWCO 1000 Da) against deionised water to remove un-reacted substrates and then lyophilized. The terminal carboxylic acid group of the COOHPEGFA conjugate (25 mg, 0.0066 mM) was also activated with DCC/NHS chemistry in DMSO and conjugated to primary amine groups of ATMC15H derivative (50 mg). The reaction was carried out at room temperature under nitrogen for 1 h. The reacted conjugate was dialyzed (MWCO 12,000 Da) against deionized water and freeze dried.

3.1.7 Preparation of HTMCPEGFA (HTFP) conjugates.

The HTMC15HPEGFA (HTFP15H) conjugate was synthesized according to the method described elsewhere (Hwa Kim et al. 2005). Briefly, folate (15 mg, 0.0375 mM), DCC (7.5 mg, 0.0375 mM), and NHS (4.25 mg, 0.0375 mM) were dissolved in anhydrous DMSO. The activation reaction proceeded under nitrogen for 1 h at room temperature. The insoluble dicyclohexylurea was removed by filtration. A hetero-functional PEG derivative (COOHPEGNH2, 44.5 mg, 0.0125 mM) dissolved in DMSO was added into the activated folate solution. The PEGFA conjugate was dialyzed (MWCO 1000 Da) against deionised water to remove un-reacted substrates and then lyophilized. The terminal carboxylic acid group of the COOHPEGFA conjugate (25 mg, 0.0066 mM) was also activated with DCC/NHS chemistry in DMSO and conjugated to primary amine groups of HTMC15H derivative (50 mg). The reaction was carried out at room temperature under nitrogen for 1 h. The reacted conjugate was dialyzed (MWCO 12,000 Da) against deionized water and freeze dried.

3.1.8 Characterisation of the polymers.

3.1.8.1 Determination of molecular weight by intrinsic viscosity method.

The molecular weights of the depolymerised chitosans were determined by the intrinsic viscosity method as described by Kassai et al. (Kasaai, Arul & Charlet 2000) Briefly, Intrinsic viscosity of chitosans in 2% HAc/0.2 M NaAc were measured using an automated Ubbelohde capillary viscometer (Model Schott AVS-360, Germany) in a constant-temperature water bath at 25±0.01 °C in triplicate. Solution concentrations were adjusted based on the viscosity of the samples and the flow through time was kept in the range of 100-150 s. Six different

concentrations were tested for each sample. The intrinsic viscosity was determined by the common intercept of both Huggins (η_{sp}/C~C) and Kraemer (η_{inh}~C) plots on the ordinate at C=0. The intrinsic viscosity of a polymer is related to the polymer molecular weight according to the Mark- Houwink- Sakurada (MHS) equation. $[\eta]$= KM_v^a where $[\eta]$ is the intrinsic viscosity of the depolymerized chitosan, 'K' and 'a' are constants for given solute-solvent system and temperature. For chitosan, they are influenced by the degree of deacetylation, pH, and ionic strength of the solvent (Kasaai et al. 2000).

3.1.8.2 Determination of molecular weight by gel permeation chromatography (GPC).

Molecuar weight of the trimethylated chitosan were confirmed using gel permeation chromatography (GPC) (Water Corporation, Washington, USA) at 25±2 ^oC. The GPC equipment consisted of ultrahydrogel linear column, Waters 600E pump and Water 2410 refractive index detector. The eluent was 0.5 M acetate buffer. The standards used to calibrate the column were dextran (MW 10000-2,00,000).

3.1.8.3 ^{1}H NMR.

^{1}H NMR spectra of depolymerised chitosan, TMC, ATMC, HTMC, ATFP and HTFP derivative were measured in D_2O using a 300 MHz spectrometer (Bruker Avance DPX 300).

3.1.8.4 FTIR.

FTIR spectra of the samples were measured over 4000-400 cm^{-1} on a Shimadzu spectrophotometer.

3.1.8.5 Colorimetric determination of the free amine groups.

The TNBS method was used to determine quantitatively the incorporation of terminal amino groups into the modified chitosan derivatives (Azzam, Eliyahu, Makovitzki, Linial & Domb 2004). The amino-terminated polymers was dissolved in 2 mL of acetate buffer in a concentration of 1 mg/mL. Sodium hydrogen carbonate (2.0 mL) containing an excess of TNBS (0.01 M) was added to the solution, which was kept for 2 h at 37 ^oC. The amount of TNBS derivatised amines in the sample was determined from the absorbance at 345 nm, using TNBS derivatized glucosamine as reference compound. A solution of TNBS without added polymer was

treated under same conditions. Its absorbance at 345 nm was subtracted from that of the TNBS derivatized polymers to correct for its residual absorbance at this wavelength.

3.1.8.6 Acid base titration.

Polymer protonation and positive charge generation over the pH range of 10 to 4 was determined by acid base titration as previously described (Benns, Mahato & Kim 2002). Briefly 1.5 mg of each polymer was dissolved in 25 mL H_2O to give a final concentration of 60 μg/mL. The solution was then titrated to pH 10 with 0.1 M NaOH, where the pH was measured using a pH meter. The solution was then titrated with 0.1 N HCl. The pH profile was obtained for each polymer.

3.1.9 Amplification and purification of pDNA.

The pGL3 plasmid DNA grown in E. coli (JM109) cells was purified using Qiagen QIA filter plasmid Mega kit according to the manufacturers instruction and re-suspended in sterilized Milli-Q water. The purity was confirmed by 1% agarose gel electrophoresis and pDNA concentration was measured by UV absorption at 260 nm.

3.1.10 Preparation of polymer-pDNA nanoparticles.

ATMC, HTMC, ATFP and HTFP samples of different molecular weight and different degree of trimethylation was dissolved in 0.5% HCl in a concentration of 1 mg/mL. The solution is filtered through a 0.22 μm. The plasmid DNA was also prepared in the same concentration of 1 mg/mL. Nanoparticles were prepared in 5 mM PBS having pH 7.4 by mixing pDNA 10 μg/mL with appropriate polymer solution at the desired charge ratio. The system was vortexed for 15 s and incubated for 20 min at room temperature for the complete complex formation. It was noted that during complex preparation the volume of DNA was constant and volume of polymer solution was varied to adjust the theoretical charge ratio. All complexes for the characterization below were prepared in terms of this method unless otherwise stated.

3.1.11 Determination of particle size and zeta potential.

Particle size and zeta potential of the polymer-pDNA nanoparticles were determined using Zetasizer Nano ZS (Malvern Instruments Ltd., UK). The particle size and the zeta potential of

the nanoparticles were measured 20 min after preparation.

3.1.12 Transmission electron microscopy.

To examine the morphology of the ATFP/HTFP-pDNA nanoparticles, 10 μL nanoparticles suspension at N/P=2 was placed on a copper grid, the excess liquid was removed with a piece of filter paper and then the grid was air dried. Samples were visualized with a Hitachi H 7650 instrument at 100 kV.

3.1.13 Gel retardation assay.

Complex formation was evaluated by agarose gel electrophoresis. The ATFP/HTFP-pDNA nanoparticles were prepared at N/P ratios of 0.25, 0.5, 1, 1.5, 2 and 4 respectively, by varying the concentration of AFFP15H/HTFP15H derivative. The nanoparticles and the naked plasmid were loaded onto a 0.7% agarose gel in Tris Acetate- EDTA buffer at pH 8.0. The samples were run on the gel at 100 V for 30 min. The gel was stained with ethidium bromide and photographed using a MultiImageTM Light Cabinet (Alpha Innotech Corporation, San Leandro, CA, USA).

3.1.14 DNase I protection assay and blood plasma protein interaction.

ATFP/HTFP-pDNA nanoparticles at varying charge ratios such as N/P ratios of 0.5, 1, 2, 4 and 6 was incubated for 10 min at 37 ^{o}C with 2 units of DNase I. The DNase I was then inactivated by adding ethtylenediaminetetraacetic acid (EDTA) (0.5 M, pH 8) and incubated for 5 min at room temperature. The pDNA integrity was assessed by agarose gel electrophoresis. The interaction of polymer/pDNA nanoparticles with plasma protein were determined by mixing 5 μL of plasma protein with 10 μL of nanoparticles containing 1 μL of pDNA at optimum N/P ratio by varying the time of plasma intreraction such as 0.5, 1, 1.5 and 2 h respectively. The stability of pDNA is evaluated by agarose gel electrophoresis.

3.1.15 Blood compatibility.

Blood compatibility of ATFP/HTPF-pDNA nanoparticles were evaluated in terms of hemolysis by the method described elsewhere (Lee, Powers & Baney 2004). Whole blood was obtained from three healthy adults. Red blood cells (RBCs) were collected by centrifuging

whole blood. The RBCs were washed three times with a saline solution before being diluted with a buffer to prepare erythrocyte stock solutions with fixed concentrations of hemoglobin (3:11 centrifuged erythrocytes, buffer saline solution). Polymer/ pDNA nanoparticles at appropriate N/P ratios were prepared in saine solutions. One hundred microliters of an erythrocyte stock solution was added to 1 mL of the nanoparticles solution. The mixtures were left for 2 h and centrifuged. One hundred microliters of the resulting supernatant was dissolved in 2 mL of an ethanol/HCl mixture (200:5 mL (v/v)). A saline solution was used as negative control (0% lysis) and DI water used as a positive control (100% lysis). The absorption of the mixture was determined at 399 nm by an UV spectrophotometer.

Blood compatibility was also evaluated by RBC aggregation studies. The saline solution of RBC was incubated with ATFP15H/ HTFP15H-pDNA nanoparticles. 10 μL of the sample was mounted on a glass slide and visualized through phase contrast microscope (Leica DM IRB, Germany) at 40 times magnification. Since ATFP15H/pDNA and HTFP15H-pDNA nanoparticles were found to be more compatible with erythrocytes and plasma, it was again tested for platelet activation. The experiment was done as per the standard protocol [ISO 10993-4:2002(E)].

3.1.16 Cell culture.

Human cervical carcinoma cells (HeLa) and Human nasopharyngeal epidermoid carcinoma cells (KB cells) were maintained in MEM supplemented with 10% FBS and 1% penicillin-streptomycin under conditions of 5% CO_2 and 95% humidity at 37^{o}C.

3.1.17 Evaluation of cytotoxicity.

The cytotoxicity of the polymers was measured by MTT assay. KB and HeLa cell lines were used for the study. Cells were seeded in a 24-well tissue culture plate at 5x10^4 cells/well in 800 μL MEM containing 10% FBS. Cells achieving 70-80% confluence after 24 h were exposed to native polymers and the nanoparticles with pDNA in MEM. After 24 h the derivatives in medium were removed and 200 μL of MTT (0.5 mg/mL in MEM) was added and incubated for 4 h under normal growing conditions. After 4 h MTT were removed and 200 μL of DMSO were added in to each wells. The well plates were incubated for 30 min at 37 ^{o}C. After 30 min absorbance

was measured at 620 nm using a plate reader. Cells without polymers were taken as control.

$$CellViability = [Abs]sample/[Abs]ControlX100$$

Since the ATFP and HTFP derivatives found to have cell growth promoting property, it was tested for cell viability by varying the concentration of the ATFP15H and HTFP15H samples such as 5, 10,15,30,45 and 60 μg each per well.

3.1.18 *In vitro* transfection studies.

KB cells were harvested with 0.05% trypsin/0.53 mM EDTA. Cells were seeded at a density of 10^5 cells/well on a 24 well plate. Minimum essential medium (MEM) was exchanged for folate free RPMI1640 (FFRPMI) supplemented with 10% FBS and 1% penicillin-streptomycin. Folate-free medium with 10% FBS provides a concentration of folic acid similar to the physiological range. The cells were treated with a polymer/pDNA complex solution in 250 μL of RPMI 10% FBS containing 2.5 μg of plasmid DNA at optimum charge ratio for 4 h at 37 ^{o}C. After an exchange of fresh medium, the cells were further incubated for 48 h at 37 ^{o}C. Then the growth medium was removed, and the cells were rinsed with DPBS and shaken for 30 min at room temperature in 100 μL of Reporter Lysis Buffer (Promega). Luciferase activity was measured by a luminescence assay, and a protein assay was performed using Micro BCA Protein Assay Reagent Kit (Pierce). According to cell lines, 25 μL of the lysate was dispensed into a luminometer tube and the luciferase activity was integrated over 10 s with a 2 s measurement delay in a Hidex Chameleon, Driver Version Plate reader with the prior addition of 50 μL of Luciferase Assay Reagent (Promega). The final results were reported in terms of RLU/mg cellular protein. PEI having molecular weight 25 kDa and Superfect were used as positive control.

3.1.19 Cellular uptake studies.

Two and half hours after transfection with rhodamine-labelled ATMC15H, ATFP15H, HTMC 15H and HTFP15H derivative, cells were washed with PBS to eliminate non-specific bindings. Quenching of extracellular fluorescence was performed with 0.4% trypan blue for 5 min. Cellular uptake of complex were analyzed under confocal laser scanning microscope. The percentage of cellular uptake is estimated using FACS. After the incubation period, the cells

were washed with PBS twice and incubated for 2 min with 0.4% trypan blue solution to quench extracellular fluorescence. The cells were again washed with PBS. Then it was treated with trypsin-EDTA for 2 min, and was suspended in PBS. Uptake specificity was assessed by incubating the cells with 1 mM folic acid (Sigma), 1 h prior to adding the nanoparticles. The percentage of cells that had taken up nanoplexes was determined by flow cytometry after excitation with a 488 nm argon laser and detection with a 515-545 nm band pass filter. Suspensions were measured on a BD FACSAria cell sorter (BD Biosciences) and 10,000 cells were evaluated in each experiment. Data acquisition and analysis were performed using BD FACSDiva software (BD Biosciences).

3.1.20 Plasmid trafficking.

Since YOYO iodide is a high affinity DNA labeling dye that exhibits fluorescence enhancement on binding to double-stranded DNA, YOYO is used for the investigation of cellular transport of plasmid during transfection. Plasmid DNA was tagged with YOYO by incubating for 30 min and nanocomplexes of ATFP15H and HTFP15H were prepared at N/P ratio 2. The complexes were incubated with KB cells for 5 and 6 h and nuclear staining was done with Hoechst 33342. The cells were then viewed under confocal laser scanning microscope using Argon/2 and He/Ne 543

3.2 Synthesis and Characterisation of Synthetic Polymer based Nanoparticles.

3.2.1 Materials.

3-(2-aminoethylamino)propyl-methyl-dimethoxysilane was from Fluka and branched PEI (Mw 25kDa), folic acid from Aldrich. Luciferase expression plasmid pGL3 control vector, Luciferase 1000 Assay System and Reporter Lysis Buffer were purchased from Promega, GFP expression plasmid, pEGFP-N3,(Clontech) were kindly provided by Dr. E. Sreekumar at RGCB (Thiruvananthapuram, India), 1-Ethyl-3-(3- dimethylaminopropyl) carbodiimide hydrochloride (EDC), dicyclohexylcarbodiimide (DCC), N - hydroxysuccinimide (NHS), L-arginine, L-histidine and 3-[4,5- dimethylthiazol- 2-yl]-2,5 -di- phenyltetrazolium bromide (MTT), were purchased from Sigma (USA). Fetal bovine serum (FBS), Minimal Essential Medium (MEM), and Trypsin/

EDTA were obtained from Gibco (USA). RPMI 1640 (RPMI), Hoechst 33342 were from Invitrogen.

3.2.2 Synthesis of SiDA.

Oligo- (alkylaminosiloxane) was prepared according to the procedure given elsewhere (Kichler et al. 2003). Briefly, to 1.8 mM, (1eq) of 3-(2-aminoethylamino) propyl-methyl- di methoxysilane, 1 equivalent of 1 N NaOH solution was added and mixed. The sample was stirred for 20 h at room temperature. Later, the oligomers were exposed to reduced pressure to remove the volatiles. The crude sample was then diluted to 5 mL with water and neutralized to pH 7 by using 1 N HCl. The product was analyzed by ^{1}H NMR and mass spectrometry. Mass spectra were determined by micromass quattro micro API mass spectrometer. Mass: m/z= 641,143,302,321,481,802.

3.2.3 Synthesis of SiDAAr.

Arginine conjugated oligo amino alkyldialkoxymethylsilane was prepared by EDC/NHS chemistry. Briefly, the acid group of arginine (5 eq) was activated using EDC/NHS for 4 h at 4 ^{o}C in PBS at pH 8. SiDA (1eq) was added to the activated arginine and the reaction kept for 18 h at room temperature. The product was then dialyzed (MWCO 1000) against deionised water to remove unreacted substrates and lyophilized.

3.2.4 Synthesis of SiDAHs.

L- Histidine conjugated oligo amino alkyldialkoxymethylsilane was prepared by EDC/NHS chemistry. Briefly, the acid group of histidine (5 eq) was activated using EDC/NHS for 4 h at 4 ^{o}C in PBS at pH 8. SiDA (1eq) was added to the activated histidine and the reaction kept for 18 h at room temperature. The product was then dialyzed (MWCO 1000) against deionised water to remove unreacted substrates and lyophilized.

3.2.5 Synthesis of P(SiDAAr)n.

SiDAAr coupling to PEI was performed by EDC/NHS chemistry using N-BOC protected aspartic acid as the linker group. Briefly, one of the acid group of aspartic acid was activated using half the equivalents of EDC and NHS for 4 h at 4 ^{o}C in PBS of pH 8. After the acid

activation, SiDAAr (n eq) was dissolved in PBS and added into the reaction mixture. The reaction took place for 18 h at room temperature. The reaction mixture was kept for dialysis (MWCO 1000) to remove the unreacted substrates. The second acid group of the reaction mixture was again activated using EDC and NHS at 4 ^{o}C for 6 h. After acid activation, one equivalent of PEI was added into the reaction mixture and the reaction was kept for 18 h at room temperature. The resultant mixture was dialyzed (MWCO 12000) and then lyophilized.

3.2.6 Synthesis of P(SiDAHs)n.

SiDAHs coupling to PEI was performed by EDC/NHS chemistry using N-BOC protected aspartic acid as the linker group. Briefly, one of the acid group of aspartic acid was activated using half the equivalents of EDC and NHS for 4 h at 4 ^{o}C in PBS of pH 8. After the acid activation, SiDAHs (n eq) was dissolved in PBS and added into the reaction mixture. The reaction took place for 18 h at room temperature. The reaction mixture was kept for dialysis (MWCO 1000) to remove the un-reacted substrates. The second acid group of the reaction mixture was again activated using EDC and NHS at 4 ^{o}C for 6 h. After acid activation, one equivalent of PEI was added into the reaction mixture and the reaction was kept for 18 h at room temperature. The resultant mixture was dialyzed (MWCO 12000) and then lyophilized.

3.2.7 Synthesis of P(SiDAAr)5FPn.

FA-PEG-COOH was synthesized using procedure reported elsewhere with some modifications (Vaidya, Paliwal, Rai, Khatri, Goyal, Mishra & Vyas 2009). Briefly, 'n' equivalent of folic acid was activated using EDC in DMSO at room temperature for 2 h. The activated folic acid solution was added to the solution of NH_2-PEG-COOH and stirred for 16 h at room temperature. The reaction mixture kept for dialysis (MWCO 1000) to remove the un-reacted substrates for two days. The free acid group of the FA-PEG-COOH was activated again using EDC/NHS in PBS having pH 7.5 at 4 ^{o}C for 6 h. The aqueous solution of n equivalent of P(SiDAAr)5 was added in to the activated FA-PEG-COOH and the reaction kept for 16 h at room temperature. The reaction mixture was kept for dialysis (MWCO 12000) and then lyophilised.

activation, SiDAAr (n eq) was dissolved in PBS and added into the reaction mixture. The reaction took place for 18 h at room temperature. The reaction mixture was kept for dialysis (MWCO 1000) to remove the unreacted substrates. The second acid group of the reaction mixture was again activated using EDC and NHS at 4 ^{o}C for 6 h. After acid activation, one equivalent of PEI was added into the reaction mixture and the reaction was kept for 18 h at room temperature. The resultant mixture was dialyzed (MWCO 12000) and then lyophilized.

3.2.6 Synthesis of P(SiDAHs)n.

SiDAHs coupling to PEI was performed by EDC/NHS chemistry using N-BOC protected aspartic acid as the linker group. Briefly, one of the acid group of aspartic acid was activated using half the equivalents of EDC and NHS for 4 h at 4 ^{o}C in PBS of pH 8. After the acid activation, SiDAHs (n eq) was dissolved in PBS and added into the reaction mixture. The reaction took place for 18 h at room temperature. The reaction mixture was kept for dialysis (MWCO 1000) to remove the un-reacted substrates. The second acid group of the reaction mixture was again activated using EDC and NHS at 4 ^{o}C for 6 h. After acid activation, one equivalent of PEI was added into the reaction mixture and the reaction was kept for 18 h at room temperature. The resultant mixture was dialyzed (MWCO 12000) and then lyophilized.

3.2.7 Synthesis of P(SiDAAr)5FPn.

FA-PEG-COOH was synthesized using procedure reported elsewhere with some modifications (Vaidya, Paliwal, Rai, Khatri, Goyal, Mishra & Vyas 2009). Briefly, 'n' equivalent of folic acid was activated using EDC in DMSO at room temperature for 2 h. The activated folic acid solution was added to the solution of NH_2-PEG-COOH and stirred for 16 h at room temperature. The reaction mixture kept for dialysis (MWCO 1000) to remove the un-reacted substrates for two days. The free acid group of the FA-PEG-COOH was activated again using EDC/NHS in PBS having pH 7.5 at 4 ^{o}C for 6 h. The aqueous solution of n equivalent of P(SiDAAr)5 was added in to the activated FA-PEG-COOH and the reaction kept for 16 h at room temperature. The reaction mixture was kept for dialysis (MWCO 12000) and then lyophilised.

3.2.8 Synthesis of P(SiDAHs)1FPn.

FA-PEG-COOH was synthesized using procedure reported elsewhere with some modifications. Briefly, 'n' equivalent of folic acid was activated using EDC in DMSO at room temperature for 2 h. The activated folic acid solution was added to the solution of NH_2-PEG-COOH and stirred for 16 h at room temperature. The reaction mixture was kept for dialysis (MWCO 1000) to remove the un-reacted substrates for two days. The free acid group of the FA-PEG-COOH was activated again using EDC/NHS in PBS having pH 7.5 at 4 ^{o}C for 6 h. The solution of 'n' equivalent of P(SiDAHs)1 was added to the activated FA-PEG-COOH and the reaction kept for 16 h at room temperature. The reaction mixture was kept for dialysis (MWCO 12000) and then lyophilised.

3.2.9 Characterization of the polymers.

3.2.9.1 Determination of molecular weight by gel permeation chromatography (GPC).

Molecular weight of PEI conjugated and non-conjugated arginine and histidine modified oligo- alkylaminosiloxane polymers were confirmed using gel permeation chromatography (GPC) (Water Corporation, Washington, USA) at 25 ± 2 ^{o}C. The GPC equipment consisted of ultra hydrogel linear column, Waters 600E pump and Water 2410 refractive index detector. The eluent was 0.5 M acetate buffer. The standards used to calibrate the column were dextran (MW 10000-2,00,000).

3.2.9.2 ^{1}H NMR.

^{1}H NMR spectra of PEI conjugated arginine and histidine modified oligo- alkylaminosiloxane polymers and its PEG-FA derivatives were measured in D_2O using a 300 MHz spectrometer (Bruker Avance DPX 300).

3.2.9.3 FTIR.

FTIR spectra of the samples were measured over 4000-400 cm^{-1} on a Shimadzu spectrophotometer.

3.2.9.4 Colorimetric determination of the free amine groups.

The TNBS method was used to determine quantitatively the incorporation of terminal amino

groups into the PEI conjugated arginine and histidine modified oligo- alkylaminosiloxane polymers and its PEG-FA derivatives (Azzam et al. 2004). The amino-terminated polymers was dissolved in 2 mL of water in a concentration of 1 mg/mL. Sodium hydrogen carbonate (2.0 mL) containing an excess of TNBS (0.01 M) was added to the solution, which was kept for 2 h at 37 ^{o}C. The amount of TNBS derivatised amines in the sample was determined from the absorbance at 345 nm, using TNBS derivatized PEI as reference compound. A solution of TNBS without added polymer was treated under same conditions. Its absorbance at 345 nm was subtracted from that of the TNBS derivatized polymers to correct for its residual absorbance at this wavelength.

3.2.9.5 Differential scanning calorimetry (DSC).

Thermal behaviour of poly(ethylene imine) [PEI] and its siloxane conjugates have been studied using differential scanning calorimeter (DSC) measurement system (Waters Differential Scanning Calorimeter with mass flow control). Specimen of 8-10 mg were encapsulated in aluminium pans and heated at a rate of 10 ^{o}C/min from -20 to 250 ^{o}C.

3.2.9.6 Acid base titration.

Polymer protonation and positive charge generation over the pH range of 10 to 3 was determined by acid base titration as previously described (Benns et al. 2002). Briefly, 6 mg of each polymer was dissolved in 30 mL H_2O to give a final concentration of 0.2 mg/mL. The solution was then titrated to pH 10 with 0.1N NaOH, and the pH was measured using a pH meter. The solution was then titrated with 0.1N HCl. The pH profile was obtained for each polymer.

3.2.10 Amplification and purification of pDNA.

The pGL3 plasmid DNA grown in E. coli (JM109) cells was purified using Qiagen QIA filter plasmid Mega kit according to the manufacturers instruction and re-suspended in TE buffer. 1% agarose gel electrophoresis was performed to confirm purity of pDNA and concentration was measured by UV absorption at 260 nm.

3.2.11 Preparation of polymer/pDNA nanoparticles.

PEI conjugated arginine and histidine modified oligo- alkylaminosiloxane polymers and its PEG-FA derivatives at different mole ratios were dissolved in Milli Q water at a concentration of 1 mg/mL. The solution was filtered through a 0.22 μm. The plasmid DNA was also prepared at the same concentration of 1 mg/mL. Nanoparticles were prepared in 5 mM PBS having pH 7.4 by mixing 2.5 μg/mL of pDNA with the appropriate polymer solution at different weight ratios. The system was vortexed for 15 s and incubated for 10 to 15 min at room temperature for the completion of complex formation. It was noted that during complex preparation, the volume of DNA was constant and that of the polymer solution was varied to adjust the theoretical charge ratio. All complexes for the characterization below were prepared in terms of this method unless otherwise stated.

3.2.12 Fluorescamine assay.

The degree of binding between PEI conjugated arginine and histidine modified oligo- alkylaminosiloxane polymers and its PEG-FA derivatives and DNA was determined by the quantification of the free amino groups on polymers before and after complexation with DNA by the fluorescamine assay (Corsi et al. 2003). 10 μL of nanoparticle solution was added to 140 μL of 100 mm boric acid-NaOH solution, pH 8 in a 96-well plate. Wells containing only boric acid assay buffer were used to determine background fluorescence. 50 μL of a 0.01% fluorescamine solution prepared in acetone was added to each well, mixed, and incubated for 10 min at room temperature. The fluorescence was measured with TECAN Infinite M200 (Monochromotor Based) Multi mode reader- Austria, at an excitation wavelength of 390 nm and emission wavelength of 475 nm.

3.2.13 Determination of particle size and zeta potential.

Particle size and zeta potential of the polymer/pDNA nanoparticles were determined using Zetasizer Nano ZS (Malvern Instruments Ltd., UK). The particle size and the zeta potential of the nanoparticles were measured 15 min after preparation.

3.2.14 Morphology of the polymer/pDNA nanoparticles by AFM.

The morphology and size distribution of polymer/pDNA nanoparticles was analyzed by atomic force microscopy (WITEC Confocal Raman Microscope System with Atomic Force Microscope Extension, Germany). The samples were prepared by mixing 1 μg of plasmid DNA with aqueous polymer solution at optimum weight ratios to obtain a final DNA concentration of 10 ng/μL. After 15 min incubation, 10 μL of the nanoparticles suspension was examined by AFM. The nanoparticles were placed on a freshly cleaved untreated mica surface and allowed to dry for 1-2 min. Excess solution was removed using filter paper and the mica surface was further dried at room temperature for 24 h. The image mode was set to tapping mode with a scanning speed of 1-5 Hz.

3.2.15 Morphology of the polymer/pDNA nanoparticles by TEM.

The morphology and size distribution of polymer/pDNA nanoparticles was analyzed by transmission electron microscopy (Hitachi H 7650 instrument at 100 KV). The samples were prepared by mixing 1 μg of plasmid DNA with aqueous polymer solution at optimum weight ratios to obtain a final DNA concentration of 10 ng/μL. After 15 min incubation, 10 μL of the nanoparticles suspension was examined by TEM. The sample was placed on a copper grid, the excess liquid was removed with a piece of filter paper and the grid air dried. Samples were visualized with a Hitachi H 7650 instrument at 100 kV.

3.2.16 Gel retardation assay.

Complex formation was evaluated by agarose gel electrophoresis. The polymer/pDNA nanoparticles were prepared at w/w ratios of 0.25, 0.5, 1, 3, 5 and 10 respectively, by varying the concentration of derivative. The nanoparticles along with naked plasmid were loaded onto a 0.7% agarose gel in Tris Acetate- EDTA buffer at pH 8.0. The samples were run on the gel at 100 V for 30 min. The gel was stained with ethidium bromide and photographed using a phospho-imager apparatus. (FUJIFILM FLA-5100).

3.2.17 DNase I protection assay.

Polymer/pDNA nanoparticles at its optimum weight ratios were incubated for 10 min at 37 ^{o}C with 1, 2.5 and 5 units of DNase I. The DNase I was then inactivated by adding 6 μL of ethtylenediaminetetraacetic acid (EDTA) (0.5 M, pH 8) and incubated for 5 min at room temperature. 3 μL of heparin was added to release the DNA from the complex nanoparticles. The pDNA integrity was assessed by agarose gel electrophoresis.

In addition, a change in the absorbance of polymer/pDNA solutions at 260 nm was observed to detect DNA fragmentation by DNase I according to the method described elsewhere (Agarwal, Unfer & Mallapragada 2005). Polymer solution in nanopure water was added to plasmid DNA in TE buffer (pH 7.5) to get desired (w/w) ratios with 20 μg of DNA/mL final concentration (i.e. 0.4 OD of DNA at 260 nm). After incubating the polyplexes for 15 min, 100 IU of DNase I were added (5 IU/μg DNA) with 10 X DNase I buffer to make the final volume of polyplex solution to 1 mL, and the change in absorbance at 260 nm was monitored. PEI was used as the positive control and uncomplexed DNA as the negative control.

3.2.18 Blood compatibility.

Blood compatibility of polymer/pDNA nanoparticles were evaluated in terms of hemolysis by the method described elsewhere (Lee et al. 2004). Blood compatibility was also evaluated by RBC aggregation studies. The saline solution of RBC was incubated with polymer/pDNA nanoparticles. 10 μL of the sample was mounted on a glass slide and visualized through phase contrast microscope (Leica DMI 3000 B Trinocular Inverted Research Microscope, Germany) at 40 times magnification. PEG-FA derivatives of P(SiDaAr)5 and P(SiDAHs)1 were chosen for blood compatibility studies.

3.2.19 Cell culture.

Human cervical carcinoma cells (HeLa), Human cervical cancer cell lines (SiHa), Human hepatocarcinoma cells (HepG2) and Human nasopharyngeal epidermoid carcinoma cells (KB cells) were maintained in MEM supplemented with 10% FBS and 1% penicillin-streptomycin under conditions of 5% CO_2 and 95% humidity at 37 ^{o}C.

3.2.20 Evaluation of cytotoxicity.

The cytotoxicity of the polymers and its nanoparticles with pDNA were measured by MTT assay. KB cell lines were used for the study. For determining the cell viability of polymers alone, cells were seeded in a 96-well tissue culture plate at 5×10^3 cells/well in 100 μL MEM containing 10% FBS. Cells achieving 70-80% confluence after 24 h were exposed to 10 μL of native polymers having various concentrations such as 25,50,75 and 100 μg/mL in 90 μL of MEM with 10% FBS. After 24 h, the derivatives in the medium were removed and 26 μL of MTT (2 mg/mL in MEM) was added and incubated for 4 h under normal growing conditions. Four hours later, MTT was removed and 150 μL of DMSO was added into each well. The well plates were incubated for 30 min at 37 ^{o}C. After 30 min, absorbance was measured at 620 nm using a plate reader. Cells without polymers were taken as control. Similarly for polymer/pDNA nanoparticles, cells were seeded in 24 well plate at 1×10^5 cells/well in 100 μL MEM containing 10% FBS. After 24 h, the nanoparticles of each polymer at its optimum weight ratios containing 2.5 μg of DNA were added onto the cells. The medium was removed and 200 μL of MTT (0.5 mg/mL in MEM) was added after 24 h and incubated for 4 h under normal growing conditions. Later, MTT was removed and 200 μL of DMSO were added into each well and absorbance measured at 620 nm.

$$CellViability = [Abs]sample/[Abs]ControlX100$$

3.2.21 *In vitro* transfection studies.

SiHa and KB cells were harvested with 0.05% trypsin/0.53 mM EDTA. Cells were seeded at a density of 10^5 cells/well on a 24 well plate. Minimum essential medium (MEM) was exchanged for RPMI1640 supplemented with 10% FBS and 1% penicillin/streptomycin. The cells were treated with polymer/pDNA complex solution in 250 μL of RPMI 10% FBS containing 2.5 μg of plasmid DNA at optimum weight ratio for 3.5 h at 37 ^{o}C. After an exchange of fresh medium, the cells were further incubated for 48 h at 37 ^{o}C. Then the growth medium was removed, and the cells were rinsed with DPBS and shaken for 30 min at room temperature in 100 μL of Reporter Lysis Buffer (Promega). Luciferase activity was measured by the luminescence assay, and protein assay was performed using Micro BCA Protein Assay Reagent Kit (Pierce). To the luminometer tube, 25 μL of the lysate was dispensed and the luciferase activity

was integrated over 10 s with a 2 s measurement delay in a Hidex Chameleon, Driver Version Plate reader with the prior addition of 50 μL of Luciferase Assay Reagent (Promega). The final results were reported in terms of RLU/mg cellular protein. PEI having molecular weight 25 kDa and Superfect were used as positive control.

3.2.22 GFP transfection and flow cytometry.

HeLa and KB cells were seeded at a density of 10^5 cells/well in a 4-well plate in a medium containing 10% FBS. The cells were treated with polymer/pDNA nanoparticles solution containing 2.5 μg of plasmid DNA (pEGFP) at its optimum weight ratios for 3.5 h at 37 ^{o}C. After exchange of medium, cells were further incubated for 24 h, and the fluorescence of expressed GFP was viewed using confocal laser scanning microscope using Argon 2 laser. GFP expressions were quantitatively measured using flow cytometry. Transfection was performed on KB cell lines in presence of 10% serum. After 48 h of transfection, the cell suspensions were measured on a BD FACSAria cell sorter (BD Biosciences) and 10,000 cells were evaluated in each experiment. Data acquisition and analysis were performed using BD FACSDiva software (BD Biosciences). Polymers which exhibit highest luminescence expression such as P(SiDAAr)5 and P(SiDAHs)1 and its folate mediated derivatives were taken for GFP transfection. PEI/DNA nanoparticles were considered as the reference.

3.2.23 Treatment with inhibitors.

KB cells were seeded at a density of 1×10^5 cells/well in a 24-well plate. After a day of incubation in normal conditions, cells were pre-treated with genistein (200 μM), wortmannin (100 nM), and chlorpromazine (10 μg/mL) (Kim, Baek, Yoon, Choi, Kim & Park 2007*a*) for 30 min, and 1 mM folic acid for 1 h before addition of polyplexes. Polyplexes nanoparticles containing 2.5 μg of plasmid DNA, were prepared at its optimum weight ratios. After 3.5 h of polyplex incubation, all media were washed with PBS and replaced with fresh media containing 10% serum, and then cells were further incubated for 2 days before the assay. Polymers which exhibit highest luminescence expression such as P(SiDAAr)5 and P(SiDAHs)1 and its folate mediated derivatives having highest transfection were taken for inhibitor studies. PEI/DNA nanoparticles were considered as the reference.

3.2.24 Nuclear localisation of polymer/DNA nanoparticles.

Polymers having highest transfection before and after targeting was tagged with FITC and complexed with plasmid DNA. The nanoparticles were incubated with Hep G2 or KB cell lines for 4 h and nuclear staining was done with Hoechst 33342. The cells were then viewed under Leica Flurescent microscope (Leica DMI 3000 B Trinocular Inverted Research Microscope, Germany)

3.2.25 Immunohistochemical analysis of folate receptor expression.

At 24 h prior to FACS experiment, adherent KB cells were grown in 24 well culture plates in RPMI media (folic acid free) with 10% FBS and 1% penicillin-streptomycin (Sigma-Aldrich). The cells were grown until 80% confluence. The cells washed with PBS and then treated with trypsin-EDTA (120 μL trypsin, 1 mM EDTA) for 2 min, transferred to 2 mL fresh growing medium with 10% FBS and centrifuged (1500 rpm for 5 min). Cells were fixed in 3.75% paraformaldehyde at 4 ^{o}C for 20 min. The cells were washed further with PBS, the primary antibody rabbit poyclonal IgG (Santa Cruz Biotehnology,Inc., USA) selective for the R-FR was then added to each tube (20 μg/mL in 0.2% BSA/PBS (total volume 1 mL)) and the cells incubated at 4 ^{o}C for 1 h. After washing with PBS, the secondary antibody (rabbit antibody IgG, FITC conjugated, Santa Cruz Biotechnology, Inc., USA) was added to the cells (1:1000 dilution, in 0.2% BSA/PBS (total volume 1 mL)) and the cells were incubated at 4 ^{o}C for a 1 h. The cells were then washed with PBS (3 x 1 mL) and centrifuged (400 rpm for 5 min) and analyzed for their FITC fluorescence on a flow cytometer.

3.2.26 *In Vitro* targeting of the polymers.

The uptake of folate-conjugated and non conjugated P (SiDAAr) 5 and P (SiDAHs)1 was determined by flow cytometry using fluorescein isothiocyanate (FITC)-labelled derivatives. At 24 h prior to FACS experiment, adherent KB cells were grown in 24 well culture plates in RPMI media (folic acid free) with 10% FBS and 1% penicillin-streptomycin (Sigma-Aldrich). The cells were grown until 80% confluence. The FITC tagged derivatives were added in to the cells and incubated for 4 h at 37 ^{o}C. For a competitive binding assay, 1 mM, 2 mM and 3 mM free folic acid was included in the incubation media. Then, the cells were washed with PBS once and

incubated with 0.4% trypan blue solution to quench extracellular fluorescence. After that, the cells were washed three times with PBS and fixed in 1% paraformaldehyde solution for 30 min at 4 ^{o}C. The fixed cells were washed twice with PBS. Complex uptake in KB cells was analyzed by a flow cytometer.

3.2.27 Statitical analysis.

All quantitative data are expressed as mean standard deviations. Statistical analysis was performed with Students t-test. Differences were considered statistically significant with P $<$ 0.05.

3.3 In Vivo Tumor Targeting.

2×10^6 KB cells in HBSS were implanted into the flanks of 6-8 week old Balb/c mice for generation of subcutaneous tumors. After 2 to 3 weeks, the mice were injected intravenously via lateral tail vein with 100 μL FITC tagged P(SiDAAr)5FP2 in saline. At 2, 4, 16 and 24 h of post injection, the mice were sacrificed and tumors, livers and kidneys were excised. Frozen on liquid nitrogen and embedded in OCT embedding fluid, 10 μm thick sections cut, mounted on slides and studied by fluorescence microscopy. The polymer without targeting group was used as control.

4 RESULTS

4.1 *Synthesis and Characterisation of Natural Polymer based Nanoparticles.*

4.1.1 Synthesis and characterisation of ATMC and HTMC derivatives.

By the depolymerization of high molecular weight native chitosan, four derivatives having molecular weight 15 kDa (Mv $\approx$ 15404.0Da), 50 kDa (Mv $\approx$ 51358.13 Da), 85 kDa (Mv $\approx$ 85519.05 Da), and 125 kDa (Mv $\approx$ 125674.58 Da) were obtained (chito 125, chito 85, chito50 and chito15 respectively). Depolymerised chitosan on trimethylation to two different degrees resulted in eight trimethylated derivatives having high (H) and low (L) degrees of trimethylation. i.e TMC15L,TMC50L, TMC85L and TMC125L were obtained by using only half the quantity of the trimethylating reagents which have been used for TMC15H, TMC 50H, TMC85H and TMC125H. The molecular weight of the depolymerised chitosans were determined using intrinsic viscosity method in 0.25 M acetic acid/0.25 M sodium acetate with k and a values of $15.7X10^{-5}$ and 0.79 (Kasaai et al. 2000). The intrinsic viscosity values for the polymers having molecular weight of 125 kDa, 85 kDa, 50 kDa and 15 kDa were found to be 1.68,1.23,0.82 and 0.30 respectively. The evaluation by viscosity method was confirmed by determining the molecular weight of the TMC derivative, TMC15H, derived from chitosan having molecular weight of 15 kDa using GPC method. The molecular weight observed was Mw of 20784Da. The increase in molecular weight from Mv of 15 kDa to Mw of 20 kDa was due to the addition of methyl group to the amino group of chitosan polymer during trimethylation. The trimethylated chitosan were further conjugated with arginine and histidine moieties using NHS/EDC chemistry. The resultant products were represented as ATMC15H, ATMC50H, ATMC85H, ATMC 125H, ATMC15L, ATMC50L, ATMC85L and ATMC125L in the case of arginine modification and HTMC15H, HTMC15L, HTMC50H, HTMC50L, HTMC85H, HTMC85L, HTMC125H and HTMC125L in case of histidine modification. The formation of the products were confirmed by determining primary amino group contents using a colorimetric assay with 2,4,6-trinitrobenzene sulphonic acid (TNBS) and Fourier Transform Infrared Spectroscopy (FTIR). From the result of TNBS experiment (Figure 4) it was observed that as the depolymerisation increases the degree of primary amine content also increases. Therefore chito 15 has found

to have highest degree of primary amine compared to all other depolymerised derivatives.

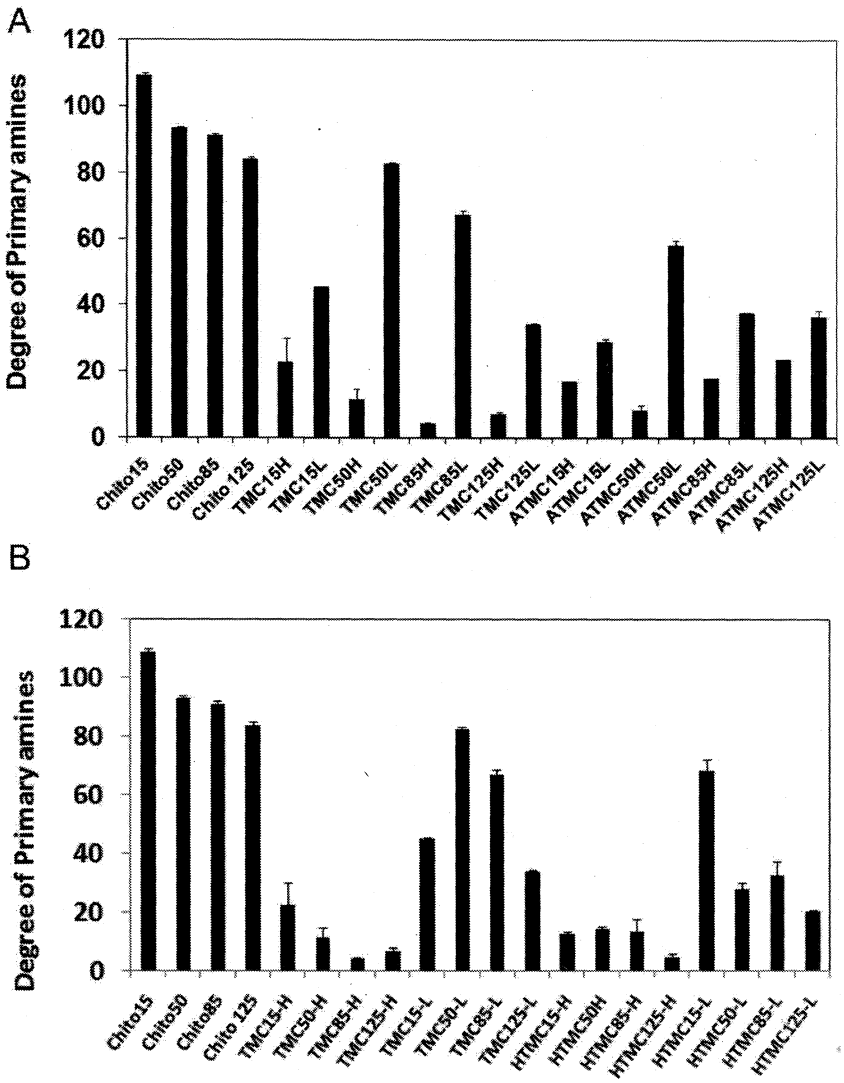

Figure 5: (A) Degree of primary amine content of depolymerised chitosans and ATMC derivatives using TNBS assay (B) Degree of primary amine content of depolymerised chitosans and HTMC derivatives using TNBS assay.

The extent of reduction of primary amines upon trimethylation was also estimated using TNBS assay. From the Figure 5, it was observed that the TMC derivatives having high degree of trimethylation exhibited low degree of primary amines. It is also observed that arginine and histidine conjugation reduced the primary amino groups of depolymerised chitosans. This may be due to the guanidine group and imidazole group of arginine and histidine respectively.

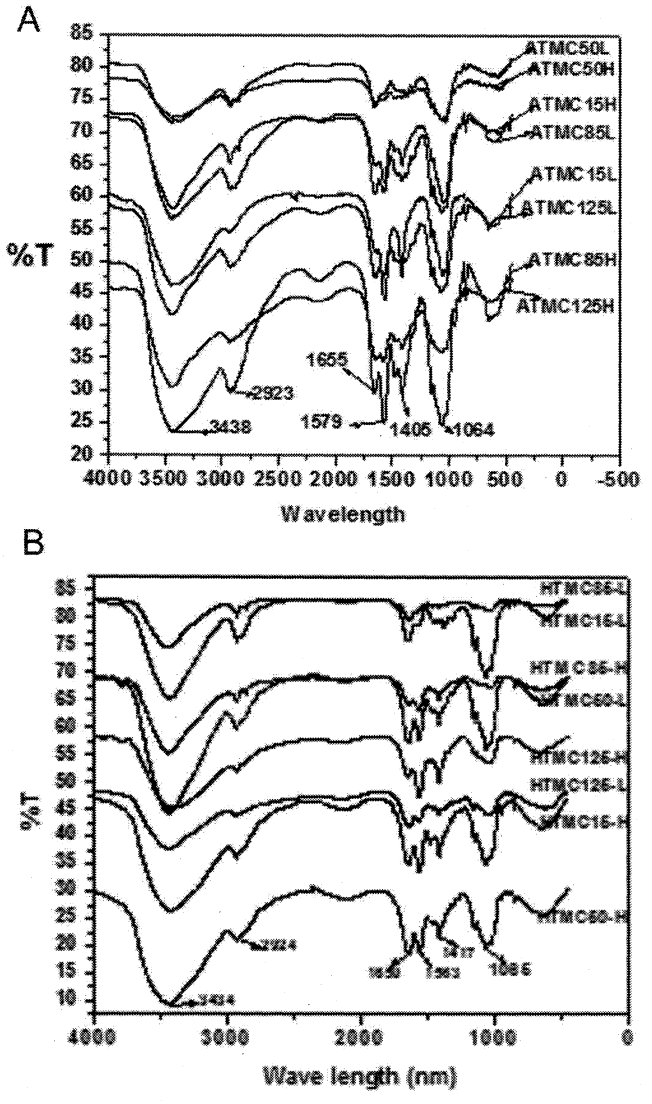

Figure 6: (A) IR spectra of ATMC derivatives (B) IR spectra of HTMC derivatives.

The results were confirmed by the FTIR spectroscopy (Figure 6). The reaction between amino groups of TMC and carboxyl groups of arginine and histidine leads to the decrease in the OH stretching vibration and $C = O$ bending vibration peaks of carboxyl groups. All ATMC and HTMC derivatives showed high intensity peaks of primary amino groups at 3434- 3438 cm^{-1}. Which also indicated the hydrogen bonded NH (amide) group. The presence of tertiary amino groups was confirmed as the peaks at 2138 cm^{-1}. In the case of ATMC derivatives the formation of $-NH - CO-$ bonds due to the conjugation of acid group of arginine and amino groups of chitosan were overlapped by stretching vibration of $C = N$ at guanidine group. In

the case of HTMC derivatives the peaks in the spectral region 1700-1500 cm^{-1} indicated the amide groups, asymmetric NH_3^+bending modes as well as imidazole ring. The peaks at 1563 cm^{-1}, 1065 cm^{-1} and 817 cm^{-1} was also due to the presence of imidazole group.

The high degree of trimethylation of TMC15H polymer is also confirmed by ^1H NMR spectroscopy (Figure 7). The integral of the hydrogens of the trimethylated amino groups at 3.3 ppm was obtained as 117.118. Therefore the degree of timethylation was found to be 71% according to the equation $DQ = [[(CH3)3/[H] \times 1/9]100$ (Verheul, Amidi, van der Wal, van Riet, Jiskoot & Hennink 2008). Similarly from the integral values of peaks due to hydrogen at 2.9 ppm (i.e. 67.05) of dimethylated amino group and at 3.5 ppm (i.e. 30) of O-methylated hydroxyl group, the degree of dimethylation (DM) and degree of 6-O-methylation were also calculated as 61% and 54% respectively from the following equations $DM = [[(CH3)2]/[H] \times 1/6] \times 100$ and $DOM = [[(CH3)/[H] \times 1/3] \times 100$. (Verheul et al. 2008).

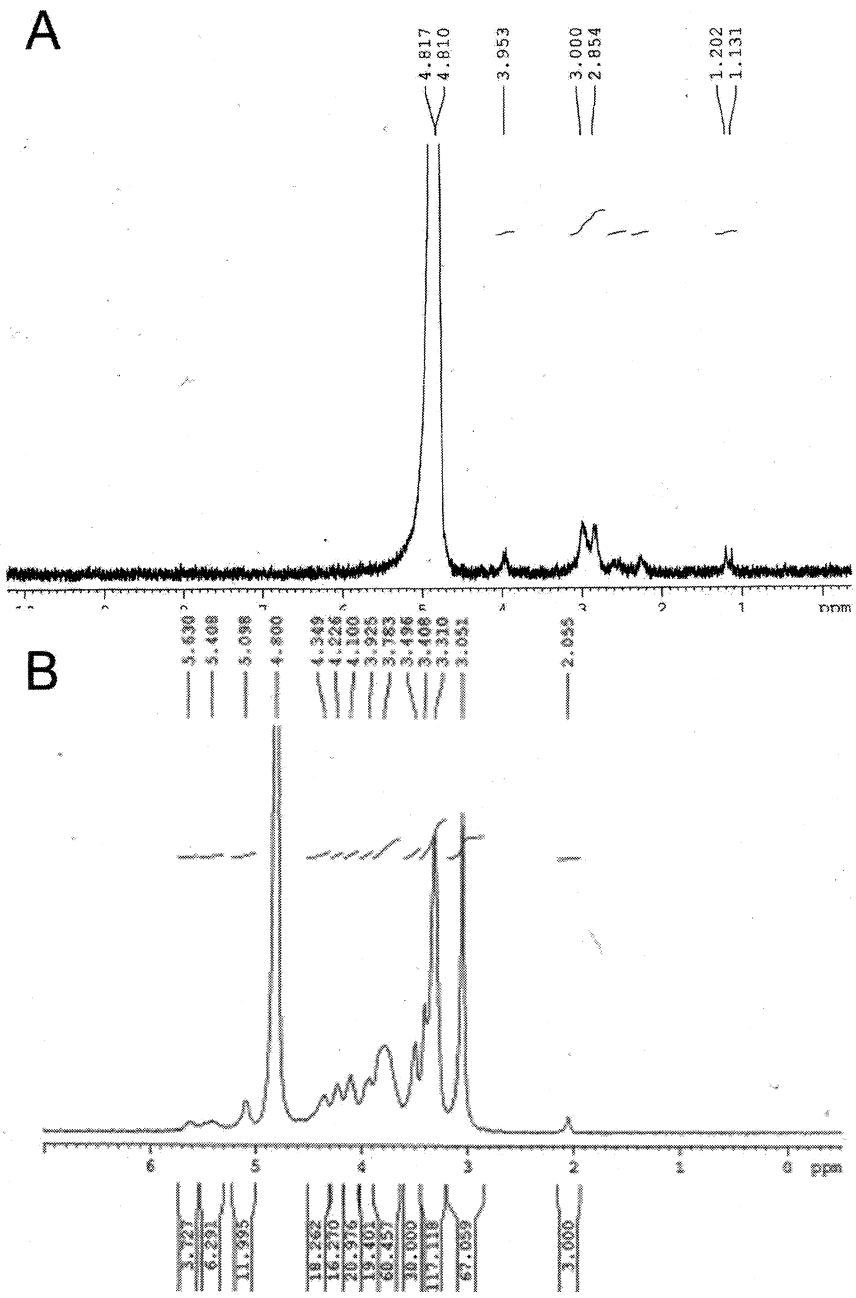

Figure 7: ^{1}HNMR spectra of (A) Chito 15 and (B) TMC15H derivatives.

The complexation of plasmid DNA with each of the eight ATMC or HTMC derivatives in PBS at pH=7.4 resulted in the formation of complex nanoparticles. The zeta potential and diameters of the complex nanoparticles formed at various charge ratios were measured by dynamic light scattering technique (DLS). Table 2 to Table 5 showed the particle sizes and zeta potentials of ATMC/pDNA and HTMC/pDNA complexes. All ATMC and HTMC derivatives showed a similar

pattern. At N/P= 0.5 particle size was found to be below 200 nm. As the ratio became N/P=1, the size reached to a micro level. On further increase in the charge ratio, the particle size decreased and attained a minimum value. The minimum sizes of the derivatives were found to be 205 nm, 196 nm, 130 nm, 212 nm, 209 nm, 184 nm, 191 nm, and 194 nm for ATMC15H, ATMC15L, ATMC50H, ATMC05L, ATMC 85H, ATMC 85L, ATMC 125H and ATMC125L respectively. Similarly in the case of HTMC derivatives the minimum sizes of the derivatives were found to be 230, 212,291,179,231,205,213, and178 nm for HTMC15H, HTMC15L HTMC50H HTMC50L, HTMC 85H, HTMC 85L, HTMC 125H, HTMC'125L respectively. The zeta potential of ATMC/pDNA and HTMC/pDNA complexes in Table 3 and 5 showed that all complexes had high zeta potential at charge ratio of N/P=3 and 2.5 respectively. On increasing the polymer ratio, the zeta potential was found to approach a plateau. The highest zeta potential of all derivatives were 13.9 mV, 19.6 mV, 11.9 mV, 13.1 mV,24.2 mV,6.83 mV,7.58 mV, 7.58 mV and 12.8 mV for ATMC15H, ATMC15L, ATMC50H, ATMC50L, ATMC85H, ATMC 85L, ATMC125H, and ATMC125L respectively. And in the case of HTMC derivatives the highest zeta potential of all derivatives were 23.3mV, 21.6 mV, 24.9 mV, 22.5 mV, 17.2 mV, 17.1 mV, 20.1 mV and 18.8 mV for HTMC15H, HTMC15L, HTMC50H, HTMC50L, HTMC85H, HTMC 85L, HTMC125H and HTMC125L respectively. The ratio providing the lowest particle size and highest positive charge were considered as optimum for further studies. For all the ATMC derivatives, the ratio of N/P=3 was taken to be the optimum ratio and for all HTMC derivatives it was 2.5.

Table 2: Particle size (nm) of ATMC derivatives at various charge ratios(Standard Deviation given in bracket)

N/P ratio	ATMC15H	ATMC15L	ATMC50H	ATMC50L	ATMC85H	ATFP85L	ATFP125H	ATFP125L
0.25	1036(8.48)	1148(11.3)	824(12.7)	465(12.0)	360(9.1)	1358(18.3)	442(14.1)	560(10.6)
0.5	876(15.5)	1037(19.7)	523(10.6)	214(8.2)	146(35.3)	281(12.7)	323(16.9)	227(9.8)
1	1343(9.89)	1462(21.2)	3144(35.3)	1714(21.2)	2468(39.0)	1825(43.0)	2638(36.0)	1151(24.0)
1.5	1066(7.07)	1308(10.6)	129(4.24)	461(13.7)	171(12.0)	586(15.5)	731(9.8)	252(12.7)
3	205(5.65)	196(4.2)	130(2.82)	212(4.94)	209(5.65)	184(2.8)	191(3.5)	194(4.2)
5	378(18.3)	245(7.07)	221(5.65)	306(8.48)	341(8.48)	212(7.07)	383(7.07)	335(8.4)

Table 3: Zeta Potential (mV) of ATMC derivatives at various charge ratios (Standard Deviation given in bracket)

N/P ratio	ATMC15H	ATMC15L	ATMC50H	ATMC50L	ATMC85H	ATFP85L	ATFP125H	ATFP125L
0.25	-72.0(3.53)	-24.2(3.67)	-21.3(4.52)	-18.0(2.67)	-22.4(4.49)	-16.69(2.05)	-18.5(1.8)	-24.6(3.46)
0.5	-12.6(2.68)	-13.4(3.25)	-12.3(3.39)	-11(3.39)	-12.4(2.96)	-6.39(1.07)	-6.49(3.67)	-20.7(4.69)
1	1.2(0.98)	0.03(1.27)	-2.53(0.48)	-1.3(0.80)	-0.01(0.50)	-2.32(0.76)	-1.06(2.26)	5.09(1.76)
1.5	6.0(1.97)	5(1.97)	4.0(0.79)	7(2.82)	12(0.59)	11.2(1.69)	7.53(0.48)	4.4(3.3)
3	13.9(0.70)	19.6(0.7)	11.9(1.06)	13(0.48)	24.2(2.47)	6.83(1.38)	7.58(0.38)	12.8(0.79)
5	18.4(1.69)	22(2.96)	19.7(0.35)	16(0.7)	31.2(2.63)	8.95(2.26)	12.9(1.89)	19.2(0.45)

Table 4: Particle size (nm) of HTMC derivatives at various charge ratios (Standard deviation given in bracket)

N/P ratio	HTMC15H	HTMC15L	HTMC50H	HTMC50L	HTMC85H	HTMC85L	HTMC125H	HTMC125L
0.5	955(111)	560(113)	434.5(30)	409.5(67)	907.5(3)	224(15)	578(45)	553.5(9)
1	2033(65)	1059(18)	1147.5(137)	1097.5(76)	1520(32)	1103(31)	2364(61)	1859(7)
1.5	937.5(60)	772.5(23)	532(33)	400(49)	321(4)	529.5(34)	850(36)	749.5(21)
2	360(70)	350(35)	446(19)	371.5(72)	260(21)	312.5(12)	330.5(13)	336.5(16)
2.5	255(35)	207(7)	287.5(4.9)	174(7)	238.5(10)	224(26)	209.5(4)	171.5(9)
3	777(11)	523.5(12)	365(12)	460.5(9)	282.5(12)	513.5(50)	566.5(33)	431.5(4.9)

Table 5: Zeta potential (mV) of HTMC derivatives at various charge ratios (Standard deviation given in bracket)

N/P ratio	HTMC15H	HTMC15L	HTMC50H	HTMC50L	HTMC85H	HTMC85L	HTMC125H	HTMC125L
0.5	-23.55(1.2)	-19.8 (1.2)	-15.35(1.9)	-18.2(0.84)	24.4(1.69)	17.85(1.06)	12.95(3.18)	-9.95(0.35)
1	1.175 (0.4)	1.34(0.36)	0.135(1.9)	2.41(1.18)	3.05(0.77)	3.555(2.02)	0.825(21)	1.615(0.35)
1.5	3.94(0.87)	11.7(1.2)	15.85(1.5)	18(0.28)	12(0.28)	16.5(0.84)	13.1(0.84)	10.1(0.56)
2	16.95(0.21)	15.8(0.84)	25(0.7)	27.1(0.42)	15(0.14)	26(0.14)	17.15(0.49)	14.85(0.91)
2.5	22.95(0.49)	21.95(0.49)	25(1.4)	22.2(0.42)	17(0.28)	16.9(0.28)	20.85(1.06)	17.8(1.41)
3	26.05(1.06)	24.45(1.06)	16.35(0.63)	33.35(0.63)	14.5(0.70)	27.8(0.56)	27.75(1.43)	25.7(0.14)

Since our major focus was to induce tumor targeting ability, ATMC15H and HTMC15H were selected based on transfection efficiency for further modification (Figure 8). Transfection studies were performed on KB oral epidermoid cells by using pGL3-Luc as the reporter gene in presence of 10% FBS. The gene transfection activity of the polymers was evaluated in terms of luciferase assay. From the Figure 8A and B the highest transfection was observed for ATMC15H and HTMC15H derivatives. As the molecular weight increased, correspondingly transfection efficiency was decreased. Therefore ATMC15H and HTMC15H derivatives were chosen for inducing tumor targeting ability.

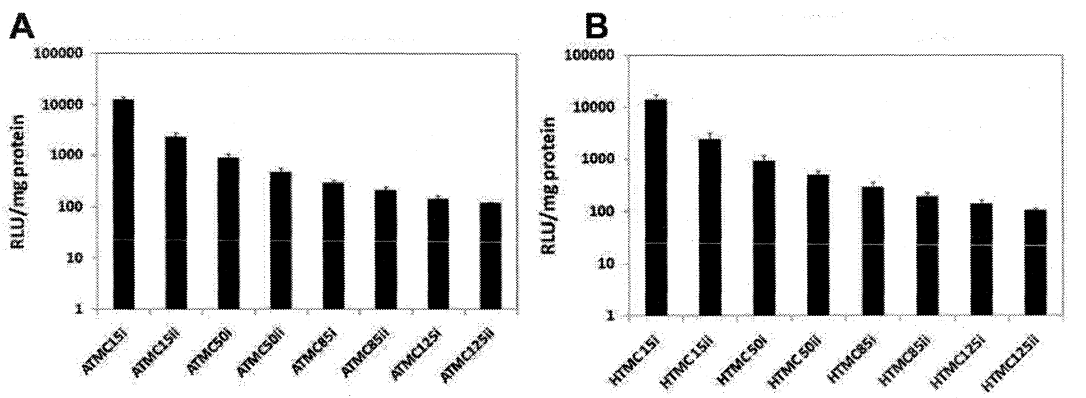

Figure 8: *In vitro* transfection of (A) ATMC and (B) HTMC derivatives into cultured KB oral epidermoid cells. Cells were incubated with polymer/pGL3 complexes.

4.1.2 Synthesis and characterization of ATFP15H and HTFP15H derivatives.

The PEG-FA conjugated ATMC15H and HTMC15H derivative (ATFP15H & HTFP 15H) (Figure 9) was characterized physico chemically by determining primary amino group contents using a colorimetric assay with 2,4,6-trinitro benzenesulphonic acid (TNBS), Fourier transform infrared spectroscopy (FTIR), ^{1}HNMR and acid base titration method.

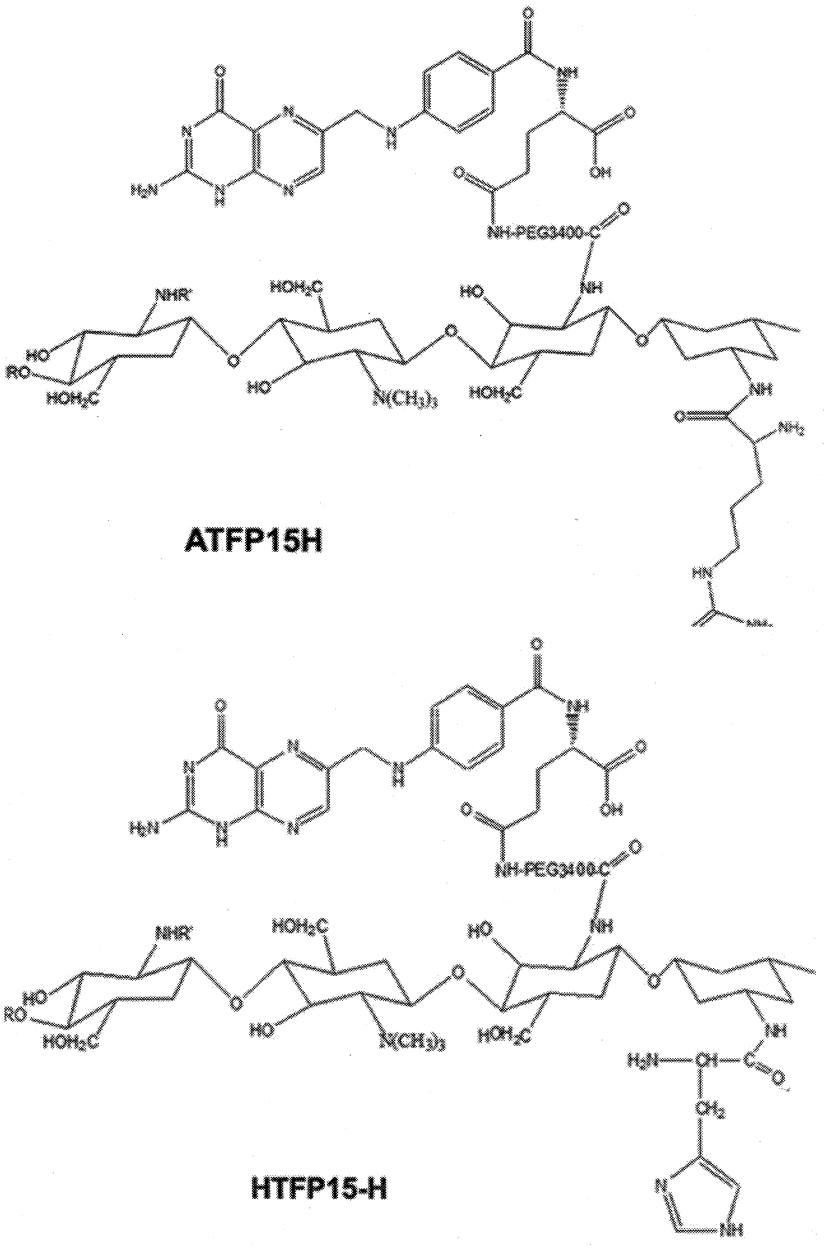

Figure 9: Schematic representation of ATFP and HTFP derivatives.

From the Figure 10, it was observed that upon conjugation with PEG-FA, the degree of primary amine content increased. The increase in primary amine was due to the presence of folic acid. This observation was confirmed by IR spectra also.The formation of $-NH-CO-$ bonds due to the conjugation of folic acid was confirmed by the presence of high intensity peak at 1631-1639 cm^{-1}. This peak was overlapped by stretching vibration of $C=N$ at guanidine group in case of ATFP15H derivative.

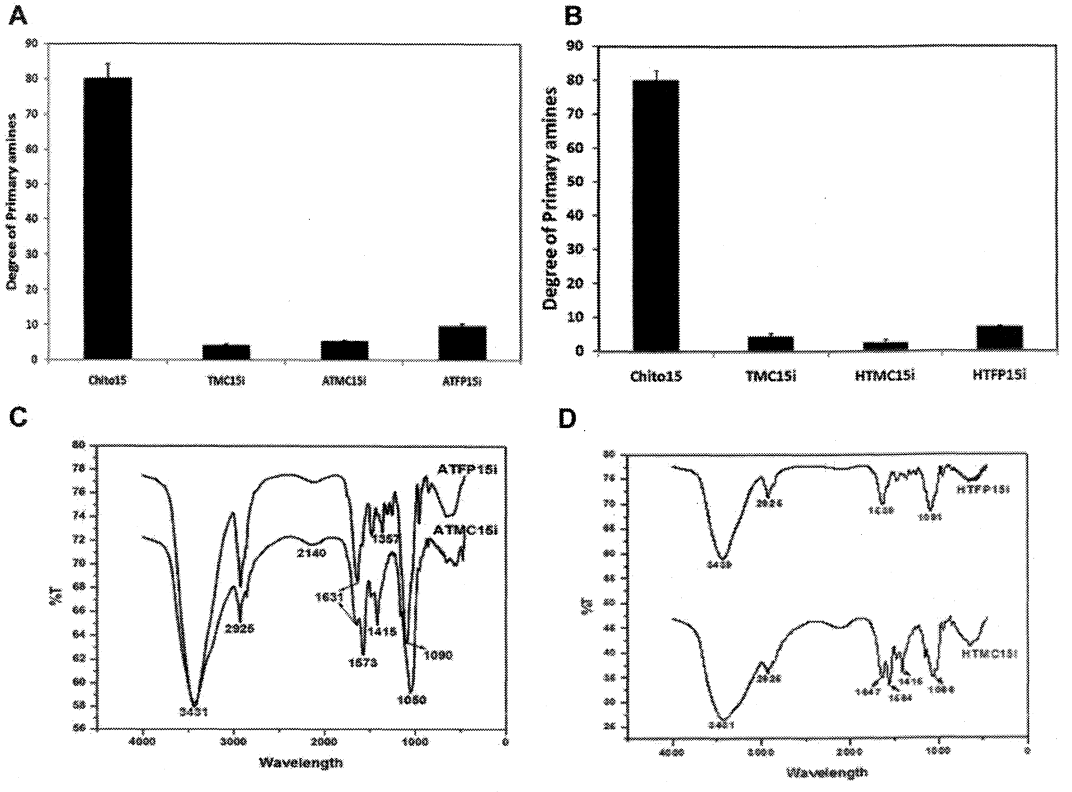

Figure 10: (A) Degree of primary amine content of ATFP derivatives using TNBS assay (B) Degree of primary amine content of HTFP derivatives using TNBS assay. (C) IR spectra of ATFP derivatives, (D) IR spectra of HTFP derivatives.

The NMR spectra also confirm the presence of PEG group from the PEG (CH_2CH_2O) signals at 3.645 ppm. Coupling of the folate residue to PEG grafted chitosan was confirmed by the appearance of signals at 8.3 ppm, which correspond to the aromatic protons of folic acid. Due to the presence of polymeric protons of PEG, the relevant signals of folate are much weaker (Figure 11A&B). Both the ATFP15H and HTFP15H derivatives showed much more buffering capacity than that of their parent compounds and PEI. So the targeted derivative can be expected to retain an endosomal disruption capacity over the entire pH range (Figure 11 C&D).

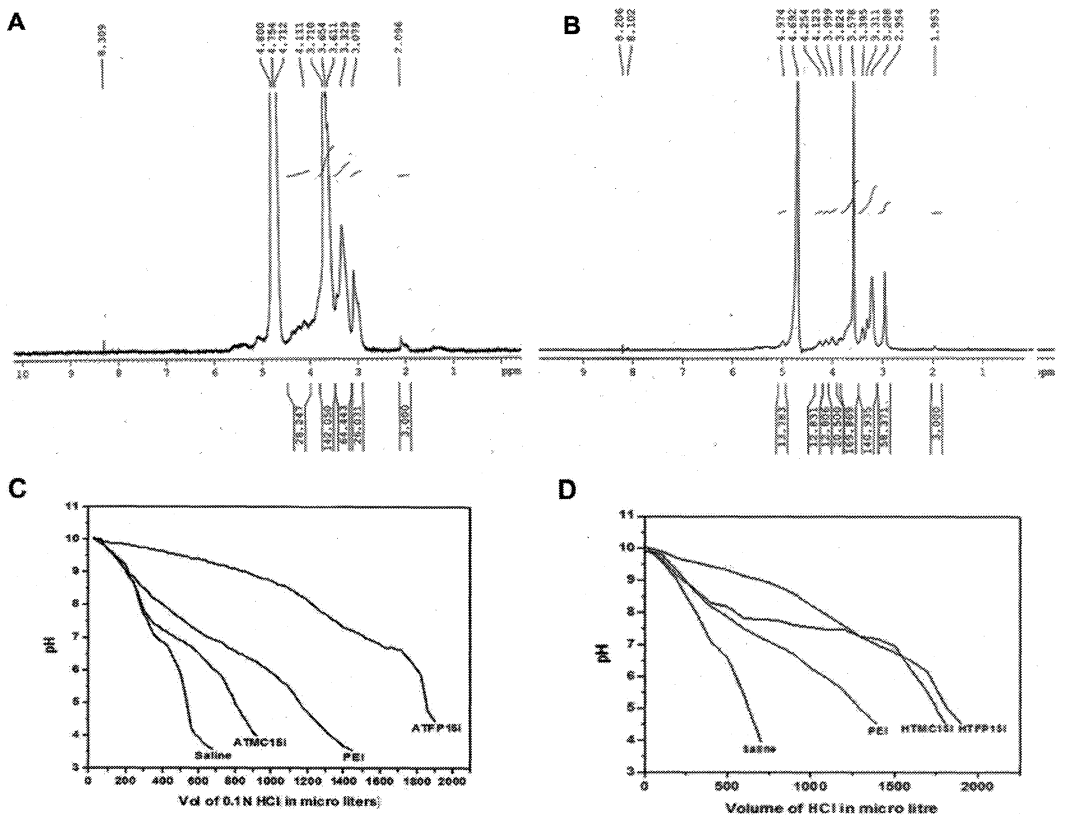

Figure 11: ^{1}HNMR spectra of (A)ATFP15H and (B)HTFP15H derivatives. (C) and (D) Acid/ base titration of ATFP and HTFP derivatives respectively, PEI was considered as positive control. pH profile is taken from initial alkalinity to final acidic conditions.

4.1.3 Formation of polymer/pDNA complex nanoparticles and its characterization.

The particle size and zeta potential of ATFP15H and HTFP15H derivatives were shown in Table 6. At N/P=1 the nanoparticles showed highest size and almost neutral charge. Then the size decreased to an average value of 175 nm and corresponding charge was found to be +12.5 mV at N/P=2, in the case of ATFP15H/pDNA and average size of 196 nm and corresponding charge of +15.48 mV in the case of HTFP/pDNA nanoparticles, which was considered as optimum value for further analysis. The size and morphology of the complexed nanoparticles were again confirmed using TEM micrographs (Figure 12 A&B). The particles were appeared in the form of well known core-shell nanostructure having size of around 100 nm.

Table 6: Particle size (nm) and Zeta potential (mV) of ATFP and HTFP derivatives at various charge ratios (Standard deviation given in bracket)

N/P ratio	Particle size (nm) Of ATFP15H derivatives	Zeta potential (mV) Of ATFP15H derivatives	Particle size (nm) Of HTFP15H derivatives	Zeta potential(mV) Of HTFP15H derivatives
0.5	238(14.14)	-30.5(2.68)	284 (14.1)	-27.65 (6.1)
1	1660(21.2)	-0.98(0.6)	1764 (28.2)	-0.88 (0.14)
2	175(4.2)	12.6(1.6)	196 (9.8)	15.48 (1.8)
3	228(7.0)	14.2(2.4)	284 (8.9)	14.2 (1.1)
4	275(7.9)	15.2(1.3)	341(8.3)	12.58 (0.8)
5	315(4.8)	13.2(2.9)	339 (24.0)	12.8 (1.13)

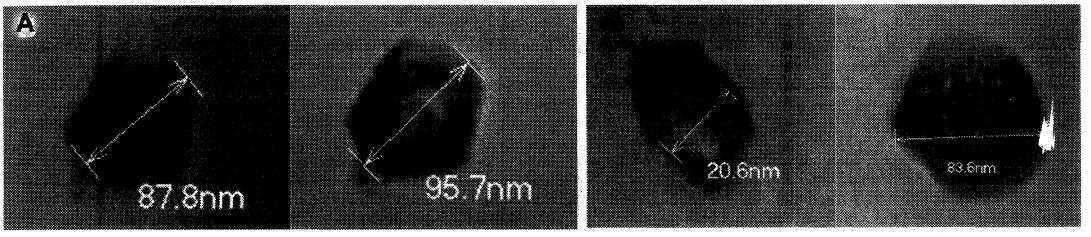

Figure 12: (A) and (B) TEM micrographs of ATFP15H/pDNA and HTFP15H/pDNA core-shell nanoparticles at their optimum charge ratios respectively.

The agarose gel electrophoresis have done at six different N/P ratios such as N/P=0.25, 0.5, 1, 1.5, 2 and 4. The result showed that for ATFP15H derivatives, due to the slight negative charge of the nanoparticles at N/P=1, there was a migration of DNA until that ratio. The plasmid DNA were effectively retarded at N/P ratio of 1.5 and onward (Figure 13 A). While in the case of HTFP15H derivatives plasmid DNA were effectively retard at N/P ratio of 2 onwards (Figure 13 B). ATFP15H and HTFP15H derivatives were examined for DNase 1 degradation and plasma protein interaction using gel electrophoretic shift assay. The DNase I degradation experiments were performed at N/P ratios of 0.5, 1, 2, 4 and 6 respectively. Figure 13C and D showed that 1 μg of naked pDNA was completely degraded without any smear with 2 unit of DNase I (Lane 2) (Thakor, Teng & Tabata 2009). While at the same concentration of DNase I the pDNA was protected from degradation by the ATFP15H and HTFP15H derivatives much effectively from N/P=2 an onwards. Below N/P ratio of 2, the protection was not found to be effective. In the absence of DNA releasing agents like heparin, the protected pDNA remained in the well and the eroded pDNA moved away from the well.

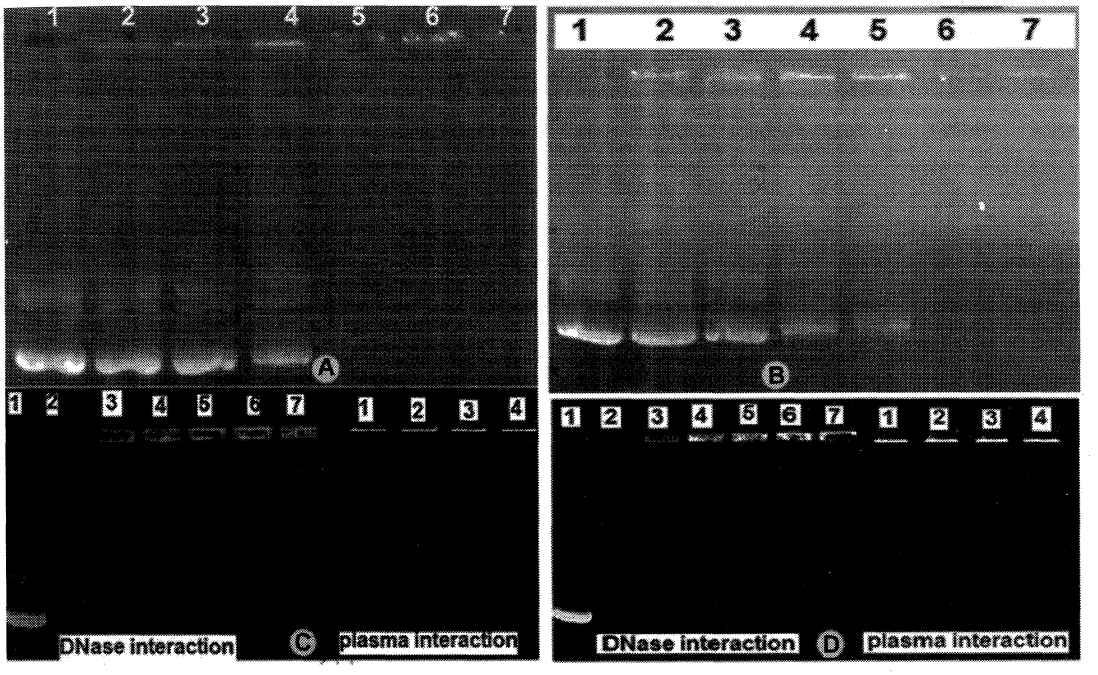

Figure 13: (A) & (B) Agarose gel electrophoresis representing pDNA binding studies with ATFP15H and HTFP15H derivatives respectively at different N/P ratios. Lane 1: pDNA alone, Lanes 2-7 are polymer/pDNA at N/P ratios of 0.25, 0.5, 1, 1.5, 2 and 4. (C) & (D) Protection of pDNA against DNase I after complexation with ATFP15H or HTFP15H derivatives respectively with DNA nanoparticles. Lane 1: pDNA alone; Lane 2 pDNA alone with 2 unit of DNase., Lane 3-7 ATFP15H/pDNA at N/P= 0.5, 1, 2, 4 and 6. & Interaction of plasma proteins with polymer/pDNA nanoparticles at N/P=2. Lane 1-4 plasma interaction at time intervals of 0.5, 1, 1.5 and 2 h respectively.

Figure 13 C and D also revealed the effect of protection of ATFP15H and HTFP15H derivatives from DNA release by the influence of negatively charged plasma protein. Interaction of plasma proteins on the polymer/pDNA complex was investigated in vitro by incubating the complexed nanoparticles at N/P=2 with the plasma protein. The extent of pDNA in the complex after interaction with plasma protein was observed using agarose gel electrophoresis. The incubation was performed for four periods of time such as 0.5, 1, 1.5 and 2 h respectively. From Figure 13 C and D, it is clear that even after 2 h, the ATFP 15H and ATFP 15H derivative protected the nanoparticles from disassembly of the complex.

4.1.4 Blood compatibility and cytotoxicity of ATFP15H and HTFP15H derivatives.

Figure 14 and 15 demonstrates the blood compatibility of ATFP15H and HTFP15H derivatives in terms of erythrocytes lysis and aggregation. 50 μg of the derivative alone and its complexed nanoparticles with DNA at its optimum charge ratio were used for incubation with

erythrocytes for 2 h. DI water and saline solution were used as a positive and negative control, respectively. From the Figure 14 and 15 it is observed that upon conjugation with PEG-FA, the hemolysis percentage of ATFP15H and HTFP15H derivative was significantly reduced compared to the parent compounds. Upon complexation with DNA also, the hemolysis level was within the acceptable level of 5% in the case of ATFP15H derivative. So the ATFP15H and HTFP15H derivative were again tested for erythrocyte aggregation and platelet activation. Microscopic images of the erythrocytes were shown in Figure 14&15. Nanoparticles were complexed at the optimum charge ratios of respective polymers. From the Figure 14 and 15 it was very clear to note that upon conjugation with PEG-FA, it behaved similar to that of the reference such as normal saline. That is, the ATFP15H and HTFP15H did not cause any RBC aggregation. To evaluate the platelet activation tendency of the polyplexes, the nanoparticles at N/P=2 were exposed to platelet rich plasma (PRP) and the percentage of activated platelets were assessed by flow cytometric determination of reduced platelet activation marker P-selectin (CD62). From the results it was found that there was only 0.03% and 0.025% change in the mean fluorescence intensity of CD62Ab in the ATFP15H and HTFP15H samples respectively before and after the incubation of materials compared to PEI which caused a change in fluorescence of 7.8%. Therefore it was clear that the ATFP15H and HTFP15H polymer did not activate platelets and the values were similar to that of saline control.

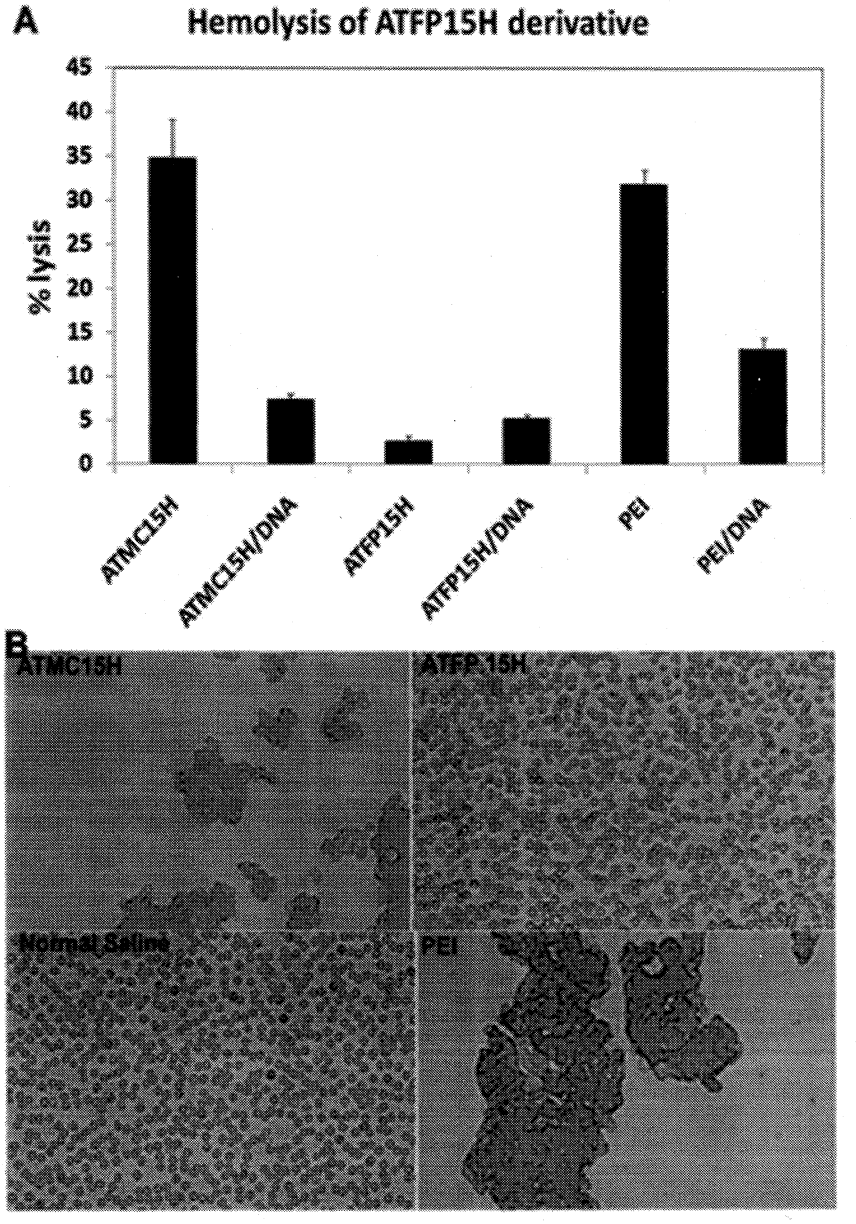

Figure 14: (A) Hemolysis of ATMC15H and ATFP15H derivatives alone and its complex with pDNA; $n = 3$ (B) RBC aggregation studies with nanoparticles of ATMC15H and ATFP15H derivatives with pDNA at its optimum charge ratios (40 times magnification for RBC).

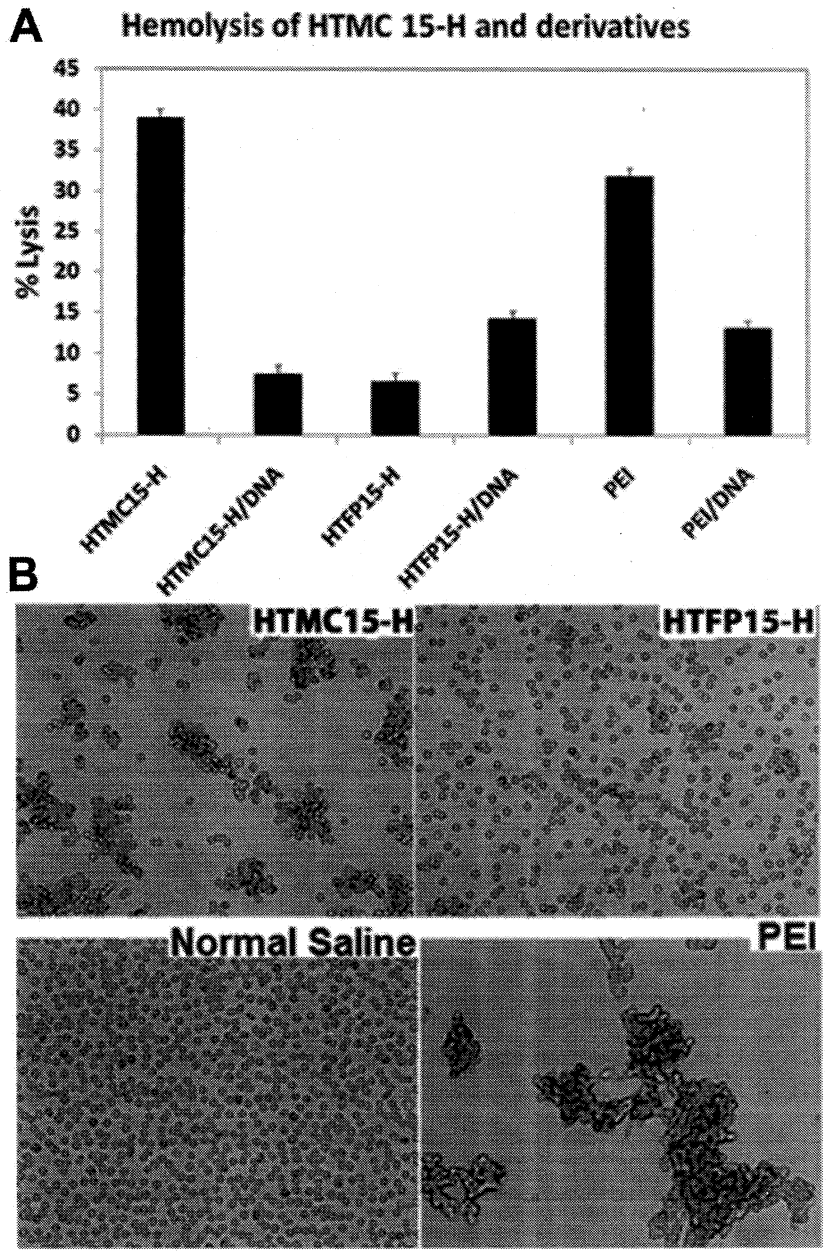

Figure 15: (A) Hemolysis of HTMC15H and HTFP15H derivatives alone and its complex with pDNA; $n = 3$ (B) RBC aggregation studies with nanoparticles of HTMC15H and HTFP15H derivatives with pDNA at its optimum charge ratios (40 times magnification for RBC).

The cytotoxicity of the ATFP15H/pDNA and HTFP15H/pDNA nanoparticles was tested in KB cell lines in which the transfection have been done. From the Figure 16A and 17A the cell viability of PEGylated nanoparticles were increased compared to the control. So we have studied the optimum concentration of ATFP15H and HTFP15H derivative which promote maximum cell growth by varying the concentration of the polymer such as 5, 10, 15, 30, 45 and 60

μg each. And it was found that at 10 μg of the ATFP15H and HTFP15H derivatives the KB cell lines showed maximum cell growth. This improvement in cell viability of the derivatives may again due to the presence of PEG which reduces the interaction of amine groups with external macromolecules or surfaces.

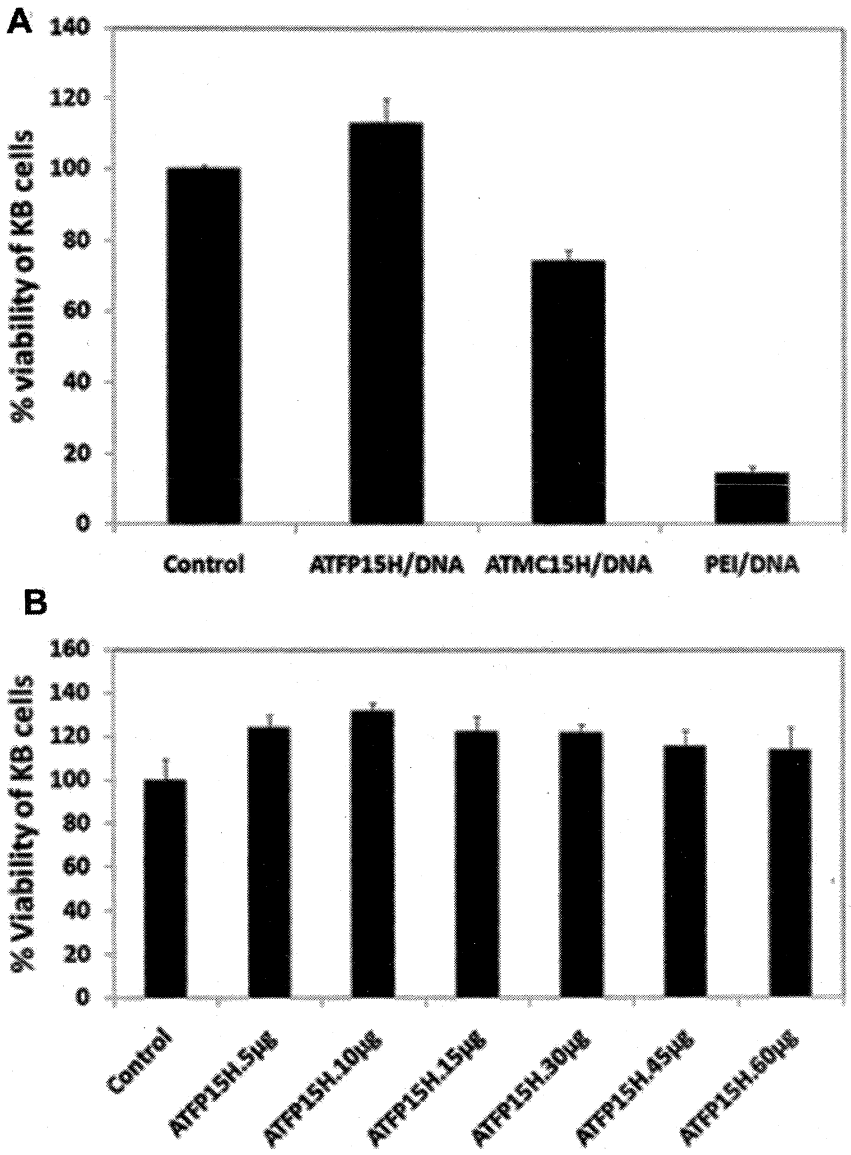

Figure 16: (A) Viability of KB cell lines at ATFP15H/pDNA and ATMC15H/ pDNA complexes: $n = 3$. (B) Viability of KB cell lines at varying concentration of ATFP15H derivatives: $n = 3$.

μg each. And it was found that at 10 μg of the ATFP15H and HTFP15H derivatives the KB cell lines showed maximum cell growth. This improvement in cell viability of the derivatives may again due to the presence of PEG which reduces the interaction of amine groups with external macromolecules or surfaces.

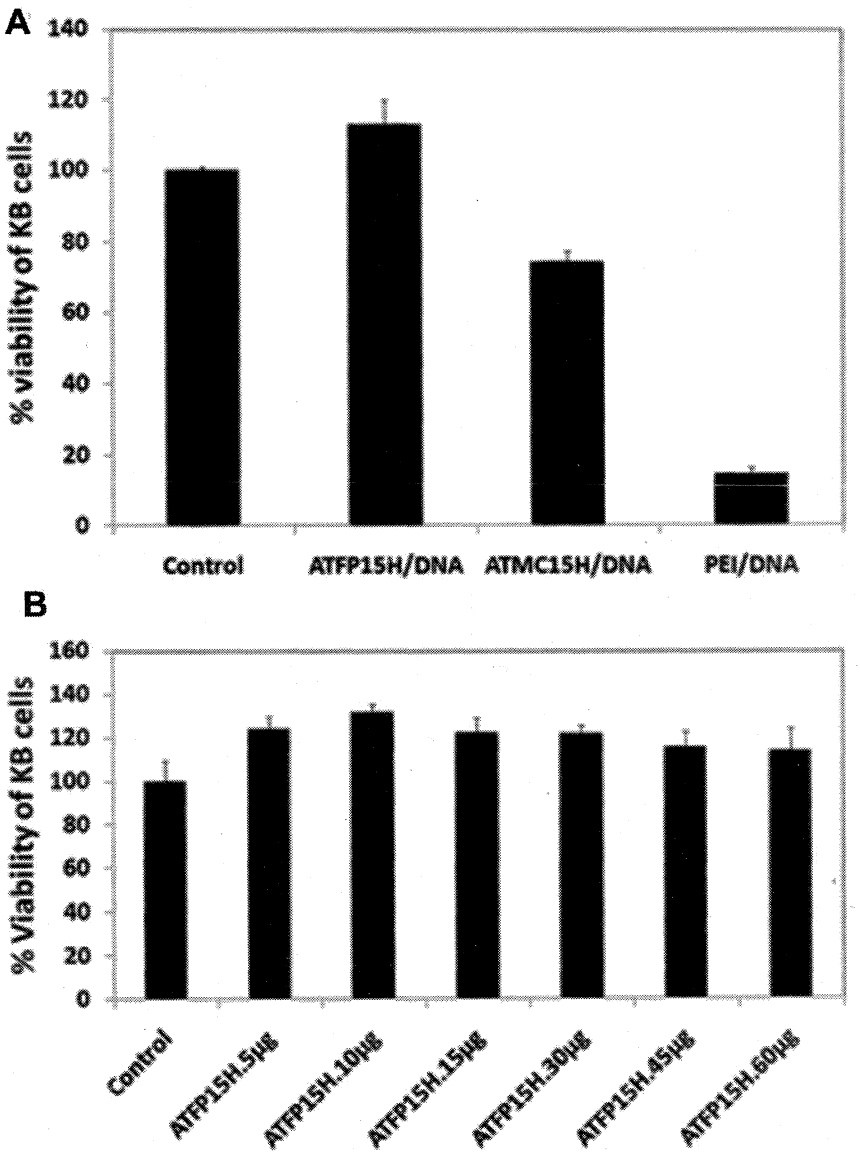

Figure 16: (A) Viability of KB cell lines at ATFP15H/pDNA and ATMC15H/ pDNA complexes: $n = 3$. (B) Viability of KB cell lines at varying concentration of ATFP15H derivatives: $n = 3$.

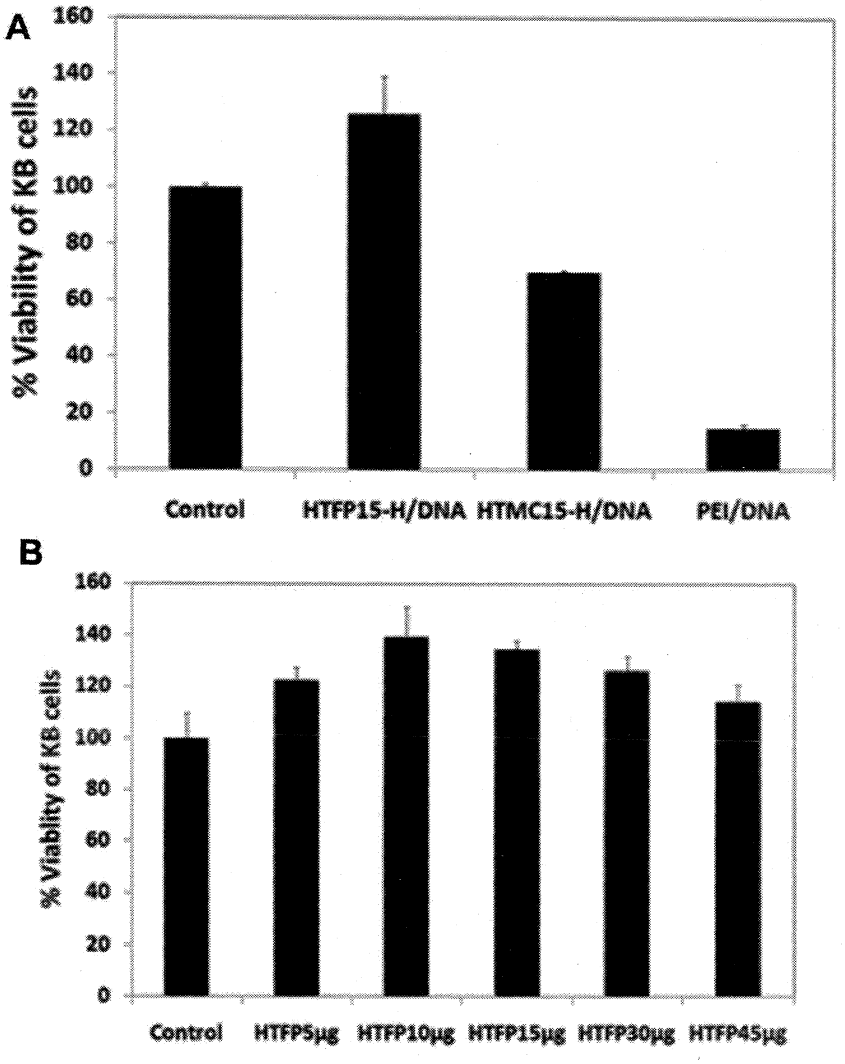

Figure 17: (A) Viability of KB cell lines at HTFP15H/pDNA and HTMC15H/ pDNA complexes: $n = 3$. (B) Viability of KB cell lines at varying concentration of HTFP15H derivatives: $n = 3$.

4.1.5 Transfection efficiency and the cellular uptake of the complexes.

To investigate *in vitro* gene transfer capability of ATFP15H and HTFP15H derivatives, transfection studies were performed on KB oral epidermoid cells by using pGL3-Luc as reporter genes in presence of 10% serum. Superfect and PEI (25 kDa) has been considered to be the highly effective gene transfecting agents, was used as the positive control. The parent polymers having no targeting group were used as negative control. From the Figure 18A&B it is interesting to note that ATFP15H and HTFP15H derivative showed one order of increased transfection than the negative controls such as ATMC15H and HTMC15H. The increase in transfection efficiency of the targeted derivative compared to the control group may due to the

presence of folic acid in the polymer which has good binding capacity to the cells having folate receptor. So we have checked the cell internalization ability of targeted derivatives compared to non-targeted derivatives by staining the polymer using rhodamine and observed the internalized nanoparticles after 2.5 h of transfection by confocal laser scanning microscopy. From the Figure 18C&D, the rapid cell internalization ability of targeted derivatives were clearly visible compared to ATMC15H and HTMC15H derivatives. Therefore the percentage of cell internalization was estimated using flow cytometry.

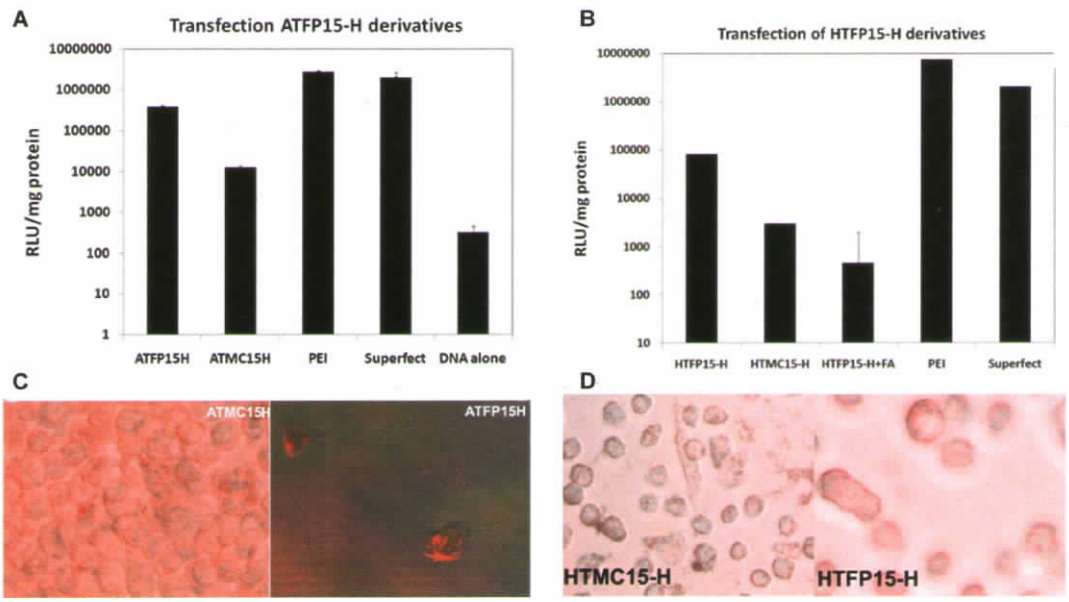

Figure 18: (A) *In vitro* transfection of ATFP15H derivatives into cultured KB oral epidermoid cells. (B) *In vitro* transfection of HTFP15H derivatives into cultured KB oral epidermoid cells (C) & (D) Cellular uptake of polymer/DNA complex. Merged images of light microscope (gray) and fluorescence microscope. Rhodamine-labeled polymer is complexed with DNA and transfected in KB cell lines. The quenching reagent trypan blue was added 2.5 h after transfection.

In order to establish the targeting ability of the ATFP15H and HTFP15H polymer, the uptake study was also performed with the derivatives in KB cell line with excess of free folic acid. From the Figure 19 & 20 it was demonstrated that 80-85% of the cells in ATFP15H derivative and 68% of the HTFP15H derivatives were fluorescently labeled. And it was interesting to note that even in the presence of 1 mM folic acid only 6% of reduction in cellular uptake was observed in the case of ATFP15H derivative and 12% reduction in HTFP15H derivative.

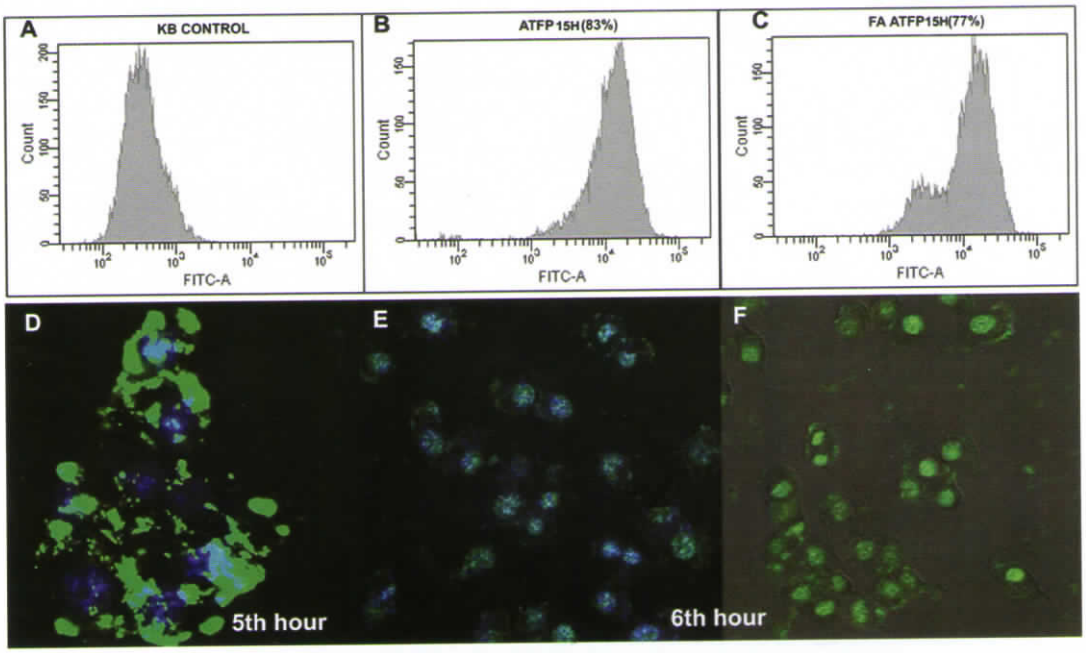

Figure 19: (A) KB control cell for Cellular uptake study of ATFP15H derivative quantified by flow cytometry in the absence (B) and presence (C) of free folic acid inhibitor. (D) Fluorescence microscopic image of YOYO labelled DNA/ATFP15H nanoparticles in KB cells after 5 h of transfection. (E&F) Confocal fluorescent microscopic images after 6 h of transfection in two fields (E) The merged image of blue staining of nucleus and green staining of YOYO labelled DNA, (F) The merged image of green staining of YOYO labelled DNA in bright field.

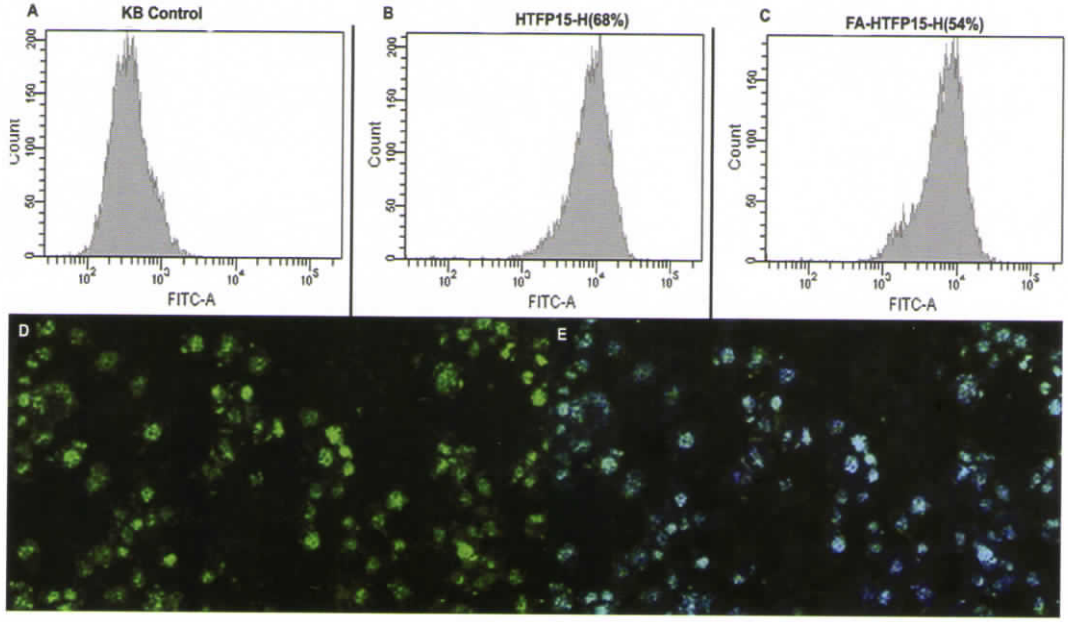

Figure 20: (A) KB control cell for Cellular uptake study of HTFP15H derivative quantified by flow cytometry in the absence (B) and presence (C) of folic acid inhibitor . (D) Confocal Fluorescence microscopic image of YOYO labelled DNA/HTFP15H nanoparticles in KB cells after 6 h of transfection. (Green filter) (E) Merged Confocal fluorescent microscopic images of Hoechst 33342 stained nucleus (blue filter) and of YOYO labelled DNA (green filter) at the same field.

Since the material was found good for cellular uptake, it was further studied by confocal microscopy for sub cellular localization of polyplexes. Plasmid DNA was labelled using YOYO and incubated with the cells for 5 and 6 h. As found with flow cytometry, the complexes of targeted derivatives were internalised in the cells and uniformly distributed to a high extent. However at 5^{th} hour, the complexes were found only near the nucleus (Figure 19 and 20). While at the 6^{th} hour majority of the YOYO labelled DNA were found inside the nucleus. This may be mainly due to the nuclear localisation ability of arginine and histidine residue along with the presence of folic acid.

4.2 Synthesis and Characterisation of Synthetic Polymer based Nanoparticles.

4.2.1 Synthesis and preliminary characterisation of P(SiDAAr)n and P(SiDAHs)n.

The oligoaminosiloxanes were synthesized using 3-(2- aminoethylamino) propyl- methyl-dimethoxysilane as the starting compound and 1 N aqueous NaOH as the hydrolysing agent

according to the method mentioned earlier (Kichler et al. 2003). After reaction for 20 h at room temperature, the mixtures were neutralized and lyophilised. The oligomers were designated as SiDA (Figure 21) and characterised using IR, NMR and mass spectroscopy.

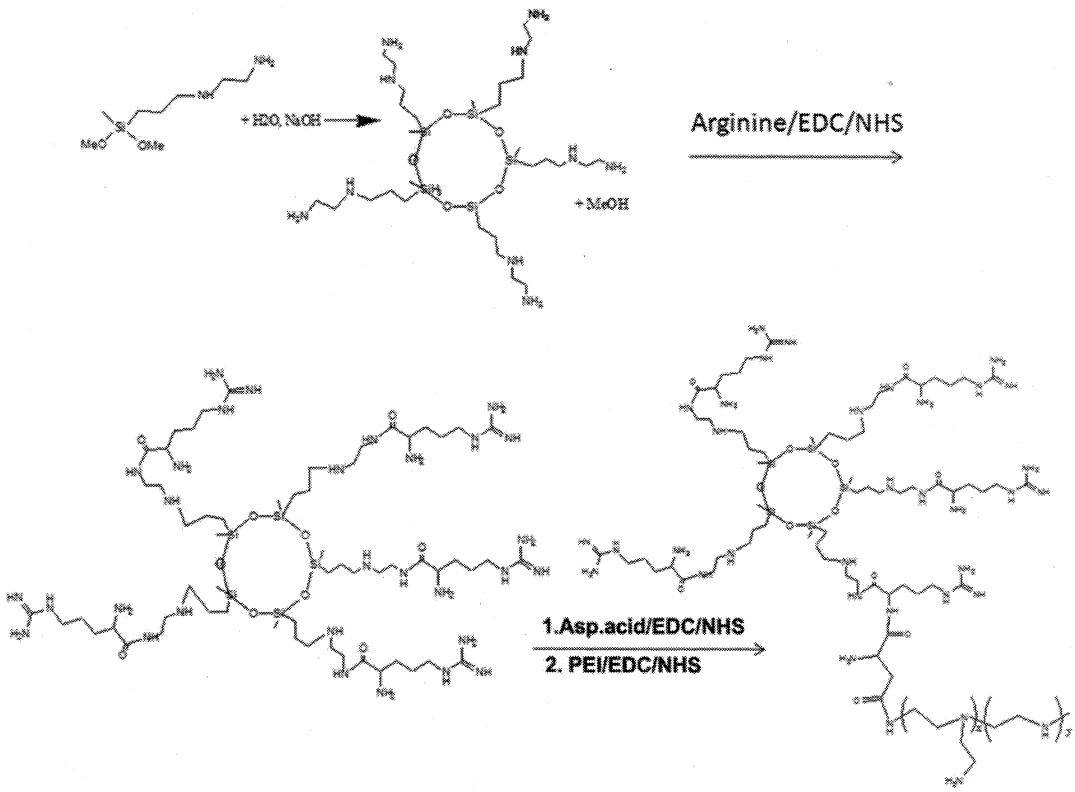

Figure 21: The reaction scheme of P(SiDAAr)1 derivative.

The m/z peak at 802 indicated a cyclic siloxane having 5 Si atoms. Thus for further reactions, 5 equivalents of arginine or histidine residue were used to conjugate with 1 equivalent of SiDA. Arginine and histidine conjugation was carried out using EDC/NHS chemistry. Synthesis of SiDAAr and SiDAHs was confirmed using IR and ^{1}HNMR spectroscopy. Finally, 1 eq of PEI was conjugated to 'n' equivalents of SiDAAr or SiDAHs molecule to obtain the four final products such as P(SiDAAr)1, P(SiDAAr)5, P(SiDAAr)10 and P(SiDAAr)15, in the case of arginine conjugation and P(SiDAHs)1, P(SiDAHs)5, P(SiDAHs)10, and P(SiDAHs)15, in case of histidine conjugation (Figure 22). The numbers, 1,5,10 and 15 indicates the various ratios of SiDAAr or SiDAHs residue keeping the composition of PEI as constant.

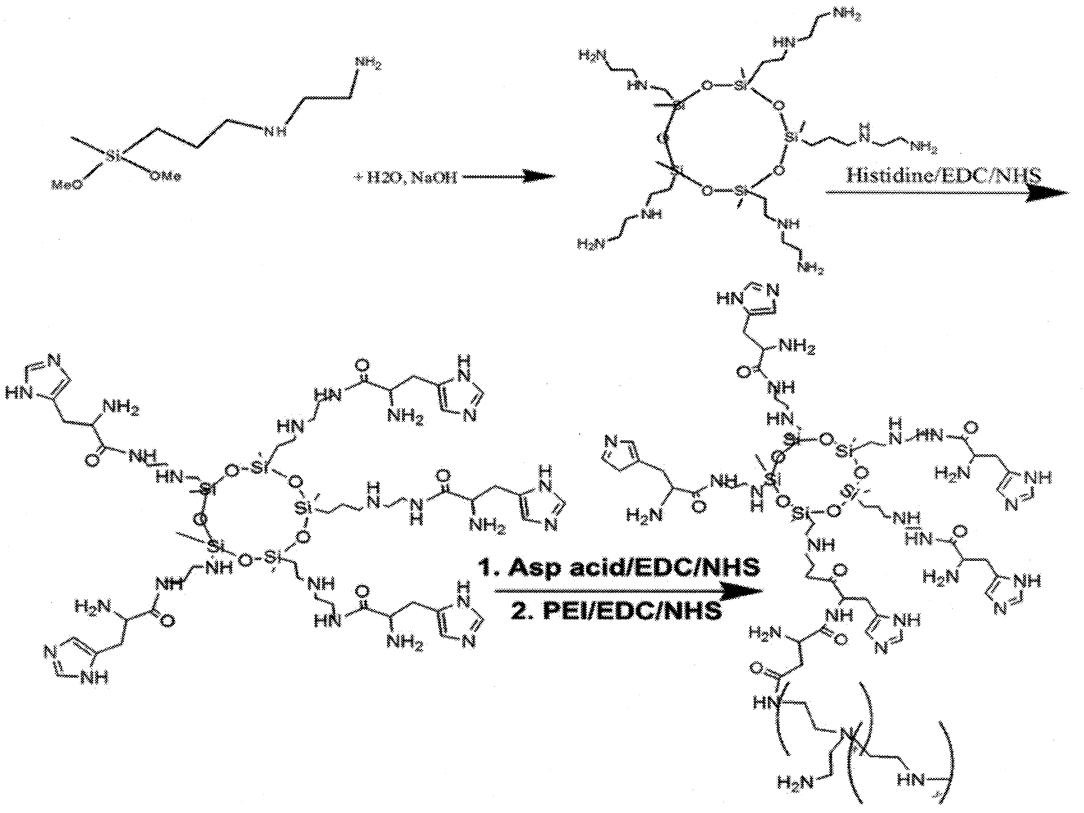

Figure 22: The reaction scheme of P(SiDAHs)1 derivative.

On further increasing the SiDAAr or SiDAHs to PEI ratio, the product became an insoluble gel like material. The molecular weight and polydispersity index of the synthesized product and its parent compound PEI were determined by GPC. Molecular weight of P(SiDAAr)5 were determined as the representative polymer. From the above result (Figure 23), it was observed that change in peak molecular weight of parent and daughter polymers were 6284 Da which was approximately equivalent to 5 SiDAAr molecules.

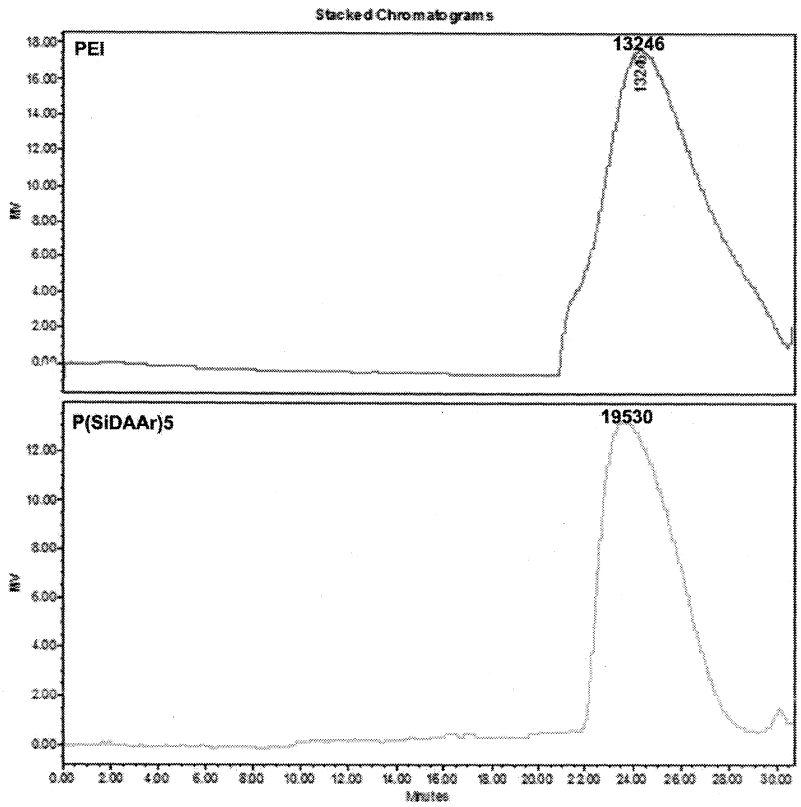

Figure 23: GPC chromatogram of PEI and P(SiDAAr)5

The formation of P(SiDAAr)n and P(SiDAHs)n polymers were confirmed using IR, NMR, DSC and also by determining primary amino group contents using colorimetric assay with 2,4,6-trinitrobenzenesulphonic acid (TNBS). The formation of $-NH-CO-$ bonds due to the conjugation of PEI and SiDAAr/Hs via the linker group aspartic acid was confirmed by the presence of IR absorption band in the range 1630-1645 cm^{-1}. The peak was more prominent as the ratio of SiDAAr/Hs to PEI increased (Figure 24 and Figure 25). In the case of P(SiDAAr)n this peak was overlapped by stretching vibration of $C=N$ at guanidine group. The bending vibration of $C-N$ of amide bond which appeared between 1364 and 1298 cm^{-1} revealed the reaction between carboxyl groups and amino groups. At lower ratios these peaks were not dominant. However in the case of P(SiDAHs)n polymers peaks in the spectral region 1700-1500 cm^{-1} indicated the amide groups, asymmetric NH_3^+ bending modes as well as the imidazole ring. The bending vibration of C-N of amide bond which appeared between 1369 and 1298 cm^{-1} revealed the reaction between carboxyl groups and amino groups. The peaks

at 1560 cm^{-1} 1065 and 970 cm^{-1} was also due to the presence of imidazole group. The formation of the product was also confirmed by the change in thermal behaviours of the parent compound and its derivatives (Table 7 and 8). The parent polymer PEI showed a melting temperature in the range of 93.74 ^{o}C. On the other hand, the melting temperature and glass transition temperature of its siloxane derivative increased as the ratio of siloxane residue to PEI increased.

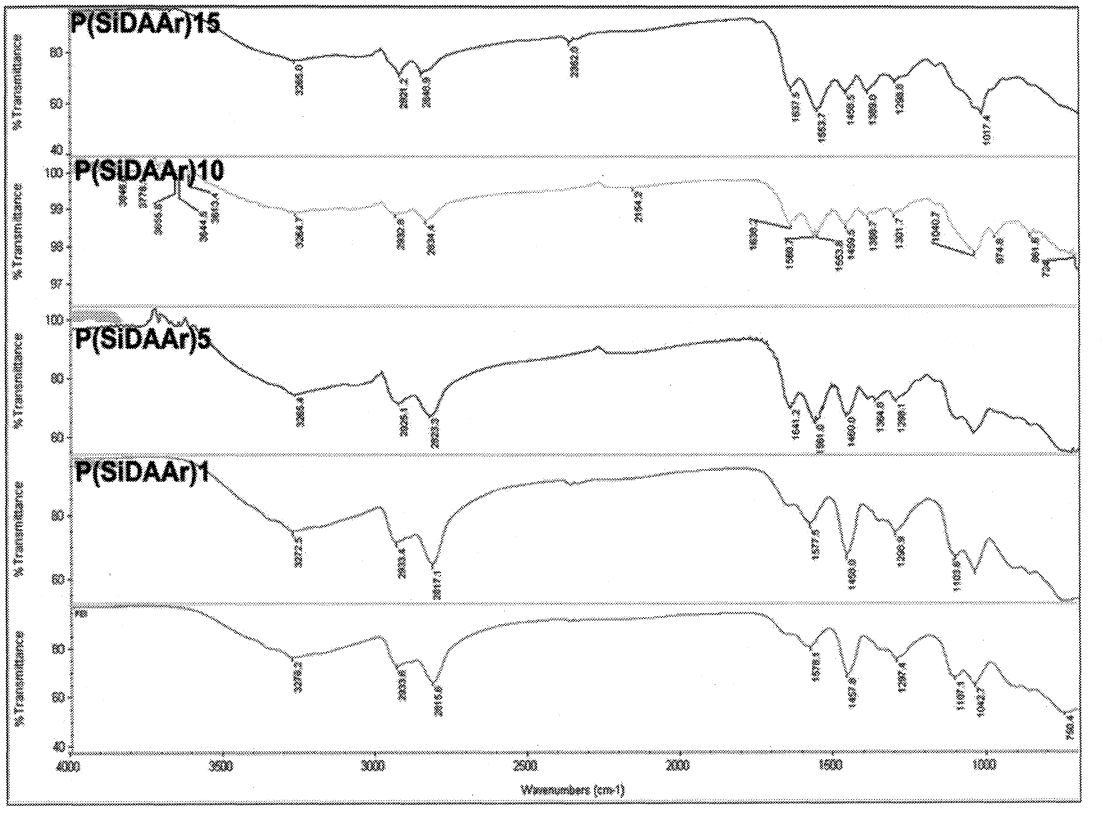

Figure 24: IR spectra of P(SiDAAr)n polymers.

Table 7: DSC data of P(SiDAAr)n polymers.

Polymer	Tg	Tm
PEI		93.74
P(SiDAAr)1	109.94	133.47
P(SiDAAr)5	141.92	170.7
P(SiDAAr)10	145.39	171.76
P(SiDAAr)15	146.99	173.36

Table 8: DSC data of P(SiDAHs)n polymers.

Polymer	Tg	Tm
PEI		93.74
P(SiDAHs)1	102.93	122
P(SiDAHs)5	113	130
P(SiDAHs)10	132.36	167.23
P(SiDAHs)15	141.68	170.54

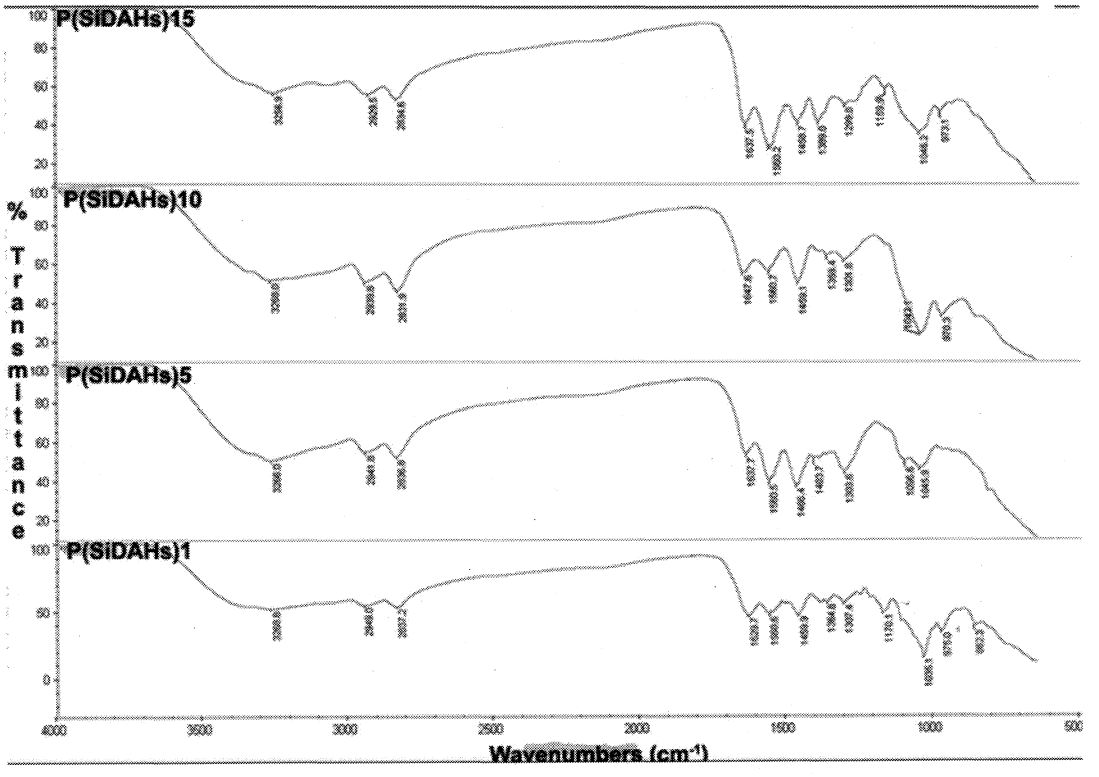

Figure 25: IR spectra of P(SiDAHs)n polymers.

The conjugation of PEI to arginine and histidine conjugated siloxane was confirmed by ^{1}HNMR spectroscopy. P(SiDAAr)1 and P(SiDAAr)5 in arginine groups and P(SiDAHs)1 and

P(SiDAHs)10 were analysed as representative polymers. The signals by PEI, siloxane methylene groups and arginine protons were observed as in Figure 26. Due to the presence of protons of high molecular weighed PEI polymer, the proton signal due to arginine molecules were not clearly visible for the product P(SiDAAr)1 but was more visible in the P(SiDAAr)5 spectra. The peaks observed in Figure 26 were, 1H NMR (D_2O): δ(ppm): 0.1-(bs, $SiCH_3$), 1.66-arginine (-$HCCH_2C\mathbf{H_2}CH_2NH$-); 1.86-arginine(-$HCC\mathbf{H_2}CH_2CH_2NH$-); 3.24-arginine (-$HCCH_2CH_2C\mathbf{H_2}NH$-); 3.86-arginine (-$\mathbf{H}CCH_2$ CH_2CH_2NH-); 3.32.5 ($NHCH_2CH_2$, PEI ethylene). In Figure 27 the peak at 7.9 ppm in P(SiDAHs)10 showed the hetero- aryl NH_2 groups of histidine residue.

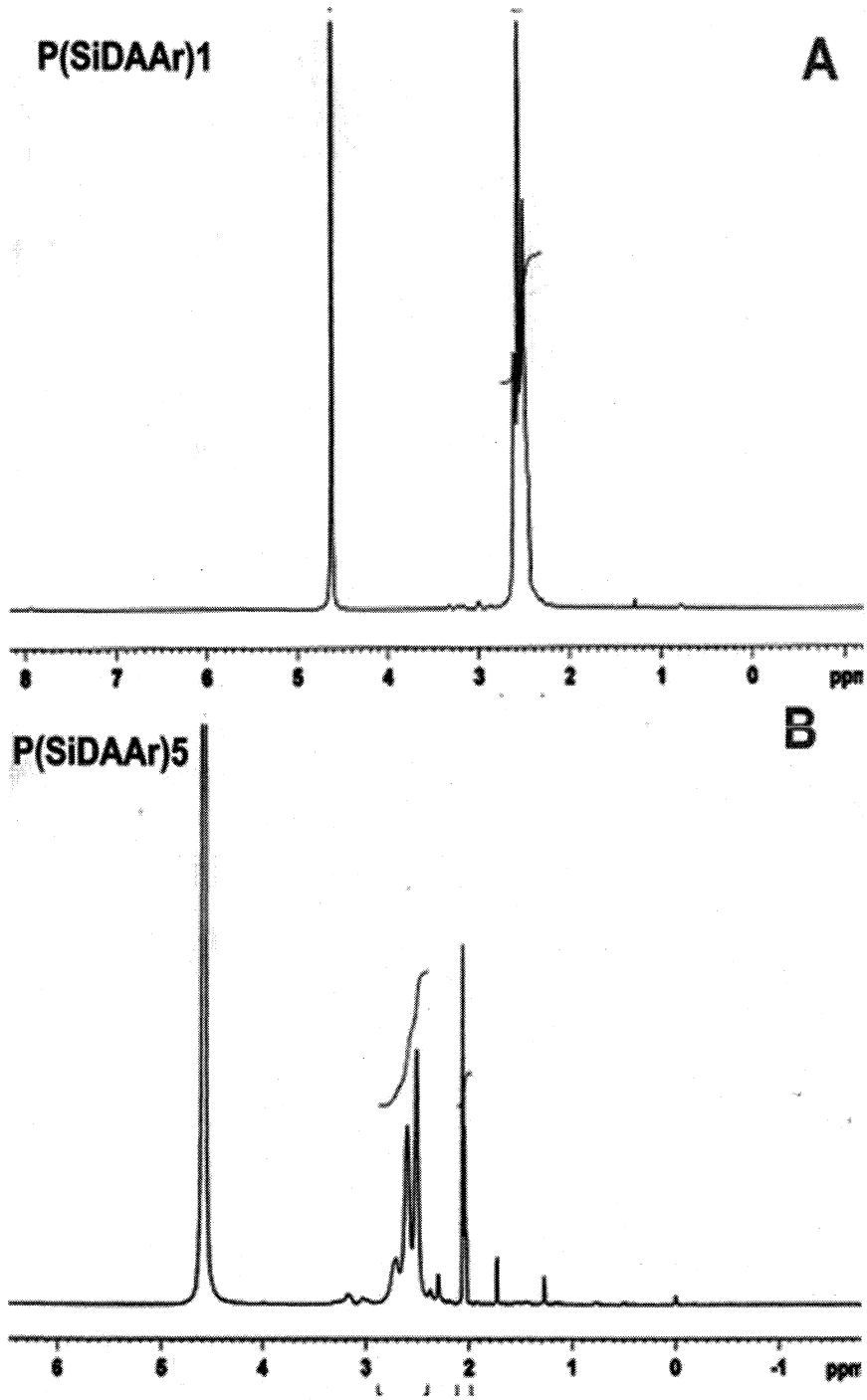

Figure 26: ^{1}HNMR spectra of (A) P(SiDAAr)1 (B) P(SiDAAr)5 derivatives.

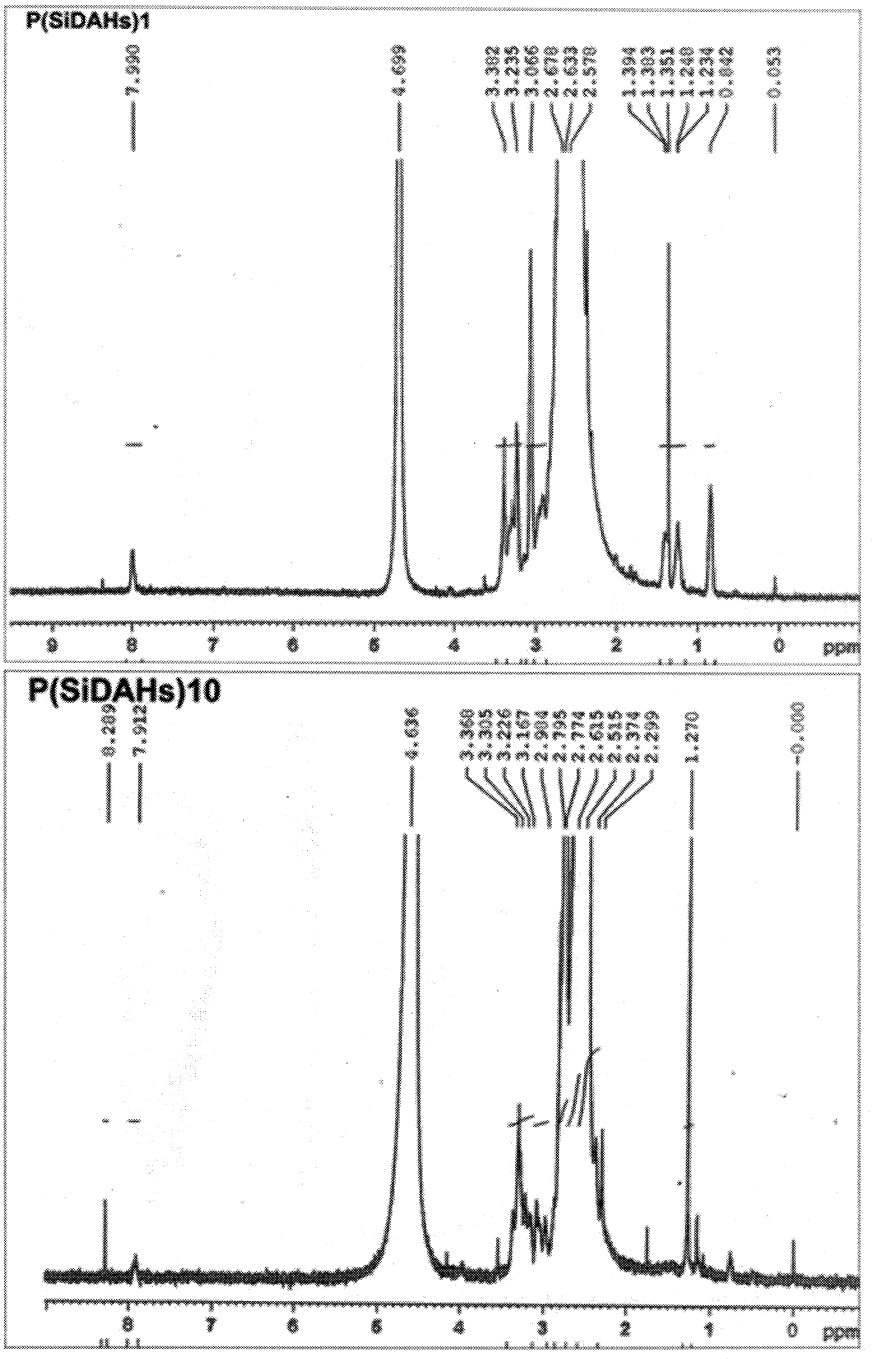

Figure 27: ^{1}HNMR spectra of (A) P(SiDAHs)1 (B) P(SiDAHs)10 derivatives.

The acid base titration profile obtained for PEI and its siloxane conjugates were shown in Figure 28. The P(SiDAAr)1 showed highest buffering capacity when compared to PEI. On increasing the ratio of SiDAAr to PEI, a moderate decrease in buffering capacity was observed. P(SiDAAr)5 polymer exhibited a similar endosomal disruption capability as that of PEI. Be-

cause of the high pKa value of imidazole group of histidine residue P(SiDAHs)n derivatives showed high buffering capacity, even higher than PEI. Even though at high composition, histidine residues does not improved the buffering capacity.

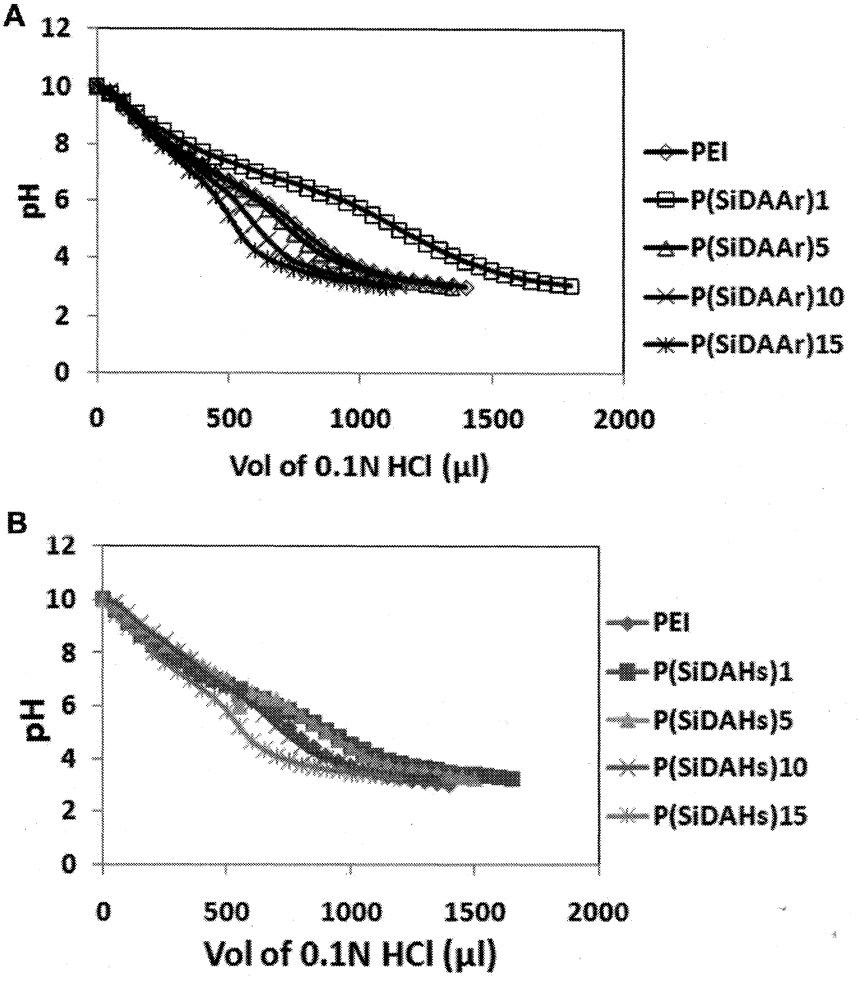

Figure 28: Acid/base titration of (A) P(SiDAAr)n and (B) P(SiDAHs)n derivatives. PEI is considered as positive control.

Quantification of the free amino groups of PEI and its arginine or histidine conjugated siloxane derivative were determined using TNBS assay, and also by fluorescamine assay as depicted in Figure 29. From both experimental data, it was clearly observed that, P(SiDAAr)1 had the highest number of primary amino groups. On increasing the composition of arginine conjugated siloxane oligomers, the amount of primary amino group decreased due to the presence of guanidine group of arginine residue. The lowest number of primary amino group was observed for PSiDAAr)15 polymer and highest for P(SiDAAr)1. Similarly in the case of histidine

derivatives also on increasing the conjugation of SiDAHs group to PEI, the free amino group density again reduced. This is due to the conjugation of SiDAHs group to the free amino groups of PEI. In both the cases TNBS assay and fluorescamine assay showed a similar pattern.

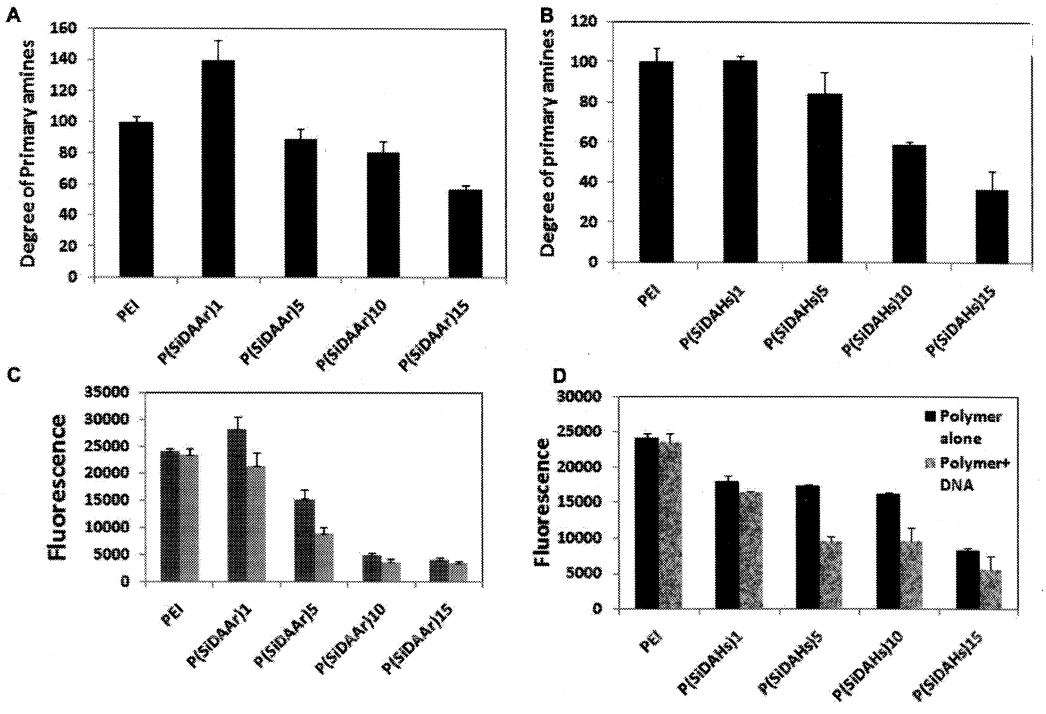

Figure 29: (A) & (B) Degree of primary amine content of P(SiDAAr)n & P(SiDAHs)n derivatives respectively using TNBS assay. (C) & (D) Free amino groups on P(SiDAAr)n and P(SiDAHs)n derivatives respectively before and after interaction with DNA determined using fluorescamine assay. Data were expressed as mean $\pm$ standard deviation. $(n = 3)$

4.2.2 Formation of polymer/pDNA complex nanoparticles and its characterization.

Nanoparticles of plasmid DNA were prepared by complexing pDNA with varying weight ratios of polymer. Fluorescamine assay can also be used to monitor the interaction between DNA and the polymer since it doesnt interact with amino groups after being bound to DNA (Corsi et al. 2003). From Figure 29, adequate amount of primary amines were detected after complexation with DNA which provided the excess positive charge for the nanoparticles. The result was found to be in good agreement with that obtained from dynamic light scattering (DLS) experiment as listed in Table 9, 10, 11 and 12.

Table 9: Particle size (nm) of P(SiDAAr)n polymers at different weight ratios. Standard deviation is given in bracket.

w/w ratio	P(SiDAAr)1	P(SiDAAr)5	P(SiDAAr)10	P(SiDAAr)15
0.5	178(13.08)	1156.5(67.17)	756.5(130.8)	1354(67.88)
1	545(7.07)	382(18.38)	294.5(36.06)	251(57.98)
2	228.5(61.51)	185(18.38)	467(70.71)	216.5(53.03)
3	273(21.21)	420(42.42)	452(39.59)	175.5(33.23)
4	152(32.52)	199(45.25)	178.5(33.23)	194(21.21)
5	271(14.14)	235(1.41)	195(87.68)	140(1.41)

Table 10: Zeta Potential (mV) of P(SiDAAr)n polymers at different weight ratios. Standard deviation is given in bracket

w/w ratio	P(SiDAAr)1	P(SiDAAr)5	P(SiDAAr)10	P(SiDAAr)15
0.5	13.5(1.55)	0.47(0.38)	9.24(0.97)	0.465(0.11)
1	10.77(4.42)	14.85(2.47)	10.04(2.34)	13.5(1.27)
2	21.25(0.21)	11.35(0.49)	4.99(0.15)	11.25(1.20)
3	22.15(0.63)	10.1(0.707)	8.36(0.12)	13.5(1.13)
4	15(3.53)	9.735(3.20)	8.45(1.41)	8.995(0.23)
5	23.2(0.98)	8.28(0.86)	11(1.41)	10.25(1.62)

DLS measurements revealed that at weight ratios of the polymer/DNA around 3 and above, it formed positively charged uniform sized nanoparticles. As observed from the fluorescamine assay, the P(SiDAAr)1 and P(SiDAHs)1 polymer showed high positive charge compared to higher ratios. The weight ratio at which the particles showed lowest particle size and highest zeta potential was considered as the optimum for further analysis. Due to the difference in composition of polymers, each derivative showed different weight ratios as optimum. For arginine modified derivatives the optimum weight ratios used for further studies were, w/w=2.5,2.5,4 and 5 for P(SiDAAr)1, P(SiDAAr)5, P(SiDAAr)10, and P(SiDAAr)15 respectively. While for histidine modified derivatives the optimum weight ratios used for further studies were, w/w= 3.04, 5, 5 and 5.2, for P(SiDAHs)1, P(SiDAHs)5, P(SiDAHs)10, and P(SiDAHs)15. It is important to evaluate the size and morphology of the complex nanoparticles for gene delivery. In the present study, the size and morphology of the polymer/DNA nanoparticles were determined using atomic force microscopy (AFM). Figure 30 demonstrated a homogeneous distribution of the spherical nanoparticles with a mean size lesser than 100 nm. The result was further confirmed by transmission electron microscopy (TEM) as shown in Figure 30.

4.2.3 Physical integrity of the polymer/pDNA complex and its protection against nuclease degradation.

The ability of P(SiDAAr)n polymers to complex with DNA was evauated by gel retardation assay as shown in Figure 31. The experiment was carried out using six different weight ratios such as 0.25, 0.5, 1, 3, 5 and 10. The results demonstrated that in the case of arginine modified polymers all polymers could retard the migration of plasmid DNA (pGL3 Luciferase reporter vector) by forming polyplexes at a weight ratio of 0.5 onwards except for P(SiDAAr)5, which could retard DNA migration even at a ratio of 0.25 onwards. However in the case of histidine the polymers P(SiDAHs)1and P(SiDAHs)5 retard DNA at weight ratio of 0.25 onwards, while the polymers P(SiDAHs)10 and P(SiDAHs)15 retards the DNA at w/w ratio of 0.5 onwards. Non-migration of DNA in the gel indicates condensation of DNA by the polymers.

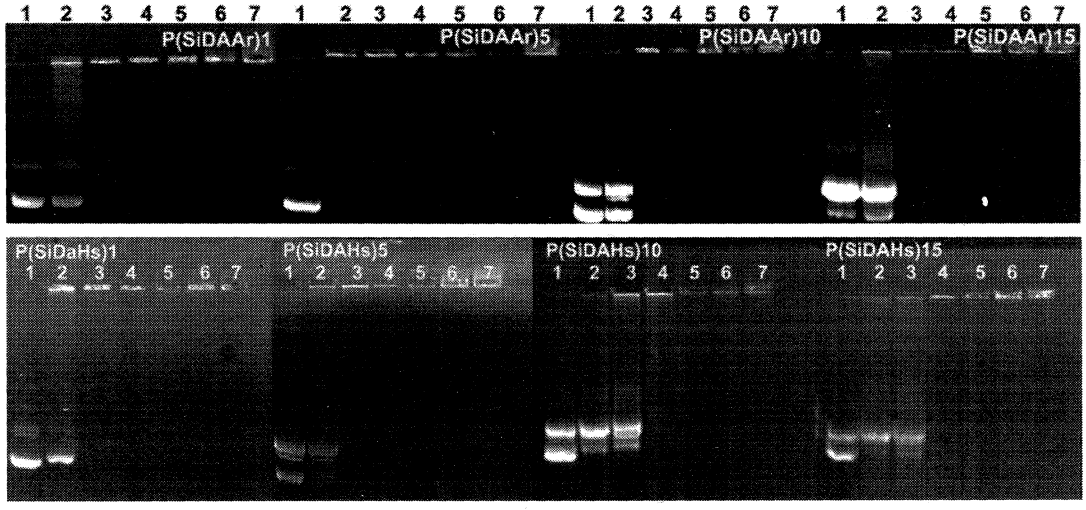

Figure 31: (A) Agarose gel electrophoresis representing pDNA (pGL3 Luciferase reporter vector) binding studies with four P(SiDAAr)n and P(SiDAHs)n derivatives at different w/w ratios. Lane1: pDNA alone, Lanes 2-7 are polymer/pDNA at w/w ratios of 0.25, 0.5, 1, 3, 5 and 10.

4.2.4 Evaluation of cytotoxicity.

The cytotoxicity of P(SiDAAr)n and P(SiDAHs)n polymers and its nanoparticles with plasmid DNA were examined on KB cell lines by MTT assay. PEI was used as control. Cytotoxicity of each polymer derivative was examined at four different concentrations such as 25 μg/ml, 50 μg/ml 75 μg/ml and 100 μg/ml. Figure 32A&B demonstrated that on increase in composition of SiDAAr residiues, the polymer exhibits low cytotoxicity at lower concentration. The high

charge density of P(SiDAAr)1 polymer as observed by the fluorescamine analysis and DLS measurements appeared to be responsible for the increase in toxicity as compared with PEI. However, on further increase in polymer concentration, all the derivatives become more toxic relatively. Due to the presence of high charge, very low polymer concentration was needed for the complexation of DNA. Therefore, on evaluation of cytotoxicity of the polymer/ DNA nanoparticles minimal toxicity was observed as shown in Figure 32B. The nanoparticles at its optimum weight ratios having 2.5 μg of DNA were used for the analysis. These results demonstrated that P(SiDAAr)5/DNA nanoparticles exhibits 98% cell viability in KB cell lines. On further increase in composition of SiDAAr, cell viability decreased as expected to 94% and 79% for P(SiDAAr)10 and P(SiDAAr)15 respectively. Similarly from Figure 32 C&D it is observed that for all the derivatives, high viability of cells at lower concentrations was detected. Viability decreased as the concentration increased. At the same time increased cell viability was observed for the polymers at high composition of SiDAHs to PEI. Therefore cell viability exhibited in the order of P(SiDAHs)15 > P(SiDAHs)10> P(SiDAHs)5> P(SiDAHs)1.

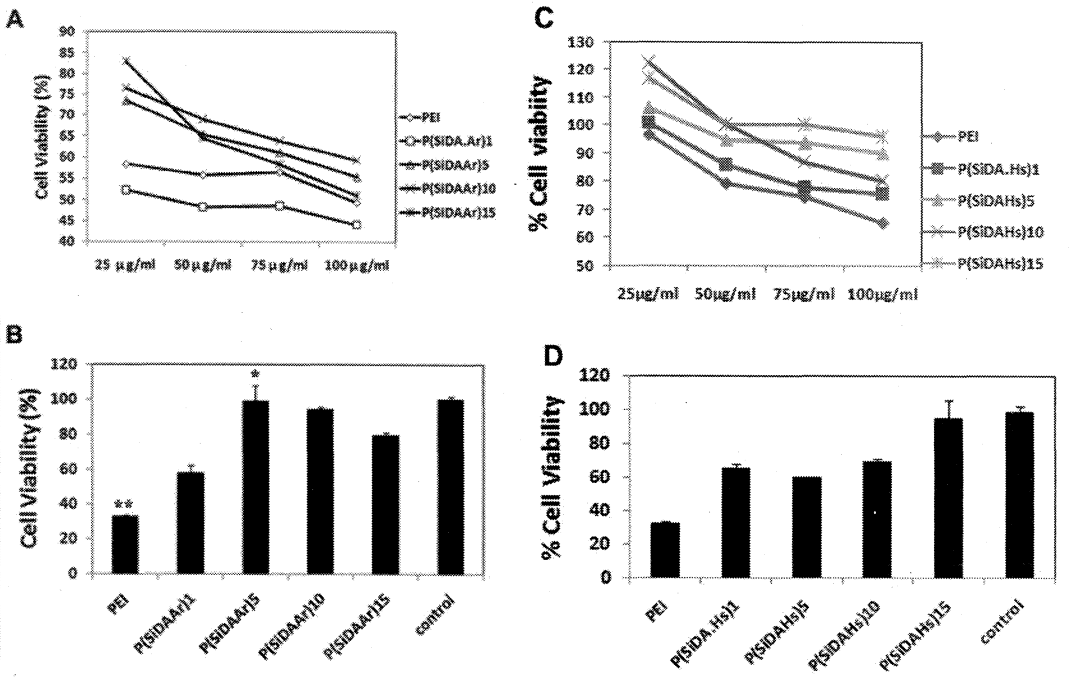

Figure 32: (A) & (C) Viability of KB cell lines at varying concentration of P(SiDAAr)n and P(SiDAHs)n derivatives respectively. PEI was used as control. (B) & (D) Viability of KB cell lines of P(SiDAAr)n / pDNA and P(SiDAHs)n/pDNA nanoparticles at its optimum weight ratios. Data were expressed as mean $\pm$ standard deviation. ($n = 3$, $^{*}P$, No statistical difference compared to control, $^{**}P < 0.05$, compared to control)

4.2.5 Estimation of transfection efficiency.

Transfection experiments were done in presence of 10% serum. Figure 33A showed the amount of luciferase protein expressed in terms of relative luminescence units (RLU). According to proton sponge mechanism, the polymer having highest buffering capacity shows highest transfection efficiency due to its highest endosomal disrupting capacity. From Figure 28A, we observed that P(SiDAAr)1 has the highest buffering capacity. However, based on its highest cytotoxicity, P(SiDAAr)1 showed almost similar protein expression to that of control PEI. The lowest cytotoxic P(SiDAAr)5 showed highest transfection efficiency compared to all other P(SiDAAr)n derivatives and controls. It also exhibited around 150% more protein expression than PEI at its optimum ratio with plasmid DNA. However, on increase in the composition of SiDAAr to PEI, the derivatives exceed the cut-off composition and hence decrease in transfection efficiency was observed. The third derivative, P(SiDAAr)10, however, showed around 65% more transfection than branched PEI at its optimum ratio with DNA. The transfection

efficiency of the polymer, P(SiDAAr)5, was again evaluated in HeLa cell line using pEGFP reporter gene and branched PEI as control. Figure 33B confirmed gene transfection efficiency of the P(SiDAAr)5 polymer even in the presence of 10% serum.

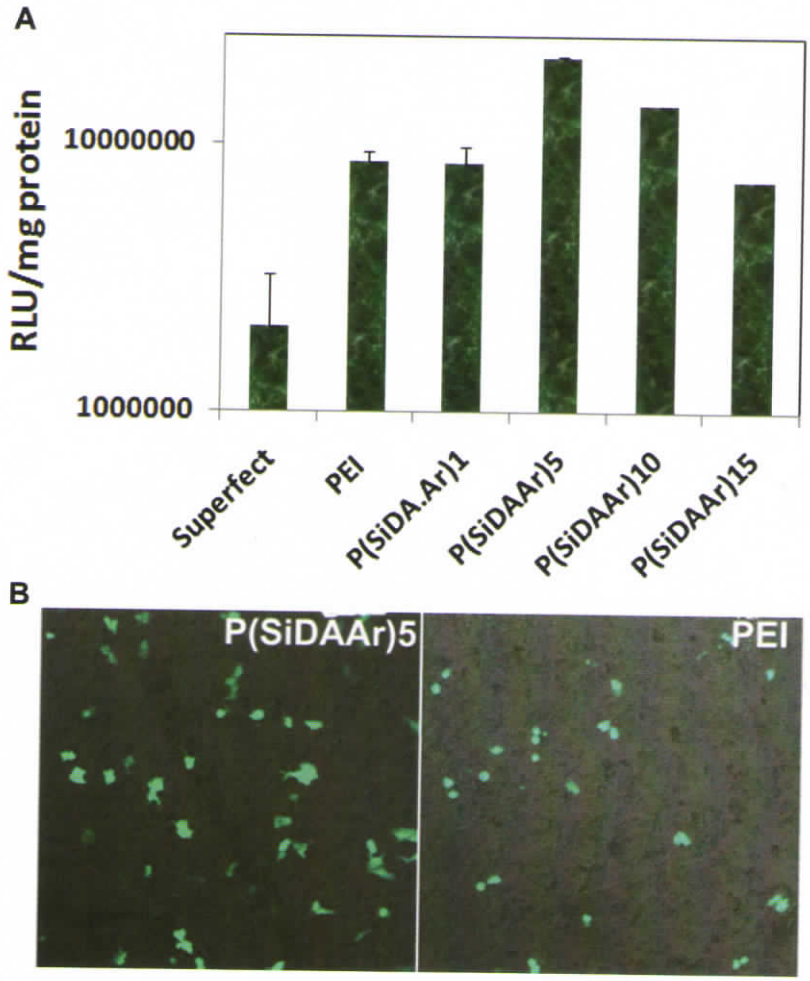

Figure 33: (A) *In vitro* transfection efficiency of P(SiDAAr)n derivatives in KB cell lines. Cells were incubated with polymer/pGL3 complexes (2.5 μg/ ml as pDNA) for 3.5 h in the presence of 10% FBS and then incubated with regular media for 48 h before measurement of luciferase activity. Luminescence activity was measured according to Experimental Procedures. Data were expressed as mean $\pm$ standard deviation. ($n = 3$, $^*P$ significantly different compared to PEI) (B) GFP expressed in HeLa cell line transfected with P(SiDAAr)5/pDNA and PEI/pDNA complexes at their optimum ratios.

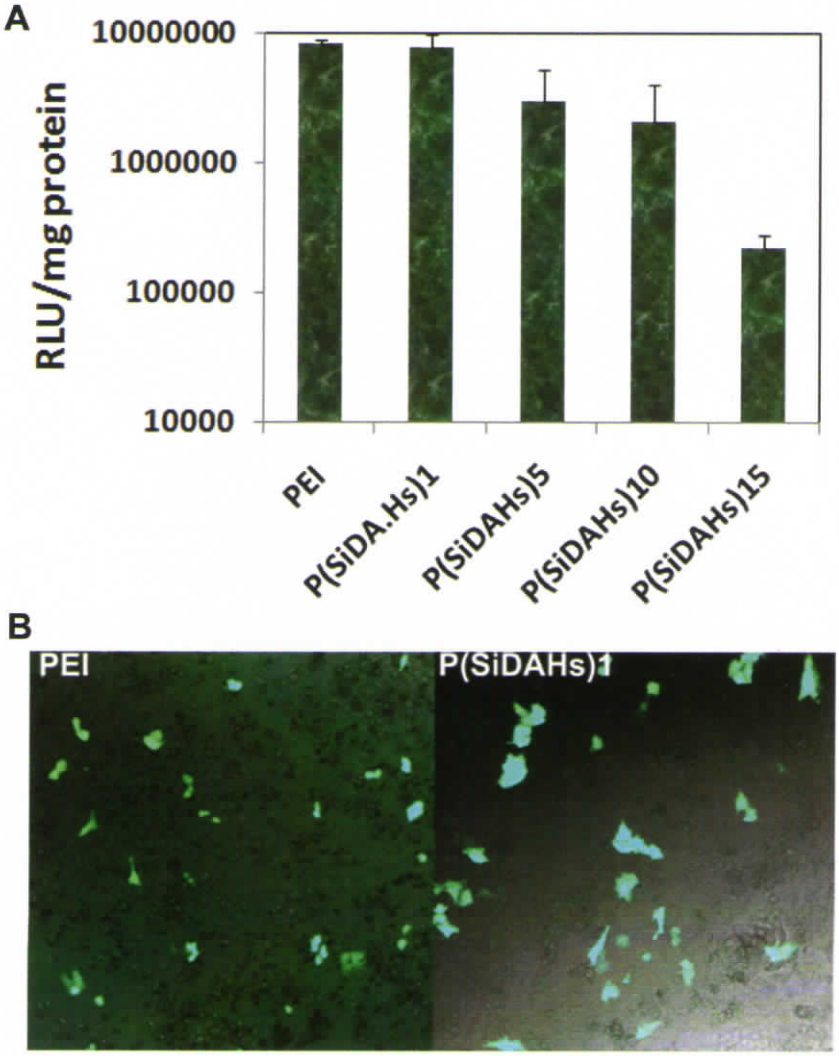

Figure 34: (A) *In vitro* transfection efficiency of P(SiDAHs)n derivatives in KB cell lines. Cells were incubated with polymer/pGL3 complexes (2.5 μg/ ml as pDNA) for 3.5 h in the presence of 10% FBS and then incubated with regular media for 48 h before measurement of luciferase activity. Luminescence activity was measured according to Experimental Procedures. Data were expressed as mean $\pm$ standard deviation. ($n = 3$, (B) GFP expressed in HeLa cell line transfected with P(SiDAHs)1/pDNA and PEI/pDNA complexes at their optimum ratios.

Figure 34A demonstrated that at 1:1 equivalents of PEI to SiDAHs i.e. P (SiDAHs)1 derivative showed almost similar protein expression to that of PEI. On increasing the equivalents of SiDAHs, transfection efficiency decreased. The efficiency was in the order of P(SiDAHs)1 >P(SiDAHs)5 >P(SiDAHs)10 > P(SiDAHs)15. Gene expression efficiency of P(SiDAHs)1 polymer were again confirmed by GFP expression as showed in Figure 34B.

4.2.6 Investigation of cellular uptake pathway and nuclear trafficking.

To confirm arginine and histidine mediated cellular uptake pathway leading to enhanced transfection efficiency compared to native PEI, transfection experiment were performed on KB cells by treatment with various cellular uptake inhibitors. Figure 35A exhibited the relative transfection efficiencies of PEI and P(SiDAAr)5 polyplexes in presence of each inhibitor. In case of PEI, wortmannin and genistein extensively reduced the efficiency. This suggests that PEI/DNA nanoparticles enter through both caveolae-mediated endocytosis and also by macropincytosis. The treatment with chloropromazin led to the enhanced transfection efficiency of PEI. On the other hand, transfection efficiency of P(SiDAAr)5/DNA polyplex was reduced in the presence of wortmannin, genestein and also by chloropromazin by 43%, 30% and 19% respectively. From Figure 35B it is observed that, transfection efficiency of P(SiDAHs)1 decreased in presence of wortmannin, genistein and chloropromazin by 55%, 60%, and 56%. This reveals that most of the P(SiDAHs)1 derivative enters the cells via all these cellular uptake pathways.

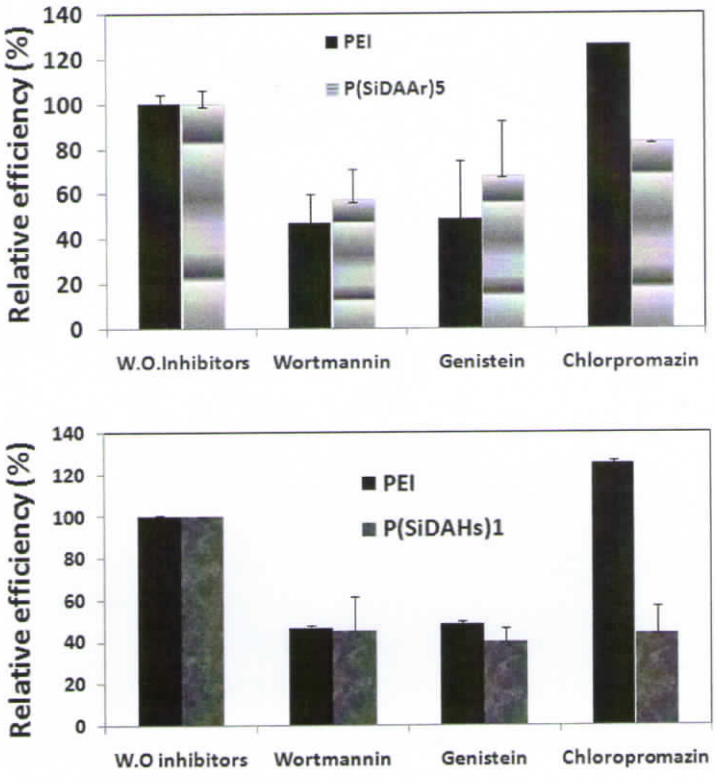

Figure 35: (A)&(B) Relative transfection efficiency (RTE) of P(SiDAAr)5/pDNA and P(SiDAHs) 1/pDNA complexes respectively in treating various cellular uptake inhibitors. Polyplex of PEI was used as control. The polymers without inhibitors (W.O. inhibitors) are expressed as 100% RTE= experimental value/control value X 100 (%). Data were expressed as mean $\pm$ standard deviation. $(n = 3)$.

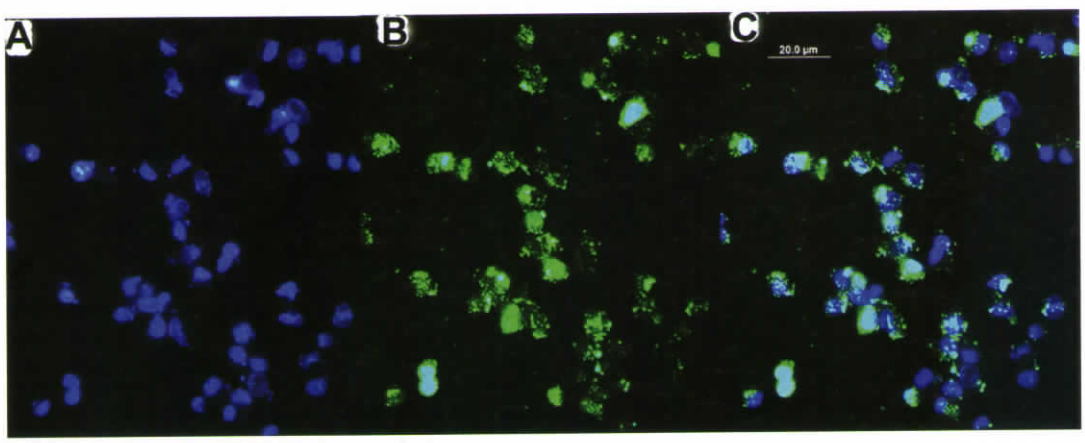

Figure 36: (A) Fluorescent microscopic image of Hoechst33342 stained nucleus (blue filter) (B) Fluorescent microscopic image of FITC stained P(SiDAAr)/pDNA (green filter) (C) Merged images of A and B.

In order to determine the nuclear localisation ability of P(SiDAAr)5, the polymer was tagged with FITC and complexed with plasmid DNA. The nanoparticles were then incubated in Hep G2 cells for 4 h. Nuclear staining was done with Hoechst 33342. Figure 36A-36C demonstrated that the FITC tagged nanoparticles were internalized into the Hoechst 33342 stained nucleus splendidly. Therefore, the enhanced transfection efficiency of the P(SiDAAr)5 derivative compared to PEI is due to the outstanding characteristics of arginine residue along with the endosomal disrupting capacity of PEI.

4.3 Synthesis and Characterisation of Targeted Derivatives of Synthetic Polymers.

4.3.1 Synthesis and preliminary characterisation of P(SiDAAr)5FPn/ P(SiDAHs)1FPn and its nanoparticles with DNA.

In order to facilitate systemic stability and tumor targeting ability, arginine or histidine modified oligo (alkylaminosiloxane) graft poly (ethyleneimine), [P (SiDAAr)n and P (SiDAHs)n] were conjugated with PEG-FA by carbodiimide chemistry using water soluble EDC as a coupling agent and N-hydroxy succinimide (NHS) as catalyst. From previous studies, the polymer having highest transfection efficiency and least cytotoxicity from each group of arginine and histidine modifications such as P(SiDAAr)5 and P(SiDAHs)1 were chosen for PEG-FA modification. By keeping the composition of P(SiDAAr)5 and P(SiDAHs)1 as constant and varying the composition of PEG-FA, two derivatives each, named P (SiDAAr)5FP2,P (SiDAAr)5FP3, P (SiDAHs)1FP2 and P (SiDAHs)1FP3, were synthesised (Figure 37&38).

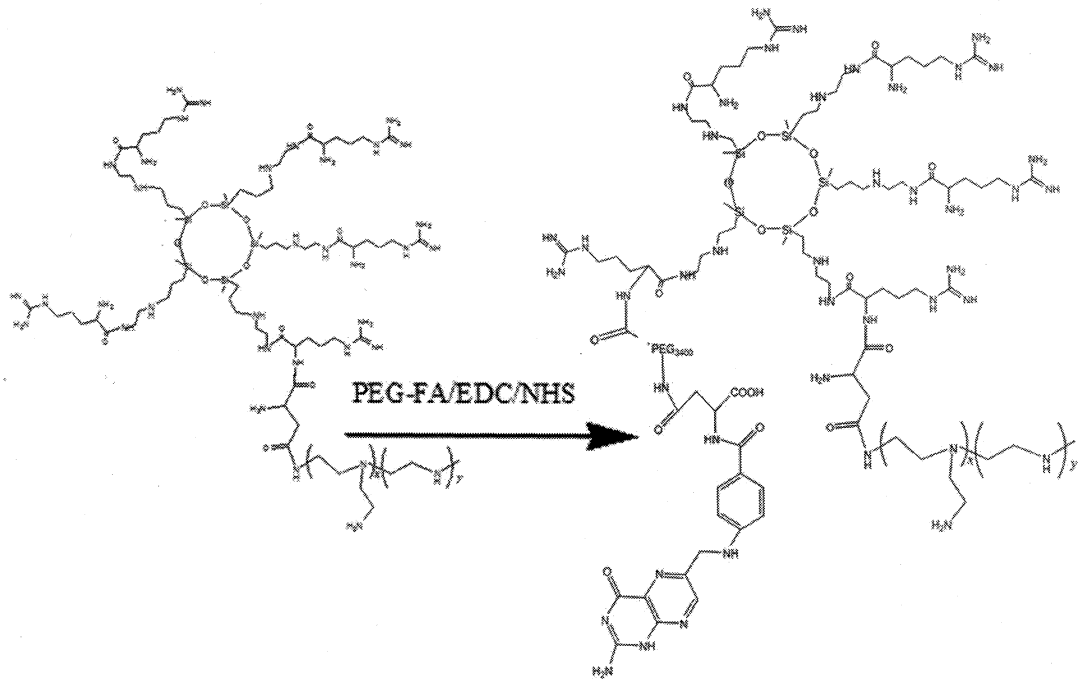

Figure 37: Synthetic scheme of P(SiDAAr)5FPn.

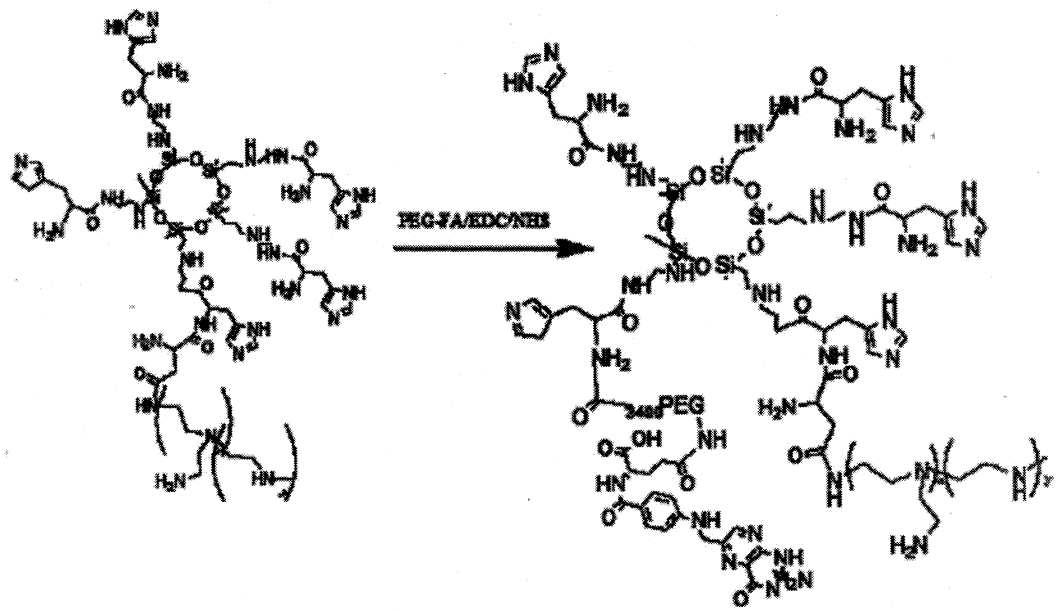

Figure 38: Synthetic scheme of P(SiDAHs)1FPn.

The conjugation of PEG-FA is examined by IR spectra and confirmed using NMR spectroscopy. From the Figure 39, the formation of $-NH-CO-$ bonds due to the conjugation of folic acid was confirmed by the shift in the peak from 1641 cm^{-1} of $C=N$ at guanidine group to 1637 cm^{-1} . The new peaks of amino groups of PEG at 1342 cm^{-1} and 1305 cm^{-1} in the derivatives P(SiDAAr)5FP2 and P(SiDAAr)5FP3 confirms its conjugation with PEG-FA . In the case of histidine conjugated derivatives due to the formation of $-CO-NH-$ bonding of PEG-FA, the peak at 1629 cm^{-1} is shifted to 1647 cm^{-1}. The new peaks of amino groups of PEG at 1342 cm^{-1} in the derivatives P(SiDAHs)1FP2 and P(SiDAHs)1FP3 confirms its conjugation with PEG-FA (Figure 40).

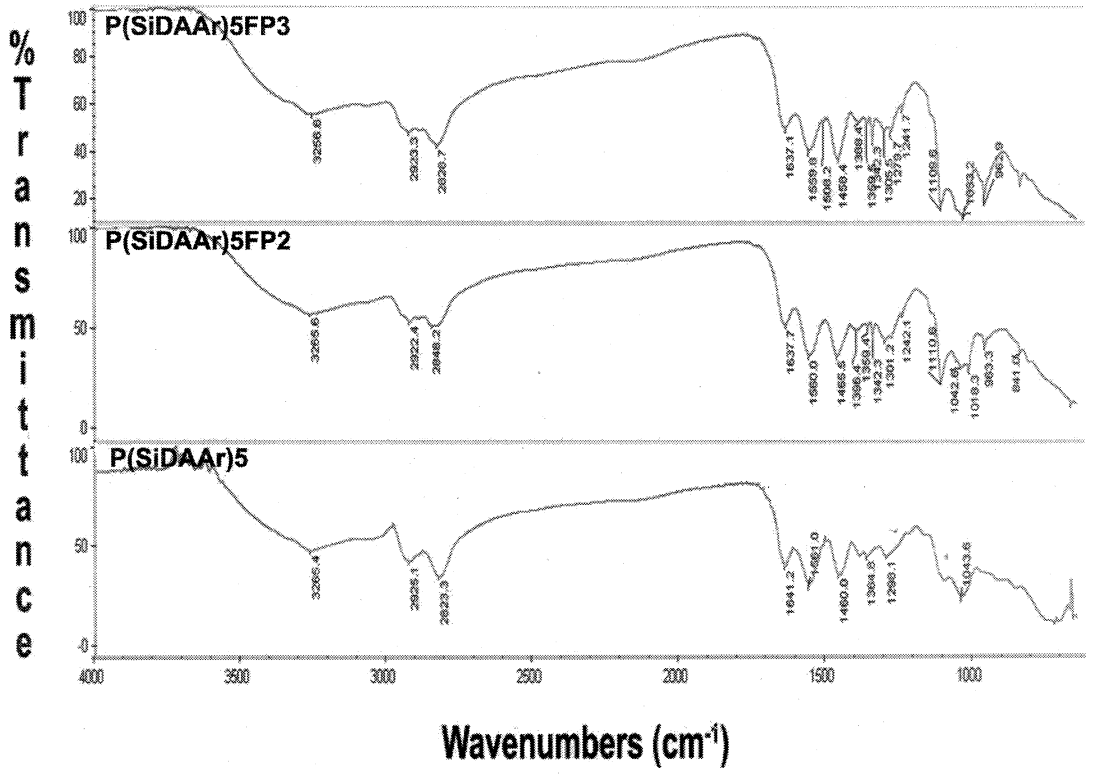

Figure 39: IR spectra of P(SiDAAr)5FPn polymers with its parent polymer P(SiDAAr)5

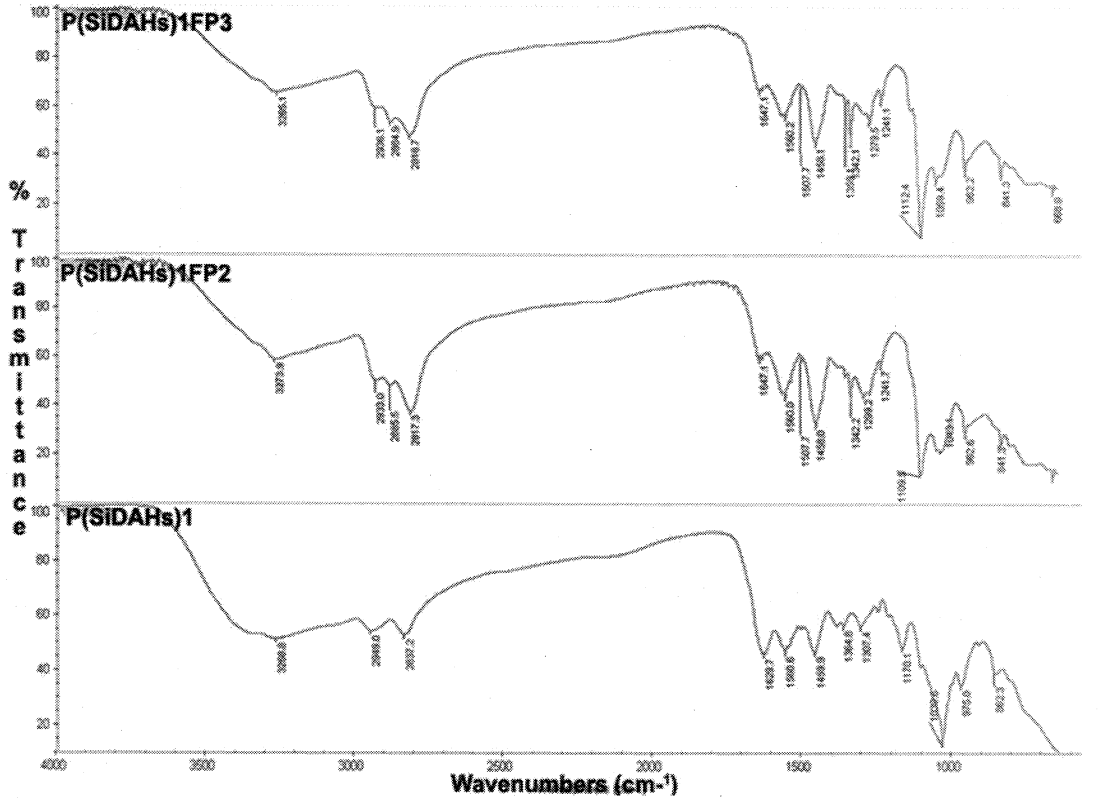

Figure 40: IR spectra of P(SiDAHs)1FPn polymers with its parent polymer P(SiDAHs)1.

The folic acid conjugation was revealed by the presence of aromatic proton signals at 6.75 to 8.5 ppm in the ^{1}HNMR spectrum (Figure 41). The signals at 3.19 - 3.547 ppm of -CH_2CH_2O- confirms the presence of PEG group. Similarly the peaks corresponding to the -CH_2- group of PEI at 2.78 to 3.17 ppm was also confirmed. The conjugation of folic acid was proved by the absorbance at 363 nm in the UV spectrum of the copolymer. From the UV spectra, the folate content of P(SiDAAr)5FP2 was calculated as 0.00825 mMg^{-1} and of P(SiDAAr)5FP3 as 0.0524 mM g^{-1} polymer. Similarly the folate content of P(SiDAHs)1FP2 was calculated as 0.016944 mM g^{-1} and of P(SiDAHs)1FP3 as 0.043032 mM g^{-1} polymer.

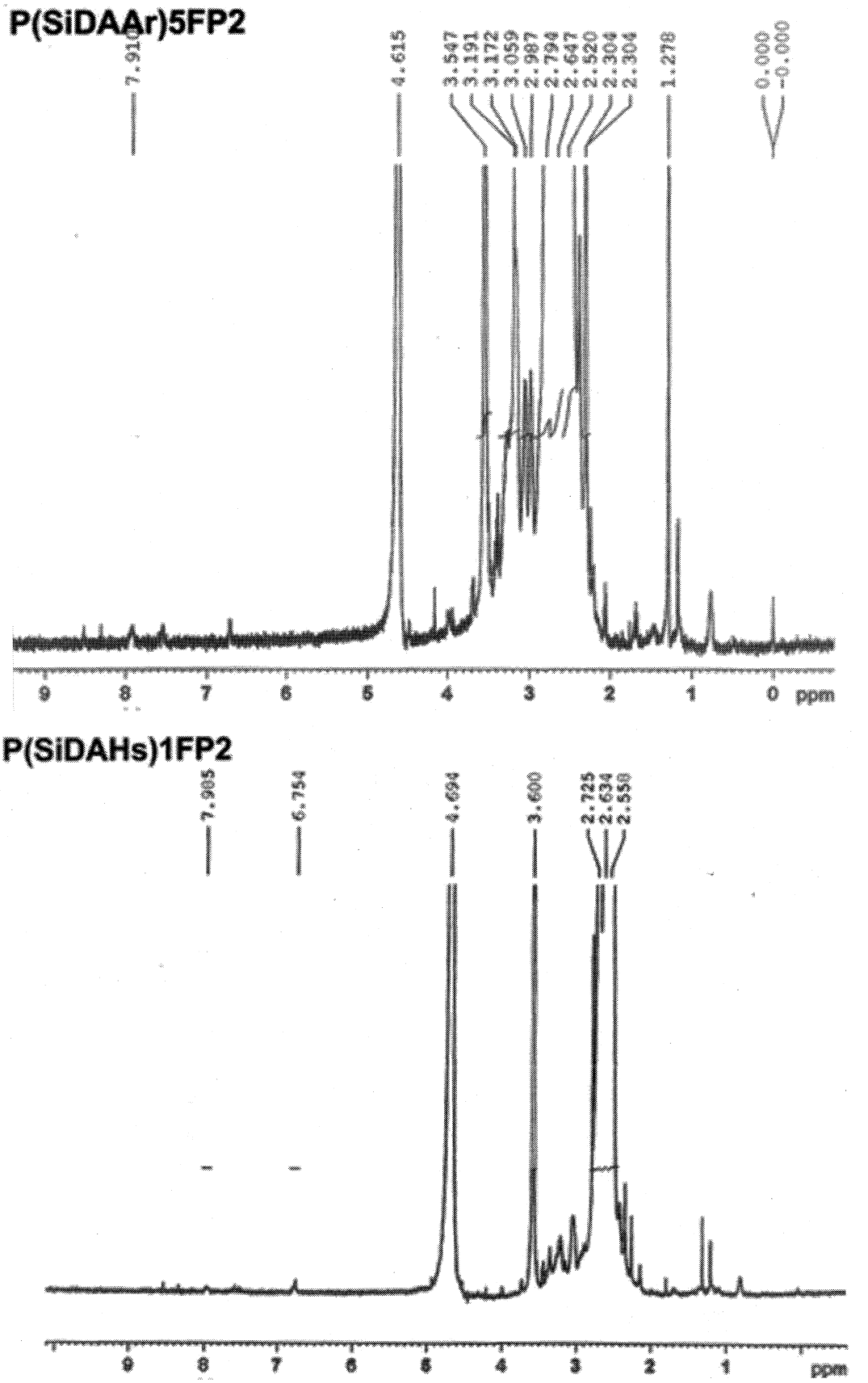

Figure 41: ^{1}HNMR spectra of P(SiDAAr)5FP2 and P(SiDAHs)1FP2.

The endosomal disruption capacity of the polymers was examined by the acid base titration method. Figure 42A showed that at lower composition of PEG-FA, i.e P(SiDAAr)5FP2 derivative showed similar buffering capacity to that of PEI, while P(SiDAAr)5FP3 showed lower buffering capacity. Because of the high pKa value of imidazole group of histidine residue P(SiDAHs)n derivatives showed high buffering capacity, even higher than PEI. The conjugation of PEG-FA to P(SiDAHs)1 also reduced the buffering capacity of P(SiDAHs)1 derivative. However it was more or less equivalent to that of PEI (Figure 42B).

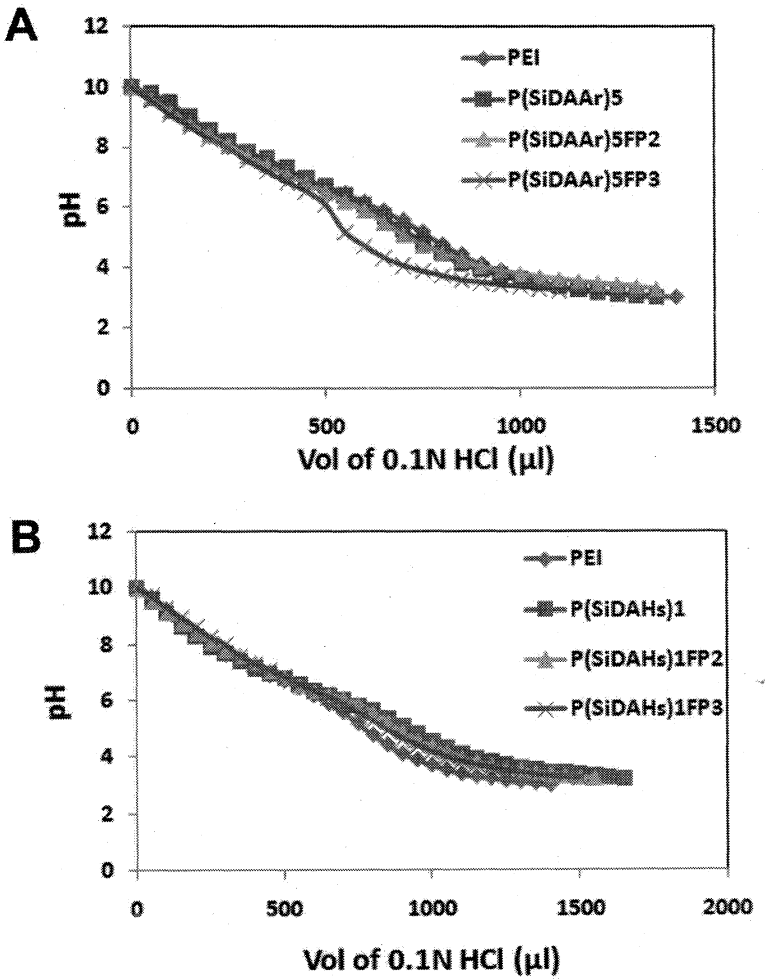

Figure 42: (A) Acid /base titration of P(SiDAAr)5 and its targeted derivatives. PEI is considered as positive control. (B) Acid /base titration of P(SiDAHs)1and its targeted derivatives. PEI is considered as positive control.

The amount of free amino groups of the derivatives before and after complexation with DNA was determined using fluorescamine assay. Figure 43A revealed that when the PEG-FA was

conjugated to the P(SiDAAr)5 derivative the amount of free amino groups decreased. From this observation it is clear that the PEG-FA is conjugated to the free amino groups of P(SiDAAr)5 derivatives. The decrease in free amino groups may also be due to the masking effect of PEG group. At higher composition, the masking of the free amino group increased. From Figure 43A it was also confirmed that even after complexation with DNA, there were adequate amount of free amino groups which provided sufficient positive charge for the nanoparticles. Similar pattern is observed in the case of histidine conjugated derivatives also (Figure 43B).

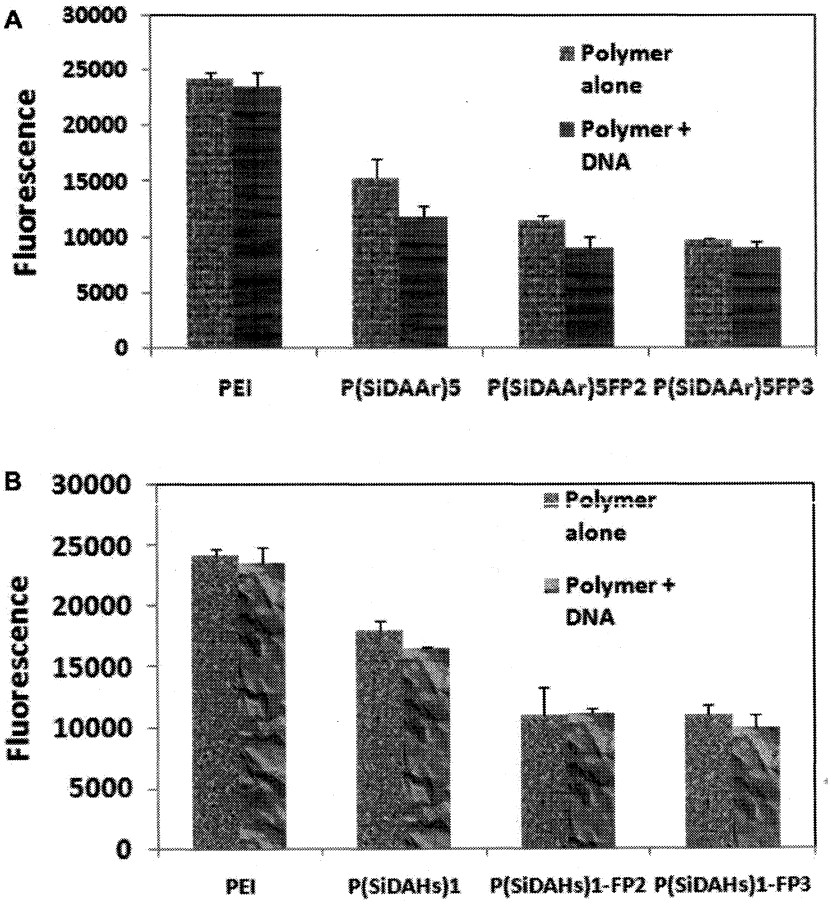

Figure 43: (A) & (B) Free amino groups on P(SiDAAr)5 and P(SiDAHs)1 respectively and its targeted derivatives before and after interaction with DNA determined using fluorescamine assay. Data were expressed as mean $\pm$ standard deviation. $(n = 3)$.

The particle size and surface charge of the nanoparticles after complexation with DNA was examined by dynamic light scattering technique as depicted in Table 13, 14, 15 & 16. The hydrodynamic diameters of the polymer/DNA complexes at various weight ratios were deter-

mined by keeping the concentration of DNA constant. From Table 13, it was observed that both the PEG-FA conjugated polymer formed nanosized complexes at higher weight ratios, even higher than the parent polymer. Similarly, higher positive charge was also observed at higher weight ratios. The nanoparticles having lower size and high surface charge were considered as optimum weight ratio for further studies. The weight ratios optimised for the polymers P(SiDAAr)5, P(SiDAAr)5FP2 and P(SiDAAr)5FP3 were 2.56, 2.88 and 2.72 respectively. Similarly the weight ratios of 3.12, and 3 were considered as optimum for P(SiDAHs)1FP2, and P(SiDAHs)1FP3 derivatives.

Table 13: Particle size (nm) of P(SiDAAr)5FPn derivatives at different weight ratios. Standard deviation given in bracket.

w/w ratio	**P(SiDAAr)5FP2**	**P(SiDAAr)5FP3**
0.5	505.5(40.3)	1056.5(361)
1	280(28.2)	2613.5(91)
2	288(15.5)	445.5(74)
3	213(83.4)	299.5(43.1)
4	193(33.2)	295.5(53.0)
5	176.5(40.3)	199(49.49)

Table 14: Zeta Potential (mV) of P(SiDAAr)5FPn derivatives at different weight ratios. Standard deviation given in bracket.

w/w ratio	**P(SiDAAr)5FP2**	**P(SiDAAr)5FP3**
0.5	-5.98(4.63)	-3.51(0.93)
1	3.65(0.53)	-0.74(1.04)
2	8.20(0.23)	9.51(1.68)
3	6.9(2.47)	12.5(1.69)
4	9.995(0.28)	13.9(0.56)
5	9.92(0.53)	14.9(0.56)

Table 15: Particle size (nm) of P(SiDAHs)1FPn derivatives at different weight ratios. Standard deviation given in bracket.

w/w ratio	**P(SiDAHs)1FP2**	**P(SiDAHs)1FP3**
0.5	373(39.5)	520(11.31)
1	343.5(27.5)	357.5(34.6)
2	431.5(0.70)	145.5(6.36)
3	169(9.89)	164(39.5)
4	348(32)	171.5(40.3)
5	351(7.07)	288(19.7)

Table 16: Zeta Potential (mV) of P(SiDAHs)1FPn derivatives at different weight ratios. Standard deviation given in bracket.

w/w ratio	P(SiDAHs)1FP2	P(SiDAHs)1FP3
0.5	-9.115	-3.405
1	-4.485	7.73(1.42)
2	5.95(4.08)	8.65(2.19)
3	11.95(0.91)	10.8(1.24)
4	11.6(0.56)	12.7(0.560
5	10.65(0.77)	11.6(0.98)

The nano size of the polymer at its optimum weight ratios were confirmed using atomic force microscopy (AFM). Figure 44A&B reveals the formation of nanoplex at size around 200 nm for both the arginine and histidine conjugated derivatives.

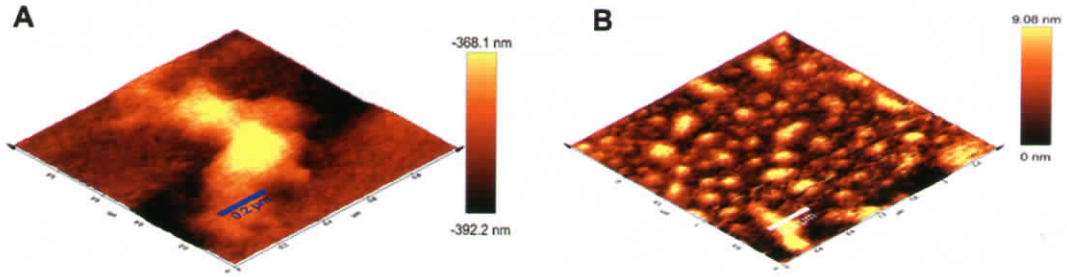

Figure 44: (A) & (B) 3D AFM image, in the tapping mode of the P(SiDAAr)5FP2/ pDNA and P(SiDAHs)1FP3/ pDNA complex respectively at their optimum weight ratios.

4.3.2 Physical integrity of the polymer/pDNA complex and its protection against nuclease degradation.

The polymer's ability for the formation of complex nanoparticles with pDNA (pGL3 Luciferase reporter vector) and its integrity was determined by gel retardation assay as shown in Figure 45. The complexation was done at weight ratios such as 0.25, 0.5, 1, 3, 5 and 10. From the Figure 45A, it was observed that both the arginine modified targeted polymers complexed DNA effectively from ratio 0.5 onwards while the parent polymer was capable to complex DNA even from 0.25 onwards as reported earlier. In the case of histidine conjugated targeted derivatives P(SiDAHs)1FP3 could retard the DNA from 0.5 onwards and the derivative P(SiDAHs)1FP2 from 0.25 onwards. Due to the masking effect of PEG group, adequate

positive charge was obtained at higher weight ratios onwards.

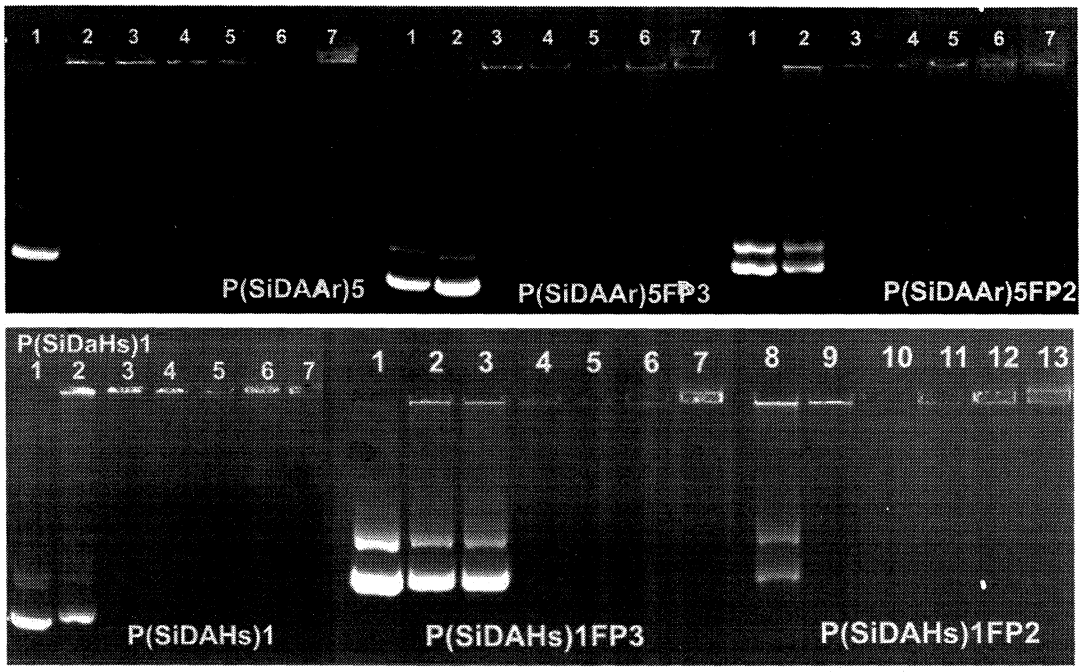

Figure 45: Agarose gel electrophoresis representing pDNA (pGL3 Luciferase reporter vector) binding studies with P (SiDAAr)5 and P (SiDAHs)1 and its targeted derivatives at different w/w ratios. Lane1: pDNA alone, Lanes 2-7 are polymer/pDNA at w/w ratios of 0.25,0.5,1,3,5 and 10.

The protection of DNA from degradation by cellular nucleases was determined by interacting the complex nanoparticles with DNase 1. As the representative polymer, one of the targeted derivative from each group such as P(SiDAAr)5FP2 and P(SiDAHs)1FP3 was analysed. Naked DNA was taken as the negative control and PEI was taken as the positive control. The complex was prepared at the optimum weight ratios of each polymer. When 100 IU of DNase 1 was added to the complexed DNA (5 IU/μg of DNA), irrespective of the sample having DNA alone, no degradation was observed for the targeted polymer similar to control polymers (Figure 46). This indicated that even after PEGylation, the polymer was effective in protecting plasmid DNA against degradation by DNase 1 at its optimum charge ratio.

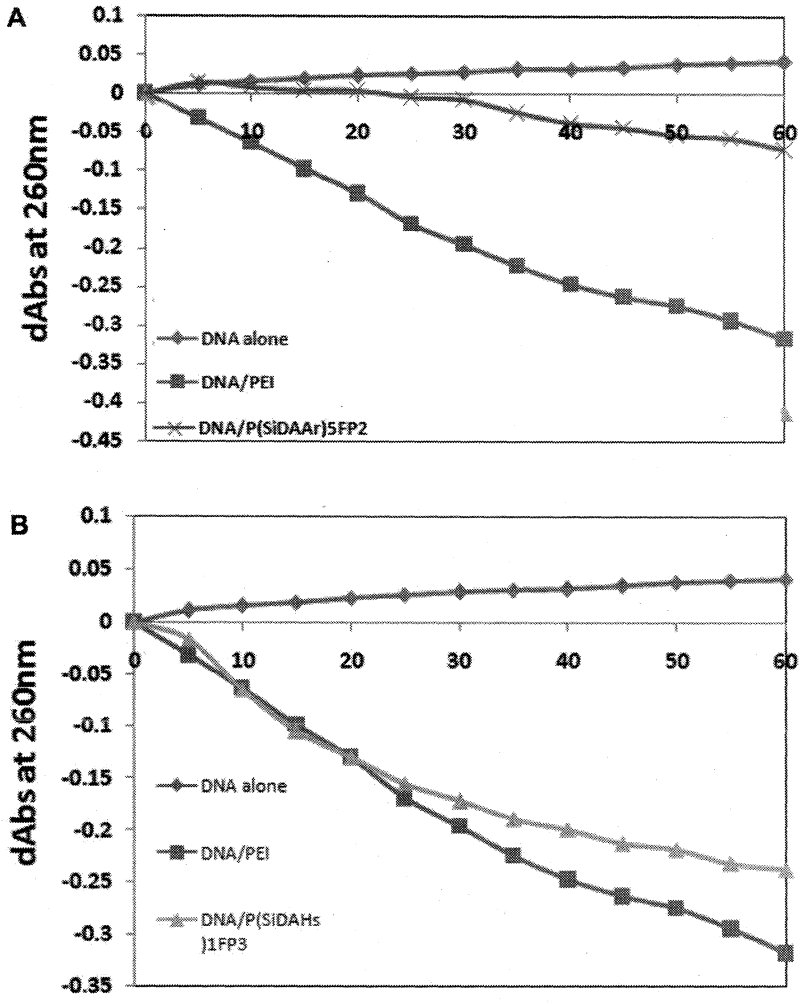

Figure 46: (A) Nuclease resistance of P(SiDAAr)5FP2/ pDNA complex against DNase I activity at w/w ratio of 2.5. (B) Nuclease resistance of P(SiDAHs)1FP3/ pDNA complex against DNase I activity at w/w ratio of 3. DNase of 5 IU/μg of DNA were used. PEI/DNA complex was used as positive control at its optimum ratio. Unprotected pDNA is used as negative control. The DNA used was pGL3 Luciferase reporter vector.

4.3.3 Evaluation of biocompatibility.

The biocompatibilities of the targeted polymers were evaluated in terms of RBC lysis, RBC aggregation and also by evaluating cell viability in presence of polymer alone and with polyplexes. The complexed nanoparticles of each polymer at its optimum charge ratios were incubated with washed RBC and incubated for 2 h at 37 ^{o}C. Due to the presence of PEG group, a drastic decrease in RBC lysis was observed for the P(SiDAAr)5FP2 compared to the parent polymer P(SiDAAr)5 and the positive control PEI (Figure 47). While in the case of P(SiDAAr)5FP3 polymer, the nanoparticles induced more cell lysis. In the case of histidine

conjugated derivatives also high extent of RBC lysis was observed. This may be due to the presence of more folic acid which provides more positive charge to the polymer. Therefore RBC aggregation experiment was done only for arginine conjugated derivatives. Similar trend was observed in the case of RBC aggregation experiment also. The P(SiDAAr)5FP2 polymer showed least aggregation compared to P(SiDAAr)5FP3 and the parent polymer P(SiDAAr)5.

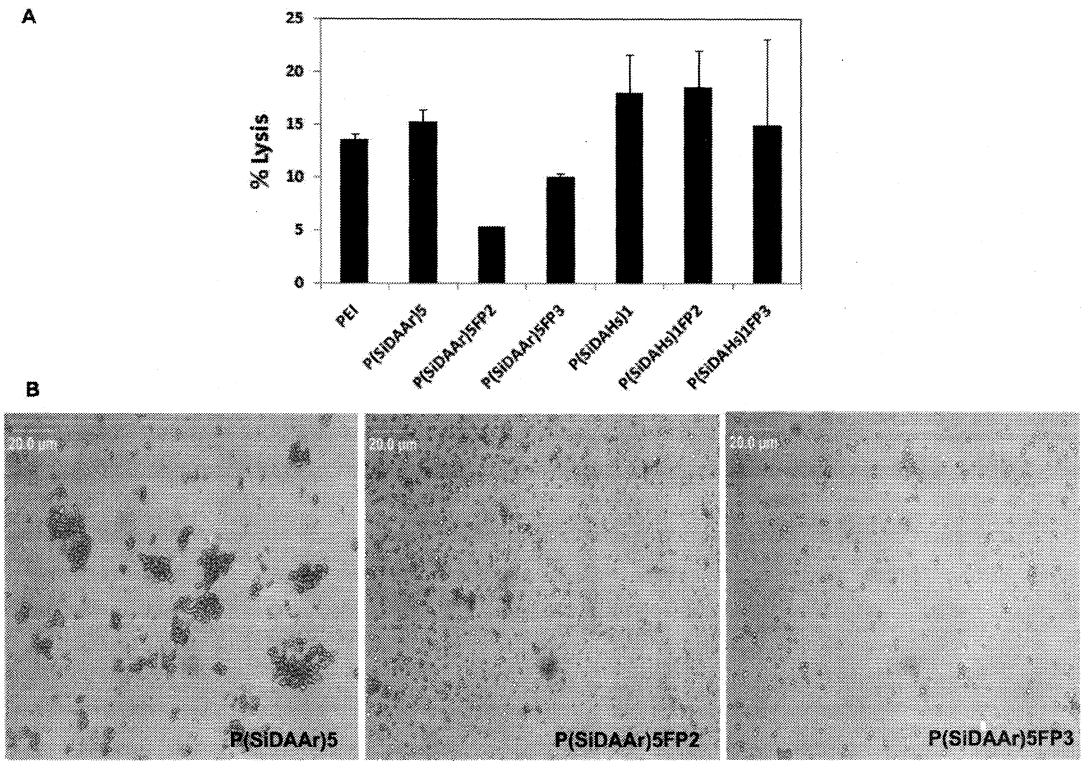

Figure 47: (A) Hemolysis of the DNA complexes of P(SiDAAr)5, P(SiDAHs)1 and its targeted derivatives; $(n = 3)$ (B) RBC aggregation studies of P(SiDAAr)5FP2/ pDNA and P(SiDAAr)5FP3/ pDNA. Aggregation of P(SiDAAr)5/pDNA is taken as control (40 times magnification for RBC).

The cell viability of KB cell lines in presence of each polymer was evaluated at different concentrations such as 25 μg/ml, 50 μg/ml, 75 μg/ml and 100 μg/ml. From Figure 48A& 49A, it was observed that at lower concentration, both the arginine and histidine conjugated targeted polymers were almost non-toxic compared to the parent polymers and the positive control PEI. At higher concentrations, the polymers exhibited toxicity to the cells.

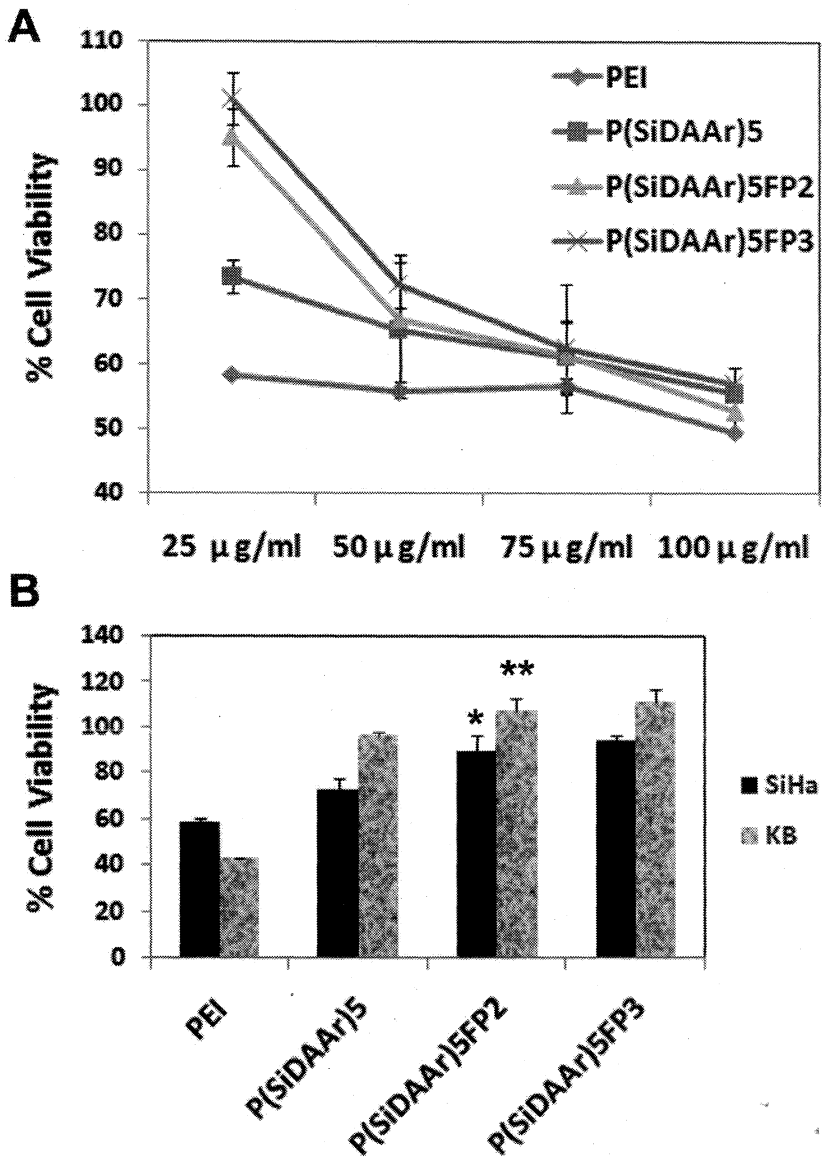

Figure 48: (A) Viability of KB cell lines at varying concentration of P(SiDAAr) 5FPn derivatives. PEI and P(SiDAAr)5 were used as control. (B) Viability of KB and SiHa cell lines of P(SiDAAr)5FPn/ pDNA nanoparticles at its optimum weight ratios. Data were expressed as mean $\pm$ standard deviation. ($n = 3$,$^{*}P, < 0.05$, compared to PEI and $^{**}P < 0.05$, compared to PEI).

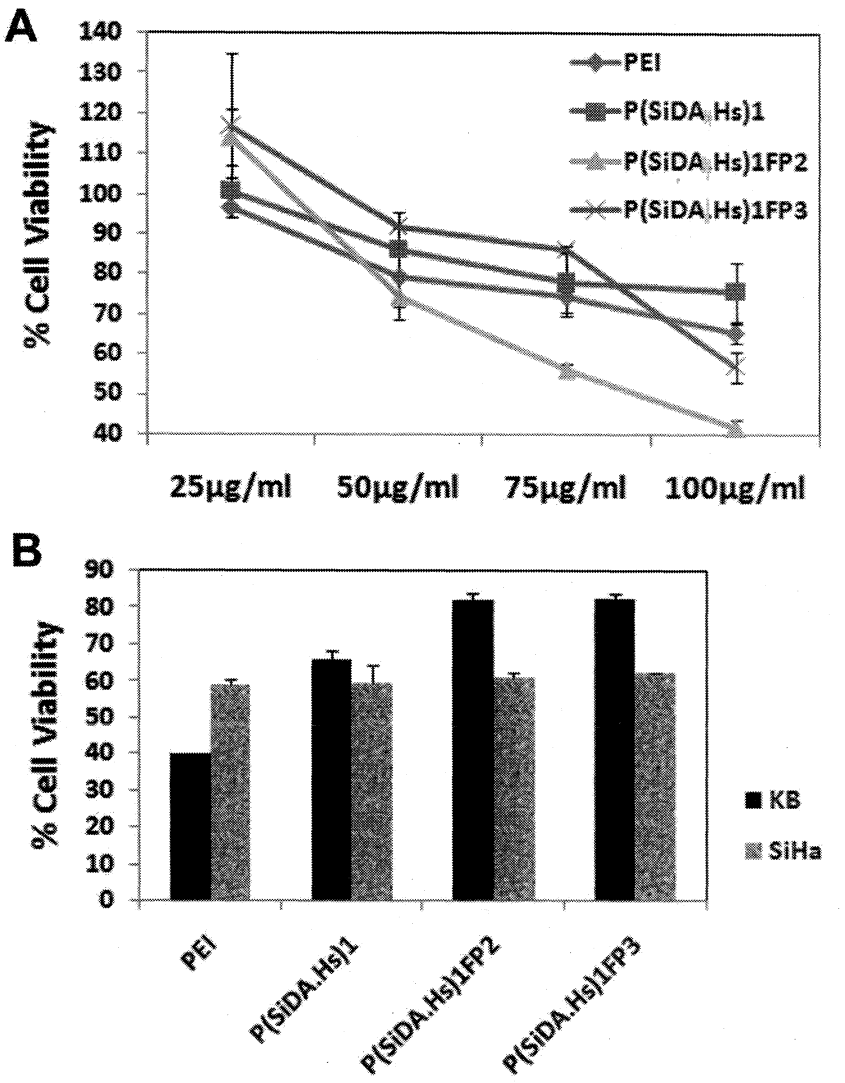

Figure 49: (A) Viability of KB cell lines at varying concentration of P(SiDAHs) 1FPn derivatives. PEI and P(SiDAHs)1 were used as control. (B) Viability of KB and SiHa cell lines of P(SiDAHs) 1FPn/ pDNA nanoparticles at its optimum weight ratios. Data were expressed as mean ± standard deviation.

The cell viability of KB and SiHa cell lines were estimated in presence of polymer/DNA nanoparticles at transfection conditions. The nanoparticles were incubated with the cell lines in presence of 10% FBS for 24 h. The polymers showed almost similar pattern of cell viability in both the cell lines, while KB cell lines were more viable compared to SiHa cells (Figure 48B&49B). In the presence of both the targeted polymers, KB cell lines showed almost 100% viability while SiHa cell lines showed more than 90% viability. In both the cell lines, targeted polymers showed more viability than the parent polymer P(SiDAAr)5. The P(SiDAAr)5 polymer

showed 98% viability in KB cell line, however in SiHa cell, it showed only 72% viability. In the case of hystidylated derivatives after complexation with DNA, both the targeted derivatives exhibited around 85% cell viability in KB cell lines.

4.3.4 Evaluation of transfection efficiency.

Transfection efficiency of the targeted polymers and its parent polymer were evaluated in KB oral epidermoid cells and SiHa cell lines using pGL3 and pEGFP reporter genes. Branched PEI having molecular weight of 25 kDa, widely used as "gold standard" have been taken as positive control. The nanoparticles of each polymer at its optimum weight ratios were used for transfection studies with pDNA concentration of 10 μg/ml. All experiments were carried out at 10% serum conditions. Figure 50 showed the amount of luciferase protein expressed in two cell lines, in terms of relative luminescence units (RLU) by arginine conjugated polymers. In agreement with the results of cytotoxicity evaluation, the KB cell line which was more viable in presence of polymeric nanoplexes showed high rate of transfection compared to the SiHa cell lines which was more toxic. In KB cell line, the parent polymer P(SiDAAr)5, showed highest transfection than the targeted polymers and even higher than the control PEI. Among the targeted polymers, P(SiDAAr)5FP2 showed better transfection. The decrease in transfection of the targeted polymers compared to the parent polymer may be due to the masking effect of PEG group. However, in SiHa cell lines the masking effect of PEG group becomes advantageous for better transfection. Since PEI and P(SiDAAr)5 were more toxic to the SiHa cells, its transfection was also reduced than the targeted derivatives eventhough the rate of transfection was higher in KB cell lines. Thus the transfection with pEGFP plasmids were carried out in KB cell lines. In agreement with the pGL3 transfection, the pEGFP transfection also showed better efficiency for the parent polymer P(SiDAAr)5 than the targeted derivative. It fluorescently activated more percentage of cells (Figure 50B). However, the confocal micrograph (Figure 50C-E) reveals that irrespective of the number of activated cells, more protein was produced by the targeted polymer P(SiDAAr)5FP2. On the basis of the results of transfection and biocompatibility studies, P(SiDAAr)5FP2 was selected for further studies.

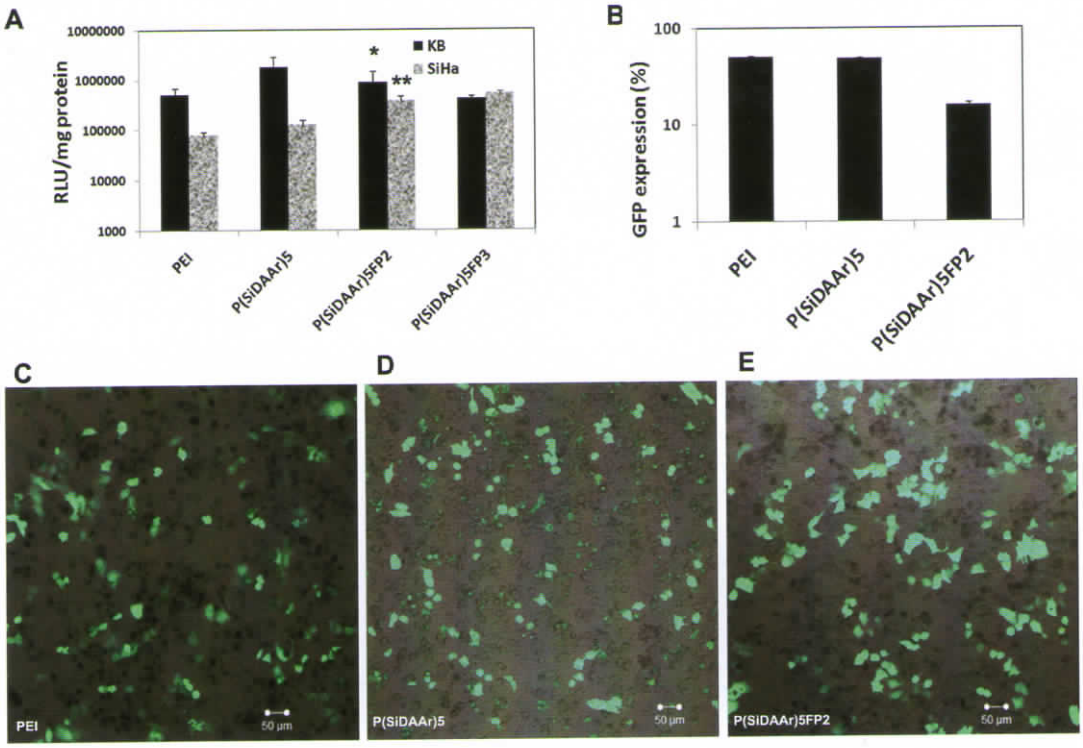

Figure 50: *In vitro* transfection efficiency in terms of luminescence activity of P(SiDAAr)5FPn derivatives in KB and SiHa cell lines. Data were expressed as mean $\pm$ standard deviation. ($n = 3$, $^*P$ significantly different compared to PEI) (B) Percentage of GFP expressed KB cell line measured by flow cytometry. (C-E) Confocal micrographs of GFP expressed KB cells.

In the case of hystidylated derivatives, On inducing the targeting via PEG-FA conjugation the transfection efficiency of the polymer P(SiDAHs)1 was decreased (Figure 51). In both the KB and SiHa cell lines, the decrease in transfection efficiency of the targeted polymers were observed. This may be due to the masking effect of PEG group. In the case of GFP expression also similar pattern was observed, however, the confocal micrographs revealed a change in morphology of the cells in the case of PEI and P(SiDAHs)1 compared to P(SiDAHs)1FP3. The unchanged morphology of cells may due to the low cytotoxicity of the P(SiDAHs)1FP3 derivative.

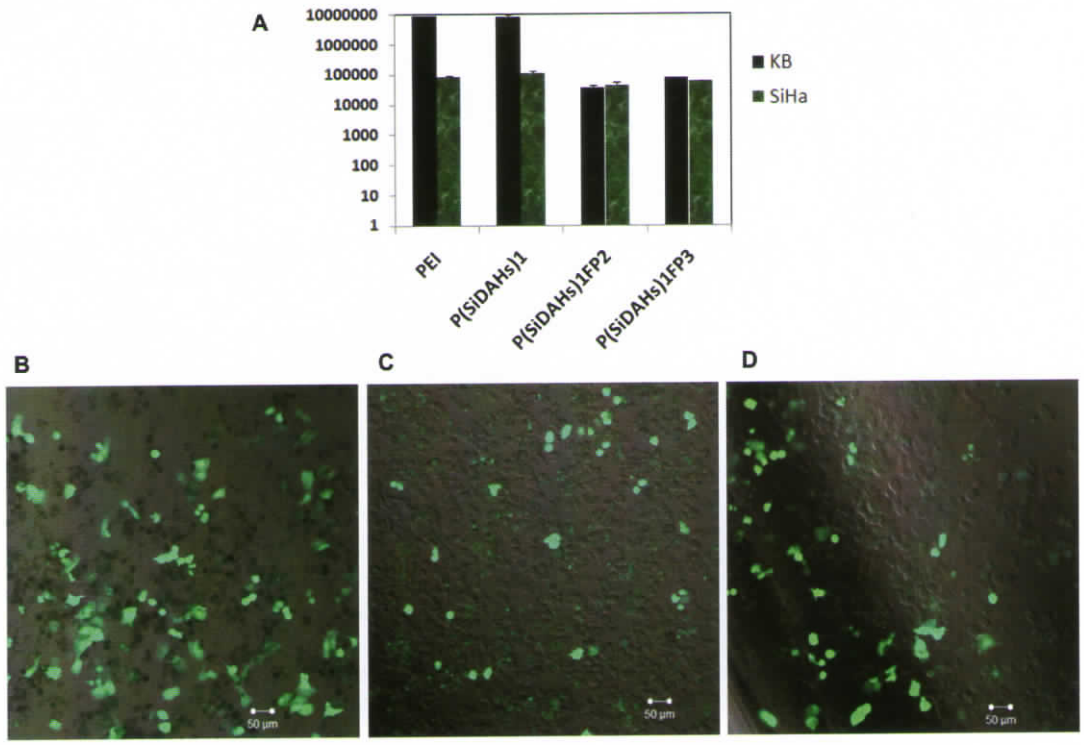

Figure 51: (A) *In vitro* transfection efficiency of P(SiDAHs)1 and its targeted derivatives in KB and SiHa cell lines. Data were expressed as mean $\pm$ standard deviation $(n = 3)$. (B-D) Confocal micrographs showing GFP expressed in KB cell line transfected with PEI/ pDNA, P(SiDAHs)1/ pDNA and P(SiDAHs)1FP3/ pDNA complexes at their optimum ratios.

4.3.5 Investigation of nuclear trafficking and clearance.

Therefore, the cellular uptake and its clearance of the polymer was evaluated by tagging P(SiDAAr)5FP2, P(SiDAHs)1FP3 and DNA separately and viewing through fluorescent microscopy at different time intervals such as 4 h, 24 h and 48 h. At first, DNA alone was tagged with YOYO and nucleus was stained with Hoechst 33342. Figure 52 A1, A2 and A3 reveals the cellular and nuclear uptake of P(SiDAAr)5FP2 complexed DNA at fourth hour after the addition of nanoparticles in to cells. The experiment was repeated by tagging the polymer with FITC. Figure 52 B1, B2 and B3 revealed the high accumulation of polymer/DNA nanoparticles inside the cell as well as in the nucleus. This indicates that the un-packaging of the polymer/DNA complex and release of DNA is expected to happen inside the nucleus. In order to confirm the un-packaging of the polymer from the DNA and its clearance, the fluorescent micrographs were taken at 24^{th} and 48^{th} h of nanoparticles incubation. Figure 52 C1, C2 and C3, clearly showed that, at 24 h, the polymer begins clearance from the cell, because the fluorescence

was observed at the boundary of the cells. And at the 48^{th} h, almost the entire polymer was evacuated from the cell (Figure 52 Figure 6-D1, D2 and D3). From the experiment, it was demonstrated the targeted polymer was capable for the delivery of the gene inside the cell as well as nucleus and subsequent release after its purpose.

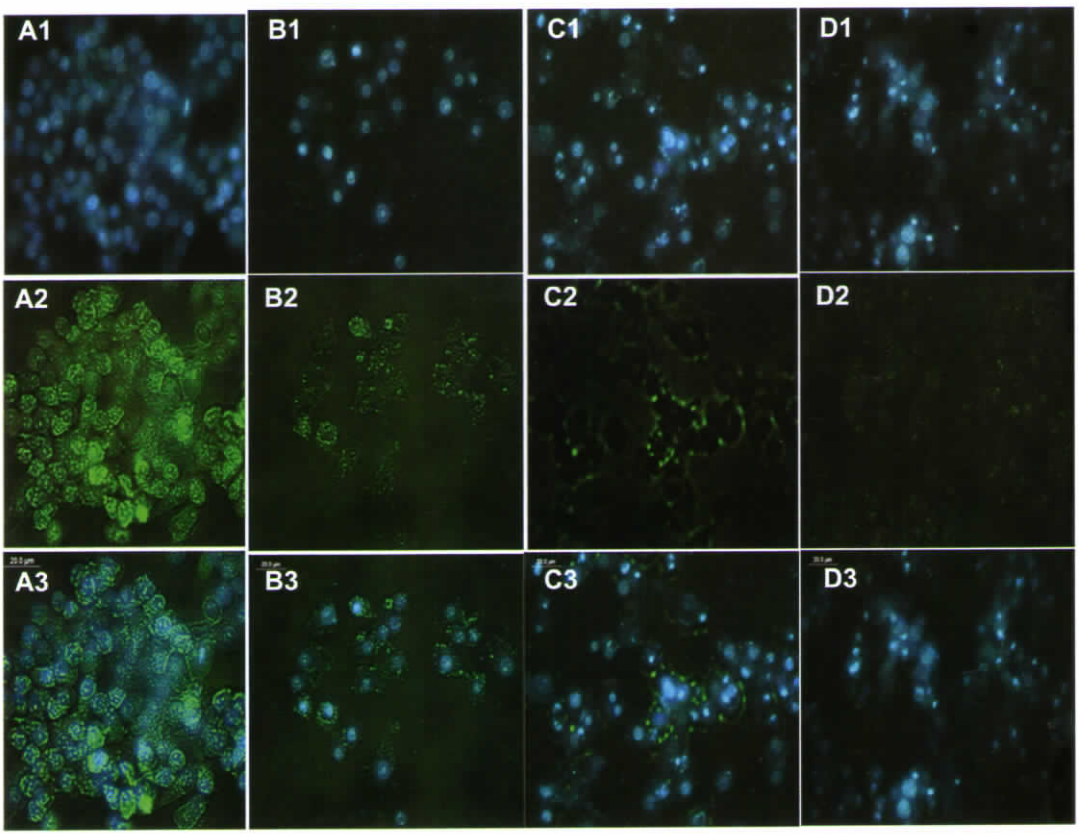

Figure 52: Nuclear uptake study of polyplexes using FITC stained P(SiDAAr) 5FP2 and YOYO stained pDNA. A1, A2, and A3 indicates fluorescent microscopic image of Hoechst33342 stained nucleus (blue filter) YOYO stained DNA complexed with unstained P(SiDAAr) 5FP2 and merged images of A1 and A2 respectively. B1, C1 and D1 indicate fluorescent microscopic images of Hoechst33342 stained nucleus at 4^{th} h, 24^{th} h and 48^{th} h respectively. B2, C2 and D2 indicates fluorescent microscopic image of nanoparticles of FITC stained P(SiDAAr)5FP2 with unstained pDNA (green filter) , B3,C3 and D3 indicates the merged images.

Similarly Figure 53 A1, B1 and C1 revealed the cellular and nuclear uptake of the P(SiDAHs) 1FP3/ pDNA nanoplexes at 4^{th} h. At 24h of post incubation, decreased green fluorescence is observed which may be due to the slow clearance of the polymer after release of the pDNA. The clearance was almost completed at 48^{th} h. Figure 52 A3, B3 and C3 showed very feeble green fluorescence inside the cell and nucleus.

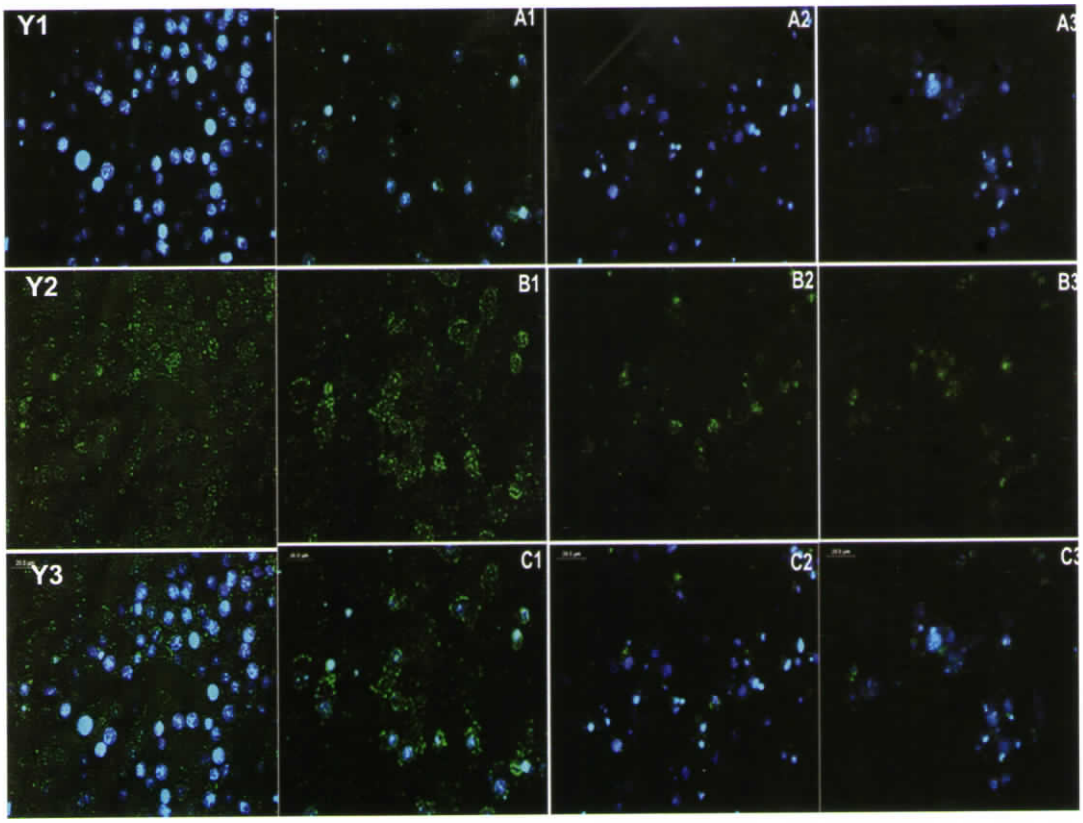

Figure 53: Nuclear uptake study of polyplexes using FITC stained P(SiDAHs) 1FP3 and YOYO stained pDNA. Y1, Y2 and Y3 indicates fluorescent microscopic image of Hoechst33342 stained nucleus (blue filter) YOYO stained DNA complexed with unstained P(SiDAAr) 5FP2 and merged images of Y1 and Y2 respectively. A1, A2, and A3 indicate fluorescent microscopic images of Hoechst33342 stained nucleus at 4^{th} h, 24^{th} h and 48^{th} h of post incubation respectively. B1, B2 and B3 indicates fluorescent microscopic image of nanoparticles of FITC stained P(SiDAHs)1FP3 complexed with unstained pDNA (green filter), C1,C2 and C3 indicates the merged images.

4.3.6 Cellular uptake pathway and *in vitro* tumor targeting.

In order to examine the cellular uptake capability of targeted polymers, the transfection efficiency of the targeted (P(SiDAAr)5FP2 & P(SiDAHs)1FP3) and non- targeted (P(SiDAAr)5) & P(SiDAHs)1) polymers in presence of various cellular uptake inhibitors such as genistein, wortmannin, chlorpromazine and folic acid have been performed. For arginine conjugated derivatives Figure 54A showed that as observed in the parent polymer, the targeted polymer also showed reduced transfection in presence of genistein, wortmannin and chlorpromazine by 45%, 44% and 9% respectively while the transfection was highly reduced in presence of folic acid inhibitor of about 82%. Similarly for histidine conjugated derivatives from Figure 54B it is observed that, transfection efficiency of both non- targeted and targeted polymers decreased

in presence of wortmannin, genistein and chloropromazin by 55%, 60%, and 56% for non-targeted polymer and 49%,32% and 22% for targeted polymers. This reveals that most of the non targeted polymer, P(SiDAHs)1 enters the cells via all these cellular uptake pathways than the targeted polymers. While in the case of targeted polymer P(SiDAHs)1FP3, the transfection efficiency was decreased to 62% in presence of folic acid inhibitor. This indicates that both the targeted derivatives undergoes cellular uptake mainly by folate receptor mediated pathway. In addition to the presence of arginine and histidine moiety, the polymer has the ability to enter the cells via multiple pathways in some extent.

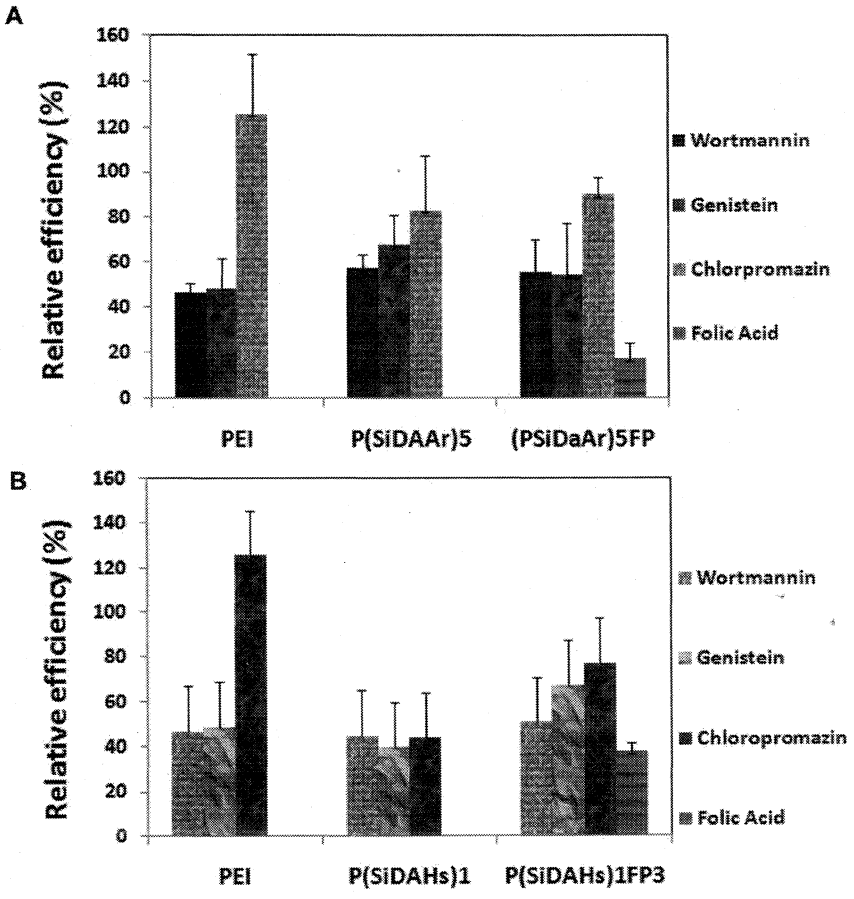

Figure 54: (A) & (B) Relative transfection efficiency (RTE) of P(SiDAAr)5FP2/ pDNA and P(SiDAHs)1FP3/ pDNA complexes respectively in treating various cellular uptake inhibitors. Polyplexes of parent polymers P(SiDAAr)5, P(SiDAHs)1 and PEI were used as control. The polymers without inhibitors are considered as 100%. RTE= experimental value/control value X 100 (%). Data were expressed as mean $\pm$ standard deviation. $(n = 2)$.

Based on the above experiments arginine conjugated targeted derivatives were chosen for

further studies. In order to establish the folate receptor expression of KB cell lines, immunostaining was carried out with rabbit polyclonal antibody IgG specific for folate receptors. After one hour of post incubation, a secondary FITC labelled antibody was incubated with the cells. Then the cells were fixed and analysed by flow cytometry. From the FACS analysis, it was found that KB cell lines exhibited around 60% of folate expression (Figure 55). In order to examine the cellular uptake of targeted and non-targeted polymers, the polyplexes of FITC stained P(SiDAAr)5FP2 and P(SiDAAr)5 polymers were incubated with KB cell line for 4 h in presence of 10% FBS. After incubation, the cells were fixed and analysed by flow cytometry. It was observed from Figure 55 that around 10% increase in cellular uptake took place in the case of folate targeted polyplexes compared to non-targeted polyplexes. To confirm that the uptake was mediated via the folate receptor, a competitive analysis using different amounts of free folic acid in the cell medium was performed on FITC stained P(SiDAAr)5FP2 polymers. The flow cytometry analysis in Figure 55 revealed the decrease in the internalised particles with increasing concentration of free folic acid. In agreement with the previous report (Rosenholm et al. 2009), at a free folic acid concentration of 3 mM the mean fluorescence intensity value decreased to a value of about 1/3 of the value of that measured in the absence of free folic acid. This experiment demonstrated that the particle uptake was mediated by the folate receptor. Based on these facts, we have chosen the targeted derivative P(SiDAAr)5FP2 for in vivo tumor targeting experiment.

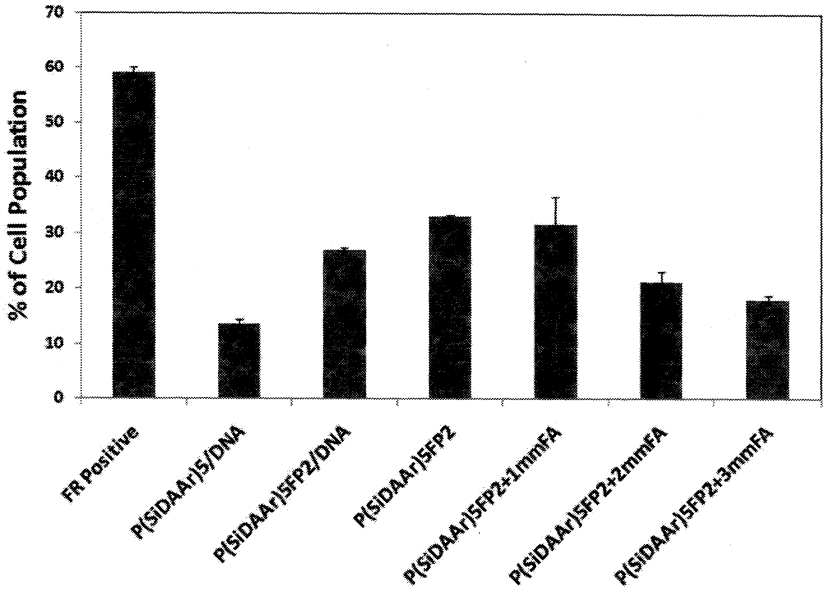

Figure 55: In vitro folate receptor mediated cellular uptake of P(SiDAAr)5FP2 derivatives. 1^{st} bar indicates folate receptor expression of KB cell lines were measured by FACS analysis. 2^{nd} and 3^{rd} bar indicates nanoparticles uptake of FITC stained non targeted and targeted polymers. 4^{th} to 7^{th} bar indicates competitive inhibition of folic acid to cellular uptake of FITC stained P(SiDAAr)5FP2 in KB cell lines $(n = 2)$

From all of the above characterisation, the natural and synthetic polymers can be comparatively evaluated as described on the table 17.

Table 17: Comparative evaluation of natural and synthetic polymer based nanoparticles.

	ATFP15H	**HTFP15H**	**P(SiDAAr)5FP2**	**P(SiDAHs)1FP3**
pGL3 expression (RLU/mg)	$3x10^5$	$8x10^4$	$1.3x10^6$	$7x10^4$
pEGFP expression (%)	-	-	15.5	-
Cell viability (%)	125	113	111	82
Hemolysis (%)	5.38	14.29	5.3	14.9
Cellular uptake (%)	77	54	33	43

Based on transfection, cell viability, blood compatibility and cellular uptake studies it can be concluded that arginine conjugated natural and synthetic polymers shows better properties than histidine conjugated natural as well as synthetic polymers. Among the arginine conju-

gated natural and synthetic polymers, synthetic polymers showed better results. Therefore it was chosen for further in vivo studies.

4.4 In Vivo Tumor Targeting

In order to find out the folate mediated in vivo targeting, FITC stained folate targeted polymer P(SiDAAr)5FP2 and non targeted control polymer P(SiDAAr)5 were prepared in normal saline and injected through tail vein of tumor bearing mice. Post injection of 2, 4, 16 and 24 h, the mice were sacrificed; the tumor, liver and kidney was excised, frozen, sectioned and fixed for confocal microscopic evaluation. Figure 56-58, presents microscopic images of sectioned tumor liver and kidney at various time of post injection. The presence of intense green fluorescence from these sections indicates the accumulation of the targeted polymers in the tissue. Figure 56&57 indicates the accumulation of targeted polymers in the tumor at 2^{nd}, 4^{th}, 6^{th} and 24^{th} hour of post injection. It is interesting to note that just 2 h post i.v. injection the active targeting effect was obvious. Similar results are observed at 4^{th} and 16^{th} h also. But in agreement with the in vitro clearance experiment illustrated in Figure 55, low level of fluorescence is observed at 24^{th} h. Moderate to high level of fluorescence in liver at 16 h and kidney at 24 h indicates detoxification and renal excretion of the polymer from the blood.

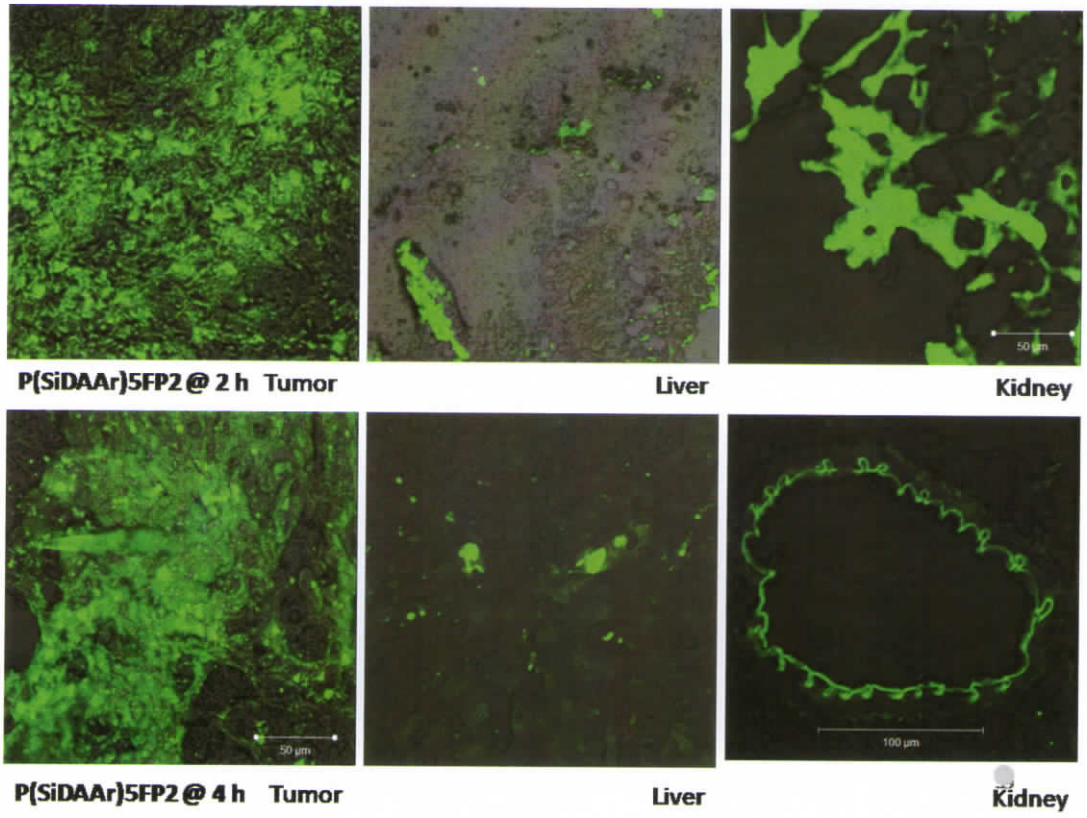

Figure 56: Confocal microscopic images of sectioned tissues at 2 h and 4 h post injection of FITC stained P(SiDAAr)5FP2.

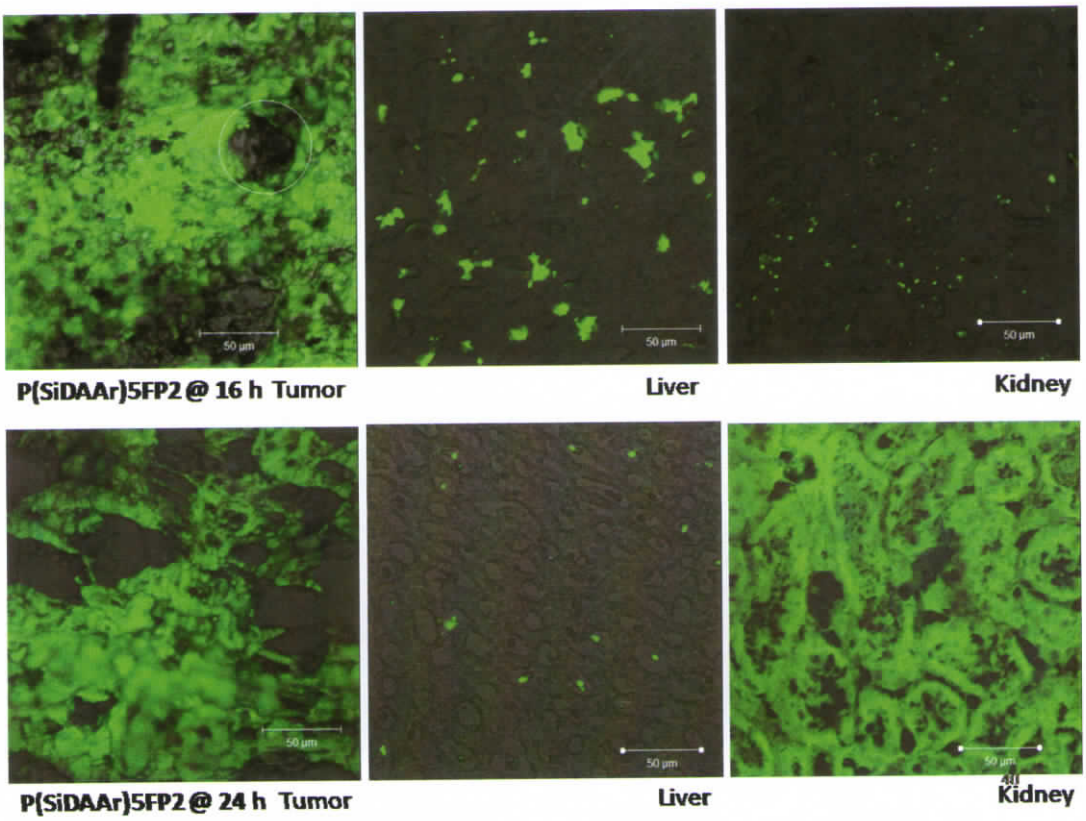

Figure 57: Confocal microscopic images of sectioned tissues at 16h and 24 h post injection of FITC stained P(SiDAAr)5FP2.

This means that the targeted polymer accumulated in the tumor tissues may start clearance from 24 h onwards. While in the case of non- targeted polymers low level of tumor accumulation is observed from 4^{th} and 16^{th} h and almost total clearance was seen at the 24^{th} h (Figure 58). This may be due to the immediate clearance of the majority of the non- targeted polymer in absence of PEG group.

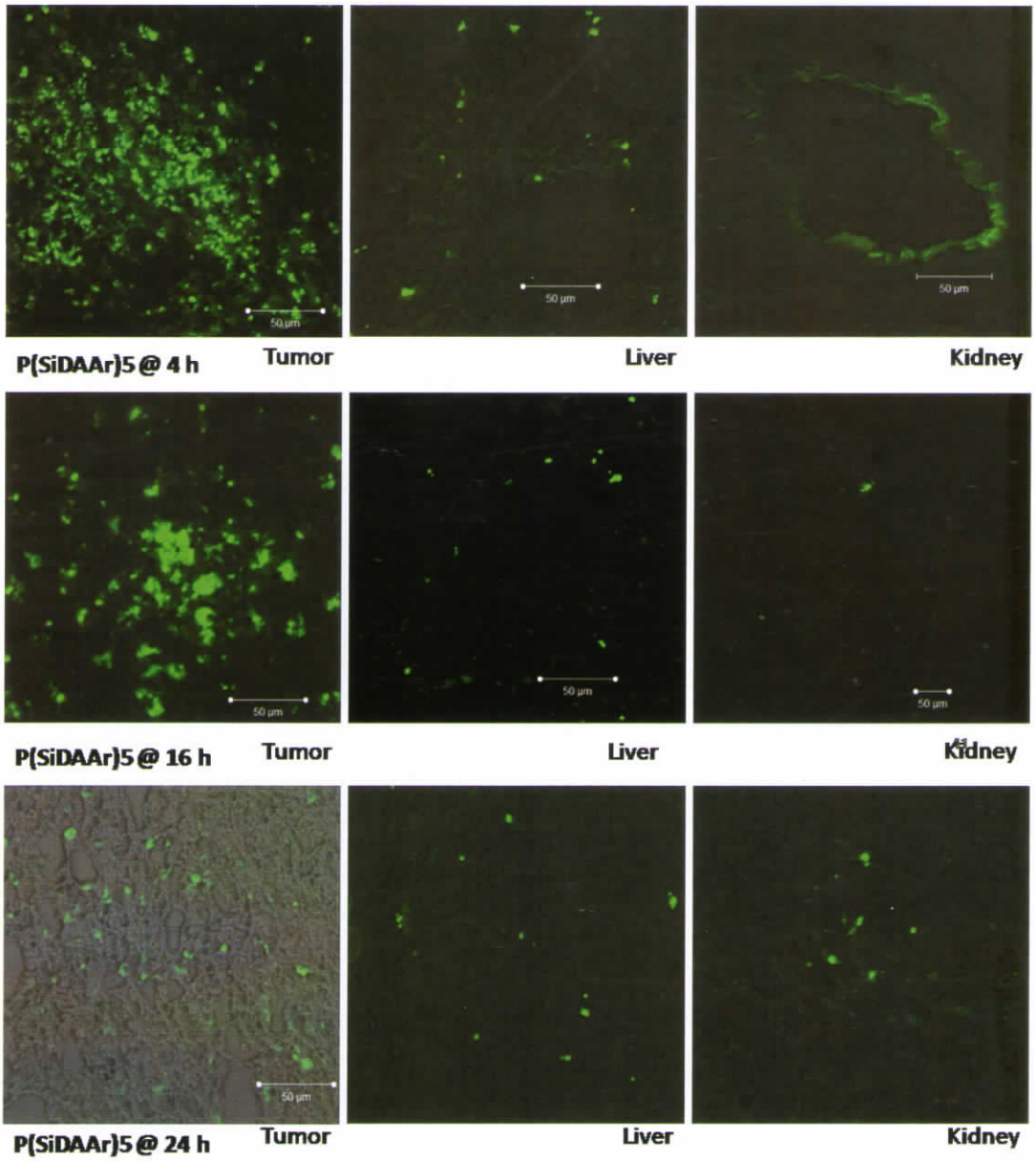

Figure 58: Confocal microscopic images of sectioned tissues at 4 h, 16 h and 24h post injection of FITC stained P(SiDAAr)5 as control polymer.

Besides the tumor accumulation a slow diffusion of the derivative across endothelium, moving out of the endothelial cells into the vascular lumen was observed in kidney at 4^{th} h and tumor at 24^{th} h (Figure 56). Fig. 59 showed the depth scan analysis with serial confocal slices of tumor at 24^{th} h, which clearly depicts the diffusion of derivative across the endothelium. Even though there is a structural difference between the brain capillaries and the non-brain capillary endothelium associated with the endothelial tight junctions (Kaur, Bhandari, Bhan-

dari & Kakkar 2008), we have tried the possibility of the derivatives to cross the blood brain barrier (BBB). Interestingly, we found that the material gets transported across the barrier and reaches the brain (Figure 60). This may be the combined effect of arginine moiety, which enables cellular uptake and long circulation time of PEG-FA. Further scientific research is going on in this area.

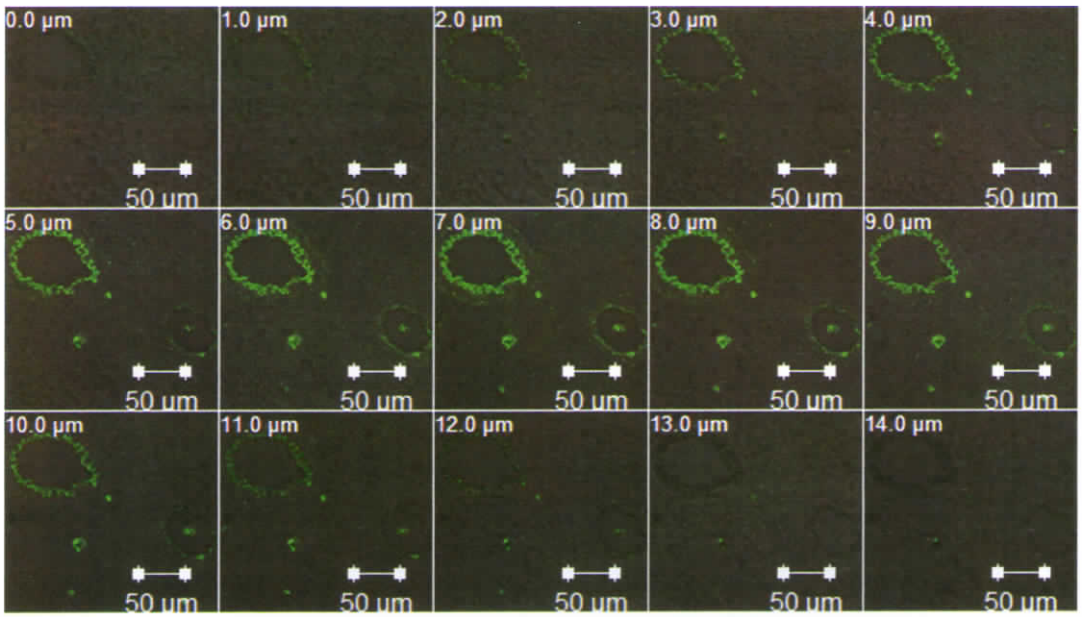

Figure 59: Serial depth scan confocal image of sectioned tumor at 24 h post injection of FITC stained P(SiDAAr)5FP2.

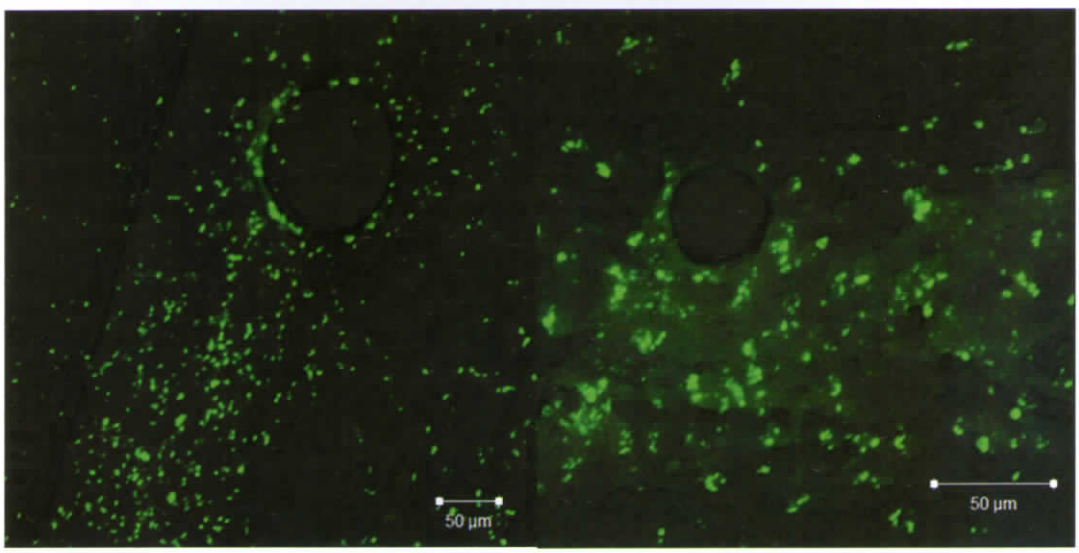

Figure 60: Confocal microscopic image of sectioned brain at 4h post injection of FITC stained P(SiDAAr)5FP2.

5 DISCUSSION

The development of safe and efficient gene delivery vectors is a prerequisite for the treatment of human genetic and acquired diseases. Non- immunogenicity, unrestricted plasmid size, and possibility of repeated administration makes non-viral gene delivery systems a safer alternative to viral vectors (Yamanouchi et al. 2008) (Pouton & Seymour 2001). Ligand targeted gene therapies offer several advantages such as site specific delivery of the gene in high concentration, receptor mediated endocytosis, flexibility and adaptability over conversional non targeted therapies (Xia & Low 2010) (Beduneau, Hindre, Clavreul, Leroux, Saulnier & Benoit 2008) (Chan et al. 2007). Since the reduced form of folic acid (Vit. B9) is essential for rapidly dividing cells including cancer cells for numerous bodily functions, an elevation in the appetite for physiological folates permit the cells to over express folate receptors (Leamon & Low 2001). Many human tumors including cancers of the brain, lung, ovary, uterus, kidney, testis, colon and myelocytic blood cells, are over expressed by folate receptors (Parker, Turk, Westrick, Lewis, Low & Leamon 2005) (Park, Lee & Lee 2005*a*). Similarly, folate receptor density appears to increase as the stage or grade of the cancer worsens. These factors enlighten the use of folate mediated gene delivery vectors in the treatment of cancers which are difficult to treat by classical methods. The conjugation of folic acid (FA) ligand to neutral polymer like poly (ethylene glycol) (PEG) assists in the achievement of both systemic stability and tumor targeting simultaneously (Zhao & Lee 2004). Therefore, in the present study we have used PEG-FA conjugation of a cationic polymeric system based on natural and synthetic polymers. From the physicochemical and biological characterisations, we have comparatively evaluated significance of natural and synthetic polymeric vectors for tumor targeted gene delivery.

5.1 Synthesis and Characterisation of Natural Polymer based Nanoparticles.

5.1.1 Synthesis and characterisation of ATMC and HTMC derivatives.

Among the cationic polymeric vectors, chitosan was found to be an attractive vector for gene delivery because of its high positive charge density and relatively low cytotoxicity. The transfection efficiency of chitosan depends on various factors such as molecular weight, de-

gree of deacetylation, and pH of the transfecting medium. In our previous studies, we have observed that chitosan with medium molecular weight (49-51 kDa) and high degree of deacetylation (DD) provided stable uniform sized nanoparticles, whereas low molecular weight chitosans in spite of having good affinity towards DNA, formed aggregates easily (Morris, Neethu, Abraham, Pillai & Sharma 2009). However, reduction in aggregation tendency of chitosan at low molecular weight by quaternization was shown by Germershaus et al. (Germershaus et al. 2008*a*). Several advantages of trimethylation including increase in solubility over a wide range of pH has been limited by toxicity (Germershaus et al. 2008*a*). In view of the above studies, the molecular weight range and degree of trimethylation was optimized in order to induce further modifications. In the present work, the creation of an effective gene delivery vector has been explored by coupling arginine (Morris & Sharma 2010*c*) and histidine (Morris & Sharma 2010*b*) residues onto the trimethylated chitosan derivatives. The main objective of arginine modification on complexation with DNA was to enhance cellular uptake which resulted in increased transfection efficiency (Choi et al. 2004). In several approaches, modification of amino groups of polymer using histidine or other imidazole containing structures showed a significant enhancement of gene expression compared to the parent polymer (Midoux & Monsigny 1999) (Lo & Wang 2008). Arginine and histidine were effectively conjugated to trimethylated depolymerised chitosan (TMC) using NHS/EDC chemistry. TMC derivatives of varying in molecular weight such as 125, 85, 50 and 15 kDa (chito 125, chito 85, chito50 and chito15 respectively) were obtained by depolymerization of the high molecular weight chitosan using sodium nitrite (Mao et al. 2004). The formations of the products were confirmed by using TNBS method, IR and NMR spectra.

One of the most important requirements for gene delivery is the formation of complex nanoparticles using the cationic polymers and plasmid DNA. Thus, several parameters affecting the complex formation of the vector with plasmid DNA were examined. Surface charges and size are the two important properties necessary to assure nanoparticles uptake by cells. It was reported that cells typically take in particles ranging from about 50 to several hundred nano meters (Lu, Wang, Wu, Li, Zhang & Zhuo 2009). From the particle size and zeta potential result of ATMC and HTMC derivatives in table 2 and 3, it was observed that at N/P=1 all the

derivatives showed very large size. At this ratio, for all the derivatives, the zeta potential was found to be almost zero. This effect might probably be due to the "re-entrant condensation" and "charge "inversion" (Bordi, Cametti, Sennato & Viscomi 2007) occurring in polyion induced aggregation. The ratio at which lowest size and high positive charge observed were considered as optimum for further studies. For all the ATMC and HTMC derivatives, N/P=3 and 2.5 respectively was found to be optimum.

For inducing tumor targeting property, the derivatives having highest transfection efficiency have been selected out of all ATMC and HTMC derivatives. Transfection studies were performed on KB oral epidermoid cells by using pGL3-Luc as reporter genes in presence of 10% serum. Out of ATMC and HTMC derivatives, histidine modified chitosan having low molecular weight and highest trimethylation (ATMC15H and HTMC15H) was found to have highest transfection compared to all the other derivatives (Figure 8). Since this result was in good agreement with the literature (KÃping-HÃggÃrd et al. 2004) we have selected those derivatives for further modification.

5.1.2 Synthesis and characterization of ATFP15H and HTFP15H derivatives.

In order to introduce tumor targeting efficiency PEG-FA was effectively conjugated to ATMC 15H and HTMC15H derivative by DCC/NHS chemistry. The ^{1}HNMR and IR spectra confirm the conjugation of PEG-FA group with the ATMC and HTMC derivative. According to proton sponge mechanism, cationic polymers like PEI are assumed to induce endosomal escape due to the uptake of protons by the amino groups and overall increase in gene transfection efficiency (Lu et al. 2009). One of the important factors is that the high density of primary, secondary and tertiary amino groups, which exhibiting protonation only on every third or fourth nitrogen at pH 7 confers significant buffering capacity to the polymers over a wide pH range. By introducing quaternisation and arginine and histidine conjugation in chitosan, the presence of primary secondary and tertiary amino groups in the molecule increases which promotes the buffering capacity of the polymer. However, it was very interesting to observe that the HTFP derivative showed much greater buffering capacity compared to PEI than ATFP derivatives.

The particle size and zeta potential of ATFP and HTFP derivative was shown in Figure 12 A&B. At N/P=1 the nanoparticles showed very larger size and slight negative charge. On

increase in charge ratio, the particle size reduced to optimum value. The size of the complexed nanoparticles was confirmed using TEM micrographs (Figure 12 C&D). TEM micrographs also revealed the morphology of the nanoparticles. The particles were found to be well known core shell nanostructure having size less than 100 nm.

Physical integrity of the DNA after complexation is a prerequisite for biological activity of the DNA to mediate successful transfection. The ability of ATFP 15H and HTFP15H derivatives to form complexes with DNA was confirmed by gel retardation assay. From the Figure 13A&B it was observed that ATFP 15H and HTFP15H derivative retard the plasmid DNA effectively from N/P ratio of 1.5 and 2 and onwards respectively. This result was in good agreement with the zeta seizer measurement. For a useful gene delivery system, the carriers must be able to protect DNA from degradation by cellular nucleases abundant in serum and extracellular matrix. From Figure 13C&D it was clear that from N/P=2 onwards the ATFP 15H and HTFP15H derivative could protect the DNA from degradation by DNase I. Figure 13C&D also revealed the effect of protection of ATFP 15H and HTFP15H derivatives from disassembly of nanoparticles by the influence of negatively charged plasma protein. When artificial materials were exposed to fluids such as plasma and serum, proteins adsorbed on the surface of the material. It may cause the disassembly of the complexed nanoparticles unless the polymer derivatives are effective for protection. So the aim of our study was to find out any disassembly in the complex in the presence of this negatively charged protein. From Figure 13C&D, it is clear that even after 2 h, the ATFP15H and HTFP15H derivative protected the nanoparticles from disassembly of the complex.

In vitro erythrocyte-induced hemolysis is considered to be a simple and reliable measure for estimating blood compatibility of materials (Lee et al. 2004). The behaviour of ATFP15H and HTFP15H/pDNA nanoparticles *in vivo* can be predicted by examining the degree of hemolysis *in vitro*. The results (Figure 14 & 15) revealed that due to PEGylation, both ATFP15H and HTFP15H derivatives become more compatible with erythrocytes than that of the parent polymers. So the derivative was further examined for erythrocyte aggregation platelet activation and complement activation studies. The nanoparticles induced aggregation of erythrocyte under in vitro conditions was analyzed as a prerequisite for the intravenous administration of

complexed nanoparticles in animals or humans. The ATFP15H and HTFP15H derivative again showed minimal aggregation potential. It is again reported that cationic polymers induce activation of platelets. The results of platelet activation and complement activation also revealed the negligible activation of platelets and complements. So the enhanced blood compatibility of ATFP15H and HTFP15H derivatives in terms of hemolysis, erythrocyte aggregation platelet activation and complement activation compared to the parent compound ATMC15H, HTMC15H and the positive control PEI might be due to the presence of PEG which protects the cationic sites from interacting with the blood components.

It is reported that cytotoxicity of gene delivery carriers is known to arise from the accumulation of non-degraded and non-discharged polymers with large molecular weight and charge (Lu et al. 2009). MTT assay was used to investigate the cytotoxicity of ATFP15H and HTFP15H derivatives in the KB cell lines. The improvement in cell viability of the derivatives compared to the control and the parent compounds may again be due to the presence of PEG which reduces the interaction of amine groups with external macromolecules or surfaces (Figure 16 & 17).

To investigate in vitro gene transfer capability of ATFP15H and HTFP15H derivatives, transfection studies were performed on KB oral epidermoid cells by using pGL3-Luc as reporter genes in presence of 10% serum. FR-expressing KB cells were used as these cell lines are commonly used for folate targeting (Benns et al. 2002) (Yang, Li, Zhou, Yuan & Li 2004). The gene transfection activity of the polymers was evaluated in terms of luciferase assay, which is a more sensitive method than fluorescence intensity determination (Lu et al. 2009). PEI (25 kDa) has been considered to be the highly effective cationic gene vector, which was used as the control in order to compare the gene transfection efficiency with other non-viral gene vectors. Superfect, a commercially available gene transfecting reagent, was also used as the control. Culture with excess of free folic acid was used as the negative control over the culture without free folic acid. From the Figure18A&B the ATFP15H and HTFP15H derivatives showed one and two orders of magnitude more transfection than ATMC15H and HTFP15H with excess folic acid respectively. This decrease in transfection may due to the competitive displacement of the nanoparticles on the folate receptors by excess of free folic acid. In order to confirm the rapid

cell internalisation efficiency of targeting group, it was examined using confocal microscopy. Figure 18C&D showed rapid cell internalisation of ATFP15H and HTFP15H compared to non targeted derivatives. From the flow cytometric analysis given in Figure 19 and Figure 20 revealed the folic acid induced targetability of the ATFP15H and HTFP15H derivative. In the case of ATFP15H derivative reduction in cellular uptake compared to non- targeted polymers were less than the HTFP15H derivatives. The result was in good agreement with the finding of Kim et al. (Kim et al. 2007*b*). They reported that the arginine conjugated polyplexes undergo cellular uptake leading to effective transfection by multiple pathway. Therefore by modification of the ATMC derivative by folic acid, one more pathway for cellular uptake is opened. It is also reported that PEGylation led to improved colloidal stability of polyplexes which gives rise to significant increase in cellular uptake compared to unmodified trimethyl chitosan (Jayakumar, Chennazhi, Muzzarelli, Tamura, Nair & Selvamurugan 2010). Since the folic acid conjugated to the ATMC15H derivative through PEG chain, the colloidal stability and thereby cellular uptake is enhanced.

Again from the Figure 19B and 20B, the derivative showed the high level of localisation of plasmid DNA inside Hoechst 33342 stained nucleus after 6th hour of transfection. Since the folic acid conjugated derivatives has very good endosomal disruption capacity, it may go through rapid endosomal escape and nuclear uptake.

From the above studies it can be concluded that both ATFP15H and HTFP15H derivatives exhibited endosomal disrupting capacity more than that of PEI. Due to the presence of PEG group, both the derivatives were found to be compatible with blood in terms of percentage hemolysis, and erythrocyte aggregation. The PEG group could also improve the colloidal stability of polyplexes and cell viability to an extent of greater than 125% compared to control at the concentration of 10 μg of the derivative. Finally due to the large extent of cellular uptake and nuclear trafficking, ATFP15H and HTFP15H derivatives were found to exhibit improved transfection efficiency in KB cell lines even in the presence of 10% serum compared to native polymers as ATMC15H and HTMC15H respectively. The outstanding characteristics observed for ATFP15H derivative was itsmembrane permeabilityand nuclear localization ability. Similarly, HTFP15H derivative was characterised by its enhanced buffering capacity. Even though the

derivatives exhibited better systemic stability and cell viability, the transfection efficiency of both the polymers were not better than the control PEI.

5.2 *Synthesis and Characterisation of Synthetic Polymer based Nanoparticles.*

Polyethyleneimine (PEI) is regarded as the most effective one among non-viral vectors (Deng et al. 2009). But the major drawbacks of PEI are its non-degradability, cytotoxicity and aggregation. High transfection efficiency of PEI, along with its cytotoxicity strongly depends on its molecular weight. The commercially available branched PEI having a molecular weight of 25 kDa, has been widely used as "gold standard", but high toxicity of this homopolymer strictly limits its application in gene therapy (Yang et al. 2007). Many studies have been attempted to reduce its cytotoxicity and maintain the transfection efficiency. Several research groups have been reported the advantages of mesoporous silica matrix in carrying, protecting and releasing large amounts of genes (Slowing et al. 2007) (Rosenholm et al. 2007). Similarly numerous studies conducted by conjugating arginine residues on polymers and dendrimers for enhancing their transfection efficiency (Zhao & Weissleder 2004) (Tung & Weissleder 2003).

5.2.1 Synthesis and characterisation of P(SiDAAr)n and P(SiDAHs)n derivatives.

A non-viral system have been designed comprising reduced toxicity and adsorptive endocytosis of siloxane derivative, endosomal disrupting capacity of branched PEI, along with membrane permeability and nuclear localization ability of arginine or histidine residues. Our objective has been attained by the synthesis of arginine or histidine modified oligo- (alkylaminosiloxane) and its conjugation with PEI at different compositions (Figure 61). Formation of the derivatives were confirmed by structural characterisations like IR, ^{1}H NMR, by analysing thermal behaviours using DSC, and also by estimating molecular weight using GPC. From TNBS and fluorescamine assay, it was observed that P(SiDAAr)1 has the highest percentage of free primary amino groups compared to all other arginine and histidine conjugated derivatives. The decrease in percentage of free amino groups at higher composition of siloxane derivatives may due to the conjugation of siloxane derivatives on the primary amino groups of PEI.

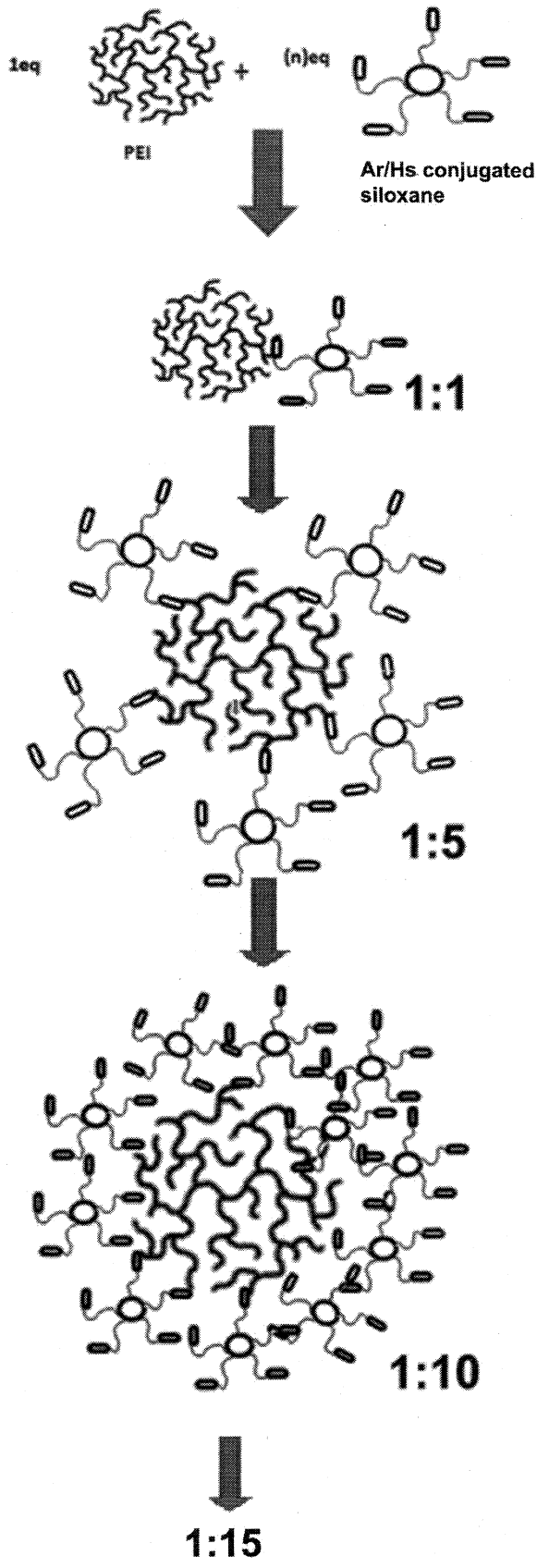

Figure 61: The synthetic scheme of P(SiDAAr)n/ P(SiDAHs)n derivatives.

Physicochemical properties of the nanoparticles with DNA were thoroughly characterised. The positive charge of the polymer-pDNA nanoparticles acts as the driving force for the complex to interact with cells (Nishikawa & Huang 2001). From the fluorescamine assay after DNA complexation and also by zeta potential determination it was evident that derivatives exhibited high positive charge density at high weight ratios with DNA. In addition to charge, the size of the polymer- pDNA complex is of crucial importance to tissue distribution, cellular uptake and nuclear entry. It is reported that the transport of nucleic acid through cytoplasm depends mainly on the size and spherical structure of the molecule (Ward, Read & Seymour 2001). The particle size determination by DLS and TEM micrographs revealed the formation of uniform sized nanoparticles by the derivatives. It is also reported that the delivery of polycation/DNA nanoparticles into the cells via endocytosis or pinocytosis requires the order of the particle size to be 200 nm or less (Wolfert & Seymour 1996). Based on the above report, the polyplexes thus prepared were found to be appropriate for cell entry.

Physical integrity of the DNA after complexation is a prerequisite for the biological activity of DNA to mediate successful transfection. From the gel electrophoretic shift assay, it was found that all the derivatives could retard and protect the DNA. Out of all the arginine and histidine conjugated derivatives P(SiDAAr)5 was found to protect DNA from weight ratio of 0.25 onwards.

The toxicity studies by MTT assay revealed that nanoparticles P(SiDAAr)5 with DNA was least toxic compared all other derivatives. In the case of arginine conjugated derivatives, again on increasing the arginine conjugated siloxane to PEI increases the toxicity and a reverse pattern is observed in the case of histidine conjugated derivatives. Therefore in the case of hystidylated derivatives the nanoparticles of P(SiDAHs)15 was found to be least toxic. The first result was in good agreement with the report by Kichler et al. They demonstrated that large amount of aminosilicons resulted in an increased cytotoxiciy (Kichler et al. 2003).

In order to find out the best polymeric vector for gene delivery application, transfection efficiency of all the P(SiDAAr)n and P(SiDAHs) polymers were evaluated in KB oral epidermoid cells and HeLa cell lines using pGL3 and pEGFP reporter genes respectively. Superfect and branched PEI (25 kDa) has been considered to be the highly effective cationic gene vec-

tor, which was used as the control so as to compare gene transfection efficiency with other non-viral gene vectors. Amount of luciferase protein expressed in terms of relative luminescence units which is a more sensitive method than fluorescence intensity determination (Lu et al. 2009). From the results, it is observed that arginine moiety enhances the transfection efficiency otherthan histidine. In other words, histidine itself does not create any improvement in transfection efficiency. Therefore as the composition of histidine conjugated siloxane increases, transfection efficiency also decreases. While in the case of arginine conjugated siloxane, at a composition of 1:5 the derivative P(SiDAAr)5 showed around 150% more transfection comared to the control PEI (Morris & Sharma 2010*a*). Again on increasing the arginine conjugated siloxane transfection efficiency slightly reduced. It may be due to increase in toxicity. The enhanced transfection efficiency of arginine conjugated polymers compared to PEI in presence of serum was also reported earlier (Choi et al. 2004) (il Kim et al. 2009). From the above results, it was assumed that the enhanced transfection activity may be due to the uniformly distributed arginine residues via the siloxane arms present on the surface of the PEI molecule as represented in Figure 61.

To confirm arginine and histidine mediated cellular uptake pathway leading to enhanced transfection efficiency compared to native PEI, we performed transfection experiment on KB cells by treatment with various cellular uptake inhibitors and compared the result. Genistein is reported to inhibit caveolae-mediated uptake processes (Liu & Anderson 1999). Wortmannin is an inhibitor of phosphatidyl inositol-3-phosphate (PI3) kinase competing macropinocytosis (GonÃalves, Mennesson, Fuchs, Gorvel, Midoux & Pichon 2004) and chlorpromazine is known to block clathrin-mediated endocytosis (Wang, Rothberg & Anderson 1993). The result was found to be in good agreement with the report by Kim et al (Kim et al. 2007*a*). They stated that the cellular uptake leading to effective transfection of arginine grafted polyplexes is not dependent on any exclusive pathway but has the possibility of a combination of multiple pathways. From the enhanced transfection efficiency of arginine conjugated polymers compared to histidine modified polymers it was demonstrated that apart from membrane permeability, nuclear localisation is another exceptional feature. (il Kim et al. 2009) (Morris & Sharma 2010*c*).

5.3 Synthesis and Characterization of Targeted Derivatives of Synthetic Polymers.

5.3.1 Synthesis and characterisation of P(SiDAAr)5FPn / P(SiDAHs)1FPn and its nanoparticles with DNA.

In order to induce targeting ability we have selected one derivative from each group of arginine and histidine modified siloxane conjugated PEI derivatives. Thus P(SiDAAr)5 and P(SiDAHs)1 were selected depending on their enhanced targeting ability compared to other members of each group. The derivatives were conjugated with PEG-FA by keeping the composition of P(SiDAAr)5 and P(SiDAHs)1as constant and varying the composition of PEG-FA. Two derivatives from each group were prepared such as P(SiDAAr)5FP2, P(SiDAAr)5FP3, P(SiDAHs)1FP2 and P(SiDAHs)1FP3. Formation of the products were characterised and confirmed by IR,NMR, DSC and also by the determination of primary amino groups. The polymer complexed the DNA into uniformly shaped positively charged nanoparticles which was evaluated by dynamic light scattering techniques and confirmed by AFM analysis. It has been reported that the nanoplexes at around 200 nm or less is appropriate for cellular entry via endocytosis or pinocytosis (Kichler et al. 2003). Therefore, nanoparticles formed by the interaction of targeted derivatives with DNA are suitable for the cellular entry. All the targeted derivatives retard and protected DNA at its optimum weight ratios. While compared to arginine modified siloxane derivatives, histidine modified siloxane derivatives exhibited high erythrocyte lysis. Therefore RBC aggregation studies were performed only with arginine modified siloxane derivatives. From the microscopic results it was observed that P(SiDAAr)5FP2 showed less erythrocyte aggregation than P(SiDAAr)5FP3.

Even if the branched PEI having a molecular weight of 25 kDa, has been widely used as "gold standard", toxicity of this homopolymer strictly limits its application in gene therapy (Yang et al. 2007). Cell viability studies of the targeted derivatives using MTT assay revealed least toxicity of the targeted derivatives compared to the parent derivatives. The increased cell viability of the targeted polymers may be due to the presence of PEG group which reduces nonspecific interaction of positively charged amino groups with cellular components and surfaces (Park, Han, Han, Cho, Nah, Choi & Cho 2005*b*).

Transfection efficiency of the targeted derivatives was evaluated in terms of luminescence

and green fluorescence expression. KB and SiHa cell lines were used for the study. Since KB cells lines over expressed the folate receptors, targeted derivatives exhibited more gene expression than the SiHa cell lines. However, irrespective of the parent polymers, targeted derivatives were less toxic in KB cell lines than in SiHa cell ines. Therefore the parent polymers were found to exhibit more gene expression in KB than in SiHa cells. Based on the pGL3 expression P(SiDAAr)5FP2 from arginine group and P(SiDAHs)1FP3 from histidine group were selected for GFP expression studies in KB cell lines. The confocal micrographs revealed that irrespective of the number of activated cells, more protein was produced by the targeted polymer. Out of two targeted derivatives, arginine modified siloxane derivative was found to be more appropriate for further analysis.

The polymer degradation and clearance of the polymer from the cell is very important for safe and efficient gene delivery. This leads to the reduction of cytotoxicity due to easy elimination by excretion pathway (Park et al. 2005*b*). Therefore the cellular uptake and its clearance of the targeted polymers were evaluated at 4, 24 and 48 h of post incubation of the FITC tagged nanoparticles in KB cell lines. From the results it is observed that both the P(SiDAAr)5FP2 and P(SiDAHs)1FP3 derivative enters into the cell as well as into the nucleus at 4^{th} hour of post incubation. More clearance from 24^{th} hour was observed for P(SiDAAr)5FP2 derivative than that of P(SiDAHs)1FP3. At 48^{th} hour, almost all the arginine conjugated derivatives cleared from the nucleus as well as from the cell. Therefore once again arginine conjugated derivative was found to be appropriate vector for further gene delivery studies.

In our previous report, we established that the enhanced transfection efficiency of the P(SiDAAr)5 polymer was due to the cellular uptake of the polymer by multiple pathway (Morris & Sharma 2010*a*). The result was in good agreement with the earlier report by Kim et. al, as stated that the arginine grafted polyplexes has the ability to enter the cells through multiple pathways (Kim et al. 2007*a*). Genistein is reported to inhibit caveolae-mediated uptake processes. Wortmannin is an inhibitor of phosphatidyl inositol-3-phosphate (PI3) kinase competing macropinocytosis and chlorpromazine is known to block clathrin-mediated endocytosis. Similarly, folic acid is expected to inhibit folate receptor mediated endocytosis (Rosenholm et al. 2009). Arginine and histidine conjugated targeted derivatives were used for the study. From

the results it was observed that both the targeted derivatives undergoes cellular uptake mainly by folate receptor mediated pathway than the other pathways.

5.4 *In Vitro and In Vivo Tumor Targeting of P(SiDAAr)5FP2 Derivative.*

Since the arginine conjugated derivatives were found to be more suitable gene delivery vector compared to histidine conjugated derivatives based on the blood compatibility, transfection, cellular uptake and its clearance studies P(SiDAAr)5FP2 derivative was taken for *in vitro* and *in vivo* tumor targeting experiments. From the various *in vitro* tumor targeting experiments, it is observed that the cellular uptake of P(SiDAAr)5FP2 derivative was mediated by folate receptors. In order to establish folate receptor mediated tissue targeting of P(SiDAAr)5FP2 derivative, *in vivo* experiments were conducted on tumor bearing Balb/c mice using FITC tagged P(SiDAAr)5FP2 derivatives. Balb/c mice bearing 14-21 days of tumor was injected with tagged P(SiDAAr)5FP2 derivatives. Non targeted P(SiDAAr)5 parent polymer was used as control.

From the confocal micrographs, it was observed that high accumulation of the targeted polymers at the tumor site from second hour onwards compared to the non- targeted polymers. In the case of non- targeted polymers, very low level of tumor accumulation was observed at 4^{th} hour onwards. Even at 16^{th} and 24^{th} hour also tumor accumulation of the non-targeted polymer was very low compared to targeted polymers. In the case of targeted polymers, tumor accumulation was maintained even at 24^{th} hour also. The low level of accumulation at 4^{th} and 16^{th} h may be due to the low concentration of polymer which undergoes recirculation and several passages before accumulating in the tumor (Park et al. 2005*b*). From these results, it can be concuded that the PEG group of the targeted polymer provides enhanced systemic residence time in the blood stream (Kim et al. 2007*a*) and folic acid facilitate receptor binding targeting, which in together enables high level of tumor accumulation.

Moderate to high level of fluorescence in liver at 16 h and kidney at 24 h for targeted derivatives indicates detoxification and renal excretion of the polymer from the blood. This result indicated the slow clearance of the derivative from the tumor. As observed from the in vitro particle clearance experiment the derivative exhibited tissue clearance from 16- 24 h onwards.

Besides the tumor accumulation the fluorescence observed at of vascular luman may be due to the diffusion of the derivative across the endothelial cell barrier. Depth scan analysis with serial confocal slices or tumor at 24 h also clearly depicts the diffusion across the endothelium. Since this property of the derivative may be useful for the targeting of brain by diffusing through the blood brain barrier, we tried the possibility of the derivatives to cross the blood brain barrier (BBB). Interestingly, we found that the material gets transported across the barrier and reaches the brain. This may be the combined effect of arginine moiety, which enables cellular uptake and long circulation time of PEG-FA. Further scientific research is going on in this area.

From all these studies we concluded that the spatially oriented arginine moiety in arginine modified oligo (alkylaminosiloxane) graft poly (ethyleneimine) enables the cellular and nuclear uptake of the derivative. The incorporation of PEG group aid long circulation time *in vivo*, and folic acid facilitate tumor targeting. The combination of all these properties in good harmony resulted in a promising tumor targeted gene delivery vector having enhanced transfection efficiency and biocompatibility for future cancer gene therapy.

6 SUMMARY AND CONCLUSION

Delivery vectors having targeting ligands provide an imminent impact on cancer gene therapy. Targeted gene delivery enables both site specificity and cellular entry by receptor mediated endocytosis. Folate receptor mediated gene targeting provides several advantages such as delivery of high concentration of gene at specific tumor sites including brain, lung, ovary, uterus and kidney where folate receptors are over expressed. In the present study, to attain both systemic stability and tumor targeting ability, poly(ethylene glycol)-folic acid (PEG-FA) conjugate was coupled with an arginine or histidine modified natural as well as synthetic polymers. The resulting derivatives have been comparatively evaluated physicochemically and biologically in order to discover an efficient tumor targeted gene delivery vector having superior qualities.

As a natural polymer based gene delivery vector, poly(ethylene glycol)-folate (PEG-FA) was conjugated with arginine or histidine modified chitosan polymer having low molecular weight of 15 kDa and high degree of quaternisation (ATFP15H/HTFP15H). For that initially native chitosan was depolymerised and quaternised at varying degrees and modified with arginine and histidine. From the resultant derivatives, a low molecular weight polymer with high degree of trimethylation (ATMC15H/ HTMC15H) showed high transfection efficiency compared to medium and high molecular weighed chitosans, which was selected for PEG-FA conjugation. FTIR and ^{1}HNMR spectra proves the conjugation of PEG-FA group. Acid-base titration experiments reveals the endosomal disrupting capacity of ATPF15H/ HTMC15H derivatives similar to PEI. From the dynamic light scattering measurement and transmission electron micrographs it was clear that the derivatives were able to condense the plasmid DNA effectively and form positively charged core-shell nano-structured particles having a size of less than 100 nm. The derivatives was found to protect DNA from DNase I degradation and also from disassembly in presence of negatively charged plasma proteins. Due to the presence of PEG group the ATFP15H/HTFP15H derivatives was found to be compatible with blood in terms of percentage hemolysis, erythrocyte aggregation and also by platelet activation. At a concentration of 10 μg, the capability of the derivatives to enhance cell growth at normal cell growing conditions was observed. The transfection efficiency was also found to be comparable to PEI

6 SUMMARY AND CONCLUSION

Delivery vectors having targeting ligands provide an imminent impact on cancer gene therapy. Targeted gene delivery enables both site specificity and cellular entry by receptor mediated endocytosis. Folate receptor mediated gene targeting provides several advantages such as delivery of high concentration of gene at specific tumor sites including brain, lung, ovary, uterus and kidney where folate receptors are over expressed. In the present study, to attain both systemic stability and tumor targeting ability, poly(ethylene glycol)-folic acid (PEG-FA) conjugate was coupled with an arginine or histidine modified natural as well as synthetic polymers. The resulting derivatives have been comparatively evaluated physicochemically and biologically in order to discover an efficient tumor targeted gene delivery vector having superior qualities.

As a natural polymer based gene delivery vector, poly(ethylene glycol)-folate (PEG-FA) was conjugated with arginine or histidine modified chitosan polymer having low molecular weight of 15 kDa and high degree of quaternisation (ATFP15H/HTFP15H). For that initially native chitosan was depolymerised and quaternised at varying degrees and modified with arginine and histidine. From the resultant derivatives, a low molecular weight polymer with high degree of trimethylation (ATMC15H/ HTMC15H) showed high transfection efficiency compared to medium and high molecular weighed chitosans, which was selected for PEG-FA conjugation. FTIR and ^{1}HNMR spectra proves the conjugation of PEG-FA group. Acid-base titration experiments reveals the endosomal disrupting capacity of ATPF15H/ HTMC15H derivatives similar to PEI. From the dynamic light scattering measurement and transmission electron micrographs it was clear that the derivatives were able to condense the plasmid DNA effectively and form positively charged core-shell nano-structured particles having a size of less than 100 nm. The derivatives was found to protect DNA from DNase I degradation and also from disassembly in presence of negatively charged plasma proteins. Due to the presence of PEG group the ATFP15H/HTFP15H derivatives was found to be compatible with blood in terms of percentage hemolysis, erythrocyte aggregation and also by platelet activation. At a concentration of 10 μg, the capability of the derivatives to enhance cell growth at normal cell growing conditions was observed. The transfection efficiency was also found to be comparable to PEI

when transfected in KB cell line, which over expressed the folate receptor (FR) in presence of 10% fetal bovine serum (FBS). On comparison with native chitosan and trimethylated chitosan, ATFP15H/HTFP15H derivative exhibited high cellular uptake and nuclear localization. This has been ascertained by flow cytometry and YOYO labelling of plasmid DNA. From all the above characterisations the outstanding characteristics observed for ATFP15H derivative was its membrane permeability and nuclear localization ability. Similarly, HTFP15H derivative was characterised by its enhanced buffering capacity. Even though the derivatives exhibited better systemic stability and cell viability, the transfection efficiency of both the polymers were not better than the control PEI.

In order to attain high transfection efficiency by maintaining the above mentioned features of arginine and histidine, a synthetic polymer PEI based tumor targeted gene delivery system have been developed. Branched poly ethyleneimine (PEI) has been considered as the most efficient non-viral gene transfection agent. However its clinical application is confined due to its cytotoxicity. In the present study we tried to enhance the transfection efficiency and reduce the toxicity of PEI by conjugating it with arginine or histidine modified oligo(-alkylaminosiloxane) [P(SiDAAr)n/ P(SiDAHs)n]. P(SiDAAr)n/P(SiDAHs)n has been synthesised by simple reproducible reaction methods. Four products from each group were prepared using varying composition of SiDAAr/ SiDAHs, by keeping the composition of PEI as constant. All the derivatives were examined physicochemically and biologically. The experimental data demonstrated that the P(SiDAAr)n/ P(SiDAHs)n derivatives formed uniform sized nanoparticles with plasmid DNA, as evident by AFM and TEM analysis. The polymers could complex DNA very well and retard its migration during electrophoretic shift assay even at low weight ratios. Out of four derivatives from arginine conjugated siloxane group, the nanoparticles of the P(SiDAAr)5/ pDNA was found to exhibit 98% cell viability and around 150% more gene transfection than branched PEI in KB cell lines. While in the case of histidine conjugated siloxane group P(SiDAHs)1 exhibited almost similar transfection efficiency and cytotoxicity compared to PEI. Studies performed on transfection mechanism, using inhibitor study, clearly stated that the enhancement in transfection is due to the multiple pathways for cellular uptake which offered by the presence of uniformly spaced arginine moiety by oligo(-alkylaminosiloxane) arms. The

nuclear localisation ability of the arginine residue was also established by using FITC stained nanoparticles on Hoechst 33342 stained nucleus.

In order to introduce folate receptor mediated gene targeting, the best derivative from each group of arginine and histidine modified oligoalkylaminosiloxanes such as P(SiDAAr)5 and P(SiDAHs)1 were chosen. The resultant PEG-FA conjugated polymers complexed pDNA effectively and showed protection against nuclease degradation. The PEG group provided improved blood compatibility and cell viability. Uniformly oriented arginine/histidine moiety helped to enhance cellular and nuclear localisation, which led to improved transfection. Based on the pGL3 expression, P(SiDAAr)5FP2 from arginine group and P(SiDAHs)1FP3 from histidine group were selected for further studies. The polymer was capable of releasing pDNA at the nucleus and being cleared from the cell after its purpose. However more clearance from 24^{th} hour was observed for P(SiDAAr)5FP2 derivative than that of P(SiDAHs)1FP3. Transfection in presence of cellular uptake inhibitors showed multiple pathways for cellular uptake of the targeted polymer, out of which folate receptor mediated uptake was more prominent. Since the arginine conjugated derivatives were found to be more suitable gene delivery vector compared to histidine conjugated derivatives based on the blood compatibility, transfection, cellular uptake and its clearance studies, P(SiDAAr)5FP2 derivative was chosen for in vitro and in vivo tumor targeting experiments. From the various in vitro tumor targeting experiments, it is observed that the cellular uptake of P(SiDAAr)5FP2 derivative was mediated by folate receptors. Folate mediated tissue targeting was confirmed by in vivo tumor targeting studies. The high accumulation of targeted polymers in the tumor tissues of tumor bearing mice from 2^{nd} hour onwards proved the active targeting effect of the polymer. Besides tumor accumulation, the material showed capability to diffuse through the vascular endothelium. This property is expected to be beneficial for brain targeting experiments.

Future works may be focused on titrating the molecular weight of PEG group in order to get better transfection efficiency for the targeted polymer as in the case of parent polymer P(SiDAAr)5. Therefore by proper designing, P(SiDAAr)5FP2 derivative can be used as a promising vector for tumor targeted as well as brain targeted gene therapy.

References

Abuchowski, A. & Davis, F. F. (1979), 'Preparation and properties of polyethylene glycol-trypsin adducts.', *Biochim Biophys Acta*, 578(1), 41–6.

Abuchowski, A., McCoy, J. R., Palczuk, N. C., van Es, T. & Davis, F. F. (1977), 'Effect of covalent attachment of polyethylene glycol on immunogenicity and circulating life of bovine liver catalase.', *J Biol Chem*, 252(11), 3582–6.

Agarwal, A., Unfer, R. & Mallapragada, S. (2005), 'Novel cationic pentablock copolymers as non-viral vectors for gene therapy', *Journal of Controlled Release*, 103(1), 245–258.

Arote, R., Kim, T.-H., Kim, Y.-K., Hwang, S.-K., Jiang, H.-L., Song, H.-H., Nah, J.-W., Cho, M.-H. & Cho, C.-S. (2007), 'A biodegradable poly(ester amine) based on polycaprolactone and polyethylenimine as a gene carrier.', *Biomaterials*, 28(4), 735–44.

Azzam, T., Eliyahu, H., Makovitzki, A., Linial, M. & Domb, A. J. (2004), 'Hydrophobized dextran-spermine conjugate as potential vector for in vitro gene transfection.', *J Control Release*, 96(2), 309–23.

Beduneau, A., Hindre, F., Clavreul, A., Leroux, J., Saulnier, P. & Benoit, J. (2008), 'Brain targeting using novel lipid nanovectors', *Journal of Controlled Release*, 126(1), 44–49.

Benns, J. M., Choi, J. S., Mahato, R. I., Park, J. S. & Kim, S. W. (2000), 'ph-sensitive cationic polymer gene delivery vehicle: N-ac-poly(l-histidine)-graft-poly(l-lysine) comb shaped polymer.', *Bioconjug Chem*, 11(5), 637–45.

Benns, J. M., Mahato, R. I. & Kim, S. W. (2002), 'Optimization of factors influencing the transfection efficiency of folate-peg-folate-graft-polyethylenimine.', *J Control Release*, 79(1-3), 255–69.

Benns, J. M., Maheshwari, A., Furgeson, D. Y., Mahato, R. I. & Kim, S. W. (2001), 'Folate-peg-folate-graft-polyethylenimine-based gene delivery.', *J Drug Target*, 9(2), 123–39.

Biesalski, H. K., Bueno de Mesquita, B., Chesson, A., Chytil, F., Grimble, R., Hermus, R. J., KÃhrle, J., Lotan, R., Norpoth, K., Pastorino, U. & Thurnham, D. (1998), 'European con-

sensus statement on lung cancer: risk factors and prevention. lung cancer panel.', *CA Cancer J Clin*, 48(3), 167–76; discussion 164–6.

Bikram, M., Ahn, C., Chae, S., Lee, M., Yockman, J. & Kim, S. (2004), 'Biodegradable poly (ethylene glycol)-co-poly (L-lysine)-g-histidine multiblock copolymers for nonviral gene delivery', *Macromolecules*, 37(5), 1903–1916.

Blau, S., Jubeh, T. T., Haupt, S. M. & Rubinstein, A. (2000), 'Drug targeting by surface cationization.', *Crit Rev Ther Drug Carrier Syst*, 17(5), 425–65.

Blessing, T., Kursa, M., Holzhauser, R., Kircheis, R. & Wagner, E. (2001), 'Different strategies for formation of pegylated egf-conjugated pei/dna complexes for targeted gene delivery.', *Bioconjug Chem*, 12(4), 529–37.

Bordi, F., Cametti, C., Sennato, S. & Viscomi, D. (2007), 'Radiofrequency dielectric loss relaxation in polyion-induced liposome aggregates.', *J Colloid Interface Sci*, 309(2), 366–72.

Boussif, O., Lezoualc'h, F., Zanta, M. A., Mergny, M. D., Scherman, D., Demeneix, B. & Behr, J. P. (1995*a*), 'A versatile vector for gene and oligonucleotide transfer into cells in culture and in vivo: polyethylenimine.', *Proc Natl Acad Sci U S A*, 92(16), 7297–301.

Boussif, O., Lezoualc'h, F., Zanta, M., Mergny, M., Scherman, D., Demeneix, B. & Behr, J. (1995*b*), 'A versatile vector for gene and oligonucleotide transfer into cells in culture and in vivo: polyethylenimine', *Proceedings of the National Academy of Sciences of the United States of America*, 92(16), 7297.

Boveri, T. (2008), 'Concerning the origin of malignant tumours by theodor boveri. translated and annotated by henry harris.', *J Cell Sci*, 121 Suppl 1, 1–84.

Breunig, M., Lungwitz, U., Liebl, R., Fontanari, C., Klar, J., Kurtz, A., Blunk, T. & Goepferich, A. (2005), 'Gene delivery with low molecular weight linear polyethylenimines.', *J Gene Med*, 7(10), 1287–98.

Brissault, B., Kichler, A., Guis, C., Leborgne, C., Danos, O. & Cheradame, H. (2003), 'Synthesis of linear polyethylenimine derivatives for dna transfection.', *Bioconjug Chem*, 14(3), 581–7.

Brooks, H., Lebleu, B. & VivÃs, E. (2005), 'Tat peptide-mediated cellular delivery: back to basics.', *Adv Drug Deliv Rev*, 57(4), 559–77.

Chan, P., Kurisawa, M., Chung, J. E. & Yang, Y.-Y. (2007), 'Synthesis and characterization of chitosan-g-poly(ethylene glycol)-folate as a non-viral carrier for tumor-targeted gene delivery.', *Biomaterials*, 28(3), 540–9.

Choate, K. A. & Khavari, P. A. (1997), 'Direct cutaneous gene delivery in a human genetic skin disease.', *Hum Gene Ther*, 8(14), 1659–65.

Choi, J. S., Nam, K., Park, J.-Y., Kim, J.-B., Lee, J.-K. & Park, J.-S. (2004), 'Enhanced transfection efficiency of pamam dendrimer by surface modification with l-arginine.', *J Control Release*, 99(3), 445–56.

Corsi, K., Chellat, F., Yahia, L. & Fernandes, J. C. (2003), 'Mesenchymal stem cells, mg63 and hek293 transfection using chitosan-dna nanoparticles.', *Biomaterials*, 24(7), 1255–64.

Dash, P. R., Read, M. L., Fisher, K. D., Howard, K. A., Wolfert, M., Oupicky, D., Subr, V., Strohalm, J., Ulbrich, K. & Seymour, L. W. (2000), 'Decreased binding to proteins and cells of polymeric gene delivery vectors surface modified with a multivalent hydrophilic polymer and retargeting through attachment of transferrin.', *J Biol Chem*, 275(6), 3793–802.

Dass, C. R. (2002), 'Biochemical and biophysical characteristics of lipoplexes pertinent to solid tumour gene therapy.', *Int J Pharm*, 241(1), 1–25.

Delgado, C., Francis, G. E. & Fisher, D. (1992), 'The uses and properties of peg-linked proteins.', *Crit Rev Ther Drug Carrier Syst*, 9(3-4), 249–304.

Deng, R., Yue, Y., Jin, F., Chen, Y., Kung, H.-F., Lin, M. C. M. & Wu, C. (2009), 'Revisit the complexation of pei and dna - how to make low cytotoxic and highly efficient pei gene transfection non-viral vectors with a controllable chain length and structure?', *J Control Release*, 140(1), 40–6.

Dong, W., Jin, G.-H., Li, S.-F., Sun, Q.-M., Ma, D.-Y. & Hua, Z.-C. (2006), 'Cross-linked polyethylenimine as potential dna vector for gene delivery with high efficiency and low cytotoxicity.', *Acta Biochim Biophys Sin (Shanghai)*, 38(11), 780–7.

Dowty, M., Williams, P., Zhang, G., Hagstrom, J. & Wolff, J. (1995), 'Plasmid DNA entry into postmitotic nuclei of primary rat myotubes', *Proceedings of the National Academy of Sciences of the United States of America*, 92(10), 4572.

El-Aneed, A. (2004), 'An overview of current delivery systems in cancer gene therapy.', *J Control Release*, 94(1), 1–14.

Elliott, G. & O'Hare, P. (1997), 'Intercellular trafficking and protein delivery by a herpesvirus structural protein.', *Cell*, 88(2), 223–33.

Elouahabi, A. & Ruysschaert, J.-M. (2005), 'Formation and intracellular trafficking of lipoplexes and polyplexes.', *Mol Ther*, 11(3), 336–47.

Erbacher, P., Bettinger, T., Belguise-Valladier, P., Zou, S., Coll, J. L., Behr, J. P. & Remy, J. S. (1999*a*), 'Transfection and physical properties of various saccharide, poly(ethylene glycol), and antibody-derivatized polyethylenimines (pei).', *J Gene Med*, 1(3), 210–22.

Erbacher, P., Remy, J. S. & Behr, J. P. (1999*b*), 'Gene transfer with synthetic virus-like particles via the integrin-mediated endocytosis pathway.', *Gene Ther*, 6(1), 138–45.

Erbacher, P., Zou, S., Bettinger, T., Steffan, A. M. & Remy, J. S. (1998), 'Chitosan-based vector/dna complexes for gene delivery: biophysical characteristics and transfection ability.', *Pharm Res*, 15(9), 1332–9.

Fernandez, C. A. & Rice, K. G. (2009), 'Engineered nanoscaled polyplex gene delivery systems.', *Mol Pharm*, 6(5), 1277–89.

Fischer, D., Bieber, T., Li, Y., ElsÃsser, H. P. & Kissel, T. (1999), 'A novel non-viral vector for dna delivery based on low molecular weight, branched polyethylenimine: effect of molecular weight on transfection efficiency and cytotoxicity.', *Pharm Res*, 16(8), 1273–9.

Fisher, K. D., Ulbrich, K., Subr, V., Ward, C. M., Mautner, V., Blakey, D. & Seymour, L. W. (2000), 'A versatile system for receptor-mediated gene delivery permits increased entry

of dna into target cells, enhanced delivery to the nucleus and elevated rates of transgene expression.', *Gene Ther*, 7(15), 1337–43.

Frankel, A. & Pabo, C. (1988), 'Cellular uptake of the tat protein from human immunodeficiency virus', *Cell*, 55(6), 1189–1193.

Fuller, J. E., Zugates, G. T., Ferreira, L. S., Ow, H. S., Nguyen, N. N., Wiesner, U. B. & Langer, R. S. (2008), 'Intracellular delivery of core-shell fluorescent silica nanoparticles.', *Biomaterials*, 29(10), 1526–32.

Gao, H. & Hui, K. M. (2001), 'Synthesis of a novel series of cationic lipids that can act as efficient gene delivery vehicles through systematic heterocyclic substitution of cholesterol derivatives.', *Gene Ther*, 8(11), 855–63.

Gao, Y., Xu, Z., Chen, S., Gu, W., Chen, L. & Li, Y. (2008), 'Arginine-chitosan/DNA self-assemble nanoparticles for gene delivery: In vitro characteristics and transfection efficiency', *International journal of pharmaceutics*, 359(1-2), 241–246.

Gene therapy clinical trials (2010), J. Gene Med.

Germershaus, O., Mao, S., Sitterberg, J., Bakowsky, U. & Kissel, T. (2008*a*), 'Gene delivery using chitosan, trimethyl chitosan or polyethylenglycol-graft-trimethyl chitosan block copolymers: establishment of structure-activity relationships in vitro.', *J Control Release*, 125(2), 145–54.

Germershaus, O., Neu, M., Behe, M. & Kissel, T. (2008*b*), 'Her2 targeted polyplexes: the effect of polyplex composition and conjugation chemistry on in vitro and in vivo characteristics.', *Bioconjug Chem*, 19(1), 244–53.

Gershon, H., Ghirlando, R., Guttman, S. B. & Minsky, A. (1993), 'Mode of formation and structural features of dna-cationic liposome complexes used for transfection.', *Biochemistry*, 32(28), 7143–51.

Godbey, W. T., Wu, K. K. & Mikos, A. G. (1999*a*), 'Tracking the intracellular path of poly(ethylenimine)/dna complexes for gene delivery.', *Proc Natl Acad Sci U S A*, 96(9), 5177–81.

Godbey, W. T., Wu, K. K., Hirasaki, G. J. & Mikos, A. G. (1999*b*), 'Improved packing of poly(ethylenimine)/dna complexes increases transfection efficiency.', *Gene Ther*, 6(8), 1380–8.

Goldman, C. K., Kendall, R. L., Cabrera, G., Soroceanu, L., Heike, Y., Gillespie, G. Y., Siegal, G. P., Mao, X., Bett, A. J., Huckle, W. R., Thomas, K. A. & Curiel, D. T. (1998), 'Paracrine expression of a native soluble vascular endothelial growth factor receptor inhibits tumor growth, metastasis, and mortality rate.', *Proc Natl Acad Sci U S A*, 95(15), 8795–800.

GonÃalves, C., Mennesson, E., Fuchs, R., Gorvel, J.-P., Midoux, P. & Pichon, C. (2004), 'Macropinocytosis of polyplexes and recycling of plasmid via the clathrin-dependent pathway impair the transfection efficiency of human hepatocarcinoma cells.', *Mol Ther*, 10(2), 373–85.

Gorlich, D. & Mattaj, I. (1996), 'Nucleocytoplasmic transport', *Science*, 271(5255), 1513.

Gottschalk, S., Cristiano, R. J., Smith, L. C. & Woo, S. L. (1994), 'Folate receptor mediated dna delivery into tumor cells: potosomal disruption results in enhanced gene expression.', *Gene Ther*, 1(3), 185–91.

Gref, R., Minamitake, Y., Peracchia, M. T., Trubetskoy, V., Torchilin, V. & Langer, R. (1994), 'Biodegradable long-circulating polymeric nanospheres.', *Science*, 263(5153), 1600–3.

Hart, S. L., Harbottle, R. P., Cooper, R., Miller, A., Williamson, R. & Coutelle, C. (1995), 'Gene delivery and expression mediated by an integrin-binding peptide.', *Gene Ther*, 2(8), 552–4.

Hernandez, B. Y., Green, M. D., Cassel, K. D., Pobutsky, A. M., Vu, V. & Wilkens, L. R. (2010), 'Preview of hawaii cancer facts and figures 2010.', *Hawaii Med J*, 69(9), 223–4.

Hirano, S., Seino, H., Akiyama, Y. & Nonaka, I. (1990), 'Chitosan: a biocompatible material for oral and intravenous administration', *Progress in Biomedical Polymers*, pp. 283–290.

Hu, F.-Q., Zhao, M.-D., Yuan, H., You, J., Du, Y.-Z. & Zeng, S. (2006), 'A novel chitosan oligosaccharide-stearic acid micelles for gene delivery: properties and in vitro transfection studies.', *Int J Pharm*, 315(1-2), 158–66.

Huang, M., Fong, C.-W., Khor, E. & Lim, L.-Y. (2005), 'Transfection efficiency of chitosan vectors: effect of polymer molecular weight and degree of deacetylation.', *J Control Release*, 106(3), 391–406.

Hwa Kim, S., Hoon Jeong, J., Joe, C. O. & Gwan Park, T. (2005), 'Folate receptor mediated intracellular protein delivery using pll-peg-fol conjugate.', *J Control Release*, 103(3), 625–34.

Hwang, S. J., Bellocq, N. C. & Davis, M. E. (2001), 'Effects of structure of beta-cyclodextrin-containing polymers on gene delivery.', *Bioconjug Chem*, 12(2), 280–90.

il Kim, T., Ou, M., Lee, M. & Kim, S. W. (2009), 'Arginine-grafted bioreducible poly(disulfide amine) for gene delivery systems.', *Biomaterials*, 30(4), 658–64.

Issa, M. M., KÃping-HÃggÃrd, M., TÃmmeraas, K., VÃrum, K. M., Christensen, B. E., Strand, S. P. & Artursson, P. (2006), 'Targeted gene delivery with trisaccharide-substituted chitosan oligomers in vitro and after lung administration in vivo.', *J Control Release*, 115(1), 103–12.

Jayakumar, R., Chennazhi, K., Muzzarelli, R., Tamura, H., Nair, S. & Selvamurugan, N. (2010), 'Chitosan conjugated DNA nanoparticles in gene therapy', *Carbohydrate Polymers*, 79(1), 1–8.

Jeon, O., Yang, H. S., Lee, T.-J. & Kim, B.-S. (2008), 'Heparin-conjugated polyethylenimine for gene delivery.', *J Control Release*, 132(3), 236–42.

Jiang, H.-L., Kim, Y.-K., Arote, R., Nah, J.-W., Cho, M.-H., Choi, Y.-J., Akaike, T. & Cho, C.-S. (2007), 'Chitosan-graft-polyethylenimine as a gene carrier.', *J Control Release*, 117(2), 273–80.

Jiao, L. R. & Habib, N. A. (2003), 'Experimental study of large-volume microwave ablation in the liver.', *Br J Surg*, 90(1), 122.

Joliot, A., Pernelle, C., Deagostini-Bazin, H. & Prochiantz, A. (1991), 'Antennapedia homeobox peptide regulates neural morphogenesis', *Proceedings of the National Academy of Sciences of the United States of America*, 88(5), 1864.

Kalderon, D., Roberts, B., Richardson, W. & Smith, A. (1984), 'A short amino acid sequence able to specify nuclear location', *Cell*, 39(3), 499–509.

Kamaly, N., Kalber, T., Thanou, M., Bell, J. D. & Miller, A. D. (2009), 'Folate receptor targeted bimodal liposomes for tumor magnetic resonance imaging.', *Bioconjug Chem*, 20(4), 648–55.

Kasaai, M., Arul, J. & Charlet, G. (2000), 'Intrinsic viscosity–molecular weight relationship for chitosan', *Journal of Polymer Science Part B: Polymer Physics*, 38(19), 2591–2598.

Katre, N. V. (1990), 'Immunogenicity of recombinant il-2 modified by covalent attachment of polyethylene glycol.', *J Immunol*, 144(1), 209–13.

Kaur, I., Bhandari, R., Bhandari, S. & Kakkar, V. (2008), 'Potential of solid lipid nanoparticles in brain targeting', *Journal of Controlled Release*, 127(2), 97–109.

KÃping-HÃggÃrd, M., Tubulekas, I., Guan, H., Edwards, K., Nilsson, M., VÃrum, K. M. & Artursson, P. (2001), 'Chitosan as a nonviral gene delivery system. structure-property relationships and characteristics compared with polyethylenimine in vitro and after lung administration in vivo.', *Gene Ther*, 8(14), 1108–21.

KÃping-HÃggÃrd, M., VÃrum, K. M., Issa, M., Danielsen, S., Christensen, B. E., Stokke, B. T. & Artursson, P. (2004), 'Improved chitosan-mediated gene delivery based on easily dissociated chitosan polyplexes of highly defined chitosan oligomers.', *Gene Ther*, 11(19), 1441–52.

Kean, T., Roth, S. & Thanou, M. (2005), 'Trimethylated chitosans as non-viral gene delivery vectors: cytotoxicity and transfection efficiency.', *J Control Release*, 103(3), 643–53.

Kiang, T., Wen, J., Lim, H. W. & Leong, K. W. (2004), 'The effect of the degree of chitosan deacetylation on the efficiency of gene transfection.', *Biomaterials*, 25(22), 5293–301.

Kichler, A., Pages, J., Leborgne, C., Druillennec, S., Lenoir, C., Coulaud, D., Delain, E., Le Cam, E., Roques, B. & Danos, O. (2000), 'Efficient DNA transfection mediated by the C-terminal domain of human immunodeficiency virus type 1 viral protein R', *Journal of Virology*, 74(12), 5424.

Kichler, A., Sabourault, N., Décor, R., Leborgne, C., Schmutz, M., Valleix, A., Danos, O., Wagner, A. & Mioskowski, C. (2003), 'Preparation and evaluation of a new class of gene transfer reagents: poly (-alkylaminosiloxanes)', *Journal of Controlled Release*, 93(3), 403–414.

Kim, T., Baek, J., Yoon, J., Choi, J., Kim, K. & Park, J. (2007*a*), 'Synthesis and characterization of a novel arginine-grafted dendritic block copolymer for gene delivery and study of its cellular uptake pathway leading to transfection', *Bioconjugate Chem*, 18(2), 309–317.

Kim, T. H., Ihm, J. E., Choi, Y. J., Nah, J. W. & Cho, C. S. (2003), 'Efficient gene delivery by urocanic acid-modified chitosan.', *J Control Release*, 93(3), 389–402.

Kim, T.-I., Baek, J.-U., Zhe Bai, C. & Park, J.-S. (2007*b*), 'Arginine-conjugated polypropylenimine dendrimer as a non-toxic and efficient gene delivery carrier.', *Biomaterials*, 28(11), 2061–7.

Kim, T., Jiang, H., Jere, D., Park, I., Cho, M., Nah, J., Choi, Y., Akaike, T. & Cho, C. (2007*c*), 'Chemical modification of chitosan as a gene carrier in vitro and in vivo', *Progress in Polymer Science*, 32(7), 726–753.

Kim, Y. H., Gihm, S. H., Park, C. R., Lee, K. Y., Kim, T. W., Kwon, I. C., Chung, H. & Jeong, S. Y. (2001), 'Structural characteristics of size-controlled self-aggregates of deoxycholic acid-modified chitosan and their application as a dna delivery carrier.', *Bioconjug Chem*, 12(6), 932–8.

Kircheis, R., SchÃller, S., Brunner, S., Ogris, M., Heider, K. H., Zauner, W. & Wagner, E. (1999), 'Polycation-based dna complexes for tumor-targeted gene delivery in vivo.', *J Gene Med*, 1(2), 111–20.

Kircheis, R., Wightman, L., Schreiber, A., Robitza, B., RÃssler, V., Kursa, M. & Wagner, E. (2001), 'Polyethylenimine/dna complexes shielded by transferrin target gene expression to tumors after systemic application.', *Gene Ther*, 8(1), 28–40.

Kirn, D. (2002), 'Virotherapy for cancer: current status, hurdles, and future directions.', *Cancer Gene Ther*, 9(12), 959–60.

Klibanov, A. L., Maruyama, K., Torchilin, V. P. & Huang, L. (1990), 'Amphipathic polyethyleneglycols effectively prolong the circulation time of liposomes.', *FEBS Lett*, 268(1), 235–7.

Knorr, V., Allmendinger, L., Walker, G. F., Paintner, F. F. & Wagner, E. (2007), 'An acetal-based pegylation reagent for ph-sensitive shielding of dna polyplexes.', *Bioconjug Chem*, 18(4), 1218–25.

Kopatz, I., Remy, J.-S. & Behr, J.-P. (2004), 'A model for non-viral gene delivery: through syndecan adhesion molecules and powered by actin.', *J Gene Med*, 6(7), 769–76.

Kunath, K., von Harpe, A., Fischer, D., Petersen, H., Bickel, U., Voigt, K. & Kissel, T. (2003), 'Low-molecular-weight polyethylenimine as a non-viral vector for dna delivery: comparison of physicochemical properties, transfection efficiency and in vivo distribution with high-molecular-weight polyethylenimine.', *J Control Release*, 89(1), 113–25.

Kursa, M., Walker, G. F., Roessler, V., Ogris, M., Roedl, W., Kircheis, R. & Wagner, E. (2003), 'Novel shielded transferrin-polyethylene glycol-polyethylenimine/dna complexes for systemic tumor-targeted gene transfer.', *Bioconjug Chem*, 14(1), 222–31.

Leamon, C. & Low, P. (2001), 'Folate-mediated targeting: from diagnostics to drug and gene delivery', *Drug discovery today*, 6(1), 44–51.

Lechardeur, D. & Lukacs, G. (2006), 'Nucleocytoplasmic transport of plasmid DNA: a perilous journey from the cytoplasm to the nucleus', *Human gene therapy*, 17(9), 882–889.

Lee, D., Powers, K. & Baney, R. (2004), 'Physicochemical properties and blood compatibility of acylated chitosan nanoparticles', *Carbohydrate Polymers*, 58(4), 371–377.

Lee, E. S., Gao, Z., Kim, D., Park, K., Kwon, I. C. & Bae, Y. H. (2008), 'Super ph-sensitive multifunctional polymeric micelle for tumor ph(e) specific tat exposure and multidrug resistance.', *J Control Release*, 129(3), 228–36.

Lee, E. S., Na, K. & Bae, Y. H. (2005), 'Super ph-sensitive multifunctional polymeric micelle.', *Nano Lett*, 5(2), 325–9.

Lee, E. S., Oh, K. T., Kim, D., Youn, Y. S. & Bae, Y. H. (2007), 'Tumor ph-responsive flower-like micelles of poly(l-lactic acid)-b-poly(ethylene glycol)-b-poly(l-histidine).', *J Control Release*, 123(1), 19–26.

Lee, E. S., Shin, H. J., Na, K. & Bae, Y. H. (2003), 'Poly(l-histidine)-peg block copolymer micelles and ph-induced destabilization.', *J Control Release*, 90(3), 363–74.

Li, F., Liu, W. G. & Yao, K. D. (2002), 'Preparation of oxidized glucose-crosslinked n-alkylated chitosan membrane and in vitro studies of ph-sensitive drug delivery behaviour.', *Biomaterials*, 23(2), 343–7.

Li, S., Rizzo, M. A., Bhattacharya, S. & Huang, L. (1998), 'Characterization of cationic lipid-protamine-dna (lpd) complexes for intravenous gene delivery.', *Gene Ther*, 5(7), 930–7.

Liang, B., He, M.-L., Xiao, Z.-P., Li, Y., Chan, C.-Y., Kung, H.-F., Shuai, X.-T. & Peng, Y. (2008), 'Synthesis and characterization of folate-peg-grafted-hyperbranched-pei for tumor-targeted gene delivery.', *Biochem Biophys Res Commun*, 367(4), 874–80.

Lin, P., Buxton, J. A., Acheson, A., Radziejewski, C., Maisonpierre, P. C., Yancopoulos, G. D., Channon, K. M., Hale, L. P., Dewhirst, M. W., George, S. E. & Peters, K. G. (1998), 'Antiangiogenic gene therapy targeting the endothelium-specific receptor tyrosine kinase tie2.', *Proc Natl Acad Sci U S A*, 95(15), 8829–34.

Liu, P. & Anderson, R. G. (1999), 'Spatial organization of egf receptor transmodulation by pdgf.', *Biochem Biophys Res Commun*, 261(3), 695–700.

Lo, S. L. & Wang, S. (2008), 'An endosomolytic tat peptide produced by incorporation of histidine and cysteine residues as a nonviral vector for dna transfection.', *Biomaterials*, 29(15), 2408–14.

Loretz, B., Thaler, M. & Bernkop-SchnÃrch, A. (2007), 'Role of sulfhydryl groups in transfection? a case study with chitosan-nac nanoparticles.', *Bioconjug Chem*, 18(4), 1028–35.

Low, P. S., Henne, W. A. & Doorneweerd, D. D. (2008), 'Discovery and development of folic-acid-based receptor targeting for imaging and therapy of cancer and inflammatory diseases.', *Acc Chem Res*, 41(1), 120–9.

Lu, B., Wang, C.-F., Wu, D.-Q., Li, C., Zhang, X.-Z. & Zhuo, R.-X. (2009), 'Chitosan based oligoamine polymers: synthesis, characterization, and gene delivery.', *J Control Release*, 137(1), 54–62.

Lukacs, G., Haggie, P., Seksek, O., Lechardeur, D., Freedman, N. & Verkman, A. (2000), 'Size-dependent DNA mobility in cytoplasm and nucleus', *Journal of Biological Chemistry*, 275(3), 1625.

MacLaughlin, F. C., Mumper, R. J., Wang, J., Tagliaferri, J. M., Gill, I., Hinchcliffe, M. & Rolland, A. P. (1998), 'Chitosan and depolymerized chitosan oligomers as condensing carriers for in vivo plasmid delivery.', *J Control Release*, 56(1-3), 259–72.

Mansouri, S., Cuie, Y., Winnik, F., Shi, Q., Lavigne, P., Benderdour, M., Beaumont, E. & Fernandes, J. C. (2006), 'Characterization of folate-chitosan-dna nanoparticles for gene therapy.', *Biomaterials*, 27(9), 2060–5.

Mansouri, S., Lavigne, P., Corsi, K., Benderdour, M., Beaumont, E. & Fernandes, J. C. (2004), 'Chitosan-dna nanoparticles as non-viral vectors in gene therapy: strategies to improve transfection efficacy.', *Eur J Pharm Biopharm*, 57(1), 1–8.

Mao, S., Shuai, X., Unger, F., Simon, M., Bi, D. & Kissel, T. (2004), 'The depolymerization of chitosan: effects on physicochemical and biological properties.', *Int J Pharm*, 281(1-2), 45–54.

Matsumura, Y. & Maeda, H. (1986), 'A new concept for macromolecular therapeutics in cancer chemotherapy: mechanism of tumoritropic accumulation of proteins and the antitumor agent smancs.', *Cancer Res*, 46(12 Pt 1), 6387–92.

Maxfield, F. & Yamashiro, D. (1987), 'Endosome acidification and the pathways of receptor-mediated endocytosis.', *Advances in experimental medicine and biology*, 225, 189.

Mellman, I. (1996), 'Endocytosis and molecular sorting', *Annual review of cell and developmental biology*, 12(1), 575–625.

Merdan, T., Kunath, K., Fischer, D., Kopecek, J. & Kissel, T. (2002), 'Intracellular processing of poly(ethylene imine)/ribozyme complexes can be observed in living cells by using confocal laser scanning microscopy and inhibitor experiments.', *Pharm Res*, 19(2), 140–6.

Midoux, P. & Monsigny, M. (1999), 'Efficient gene transfer by histidylated polylysine/pdna complexes.', *Bioconjug Chem*, 10(3), 406–11.

Moffatt, S., Wiehle, S. & Cristiano, R. (2006), 'A multifunctional PEI-based cationic polyplex for enhanced systemic p53-mediated gene therapy', *Gene therapy*, 13(21), 1512–1523.

Moffatt, S., Wiehle, S. & Cristiano, R. J. (2005), 'Tumor-specific gene delivery mediated by a novel peptide-polyethylenimine-dna polyplex targeting aminopeptidase n/cd13.', *Hum Gene Ther*, 16(1), 57–67.

Morille, M., Passirani, C., Vonarbourg, A., Clavreul, A. & Benoit, J.-P. (2008), 'Progress in developing cationic vectors for non-viral systemic gene therapy against cancer.', *Biomaterials*, 29(24-25), 3477–96.

Moroianu, J., Blobel, G. & Radu, A. (1995), 'Previously identified protein of uncertain function is karyopherin alpha and together with karyopherin beta docks import substrate at nuclear pore complexes', *Proceedings of the National Academy of Sciences of the United States of America*, 92(6), 2008.

Morris, V. B. & Sharma, C. P. (2010*a*), 'Enhanced in-vitro transfection and biocompatibility of l-arginine modified oligo (-alkylaminosiloxanes)-graft-polyethylenimine.', *Biomaterials*, 31(33), 8759–69.

Morris, V. B. & Sharma, C. P. (2010*b*), 'Folate mediated histidine derivative of quaternised chitosan as a gene delivery vector.', *Int J Pharm*, 389(1-2), 176–85.

Morris, V. B. & Sharma, C. P. (2010*c*), 'Folate mediated in vitro targeting of depolymerised trimethylated chitosan having arginine functionality.', *J Colloid Interface Sci*, 348(2), 360–8.

Morris, V. B., Neethu, S., Abraham, T. E., Pillai, C. K. S. & Sharma, C. P. (2009), 'Studies on the condensation of depolymerized chitosans with dna for preparing chitosan-dna nanoparti-

cles for gene delivery applications.', *J Biomed Mater Res B Appl Biomater*, 89B(2), 282–92.

Mumper, R., Wang, J., Claspell, J. & Rolland, A. (1995), Novel polymeric condensing carriers for gene delivery, *in* 'Proc Int Symp Control Rel Bioact Mater', Vol. 22, pp. 178–179.

Nishikawa, M. & Huang, L. (2001), 'Nonviral vectors in the new millennium: delivery barriers in gene transfer', *Human gene therapy*, 12(8), 861–870.

Ogris, M., Brunner, S., SchÃller, S., Kircheis, R. & Wagner, E. (1999), 'Pegylated dna/transferrin-pei complexes: reduced interaction with blood components, extended circulation in blood and potential for systemic gene delivery.', *Gene Ther*, 6(4), 595–605.

Ogris, M., Walker, G., Blessing, T., Kircheis, R., Wolschek, M. & Wagner, E. (2003), 'Tumor-targeted gene therapy: strategies for the preparation of ligand-polyethylene glycol-polyethylenimine/dna complexes.', *J Control Release*, 91(1-2), 173–81.

Okuda, T., Sugiyama, A., Niidome, T. & Aoyagi, H. (2004), 'Characters of dendritic poly(l-lysine) analogues with the terminal lysines replaced with arginines and histidines as gene carriers in vitro.', *Biomaterials*, 25(3), 537–44.

O'Reilly, K., Mclaughlin, A., Beckett, W. & Sime, P. (2007), 'Asbestos-related lung disease.', *American family physician*, 75(5), 683.

Orig, M., Brunner, S., Schuller, S., Kircheis, R. & Wagner, E. (1999), 'PEGylated DNA/transferring-PEI complexes: reduced interaction with blood components, extended circulation in blood and potential for systemic gene delivery', *Gene Therapy*, 6, 595–605.

OupickÃ, D., Howard, K. A., KonÃ¡k, C., Dash, P. R., Ulbrich, K. & Seymour, L. W. (2000), 'Steric stabilization of poly-l-lysine/dna complexes by the covalent attachment of semitelechelic poly[n-(2-hydroxypropyl)methacrylamide].', *Bioconjug Chem*, 11(4), 492–501.

OupickÃ, D., Konak, C., Dash, P., Seymour, L. & Ulbrich, K. (1999), 'Effect of albumin and polyanion on the structure of DNA complexes with polycation containing hydrophilic non-ionic block', *Bioconjug. Chem*, 10, 764–772.

OMalley, B. & Couch, M. (1999), *Advanced Gene Delivery*, Hardwood Academic Publishers.

Park, E. K., Lee, S. B. & Lee, Y. M. (2005*a*), 'Preparation and characterization of methoxy poly(ethylene glycol)/poly(epsilon-caprolactone) amphiphilic block copolymeric nanospheres for tumor-specific folate-mediated targeting of anticancer drugs.', *Biomaterials*, 26(9), 1053–61.

Park, I.-K., Jiang, H.-L., Cook, S.-E., Cho, M.-H., Kim, S.-I., Jeong, H.-J., Akaike, T. & Cho, C.-S. (2004), 'Galactosylated chitosan (gc)-graft-poly(vinyl pyrrolidone) (pvp) as hepatocyte-targeting dna carrier: in vitro transfection.', *Arch Pharm Res*, 27(12), 1284–9.

Park, M., Han, K., Han, I., Cho, M., Nah, J., Choi, Y. & Cho, C. (2005*b*), 'Degradable polyethylenimine-alt-poly (ethylene glycol) copolymers as novel gene carriers', *Journal of Controlled Release*, 105(3), 367–380.

Parker, N., Turk, M. J., Westrick, E., Lewis, J. D., Low, P. S. & Leamon, C. P. (2005), 'Folate receptor expression in carcinomas and normal tissues determined by a quantitative radioligand binding assay.', *Anal Biochem*, 338(2), 284–93.

Petersen, H., Fechner, P. M., Martin, A. L., Kunath, K., Stolnik, S., Roberts, C. J., Fischer, D., Davies, M. C. & Kissel, T. (2002*a*), 'Polyethylenimine-graft-poly(ethylene glycol) copolymers: influence of copolymer block structure on dna complexation and biological activities as gene delivery system.', *Bioconjug Chem*, 13(4), 845–54.

Petersen, H., Kunath, K., Martin, A. L., Stolnik, S., Roberts, C. J., Davies, M. C. & Kissel, T. (2002*b*), 'Star-shaped poly(ethylene glycol)-block-polyethylenimine copolymers enhance dna condensation of low molecular weight polyethylenimines.', *Biomacromolecules*, 3(5), 926–36.

Pitt, C. (1973), 'Hyperconjugation and its role in group IV chemistry', *Journal of Organometallic Chemistry*, 61, 49–70.

Pluen, A., Boucher, Y., Ramanujan, S., McKee, T. D., Gohongi, T., di Tomaso, E., Brown, E. B., Izumi, Y., Campbell, R. B., Berk, D. A. & Jain, R. K. (2001), 'Role of tumor-host

interactions in interstitial diffusion of macromolecules: cranial vs. subcutaneous tumors.', *Proc Natl Acad Sci U S A*, 98(8), 4628–33.

Pollard, H., Remy, J., Loussouarn, G., Demolombe, S., Behr, J. & Escande, D. (1998), 'Polyethylenimine but not cationic lipids promotes transgene delivery to the nucleus in mammalian cells', *Journal of Biological Chemistry*, 273(13), 7507.

Pouton, C. & Seymour, L. (2001), 'Key issues in non-viral gene delivery1', *Advanced drug delivery reviews*, 46(1-3), 187–203.

Reddy, J. A. & Low, P. S. (2000), 'Enhanced folate receptor mediated gene therapy using a novel ph-sensitive lipid formulation.', *J Control Release*, 64(1-3), 27–37.

Reddy, J. A., Dean, D., Kennedy, M. D. & Low, P. S. (1999), 'Optimization of folate-conjugated liposomal vectors for folate receptor-mediated gene therapy.', *J Pharm Sci*, 88(11), 1112–8.

Reschel, T., KonÃ¡k, C., OupickÃ, D., Seymour, L. W. & Ulbrich, K. (2002), 'Physical properties and in vitro transfection efficiency of gene delivery vectors based on complexes of dna with synthetic polycations.', *J Control Release*, 81(1-2), 201–17.

Rose, N. R., Landavere, M. & Kuppers, R. C. (1996), 'Silicone binding immunoglobulins in human sera.', *Curr Top Microbiol Immunol*, 210, 269–76.

Rosenholm, J., Duchanoy, A. & Lindén, M. (2007), 'Hyperbranching Surface Polymerization as a Tool for Preferential Functionalization of the Outer Surface of Mesoporous Silicaâ ', *Chemistry of Materials*, 20(3), 1126–1133.

Rosenholm, J. M., Meinander, A., Peuhu, E., Niemi, R., Eriksson, J. E., Sahlgren, C. & LindÃn, M. (2009), 'Targeting of porous hybrid silica nanoparticles to cancer cells.', *ACS Nano*, 3(1), 197–206.

Rudolph, C., Plank, C., Lausier, J., Schillinger, U. & Rosenecker, J. (2003), 'Oligomers of the arginine-rich motif of the HIV-1 TAT protein are capable of transferring plasmid DNA into cells', *Journal of Biological Chemistry*, 278(13), 11411.

Sato, T., Ishii, T. & Okahata, Y. (2001), 'In vitro gene delivery mediated by chitosan. effect of ph, serum, and molecular mass of chitosan on the transfection efficiency.', *Biomaterials*, 22(15), 2075–80.

Schatzlein, A. (2003), 'Targeting of synthetic gene delivery systems', *Journal of Biomedicine and Biotechnology*, 3, 149–158.

Schwartz, B., Ivanov, M. A., Pitard, B., Escriou, V., Rangara, R., Byk, G., Wils, P., Crouzet, J. & Scherman, D. (1999), 'Synthetic dna-compacting peptides derived from human sequence enhance cationic lipid-mediated gene transfer in vitro and in vivo.', *Gene Ther*, 6(2), 282–92.

Schwarze, S. R., Ho, A., Vocero-Akbani, A. & Dowdy, S. F. (1999), 'In vivo protein transduction: delivery of a biologically active protein into the mouse.', *Science*, 285(5433), 1569–72.

Shiah, J. J., Sun, Y., Peterson, C. M. & Kopecek, J. (1999), 'Biodistribution of free and n-(2-hydroxypropyl)methacrylamide copolymer-bound mesochlorin e(6) and adriamycin in nude mice bearing human ovarian carcinoma ovcar-3 xenografts.', *J Control Release*, 61(1-2), 145–57.

Slowing, I. I., Trewyn, B. G. & Lin, V. S.-Y. (2007), 'Mesoporous silica nanoparticles for intracellular delivery of membrane-impermeable proteins.', *J Am Chem Soc*, 129(28), 8845–9.

Sorgi, F. L., Bhattacharya, S. & Huang, L. (1997), 'Protamine sulfate enhances lipid-mediated gene transfer.', *Gene Ther*, 4(9), 961–8.

Subr, V., KonÃ¡k, C., Laga, R. & Ulbrich, K. (2006), 'Coating of dna/poly(l-lysine) complexes by covalent attachment of poly[n-(2-hydroxypropyl)methacrylamide].', *Biomacromolecules*, 7(1), 122–30.

Sun, S., Liu, W., Cheng, N., Zhang, B., Cao, Z., Yao, K., Liang, D., Zuo, A., Guo, G. & Zhang, J. (2005), 'A thermoresponsive chitosan-nipaam/vinyl laurate copolymer vector for gene transfection.', *Bioconjug Chem*, 16(4), 972–80.

Thakor, D., Teng, Y. & Tabata, Y. (2009), 'Neuronal gene delivery by negatively charged pullulan-spermine/DNA anioplexes', *Biomaterials*, 30(9), 1815–1826.

Thanou, M., Florea, B. I., Geldof, M., Junginger, H. E. & Borchard, G. (2002), 'Quaternized chitosan oligomers as novel gene delivery vectors in epithelial cell lines.', *Biomaterials*, 23(1), 153–9.

Tung, C.-H. & Weissleder, R. (2003), 'Arginine containing peptides as delivery vectors.', *Adv Drug Deliv Rev*, 55(2), 281–94.

Vaidya, B., Paliwal, R., Rai, S., Khatri, K., Goyal, A., Mishra, N. & Vyas, S. (2009), 'Cell-selective mitochondrial targeting: A new approach for cancer therapy', *Cancer Therapy*, 7, 141–148.

Veiseh, O., Kievit, F. M., Gunn, J. W., Ratner, B. D. & Zhang, M. (2009), 'A ligand-mediated nanovector for targeted gene delivery and transfection in cancer cells.', *Biomaterials*, 30(4), 649–57.

Verheul, R., Amidi, M., van der Wal, S., van Riet, E., Jiskoot, W. & Hennink, W. (2008), 'Synthesis, characterization and in vitro biological properties of O-methyl free N, N, N-trimethylated chitosan', *Biomaterials*, 29(27), 3642–3649.

Vonarbourg, A., Passirani, C., Saulnier, P. & Benoit, J. (2006), 'Parameters influencing the stealthiness of colloidal drug delivery systems', *Biomaterials*, 27(24), 4356–4373.

Wang, C.-H. & Hsiue, G.-H. (2005), 'Polymer-dna hybrid nanoparticles based on folate-polyethylenimine-block-poly(l-lactide).', *Bioconjug Chem*, 16(2), 391–6.

Wang, L., Rothberg, K. & Anderson, R. (1993), 'Mis-assembly of clathrin lattices on endo-somes reveals a regulatory switch for coated pit formation.', *The Journal of cell biology*, 123(5), 1107.

Wang, S. & Low, P. S. (1998), 'Folate-mediated targeting of antineoplastic drugs, imaging agents, and nucleic acids to cancer cells.', *J Control Release*, 53(1-3), 39–48.

Ward, C., Read, M. & Seymour, L. (2001), 'Systemic circulation of poly (L-lysine)/DNA vectors is influenced by polycation molecular weight and type of DNA: differential circulation in mice and rats and the implications for human gene therapy', *Blood*, 97(8), 2221.

Warrant, R. W. & Kim, S. H. (1978), 'alpha-helix-double helix interaction shown in the structure of a protamine-transfer rna complex and a nucleoprotamine model.', *Nature*, 271(5641), 130–5.

Wente, S. (2000), 'Gatekeepers of the nucleus', *Science*, 288(5470), 1374.

Wightman, L., Kircheis, R., RÃssler, V., Carotta, S., Ruzicka, R., Kursa, M. & Wagner, E. (2001), 'Different behavior of branched and linear polyethylenimine for gene delivery in vitro and in vivo.', *J Gene Med*, 3(4), 362–72.

Wolfert, M. & Seymour, L. (1996), 'Atomic force microscopic analysis of the influence of the molecular weight of poly (L) lysine on the size of polyelectrolyte complexes formed with DNA.', *Gene therapy*, 3(3), 269.

Wolff, J., Malone, R., Williams, P., Chong, W., Acsadi, G., Jani, A. & Felgner, P. (1990), 'Direct gene transfer into mouse muscle in vivo', *Science*, 247(4949), 1465.

Wong, K., Sun, G., Zhang, X., Dai, H., Liu, Y., He, C. & Leong, K. W. (2006), 'Pei-g-chitosan, a novel gene delivery system with transfection efficiency comparable to polyethylenimine in vitro and after liver administration in vivo.', *Bioconjug Chem*, 17(1), 152–8.

Xia, W. & Low, P. (2010), 'Folate-Targeted Therapies for Cancer', *Journal of medicinal chemistry*, pp. 66–76.

Xu, L., Huang, C.-C., Huang, W., Tang, W.-H., Rait, A., Yin, Y. Z., Cruz, I., Xiang, L.-M., Pirollo, K. F. & Chang, E. H. (2002), 'Systemic tumor-targeted gene delivery by anti-transferrin receptor scfv-immunoliposomes.', *Mol Cancer Ther*, 1(5), 337–46.

Yamanouchi, D., Wu, J., Lazar, A., Craig Kent, K., Chu, C. & Liu, B. (2008), 'Biodegradable arginine-based poly (ester-amide) s as non-viral gene delivery reagents', *Biomaterials*, 29(22), 3269–3277.

Yang, C., Li, H., Goh, S. H. & Li, J. (2007), 'Cationic star polymers consisting of alpha-cyclodextrin core and oligoethylenimine arms as nonviral gene delivery vectors.', *Biomaterials*, 28(21), 3245–54.

Yang, L., Li, J., Zhou, W., Yuan, X. & Li, S. (2004), 'Targeted delivery of antisense oligodeoxynucleotides to folate receptor-overexpressing tumor cells.', *J Control Release*, 95(2), 321–31.

Yu, H., Chen, X., Lu, T., Sun, J., Tian, H., Hu, J., Wang, Y., Zhang, P. & Jing, X. (2007), 'Poly(l-lysine)-graft-chitosan copolymers: synthesis, characterization, and gene transfection effect.', *Biomacromolecules*, 8(5), 1425–35.

Yuan, F., Leunig, M., Huang, S. K., Berk, D. A., Papahadjopoulos, D. & Jain, R. K. (1994), 'Microvascular permeability and interstitial penetration of sterically stabilized (stealth) liposomes in a human tumor xenograft.', *Cancer Res*, 54(13), 3352–6.

Zhang, S., Xu, Y., Wang, B., Qiao, W., Liu, D. & Li, Z. (2004), 'Cationic compounds used in lipoplexes and polyplexes for gene delivery.', *J Control Release*, 100(2), 165–80.

Zhao, M. & Weissleder, R. (2004), 'Intracellular cargo delivery using tat peptide and derivatives.', *Med Res Rev*, 24(1), 1–12.

Zhao, X. B. & Lee, R. J. (2004), 'Tumor-selective targeted delivery of genes and antisense oligodeoxyribonucleotides via the folate receptor.', *Adv Drug Deliv Rev*, 56(8), 1193–204.

Zhao, X., Yu, S., Wu, F., Mao, Z. & Yu, C. (2006), 'Transfection of primary chondrocytes using chitosan-pEGFP nanoparticles', *Journal of Controlled Release*, 112(2), 223–228.

Zhu, J., Tang, A., Law, L. P., Feng, M., Ho, K. M., Lee, D. K. L., Harris, F. W. & Li, P. (2005), 'Amphiphilic core-shell nanoparticles with poly(ethylenimine) shells as potential gene delivery carriers.', *Bioconjug Chem*, 16(1), 139–46.

List of Publications

Original papers

1. **V. B. Morris** and C.P. Sharma, "Folate Mediated in vitro Targeting of Histidine Modified Oligo (-alkylaminosiloxane)-Graft-Poly (ethyleneimine) for Gene Delivery," in *Biomacromolecues*, Under Review.

2. **V. B. Morris** and C.P. Sharma, "Folate Mediated L-Arginine Modified Oligo (-alkylaminosiloxane)-Graft-Poly (ethyleneimine) for Tumor Targeted Gene Delivery," in *Biomaterials*, Under Revision.

3. **V. B. Morris** and C.P. Sharma, "Enhanced in-vitro transfection and biocompatibility of L-arginine modified oligo (-alkylaminosiloxanes) -graft- poly- ethylenimine," in *Biomaterials*, vol 31, 2010, pp. 8759-8769.

4. **V. B. Morris** and C.P. Sharma, "Folate mediated in vitro targeting of depolymerised trimethylated chitosan having arginine functionality," in *Journal of Colloid and Interface Science*, vol 348, 2010, pp. 360-368.

5. **V. B. Morris** and C.P. Sharma, "Folate mediated histidine derivative of quaternised chitosan as a gene delivery vector," in *International Journal of Pharmaceutics*, vol 389, 2010, pp. 176-185.

6. **V. B. Morris**, C.K.S. Pillai, C.P. Sharma, "Folic acid conjugated depolymerised quaternised chitosan: non-viral vector for tumor-targeted gene delivery," in *Polymer International*, Under Revision.

7. **V. B. Morris** , S. Neethu , T. E. Abraham , C. K. S. Pillai and C. P. Sharma, "The Condensation of Depolymerised Chitosans with DNA for Preparing Chitosan-DNA Nanoparticles for Gene Delivery Applications," in *Journal of Biomedical Materials Research Part B: Applied Biomaterials*, vol 89(B), 2009, pp. 282-292.

Book Chapter

- **V. B. Morris** and C.P. Sharma, "Polymeric nanoparticles for delivery of drugs and genes in cancers," in *Nanotechnology: Perspectives in the Diagnosis and Treatment of Cancers*, by Narosa International Publishers *(In Press)*.

List of Publications

Original papers

1. **V. B. Morris** and C.P. Sharma, "Folate Mediated L-Arginine Modified Oligo (-alkylaminosiloxane)-Graft-Poly (ethyleneimine) for Tumor Targeted Gene Delivery," in *Biomaterials*, In Press.

2. **V. B. Morris** and C.P. Sharma, "Enhanced in-vitro transfection and biocompatibility of L-arginine modified oligo (-alkylaminosiloxanes) -graft- poly- ethylenimine," in *Biomaterials*, vol 31, 2010, pp. 8759-8769.

3. **V. B. Morris** and C.P. Sharma, "Folate mediated in vitro targeting of depolymerised trimethylated chitosan having arginine functionality," in *Journal of Colloid and Interface Science*, vol 348, 2010, pp. 360-368.

4. **V. B. Morris** and C.P. Sharma, "Folate mediated histidine derivative of quaternised chitosan as a gene delivery vector," in *International Journal of Pharmaceutics*, vol 389, 2010, pp. 176-185.

5. **V. B. Morris**, C.K.S. Pillai, C.P. Sharma, "Folic acid conjugated depolymerised quaternised chitosan: non-viral vector for tumor-targeted gene delivery," in *Polymer International*, In Press.

6. **V. B. Morris** , S. Neethu , T. E. Abraham , C. K. S. Pillai and C. P. Sharma, "The Condensation of Depolymerised Chitosans with DNA for Preparing Chitosan-DNA Nanoparticles for Gene Delivery Applications," in *Journal of Biomedical Materials Research Part B: Applied Biomaterials*, vol 89(B), 2009, pp. 282-292.

7. **V. B. Morris** and C.P. Sharma, "Folate Mediated in vitro Targeting of Histidine Modified Oligo (-alkylaminosiloxane)-Graft-Poly (ethyleneimine) for Gene Delivery," *Communicated.*

Book Chapter

- **V. B. Morris** and C.P. Sharma, "Polymeric nanoparticles for delivery of drugs and genes in cancers," in *Nanotechnology: Perspectives in the Diagnosis and Treatment of Cancers*, by Narosa International Publishers *(In Press).*

Curriculum Vitae

Education

04/2007- present	**Ph D Scholar** at Sree Chitra Tirunal Institute for Medical Sciences and Technology. Biomedical Technology Wing, Trivandrum, Kerala, India. Advisor: Dr. Chandra P. Sharma, Ph.D.
10/2001- 03/2003	**Master of Technology in Polymer Technology**, Cochin University of Science & Technology, Kerala, India.
07/1997-04/1999	**Master of Science in Chemistry**, University of Kerala, India.
07/1994-04/1997	**Bachelor of Science in Polymer Chemistry**, University of Kerala, India.

Professional experience

10/2004-04/2007	National Institute for Interdisciplinary Science and Technology (NIIST), CSIR, India. Project advisor Dr.C.K.S. Pillai, Scientist G & Head, Chemical Sciences & Technology Division (NIIST).
10/2002-04/2003	Vikram Sarabhai Space Centre (VSSC), Indian Space Research Organisation (ISRO), Thiruvananthapuram, India Project advisor: Dr. S.Packirisamy Scientist SG PSCD, VSSC, ISRO,India.
10/1999-03/2000	Teaching Assistant, Government Engineering College, Wynad, Kerala.
06/2000-10/2004	Teaching Assistant, Fatima Mata National College, University of Kerala, India.